Micronesica 43(2): 237 – 479, 2012

Coral-reef diatoms (Bacillariophyta) from Guam: new records and preliminary checklist, with emphasis on epiphytic species from farmer-fish territories

Christopher S. Lobban[1], María Schefter

Division of Natural Sciences, University of Guam, Mangilao, GU 96923, USA
Email: clobban@uguam.uog.edu

Richard W. Jordan, Yumi Arai, Asami Sasaki

Department of Earth and Environmental Sciences, Faculty of Science, Yamagata University, Yamagata 990 8560, Japan

Edward C. Theriot, Matt Ashworth, Elizabeth C. Ruck[2]

Section of Integrative Biology, University of Texas, Austin, TX 78712, USA

Chiara Pennesi

Department of Life and Environmental Sciences, Polytechnic University of the Marche, Via Brecce Bianche, 60131 Ancona, Italy

Abstract—The marine diatom flora of the tropical western Pacific island of Guam is all but unknown. Following several taxonomic/systematic papers, this floristics paper documents 179 new records of diatoms identified from light microscopy and/or scanning electron microscopy. Samples were collected from diverse habitats for several research projects in the authors' laboratories, but the majority reported here are epiphytic, especially from pomacentrid farmer-fish territories. While many of the species are well known from other regions, some recently named, rarely seen, or poorly-described taxa include *Amphora decussata* Grunow; *Ardissonea fulgens* var. *fulgens* (Greville) Grunow and var. *gigantea* (Lobarzewsky) De Toni; *Campylodiscus humilis* Greville; *Falcula paracelsianus* Voigt; *Hyalosira interrupta* (Ehrenberg) Navarro; *Olifantiella pilosella* Riaux-Gobin; and *Triceratium pulchellum* (Grunow) Grunow. A preliminary checklist incorporating the new records and our previous records totals 237 taxa, which is a step towards the development of the regional flora. Many taxa remain to be identified from the documentation so far and few samples have been analyzed from other habitats such as sediments and mangroves. Only 28–42% of the species in this checklist also occurred in lists from the Society Islands, Mahé, Puerto Rico and The Bahamas—but all regions remain seriously undersampled. We do, however note some apparent differences in common and distinctive species.

[1]Corresponding author.
[2]Present address: Department of Biological Sciences, University of Arkansas, Fayetteville, AR 72701

Tropical marine environments, especially coral reefs, are of great biological and economic value and are degrading rapidly under local and global anthropogenic stresses (Pandolfi et al. 2003). The diversity of larger coral reef organisms, including seaweeds, is relatively well documented (e.g., Paulay 2003 for Guam) but virtually all small and microscopic species are very poorly known; their importance to the health of reef ecosystems can be supposed by analogy with freshwater and soil microorganisms. Diatoms are widely used for environmental assessment (Smol & Stoermer 2010) and have the potential to be useful in studies of living and fossil coral reefs (Lobban & Jordan 2010), but the first prerequisite is to know what species are present. One role that has been shown, however, is as food for farmer fish (territorial pomacentrids that cultivate algae), which are abundant in some reef habitats and significantly alter reef structure (Polunin 1988, Ceccarelli et al. 2001, Ceccarelli 2007); Hixon & Brostoff (1983) called them keystone species in the reef community. Their stomach contents can be 30–80% diatoms (Jones et al. 2006), yet ecological studies of these communities have focused on seaweeds, with diatoms rarely mentioned as a group and never identified to genus or species (Lobban & Jordan 2010).

Although there are many diatom species described from tropical waters, diatom floras of tropical habitats, including coral reefs, are poorly known (Lobban & Jordan 2010, Riaux-Gobin et al. 2011b). Many of the known descriptions result from the long history of collections by travelling naturalists or scientific expeditions being sent to diatomists, especially in Europe. Ecological data on these species tend to be extremely scant to non-existent, often no more than a vague locality. For instance, Hustedt (1931–1959) named many new *Mastogloia* species and gave occurrence data such as "Ocean form. Not rare in the northern Adriatic" *(M. decipiens)* and "very rare near Miang Besar, Borneo" *(M. lata)*. Even in great recent works like Witkowski et al. (2000), one cannot ascertain which species occur on coral reefs. Mann's (1925) report on the *Albatross* collections from the Philippines is an important resource for our region but is based entirely on dredge samples. More recently, diatomists have made brief collecting trips themselves and published books based on a small number of samples. For example, Foged (1987) in a quick tour of Viti Levu collected 18 samples only 7 of which were marine, but they included 287 "polyhalobe" species. Similarly, Podzorski & Håkansson (1987) had 11 marine samples from Palawan; they summarized their results in species lists by habitat. Long-term studies are uncommon but include, of most relevance to the present work, Ricard's (1974, 1975, 1977) studies in Tahiti, Giffen's (1980) checklist for Mahé, Seychelle Is., Navarro's studies in Puerto Rico (Navarro 1981a, b, 1982a–c, 1983a, b; Navarro et al. 1989), the book by Hein et al. (2008) for The Bahamas, and a series recently initiated by Riaux-Gobin in the Mascarene Islands (western Indian Ocean) and Tahiti (Riaux-Gobin & Compère 2009, Riaux-Gobin et al. 2010, 2011a, b, Riaux-Gobin & Al-Handal 2012). As far as benthic records are concerned, both Ricard's work and Navarro's early studies were based on net collections, so that benthic taxa were sampled out of context and undoubtedly undersampled. At present one can scarcely say what species of diatoms occur on coral reefs anywhere.

Besides its importance to understanding biodiversity in a very productive group of organisms, improved knowledge of tropical benthic diatom floras gives access to many taxa useful in phylogenetic and basic biology studies of diatoms and will allow them to be more extensively used in environmental monitoring. For example, comparison with *Cyclophora tenuis* Castracane of four new taxa with cup-like pseudosepta inside the valves led to a study of the ultrastructure of this feature as well as the phylogenetic implications, including the discovery of the genus *Astrosyne*, an araphid pennate with radial symmetry typical of centric diatoms, rather than bilateral symmetry typical of pennate diatoms (Ashworth et al. 2012). In addition, multigene molecular phylogenies of the diatoms including many Guam isolates have been published by Theriot et al. (2010, 2011) and Ashworth et al. (2012), where the inclusion of Guam isolates proved significant in resolving certain areas of the diatom tree, particularly the early-diverging araphid pennates.

There have been few reports of diatom taxa from the tropical Western Pacific islands. An unpublished master's thesis on diatom settlement on glass slides in Guam left no voucher specimens or illustrations (Zolan 1980), and thus the first documented records of marine diatoms in Guam were the 27 taxa included in Navarro & Lobban (2009). Following these initial records of the diatoms of Guam and Yap (Navarro & Lobban 2009) and studies by Jordan in Palau (Konno & Jordan 2008, Konno et al. 2010), the Lobban, Jordan, and Theriot laboratories began collaborative work to document the marine benthic diatom flora of the western Pacific islands, including to date significant collections from Guam, Yap (Federated States of Micronesia, FSM) and the Republic of Palau, with a few incidental samples from Chuuk (FSM) and Republic of the Marshall Islands. Several novel genera and species and additional new records have been described in separate papers (Lobban et al. 2010, Lobban et al. 2011a, b, Lobban & Navarro 2012, in press, Ashworth et al. 2012) and more new taxa are in manuscript. Pennesi contributed to identifying *Mastogloia*—the most speciose genus in our flora so far—on the basis of her global experience with the genus (Pennesi et al. 2011, 2012). The present paper is a floristic work documenting a further 179 known taxa identified to date from surveys of collections from Guam, and providing a checklist (Appendix 1) with all the published records, bringing the Guam list to 237 taxa. The new records listed here include both new sampling by the authors and new analysis of prior collections by Lobban. Two of the authors completed theses on Guam materials (Arai 2010, Sasaki 2010) and Ruck's work, particularly on Surirellales was part of her dissertation (Ruck 2010). The ongoing project is more extensively but informally documented on the ProtistCentral website (Jordan et al. 2009–2012).

Materials and methods

Study area

Guam (Fig. 1) is a small (541 km^2), limestone-capped volcanic island in the western Pacific, 13 °N, 144 °E, the southernmost of the Mariana Islands. It has a small lagoon and motu (low coral island) at the southern tip but is otherwise sur-

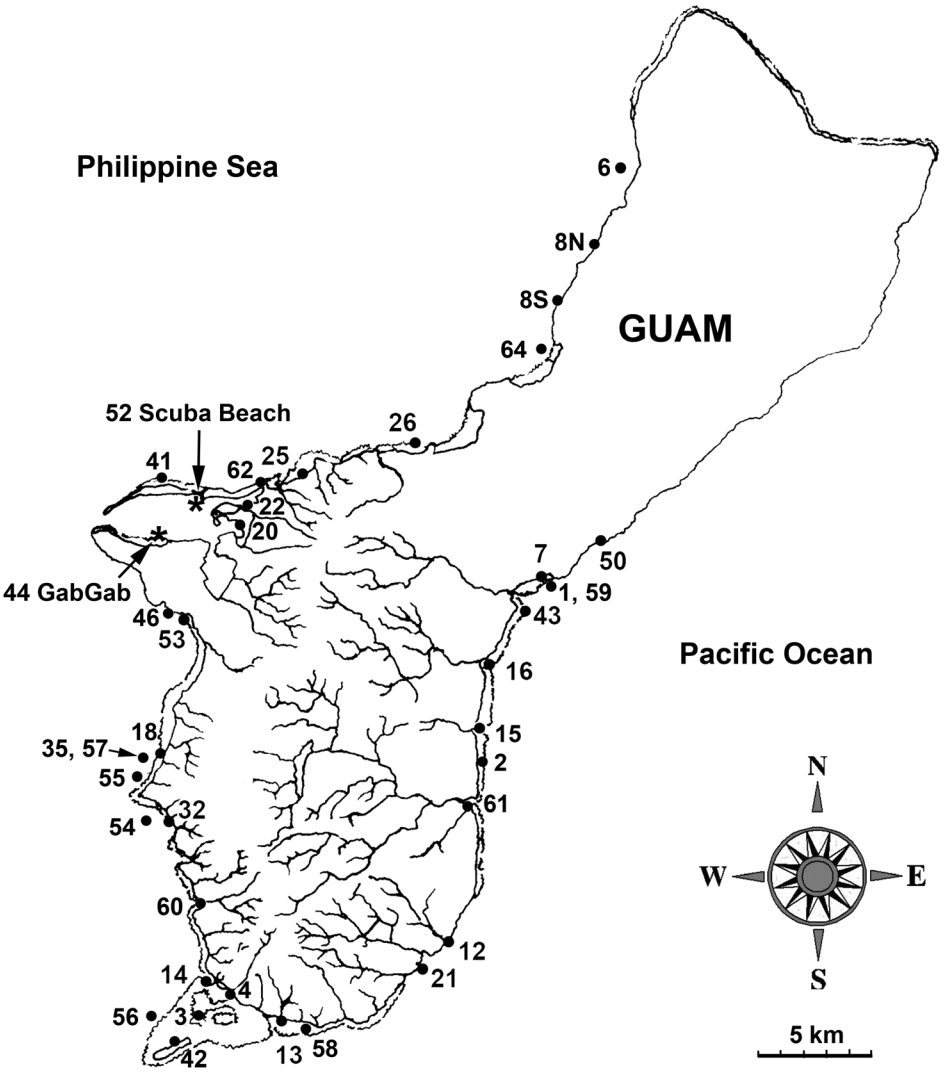

Figure 1. Map of Guam showing location of collection sites listed in Table 1. The two main study sites, GabGab and Scuba (Outhouse) Beach are named and marked with an asterisk, other sites marked with a filled circle.

rounded by fringing reef, much of it erosional. The northern half of the island is a limestone plateau extending below sea level and containing a large freshwater lens; the coastline here has some sandy beaches but is largely inaccessible cliffs and cut benches. The southern half is volcanic hills with only small patches of limestone on some of the peaks and an accessible shoreline. Thus the southern half of the island has many rivers, the northern half has no rivers but many sea-level springs. On the west (Philippine Sea) side of the island, a large deepwater harbor (Apra Harbor) exists, bordered on the south by the limestone Orote Peninsula, and

bounded on the north by Glass Breakwater, a structure built over the inner edge of a barrier reef (Luminao Reef) and extending westward beyond it. Apra Harbor has relatively small freshwater inputs and some of the island's remnant mangroves in their estuaries. Although coral diversity is low in the harbor, cover in the top 20 m is still fairly complete. Many of our samples were collected at one site on the south side (GU44 GabGab) and one site on the north side (GU52 Scuba/Outhouse Beach); these sites are described briefly as follows.

GabGab is a recreation site on U.S. Naval Base Guam, comprising a shallow dredged swimming pool with concrete walls, cut through the fringing reef and opening onto the reef slope. There is an abundance of macroalgae in the pool and on the adjacent reef flat just below low water, while the upper part of the reef slope is almost completely covered with one coral, *Porites rus* (Forskål, 1775). In the coral heads from just below low water to about 8 m are many farmer fish—territorial algae cultivators in the damselfish family Pomacentridae, which maintain closely-spaced territories and cultivate filamentous algae (see Polunin 1988, Lobban & Jordan 2010). *Stegastes nigricans* (Lacepède, 1802) is more common in the shallow water and its algal turf farms can completely cover rock surfaces and iron debris; *Plectroglyphidodon lacrymatus* (Quoy & Gaimard, 1825) is more common on the reef slope in the lower parts of the *Porites* structure and has much patchier algal turf and macroalgae in its territories. Below about 8 m there is less coral cover, more calcareous algae *(Halimeda, Peysonnelia)*, and no farmer fish.

Scuba (Outhouse) Beach is a derelict wharf stretching for 100 m along the inner side of Glass Breakwater, and our collecting sites are all within the first 5 m below low water on the boulder remains of the wharf; below that the substratum consists of sediments. There is little live coral at this site and the biota is dominated by fleshy algae, with extensive seasonal *Padina* meadows where we studied the zooxanthellate ciliate *Maristentor dinoferus* Lobban et al., 2002 over a number of years (Lobban & Schefter 2012 and references therein). There are a few farmer-fish territories, mostly *S. nigricans* on rubble with a few *S. lividus* (Forster, 1801) in a patch of *Acropora* (staghorn coral). On the outer side of Glass Breakwater, on Luminao Reef, the coral is chiefly *Acropora* spp. and the dominant farmer fish is *S. lividus*.

Procedures

Collections were made during scuba, snorkeling or beach-walking around Guam. GabGab and Scuba Beach have been repeatedly sampled by Lobban & Schefter over 5 years (to date >100 retained samples from GabGab, nearly 50 from Scuba Beach), whereas other sites have been less regularly visited. Extensive sampling was carried out by the Theriot laboratory throughout June 2008 and on several occasions by the Jordan laboratory in 2008–2009. In addition some records come from extensive collections made by Lobban in Guam in 1988–1989. A summary list of all collecting sites is given in Table 1. The Guam Diatom Herbarium as of August 2012 comprises over 650 raw samples, 1,100 permanent slide mounts in Naphrax®, 300 SEM stubs and 55,000 images. Analysis is ongoing and has so far focused primarily on samples from farmer-fish territories.

Table 1. List of all Guam sites for marine benthic diatom collections to date. See map, Fig. 1.

Site	Latitude N	Longitude E	Name
GU1	13.428	144.797	Pago Bay forereef near Marine Laboratory
GU2	13.354	144.773	Jones Beach Ipan
GU3	13.250	144.670	Cocos Lagoon
GU4	13.263	144.673	Geus River estuary
GU6	13.596	144.834	Double Reef / Haputo Point
GU7	13.428	144.799	UOG Marine Laboratory aquaria.
GU8 (south)	13.545	144.809	Tanguissan Beach
GU8 (north)	13.559	144.816	Shark's Hole (Hilaan Beach)
GU12	13.281	144.760	Pauliluc Bay, Inarajan
GU13	13.281	144.693	Suyafe River
GU14	13.268	144.664	Mamaon Channel / Merizo pier
GU15	13.367	144.770	Togcha River, Yona
GU16	13.392	144.769	Ylig River, Yona
GU18	13.356	144.750	Taleyfac River (Spanish Bridge)
GU20	13.444	144.682	Laguas River mangal
GU21	13.271	144.748	Saluglula Pools, Inarajan
GU22	13.401	144.664	Namo River estuary
GU25	13.469	144.703	Tepungan Beach, Piti
GU26	13.478	144.749	Agana Boat Basin
GU32	13.328	144.651	Sella Bay
GU35	13.357	144.638	Anae Island
GU41	13.465	144.647	Luminao Reef (Glass Breakwater)
GU42	13.239	144.648	Cocos Lagoon at Cocos I.
GU43	13.406	144.781	Tagachang Reef
GU44	13.443	144.643	GabGab reef, Apra Harbor
GU46	13.412	144.658	South Tipalao Beach
GU50	13.443	144.821	Fadian Fish Hatchery aquarium
GU52	13.464	144.656	Scuba Beach, Apra Harbor
GU53	13.405	144.661	Rizal Beach / Dadi Beach
GU54	13.336	144.641	Nathan's Dent
GU55	13.347	144.639	Pete's Reef MDA study site
GU56	13.252	144.648	Cocos West at MDA buoy
GU57	13.357	144.641	Coral Gardens (inshore side Anae I.)
GU58	13.249	144.697	Achang mangroves
GU59	13.428	144.798	Pago Bay shoreline at Marine Lab
GU60	13.299	144.659	Umatac Bay
GU61	13.336	144.763	Talofofo Bay SW corner
GU62	13.468	144.684	Cabras Channel
GU64	13.494	144.768	Agana Bay forereef, eastern end
GU65	13.444	144.656	Sumay Reef
GU66	13.444	144.644	GabGab II Reef

Samples were observed alive while fresh whenever possible and some cells were isolated into culture, yet many taxa have been seen only in acid cleaned preparations. The most intense analysis of samples has been done on the following samples: (a) GU44 (GabGab) farmer-fish territories, samples GU44I-1, GU44I-2 (29Oct07, both *Plectroglyphidodon lacrymatus* from 8m depth), GU44P-B (1Sep08, *Stegastes nigricans*), GU44Y-13 (10May09, *P. lacrymatus* from <1 m depth), and GU44Z-15 (20June09, *S. nigricans*); (b) GU26A (Agana Boat Basin, 29Nov88) algal turf on rock just below zero tide level. Light- and scanning electron microscopy and culture methods were described previously (Konno & Jordan 2008, Arai 2010, Sasami 2010, Lobban et al. 2010, Lobban et al. 2011a). Samples from farmer-fish territories are identified by boldface in the species accounts. We have included presumably-marine planktonic taxa that were found in our benthic samples, but excluded freshwater taxa that were found occasionally.

Documentation

Vouchers: permanent slides and SEM stubs for most records claimed here are presently in the Guam Diatom Herbarium (GU sample numbers) with additional materials in Jordan's collection (Arai, Sasaki samples) and Theriot's collection (ECT sample numbers). In addition many of the taxa documented below occur on strew slides and stubs that were deposited at California Academy of Sciences for type specimens (Table 2).

Table 2. Strew slides and stubs from Guam in the California Academy of Sciences Diatom Collection as of August 2012.

Sample #	Accession #	Slide #	Type species
GU7N	627384	223006	*Perideraion montgomeryi*
GU32B	627397	223012	*Mastogloia lyra*
GU44I-4	627405	223019	*Cyclophora minor*
GU44U-1A	627394	223008	*Mastogloiopsis biseriata* [paratype]
GU44V-1	627375	222100	*Climaconeis undulata* [voucher, not a type]
GU44Y-13	627373	222098	*Climaconeis guamensis*
GU44Z-15	627386	223007	*Perideraion* spp., including *P. elongatum*
GU44Z-15	627385	SEM stub	*Perideraion* spp., including *P. decipiens*; *Gato hyalinus* [isotype]
GU44Z-15	627383	223005	*Gato hyalinus*
GU44Z-15	627409	223023	*Astrosyne radiata*
GU44Z-15	627396	223010	*Hanicella moenia* [ms name]
GU44AA-5	627406	223020	*Cyclophora castracanei*
GU44AL-3	627403	223017	*Licmosphenia peragallioides*
GU54B-4	627377	SEM stub	*Licmophora flucticulata*
GU54B-4	627397	223011	*Mastogloia parlibellioides*
GU55B-4-1	627376	223001	*Climaconeis petersonii*
GU52K-2	627404	223018	*Licmosphenia albertmannii* and *L. leuduger-fortmorelii*
GU52J-3	627414	223026	*Cyclophora tabellariformis* [paratype]

Measurements are based on one to several imaged specimens and do not necessarily represent the range of size present in Guam. Measurements without a range sometimes came from several specimens; we have indicated when the record is based on a single valve. In cases where a taxon occurred in many samples from a site we have listed several records including the imaged specimens but not all. A more complete analysis of the farmer-fish territory assemblages is in progress.

Additional documentation: Many additional images of these taxa have been posted on the ProtistCentral website (Jordan et al. 2009–2012).

Terminology follows Ross et al. (1979), Round et al. (1990) and recent papers on particular genera. Several terms and corresponding acroynms are in use for the rapheless valve in monoraphid taxa including rapheless valve (RLV) (e.g., Witkowski et al. 2000), raphe-sternum valve (RSV) (e.g., Sar et al. 2003), and sternum valve (SV) (e.g., Riaux-Gobin et al. 2011b). We have adopted the latter.

Identifications

The claims made here for Guam records are based on comparison of our images with images in the literature available to us and cited for each species, and the species listed are those for which we feel confident in the comparison. Besides books cited for reference illustrations, we also found very useful the bibliographies of fine structure by Gaul et al. (1993) and Henderson & Reimer (2003). We make these claims cognizant of the risks of "force fitting" tropical specimens into European taxa (Tyler 1996, Vanormelingen et al. 2008) and modern taxa into fossil taxa and thus we illustrate all our taxa and note differences between our specimens and those reported in the literature. However, it must be recognized that there are also documented morphological continuities and even genetic identity in diatoms across broad regions of geographic and ecological space (Alverson & Kolnick 2005; Edgar & Theriot 2003; Edgar & Theriot 2004; Gallagher 1980; Sarno et al. 2005; Theriot & Stoermer 1981; Theriot & Stoermer 1984a; Theriot & Ladewski 1986; Theriot 1987; Theriot et al. 1988; Theriot & Stoermer 1984b; Theriot 1992; Zingone et al. 2005), and morphological identity even across large gaps in the stratigraphic record, as per the numerous examples of Eocene records of modern freshwater species (Wolfe & Siver 2009). Thus, we elected not to take a point of view about endemism or regionalism, but rather to simply record as best we could the (dis-)similarity between our specimens and those previously reported in the literature, mainly using qualitative morphological observations. Further qualitative morphological, quantitative morphometric and molecular studies will refine our knowledge. The value of a flora such as this is not as a final summary of knowledge, but as a guide to further research into the diverse and largely poorly known marine benthic diatom flora.

Systematic List

The systematic arrangement used is based on Round et al. (1990) (Table 3). An alphabetical listing is given in the Appendix.

Table 3. Systematic order of the taxa reported from Guam to date. Based on Round et al. 1990, and modifications in more recent publications. Orders and Families without a page reference and genera marked with * are earlier records, see Appendix 1.

THALASSIOSIRALES Glezer and Makarova	
Thalassiosiraceae Lebour: *Roundia* Makarova	p. 247
CHRYSANTHEMODISCALES Round	
Chrysanthemodiscaceae Round: **Chrysanthemodiscus* A. Mann	
MELOSIRALES Crawford	
Melosiraceae Kützing: **Melosira* C.A. Agardh	
Hyalodiscaceae Crawford: *Podosira* Ehrenberg	p. 247
PARALIALES Crawford	
Paraliaceae Crawford: *Paralia* Heiberg	p. 249
COSCINODISCALES Round and Crawford	
Hemidiscaceae Hendey *emend* Simonsen: *Actinocyclus* Ehrenberg	p. 249
Aulacodiscaceae (Schütt) Lemmermann: *Aulacodiscus* Ehrenberg	p. 249
ASTEROLAMPRALES Round and Crawford	
Asterolampraceae H.L. Smith: *Asterolampra* Ehrenberg	p. 249
STICTOCYCLALES Round	
Stictocyclaceae Round: **Stictocyclus* A. Mann	
TRICERATIALES Round and Crawford	
Triceratiaceae (Schütt) Lemmermann: *Odontella* C.A. Agardh, *Triceratium* Ehrenberg, **Lampriscus* A. Schmidt	p. 250
BIDDULPHIALES Krieger	
Biddulphiaceae Kützing: **Biddulphia* Gray, *Biddulphiopsis* von Stosch & Simonsen, *Isthmia* C.A. Agardh, *Trigonium* Cleve	p. 251
HEMIAULALES Round and Crawford	
Hemiaulaceae Heiberg: *Hemiaulus* Ehrenberg	p. 252
LITHODESMIALES Round and Crawford	
Lithodesmiaceae Round: *Lithodesmioides* von Stosch	p. 252
RHIZOSOLENIALES Silva	
Probosciaceae Jordan & Ligowski: *Proboscia* Sundström	p. 253
CHAETOCEROTALES Round & Crawford	
Chaetocerotaceae Ralfs: *Chaetoceros* Ehrenberg	p. 253
FRAGILALARIALES Silva	
Plagiogrammaceae De Toni emend Sato, Kooistra & Medlin: *Neofragilaria* Desikachary, Prasad & Prema, *Plagiogramma* Greville, *Psammoneis* Sato, Kooistra & Medlin	p. 254
Fragilariaceae Greville: **Bleakeleya* Round emend. Theriot & Lobban, *Falcula* Voigt, **Hyalosynedra* Williams & Round, **Koernerella* Ashworth, Lobban & Theriot, *Neosynedra* Williams & Round, **Perideraion* Lobban & Jordan, *Podocystis* Bailey, *Synedra* Ehrenberg, *Tabularia* (Kützing) Williams & Round	p. 255
LICMOPHORALES Round	
Licmophoraceae Kützing: **Licmophora* C.A. Agardh, **Licmosphenia* Mereschkowsky	

RHAPHONEIDALES Round
Rhaphoneidaceae Forti: *Perissonoë* Andrews & Stoelzel, *Rhaphoneis* Ehrenberg p. 258
Psammodiscaceae Round & Mann: *Psammodiscus* Round & Mann p. 258
ARDISSONEALES Round
Ardissoneaceae Round: *Ardissonea* De Notaris p. 259
TOXARIALES Round
Toxariaceae Round: *Toxarium* Bailey p. 260
RHABDONEMATALES Round & Crawford
Rhabdonemataceae Round & Crawford: *Rhabdonema* Kützing p. 261
STRIATELLALES Round
Florellaceae Navarro: *Florella* Navarro p. 261
Striatellaceae Kützing: *Hyalosira* Kützing, *Grammatophora* Ehrenberg, *Striatella* C.A. Agardh p. 261
CYCLOPHORALES Round & Crawford
Cyclophoraceae Round & Crawford: **Cyclophora* Castracane emend. Ashworth & Lobban
INCERTAE SEDIS
**Astrosyne* Ashworth & Lobban
CLIMACOSPHENIALES Round
Climacospheniaceae Round: **Climacosphenia* Ehrenberg

LYRELLALES D.G. Mann
Lyrellaceae D.G. Mann: *Lyrella* Karajeva, *Petroneis* Stickle & D.G. Mann p. 263
INCERTAE SEDIS
Olifantiella Riaux-Gobin & Compère p. 264
CYMBELLALES D.G. Mann
Rhoicospheniaceae Chen & Zhu: *Gomphonemopsis* Medlin p. 264
MASTOGLOIALES D.G. Mann
Mastogloiaceae Mereschkowsky: *Mastogloia* Thwaites ex W. Smith, **Mastogloiopsis* Lobban & Navarro, *Mastoneis* Cleve p. 265
Achnanthaceae Kützing: *Achnanthes* Bory p. 284
ACHNANTHALES Silva
Achnanthidiaceae D.G. Mann: *Planothidium* Round & Bukhtiyarova p. 285
Cocconeidaceae Kützing: *Anorthoneis* Grunow, *Cocconeis* Ehrenberg p. 286
NAVICULALES Bessey
Berkeleyaceae D.G. Mann: **Berkeleya* Greville, *Climaconeis* Grunow, *Parlibellus* E.J. Cox p. 289
Diadesmidaceae D.G. Mann: **Luticola* D.G. Mann
Diploneidaceae D.G. Mann: *Diploneis* Ehrenberg ex Cleve p. 289
Naviculaceae Kützing: *Chamaepinnularia* Lange-Bertalot & Krammer, *Cymatoneis* Cleve, *Haslea* Simonsen, *Navicula* Bory, *Trachyneis* Cleve p. 291
Pinnulariaceae D.G. Mann: *Caloneis* Cleve, *Oestrupia* Heiden ex Hustedt p. 294
Pleurosigmataceae Mereschkowsky: *Donkinia* Ralfs, *Pleurosigma* W. Smith p. 295
Plagiotropidaceae D.G. Mann: *Plagiotropis* Pfitzer emend. Paddock,

Staurotropis Meunier p. 295
Stauroneidaceae D.G. Mann: *Stauroneis* Ehrenberg p. 296
Proschkiniaceae D.G. Mann: *Proschkinia* Karayeva p. 296
THALASSIOPHYSALES D.G. Mann
Catenulaceae Mereschkowsky: *Amphora* Ehrenberg ex Kützing, *Halamphora* (Cleve) Levkov, *Undatella* Paddock & Sims p. 297
Thalassiophysaceae D.G. Mann: *Thalassiophysa* Conger p. 300
BACILLARIALES Hendey
Bacillariaceae Ehrenberg: *Bacillaria* Gmelin, *Nitzschia* A.H. Hassall, *Psammodictyon* D.G. Mann p. 300
RHOPALODIALES D.G. Mann
Rhopalodiaceae (Karsten) Topachevs'kyj & Oksiyuk: **Rhopalodia* O. Müller
SURIRELLIALES D.G. Mann
Auriculaceae Hendey: *Auricula* Castracane p. 304
Entomoneidaceae Reimer: **Entomoneis* Ehrenberg
Surirellaceae Kützing: *Campylodiscus* Ehrenberg ex Cleve, *Hydrosilicon* J. Brun, *Petrodictyon* D.G. Mann, *Plagiodiscus* Grunow & Eulenstein, *Surirella* Turpin p. 305

Roundia cardiophora (Round) Makarova Plate 3, Figs 1, 2
Syn.: *Thalassiosira cardiophora* Round
Ref. illus.: Round 1988, figs 1–12; Hernández-Becerril & Navarro 1998, figs 4–11.
Samples: **GU44I-2, GU44Z-15**; culture isolate ECT 3681.
Dimensions: Diam. 35–60 µm.
Diagnostics: The cluster of 5 rimoportulae distinguish this monospecific genus from *Thalassiosira*. The long pervalvar axis of the frustule is due to numerous girdle bands.

Podosira baldjickiana Grunow Plate 3, Figs 3–6
Ref. illus.: Grunow in Schmidt et al. 1874–1959, pl. 130, fig. 40 (type, 1888), plate 183, fig. 11 (1893); Van Heurck 1880–1887, slide 545!
Samples: **GU44I-1, GU44R-2**
Dimensions: Diam. 42 µm, areolae 15 in 10 µm.
Diagnostics: This species has elongated, flat-topped valves that resemble thimbles. Areolae are uniform, covering hexagonal loculi, except for forming rosettes around the rimoportulae (Pl. 3, Fig. 5) (also seen in other species).
Comments: We have not found other records of this species and Grunow in Schmidt et al. (1874–1959) gave no description, so we propose this identity with some hesitation. Indeed, the origin of this name is in some doubt. The specimens were collected by Weissflog, drawn by Schmidt and attributed to Grunow as the authority. There appears to be a reference to Grunow in Van Heurck (1880–1885), but it does not appear in the plates where there are several *Podosira* species, nor in the text, where there are no *Podosira* sp.). Thus the CAS Catalogue gives the type as the first illustration of it in Schmidt's Atlas. It occurs on Van Heurck's (1880–1887)

Types, slide 545, and we examined this slide from the Farlow Herbarium of Harvard University. Droop (1998) described this material as fossil, Miocene marine deposit from Paratethys Sea, collected at Baldjick (Balchik), Bulgaria, west coast of the Black Sea (43°24' N, 28°10' E). Several valves matching the Schmidt's Atlas drawing are present (Pl. 3, Figs. 6, 7), but there are also valves of a similar shape with much different valve structure (Pl. 3, Fig. 8). Whereas in the former the areolae are small and uniform, with evident rimoportulae among them, the latter has larger, irregular areolae and no evident rimoportulae.

Podosira hormoides (Montagne) Kützing Plate 4, Figs 1, 2
Ref. illus.: Grunow in Van Heurck 1880–1885, pl. 84, figs 3–6; Peragallo & Peragallo 1897-1908, pl. 120, fig. 12; Hustedt 1927–1930, figs 123–125.
Samples: **GU44I-1, GU44R-2**
Dimensions: Diam. 42– µm, areolae 15 in 10 µm.
Diagnostics: This species is distinguished from others in the European flora (Hustedt 1927–1930) by a moderately high dome and relatively coarse areolae, but the frustule is nevertheless lenticular in profile (Pl. 4, Fig. 2), whereas *P. montagnei* is ± spherical.
Comments: Cells in wild material and culture develop simple stalks near the margin of the cell. We have observed a range of lenticular valves some of which do not fit well into the species and varieties covered by Hustedt. However, the images presented here agree with the criteria for *P. hormoides* var. *hormoides*. Areola density is an important character and Hustedt (1927–1930, p. 284) expressed doubt that var. *delicatula*, which has about 22 areolae in 10 µm, fits within *P. hormoides*, which has 13–18 in the other two varieties. Bérard-Therriault et al. (1987, figs 56, 59, 60) and Hein et al. (2008, pl. 3:2) show var. *adriatica* Grunow, the former including SEM and noting an areola density of 14–18 in 10 µm. It is clear that this genus of fossil and extant taxa needs further study.

Podosira montagnei Kützing Plate 4, Figs 3–5
Ref. illus.: Grunow in Van Heurck 1880–1885, pl. 84, figs. 11, 12; Peragallo & Peragallo 1897-1908, pl. 120, fig. 11; Hustedt 1927–1930, fig. 122.
Samples: **GU44AC-4, GU44I-2, GU44Z-15, GU44R-2, GU44Q-1; GU52P-7, GU52P-2**
Dimensions: Diam. 22–47 µm, striae 21–23 in 10 µm.
Diagnostics: The deep valve is unique in this genus (Hustedt 1927–1930).
Comments: The deep valve could be confused with some *Melosira*, e.g., *Melosira moniliformis* var. *octagona* (Grunow) Hustedt (see López-Fuerte et al. 2010: pl. 7, fig. 12). However, the striae in *Melosira* are not arranged in bundles, in contrast to *Podosira* (Hustedt 1927–1930: 221). The dimensions are within the ranges given by Hustedt (1927–1930) and by Hendey (1964: 90–91), but there appear to be no SEM images of European material to compare (Gaul et al. 1993, Henderson & Reimer 2003) and this identification is made with some trepidation. Stalks appear to be multistranded and off-center (Pl. 4, Fig. 5); Peragallo & Peragallo (1897–1908) suggest a simple, off-center stalk similar to *P. hormoides*, but Round

et al.'s (1990) images suggest a multistranded, centrally located stalk. [Medlin et al. (1985) show two whole-mount SEM images of this species from Texas but no taxonomic detail is visible, and images in Round et al. (1990: 164–165) are not identified to species or origin.]

Paralia longispina Konno & Jordan Plate 4, Figs 6–8
Ref. illus.: Konno & Jordan 2008, figs 2–53
Samples: **GU44I-1, GU44K-6**; GU55B-4
Dimensions: Diam. 9–12 µm
Diagnostics: Distinguished from the widespread *P. sulcata* (Ehrenberg) Cleve by the long, tapering marginal spines on the separation valve (Pl. 4, Fig. 7) (Konno & Jordan 2008) compared to other species (e.g., Sawai et al. 2005). MacGillivary & Kaczmarska (2012) recognized a complex of species around *P. longispina* that are separated by genetic and very subtle ultrastructural differences; Guam specimens in this complex bear closer study.

Actinocyclus tenuissimus Cleve Plate 5, Figs 1, 2
Ref. illus.: Hustedt 1927–1930, fig. 305; Navarro 1981a, fig. 29
Samples: **GU44I, GU44J-2, GU44Y-13, GU44Z-15**
Dimensions: Diam. 43–68 µm; areolae 20 in 10 µm; 21–26 rimoportulae aligned almost along the pervalvar axis
Diagnostics: *Actinocyclus* is distinguished by the pseudonodulus on the margin (Watkins & Fryxell 1986).
Comments: *A. tenuissimus* has 18–20 areolae in 10 um, whereas *A. subtilis* (Gregory) Ralfs has 12–15 areolae in 10 µm (Hustedt 1927–1930).

Aulacodiscus orientalis Greville Plate 5, Figs 3–5
Ref. illus.: Schmidt et al. 1874–1959, pl. 34, figs 1, 2; Desikachary 1987, pl. 20, figs 1, 2, 6
Samples: Talofofo– ECT3746
Dimensions: Diam. 85–140 µm; areolae 5–7 in 10 µm; 9–12 rimoportulae per valve
Diagnostics: Hyaline area at valve center, striae in distinct rays aligned to the unique complex rimoportulae; 7 or more rimoportulae around the margin, each a simple tube (not "capped" – cf. Round et al. 1990: 188).
Comments: The most common comment regarding this taxon in the literature is "often confused with *A. oreganus*." Rattray (1888) listed the size and rimoportula count for both species as overlapping, with *A. orientalis* having a higher minimum number of rimoportulae (7 versus 6 for *A. oreganus*), and as of yet we have not observed fewer than 7 rimoportulae on the Guam isolates. However, this identification will probably remain in doubt until thorough morphometric analyses are conducted on the two taxa.

Asterolampra marylandica Ehrenberg Plate 5, Fig. 6
Ref. illus.: Hustedt 1927–1930, figs 270, 271; Hein et al. 2008, pl. 1, fig. 5

Samples: GU21Y; **GU44Z-15**; GU55B-4; ECT3754
Dimensions: Diam. 45–130 μm
Diagnostics: The broad central area (1/3 the diameter of the valve) and number of rays (usually 7) distinguish this from other species of the genus (Hustedt 1927–1930: 485).
Comments: The generic SEM structure illustrated by Round et al. (1990: 210–211) appears to show mostly *A. marylandica*.

Odontella aurita (Lyngbye) C.A. Agardh Plate 6, Figs 1, 2
Ref. illus.: Peragallo & Peragallo (1897–1908), pl. 98, figs 3–6; Foged 1975 pl. 2, fig. 3; Witkowski et al. 2000, pl. 8, figs 12-13 and pl. 9, figs 1–3;
Samples: GU14P; GU18–ECT3772; GU55B-4; GU61–ECT3743
Dimensions: Length (apical axis) 39–40 μm
Diagnostics: Cells with central elevation and two polar elevations, the latter bearing ocelli, in contrast to *Biddulphia*.
Comments: The valve is covered in small pores with domed occulsions, and is distinguished from *Triceratium* (q.v.) by the lack of large, irregular and incomplete chambers surrounding the pores on the valve face (pseudoloculi). The distinction between loculate valves of *Odontella* and pseudoloculate valves of *Triceratium* has been emphasized by Ross & Sims (1971) and Sims & Ross (1990). *O. aurita* is distinguished from *O. longicruris* (Greville) Hoban by the position of the rimoportulae around the central elevation (Pl. 6, Fig. 2) rather than on top of it and possessing shorter, fatter ocellus-bearing apical elevations.

Triceratium dictyotum (Roper) P.A. Sims & R. Ross Plate 6, Figs 3, 4
Syn.: *Biddulphia reticulata* Roper
Ref. illus.: Ross & Sims 1971, plate 4, figs 5, 6; Jin et al. 1985, figs 116–118; Ricard 1977, pl. 12, figs. 1–6; Navarro 1981b, figs 11, 12 (all as *Biddulphia reticulata*); Ricard 1987, figs 434–440 (as *Odontella rhombus*)
Samples: GU32B
Dimensions: Length 73–110 μm, width 40–58 μm
Diagnostics: Rimoportulae with long external tubes near the base of the ocelli. The broadly lanceolate valves distinguish this from other species of *Triceratium*.
Comments: Distinguished from *Odontella rhombus* (Ehrenberg) Kützing (Sar et al. 2007, fig. 4) by the pseudoloculi on the valve face discussed previously [compare valve structure of *O. aurita* (above) and *T. dubium* Brightwell (Navarro & Lobban 2009, figs 21–24]. *T. dictyotum* is similar to *T. dubium* in the sense that they are both ocellate and pseudoloculate with vertically-deflected mantle edges. They differ in that *T. dubium's* rimoportula is on apices separate from the ocelli, whereas *T. dictyotum* has very close-occurring ocelli and rimoportula. The nomenclatural change was made by Sims & Ross (1990: 168) because of the ocelli (Fig. 24, arrow) and pseudoloculi; but a new specific epithet was needed because *T. reticulatum* was already occupied.

Triceratium pulchellum (Grunow) Grunow Plate 6, Figs 5–7, Plate 7, Figs 1, 2

Syn: *Biddulphia pygmaea* Mann 1925, p. 44.
Ref. illus.: Grunow in Van Heurck 1880–1885, pl. 108, fig. 12, 13 (as *T. cornutum* var. *pulchella*); Grunow in Schmidt et al. 1874–1959, pl. 98, fig. 16, 17; Montgomery 1978, pl. 45, figs A–C.
Samples: GU7N
Dimensions: Diam. (across two points) 23–31 µm.
Diagnostics: Small species, pentagonal in our sample but also reported tetragonal, with 5 rimoportulae with very long external processes (Pl. 6, Fig. 5) around the central elevation (some may be missing—Pl. 7, Fig. 1), aligned with the indentations between the poles. Valve surface with many short, stout spines.
Comments: Although Mann (1925) argued that this species belonged in *Biddulphia*, and gave it a new name since *B. pulchella* Gray was already in use, the ocelli are inconsistent with *Biddulphia* and this suggestion must be rejected.

Biddulphiopsis titiana (Grunow) von Stosch & Simonsen Plate 7, Fig. 3
Ref. illus.: von Stosch & Simonsen 1984, figs 1–26; Franz & Schmid 1994, figs 1–11
Samples: **GU44I-2, GU44U-1A**; ECT 3697
Dimensions: Diam. 100–110 µm.
Diagnostics: *B. titiana* in our samples was tripolar, the corners barely elevated and with little change in pore pattern.
Comments: Distinguished by size and shape from the larger, elliptical *B. membranacea* (Navarro & Lobban 2009, figs 6, 7).

Isthmia minima Harvey & J.W. Bailey Plate 7, Figs 4–6
Ref. illus.: Montgomery 1978, pl. 49E-H; Ricard 1987, figs 320–324; Navarro 1981b, figs 16–20 (all as *I. enervis* Ehrenberg); Andresen 1995, figs 1–9; Hein et al. 2008, pl. 5, fig. 7
Samples: GU44Y-8, **GU44AR-3**
Dimensions: Diam. 67–80 µm, length 188–300 µm
Diagnostics: The asymmetric and dissimilar (alpha and beta) valves without costae and the very large areolae are characteristic of the genus; the invaginated cribra (Pl. 7, Figs 5, 6) are unique to this species.
Comments: Colonies readily observed at low magnification. Readily distinguished from *I. nervosa* Kützing (Round 1984, figs 1F, G, 3C) by the lack of costae, and from *I. inervis* (Round 1984, Figs 1I, 3D) by presence of invaginated cribra. In addition, Andresen (1995) noted that the rimoportulae have unoccluded external openings in *I. minima* and no openings in *I. nervosa* or *I. enervis*. Mann (1925) described but did not illustrate *I. minima*; in noting the "dim club-shaped bodies enclosed within the frustules" of *I. lindigiana* observed by Grunow, he suggested, "That they are no essential part of the diatom is unquestionable and they may be dropped out of consideration" in defining species. In contrast, Andresen (1995) found that invaginated cribra are diagnostic of *I. minima*. Moreover, Andresen contended that *I. lindigiana* is synonymous with *I. minima*. Invaginated cribra are also evident in Ricard's (1987) images, which must thus be included under *I. minima*.

Trigonium diaphanum A. Mann Plate 8, Figs 1, 2
Ref. illus.: Mann 1925 pl. 37, fig. 3; Navarro 1981b, fig. 22, 23
Samples: **GU44I-1, GU44I-2**
Dimensions: Width 80–89 µm
Diagnostics: This species is distinguished from *T. formosum* by the large circular area having larger areolae than the outer area, whereas in *T. formosum* the areolae are uniform.
Comments: Our specimens all quadrangular, which predominated in Mann's (1925) Philippine samples; 3- and 5-cornered specimens also occur and were the only ones found by Navarro (1981b) in Puerto Rico. In this species these shapes are not designated as separate forms, in contrast to *T. formosum* (Brightwell) Cleve, where the type form is triangular and so far in Guam we have recorded *T. formosum* f. *pentagonale* Hustedt (Navarro & Lobban 2009) commonly and *T. formosum* f. *quadrangularis* (Greville) Desikachary & Sreelatha (q.v.) only rarely.

Trigonium formosum f. *quadrangularis* (Greville) Desikachary & Sreelatha
Plate 8, Fig. 3
Ref. illus.: Hustedt 1927–1930, fig. 483 [as *Triceratium formosum* f. *quadrangularis* (Greville) Hustedt]; Navarro 1981b, fig. 25; Desikachary & Sreelatha 1989, pl. 113, figs 3, 7
Samples: ECT 3671; **GU44AR-1**
Dimensions: Width 73 µm.
Diagnostics: See *T. diaphanum*, above.
Comments: This form differs from *T. formosum* f. *pentagonale* Hustedt (reported for Guam by Navarro & Lobban 2009) only in the number of angles.

Hemiaulus hauckii Grunow in Van Heurck Plate 8, Fig. 4
Ref. illus.: Proschkinia-Lavrenko 1955, fig. 66; Ross et al. 1977, pl. 4; Moreno et al. 1996, pl. 22, figs 7–8
Samples: ECT 3753, from plankton tow in Cocos Lagoon, GPS 13° 15.273' N, 144° 38.554' E; **GU6D-2**
Dimensions: Diam. 15–20 µm.
Diagnostics: Very long linking spines; simple, small pores; single rimoportula apically-placed.
Comments: The small pores (versus larger areolae) distinguish this species from others in the genus (Round et al. 1990: 260), e.g. *H. sinensis* (Ricard 1987, figs 326–329). The apical position of the rimoportula is in contrast to *H. sinensis* and *H. membranacea* in which they are offset from center (Ross et al. 1977). The very long linking spines distinguish this genus from most others.

Lithodesmioides polymorpha von Stosch Plate 8, Figs 5, 6
Ref. illus.: Von Stosch 1987, figs 60–84
Samples: Isolated into culture: ECT 3772, from GU18
Dimensions: Width 80–100 µm

Diagnostics: This genus is distinguished from *Lithodesmium* by the reduced marginal ridge and the continuity between the pores of the valve face and apices. Four- and five- pointed forms are known. The central rimoportula has a prominent external tube (Pl. 5, Fig. 6), which internally is spade-shaped with two separate slits, hence a "bilabiate process."
Comments: This species is distinguished from *Lithodesmioides minutum* by the presence of many small spines on the valve face (Pl. 8, Fig. 6). The 4-pointed frustule is the most common morph of this taxon in the Guam material. An additional SEM of this culture is shown in Theriot et al. (2010, fig. 1C).

Proboscia alata (Brightwell) Sundström Plate 9, Figs 1, 2
Ref. illus.: Hustedt 1927–1930, fig. 344; Hendey 1964, pl. 2, fig. 2 (both as *Rhizosolenia alata*); Jordan et al. 1991, figs 1–9, 32–34; Takahashi et al. 1994, figs 2–7; Hernández-Becerril 1995, figs 2-4; Jordan & Ligowski 2004, pl. 3, figs 1, 2
Samples: **GU52J-3**
Dimensions: Diam. 10–12 µm
Diagnostics: Valve conical, asymmetrical with asymmetrical claspers (Pl. 9, Fig. 2) into which the proboscis from the adjoining cell fits; there is a notch in the apex of the proboscis. Girdle bands (often seen isolated in girdle view) spiral around the pervalvar axis (Pl. 9, Fig. 1).
Comments: The unequal claspers distinguish *P. alata* from the five other living species (Jordan et al. 1991; Takahashi et al. 1994; Hernández-Becerril 1995). A planktonic diatom, but relatively common in this benthic sample. Although Sundström (1986) redefined *P. alata* as a North Atlantic species, Jordan et al. (1991) found it in Antarctic waters and Hernández-Becerril (1995) considered it cosmopolitan in temperate and tropical waters. Sundström (1986) noted ultrastructural differences with *"Rh. alata"* from tropical waters and, given the state of knowledge of this genus in tropical waters, we regard this identification provisional, awaiting additional material from studies of planktonic diatoms from Guam.

Chaetoceros atlanticus var. *skeleton* (Schütt) Hustedt Plate 9, Fig. 3
Ref. illus.: Hustedt in Schmidt et al. 1874–1959, pl. 322, figs 5, 6, 6a, 8 (as *C. polygonus* Schütt); Hustedt 1927–1930, fig. 365; Ricard 1987, fig 490 (as *C. atlanticus*).
Samples: GU55B-4
Dimensions: Diam. 12 µm
Diagnostics: Valve extremely shallow, height only 1/10 of the length of the apical axis. Intersection point of bristles lies further outside of the chain than in the nomiate variety, so the "window" in relation to the cells is very large. Bristles thin, basal swelling inconspicuous or absent (Hustedt 1927–1930: 643–645).
Comments: Single specimen observed, presumably deposited from plankton. The specimens illustrated in Schmidt's Atlas came from Palau and New Guinea/ Philippines.

Chaetoceros peruvianus Brightwell Plate 9, Figs 4, 5
Ref. illus.: Hustedt in Schmidt et al. 1874–1959, pl. 323, figs 1–5; Hustedt 1927–1930, fig. 380; Shevchenko et al. 2006, figs 13–16; Kooistra et al. 2010, figs 80–86
Samples: **GU44U-1A, GU44AE-2; GU52J-3**
Dimensions: Diam. 15–16 μm
Diagnostics: Very coarse, distinctly striated, concave setae; setae on the anterior valve arising straight up forming a cleft before sharply bending outward.
Comments: Distinguished from *C. saltans* Cleve by the way the setae arise (cf. Hustedt 1927–1930: 635). Valves presumably deposited from the plankton but common in GU52J-3.

Neofragilaria nicobarica Desikachary, Prasad & Prema Plate 10, Figs 1, 2
Ref. illus.: Witkowski et al. 2000, pl. 22, figs 15–19; Hein et al. 2008, pl. 11, fig. 9; Sato et al. 2008c, figs 38–55
Samples: **GU44I-1, GU44AF-5**
Dimensions: Length 25–31 μm, width 8–9 μm; striae 6 in 10 μm
Diagnostics: Symmetrical lanceolate valve with very broad striae, offset on opposite sides of the narrow sternum, so the sternum appears zigzag in LM.
Comments: The symmetrical valve shape distinguish this species from several species of *Opephora* Petit. Sato et al. (2008c), who transferred this genus from Fragilariaceae to Plagiogrammaceae, noted the possibility that cells illustrated by Foged (1987, pl. 5, figs 15, 16) as *Rhaphoneis bilineata* might be synonymous with this taxon; a similar specimen under that name was shown by Podzorski & Håkansson (1987, pl. 6, fig. 17).

Plagiogramma staurophorum (Gregory) Heiberg Plate 10, Figs 3–5
Ref. illus.: Hustedt 1931–1959, fig. 635; Hendey 1964, pl. 36, fig. 1; Ricard 1977, pl. 10, figs 5, 6; Witkowski et al. 2000, pl. 11, figs 16–21
Samples: GU26A; ECT 3776
Dimensions: Length 24–40 μm, width 8–19 μm; striae 7 in 10 μm
Diagnostics: The linear-ellipic shape and the coarse areolae arranged in both transapical striae and longitudinal lines, with one pair of septa near the center separating a hyaline area (no apical septa) help distinguish this species from other *Plagiogramma* spp.

Psammoneis japonica S. Sato, Kooistra & Medlin Plate 10, Figs 6, 7
Ref. illus.: Sato et al. 2008b, figs 8, 26, 33
Samples: GU26A stub 1, GU52O (isolated into culture)
Dimensions: Length 7.4 μm, width 3.5 μm; striae 30 in 10 μm
Diagnostics: Our specimens have the combination of cell length and stria count that fit *P. japonica*, though they are near the short end of the range for that species.
Comments: *P. japonica* was recently described from Iriomote I., Okinawa, along with *P. pseudojaponica*; these are all sand-dwelling species, a habitat we have not yet explored. Morphological differences between the 3 species described by Sato et al. (2008b) are very subtle and the diagnoses include nuclear ribosomal SSU and

LSU DNA sequences and the (transapical) width of the areolar slits in nm. We have not been able to acquire these data; molecular data and measurements from more detailed images could confirm the identity, or perhaps reveal still more variation.

Falcula paracelsiana Voigt 1961 Plate 11, Figs 1–6
Ref. illus.: Voigt 1961, figs 1–6
Samples: **GU52K-4**, GU62A-7
Dimensions: Length (straight line apex to apex) 79–125 µm, width at center 7–10 µm; striae 35 in 10 µm
Diagnostics: More strongly arcuate on ventral sides and sternum not evident, in contrast to other species of *Falcula*. Apical pore field comprising 4 slits.
Comments: The plastids in this species (Pl. 11, Fig. 1), linked in 4 pairs by pyrenoids, suggest a curved *Climaconeis* (cf. Lobban et al. 2010a), but the absence of a raphe is apparent even in live cells. Voigt (1960) described *Falcula* with three epiphytic species from Europe and later (Voigt 1961) added this species from Hainan and the Paracels, tropical islands in the South China Sea. Besides the dimensions, which correspond with our species, he also noted that the very fine sternum (pseudoraphe) was often detectable only by the slight displacement of the transverse striae (Pl. 11, Fig. 4). He noted a second "pore" close to the "apical pore" at one pole; this is the rimoportula (Pl. 11, Fig 4, 5). (He also reported that the rimoportula occurs in at least two of his original species.) We have observed the rimoportula in SEM but cannot confirm that it is at one end only. Geissler & Gerloff (1963) studied *F. media* Voigt with TEM and discovered that the apical pore in that species is a series of slits and lamellae, as shown here for *F. paracelsiana*. Güttinger (1994) showed SEM images of *F. rogalli*, which differs from *F. paracelsiana* in the presence of an apical pore field in addition to the slits. Tanako (1983) described an epizoic species *F. hyalina*, and this was also studied by Prasad et al. (1989) and illustrated in Round et al. (1990) for the genus; however, the structure is significantly different from Voigt's species, particularly in the presence of an ocellulimbus at each apex, i.e., an apical field of pores sunk into a cavity. This species is evidently a different genus, but at the time of Prasad et al.'s (1989) study taxonomic revision awaited SEM images of the type species, *F. rogalli* Voigt. Güttinger's (1994) images should enable re-evaluation of *F. hyalina*.

Neosynedra tortosa (Grunow) Williams & Round Plate 12, Fig 1
Ref. illus.: Williams & Round 1986, figs 68–71; Witkowski et al. 2000, pl. 29, fig. 11; Navarro & Lobban 2009 (for Yap), figs 44, 45
Samples: **GU44Z-15; GU52K-2, GU52Q-3**
Dimensions: Length 81–95 µm, width 4 µm; striae 35 in 10 µm
Diagnostics: The undulate margins of this species are distinctive. Striae generally not resolved in LM. Colonies of zigzag chains, as in *N. provincialis*. Plastids of 4 plates.
Comments: Distinguished from *Cyclophora* spp. by the absence of pseudosepta. Giffen (1980) described *Synedra distinguenda* var. *curta*, which he distinguished from *S. distinguenda* Hustedt (Hustedt 1931–1959, fig. 707) only by being very short. Hustedt's distinctive species is extremely long and narrow (300–500 µm x 3

µm), but Giffen's form, 70–80 µm x 4 µm, is indistinguishable on the basis of his drawing and description from *N. tortosa*.

Podocystis adriatica (Kützing) Ralfs Plate 12, Figs 2, 3
Ref. illus.: Van Heurck 1896, fig. 117; Hein et al. 2008 pl. 12, fig. 6 (as *P. americana* Bailey).
Samples: GU1B-2; GU6C; **GU44W-8, GU44Y-13**
Dimensions: Length 60–71 µm, width 16–17 µm; costae 8 in 10 µm with 2–3 striae between costae; striae 15 in 10 µm.
Diagnostics: Well-developed costae separating several transapical rows of areolae; our specimens smaller and narrower than *P. spathulata* (q.v.).
Comments: Our cells fairly well match the two illustrations cited above, except for being more produced at the basal pole, but they are small, narrow and with more costae in 10 µm than typical cells as described by Hustedt (1931–1959, fig. 652) and Witkowski et al. (2000, pl. 21, figs 1–4). Much less common in our samples to date than *P. spathulata*.

Podocystis spathulata (Shadbolt) Grunow Plate 12, Figs 4–6
Ref. illus.: Hustedt 1931–1959, fig. 653; Navarro 1982a, figs 44–46
Samples: GU32B; GU42A; GU43B; **GU44K-6, GU44AR-1; GU52Q-2**
Dimensions: Length 92–118 µm, width 35–82 µm; striae 5–8 in 10 µm.
Diagnostics: Broadly spathulate valves without costae (contrast *P. adriatica*); areolae apically elongated, quadrangular, crossed by a transapical bar (Plate 6, Figs 5, 6).
Comments: *Podocystis* differ from solitary *Licmophora* spp. by the large areolae, which are frequently visible even in live cells. Other species of *Podocystis* with other valve outlines have been described by Ricard (1979) (see also Ricard 1987, figs 602–604). In the course of studying *Licmosphenia* (Lobban in press), we had cause to determine whether there is a foot-pole rimoportula on both valves of *Podocystis*, as stated by Round et al. (1990) or on only one pole as in *Licmophora* (Honeywill 1998). Examination of 25 internal views from a large population of *P. spathulata* (GU32B) counted 12 with and 13 without a rimoportula (Pl. 12, Figs 5, 6), confirming that there is the same slight heterovalvy as in *Licmophora*. All valves had a head-pole rimoportula, smaller than that at the foot pole. In *Licmophora* some species have a head-pole rimoportula on both valves (so 3 rimoportulae total), some on only one (then the opposite valve from that with the foot-pole rimoportula) (Honeywill 1998).

Synedra bacillaris (Grunow) Hustedt Plate 13, Figs 1, 2
Ref. illus.: Peragallo & Peragallo (1897–1908), pl. 79, figs 1–4 (vars); Hustedt 1931–1959, fig. 718; Sullivan & Wear 1995, figs 9–12; Hein et al. 2008, pl. 13, fig. 8 and pl. 14, figs 1, 2
Samples: **GU44I-1, GU44I-2, GU44Z-15**
Dimensions: Length 180–400 µm, width 14 µm; striae 9–14 in 10 µm.
Diagnostics: Large, bright (heavily silicified) cells with prominent areolae and a

marked central rib (Pl. 13, Fig. 2); sternum but lacking bifacial annulus (see Medlin et al. 2008), in contrast to *Ardissonea* spp.
Comments: The coarse and prominent areolae are similar to *A. formosa* (Hantzsch) Grunow (reported for Guam by Navarro & Lobban 2009), but that species has an internal silica plate in addition to the bifacial annulus (Sullivan & Wear 1995); the girdle band of *S. bacillaris* is porate, that of *A. formosa* hyaline. Although many marine species formerly in *Synedra* have been removed to new genera, leaving *Synedra* as a freshwater genus (Williams & Round 1986, Round et al. 1990), *S. bacillaris* has yet to be revised, in spite of Sullivan & Wear's (1995) observations. The internal structure (Pl. 13, Fig. 2) is not similar to *A. formosa* (Pl. 16, Fig. 2) and *A. robusta*, nor to the any of the other groups formerly in *Synedra* and currently lumped into *Ardissonea*.

Synedra lata (Giffen) Witkowski Plate 13, Figs 3, 4
Ref. illus.: Giffen 1980, figs 40, 41; Foged 1987, pl. 8, fig. 2 (both as *Synedra tabulata* var. *lata*); Witkowski et al. 2000, pl. 30, figs 9, 10
Samples: **GU44AF-5, GU44AK-1, GU44W-8**
Dimensions: Length 60 µm, width 9–13 µm; striae 15 in 10 µm
Diagnostics: Broad lanceolate valve with a very wide sternum.
Comments: The shape and broad sternum distinguish this from other species of *Synedra* except for *S. tabulata* var *acuminata* (Hustedt 1931–1959, fig. 710e, f; Hein et al. 2008, pl. 13, fig. 6), which is not as wide and has long protracted apices. Given that this species was formerly included in *S. tabulata*, it might now belong in *Tabularia*, but was not studied by Williams & Round (1986). Witkowski et al. (2000: 81) remarked that it was thus far reported only from the Seychelles and Thailand. Specimens in Hein et al. (2008, pl. 13, figs 2–6) from the Bahamas suggest that these two taxa are inadequately known.

Tabularia fasciculata (C.A. Agardh) Williams & Round Plate 13, Fig. 5
Ref. illus.: Williams & Round 1986, figs 46–52; Kaczmarska et al. 2009, figs 1–11
Samples: GU26A, GU26AD; **GU44Z-15**
Dimensions: Length 75–80 µm, width 3.5–5.5 µm; striae 11–12 in 10 µm
Diagnostics: Distinguished from other species of *Tabularia* by the broad areolae closed by complex cribra on the valve face and mantle (Pl. 13, Fig. 5).
Comments: The areolae are in contrast to the biseriate striae in *T. parva* (q.v., Pl. 13, Fig. 6). SEM images in Kaczmarska et al. (2009) indicate that this is *T. fasciculata*. However, *T. fasciculata* as shown by Williams & Round (1986, figs 46–52), differs somewhat in cell shape and the shape of the cribrate closing plates. Snoeijs (1992) studied the *T. fasciculata* complex along a (low) salinity gradient in the Baltic, and her results suggest that caution must be used in applying these names to tropical marine taxa.

Tabularia parva (Kützing) Williams & Round Plate 13, Figs 6, 7
Ref. illus.: Williams & Round 1986, figs 33–38; Kuriyama et al. 2010 figs 3–12
Samples: GU26A; **GU44Z-15; GU52Q-1**

Dimensions: Length 25–174 μm, width 4 μm; striae 20–22 in 10 μm
Diagnostics: Narrower, biseriate striae (Pl. 13, Fig. 6) nearly twice the density of those in *T. fasciculata*.

Perissonoë cruciata (Janisch & Rabenhorst) Andrews & Stoelzel
Plate 14, Figs 1, 2
Ref. illus.: Navarro 1982a, figs 53, 54 (as *Rhaphoneis crucifera*); Montgomery 1978 pl. 180E–H (as *Raphoneis amphiceros* var. *tetragona* Grunow); Round et al. 1990, pp. 414–415; Hein et al. 2008, pl. 11, fig. 7
Samples: Arai 2010 (GU44), GU14P, **GU44Y-13, GU44AF-3**
Dimensions: Width 21–22 μm; striae 8 in 10 μm
Diagnostics: Quadrate cell with four sterna not forming a perfect cross, striae radiate. Small pore fields on each corner not visible in LM.

Rhaphoneis amphiceros (Ehrenberg) Ehrenberg Plate 14, Figs 3, 4
Ref. illus.: Witkowski et al. 2000, pl. 22, figs 3–6; Hein et al. 2008 pl. 11, fig. 8; Sato et al. 2011, figs 1–3, 11, 19
Samples: **GU44I-1, GU44K-6,** GU44X-2, **GU44AF-5, GU44AK-1**
Dimensions: Length 17–27 μm; width 14–18 μm; striae radiating, 8–11 in 10 μm
Diagnostics: Very broadly rounded cell with two apices and single sternum (contrast *Perissonoë*).
Comments: There is a substantial range of size and shape in this species, with some larger and/or elliptical, as shown by Witkowski et al. (2000) (reprinted in Hofmann et al. 2011, pl. 133, figs 15–18). The genus name is currently spelled both *Rhaphoneis* and *Raphoneis*.

Rhaphoneis castracanii Grunow Plate 14, Fig. 5
Ref. illus.: Navarro 1982d, pl. 13, fig. 10; López Fuerte et al. 2010, pl. 13, figs 14, 15
Samples: GU14P
Dimensions: Length 33 μm, width 25 μm; striae 8 in 10 μm
Diagnostics: Similar size and stria pattern to *R. amphiceros* but with concave sides.

Psammodiscus nitidus (Gregory) Round & Mann Plate 14, Figs 6, 7
Ref. illus.: Witkowski et al. 2000, pl. 23, figs 12–14; Hein et al. 2008, pl. 5, figs 5, 6
Samples: **GU44W-8;** GU52K-4; GU55B-4; GU56A-2
Dimensions: Diam. 21–58 μm
Diagnostics: Circular valve, widely spaced areolae; non-cavitate valve with areolae occluded by rotae (Pl. 14, Fig. 7). Reportedly one rimoportula near the center, if any.
Comments: In LM distinguished with difficulty from *Coscinodiscus* (in which it was originally classified), but the wide spacing of the areolae distinguishes it from benthic centric taxa so far in our flora. In SEM readily distinguished by the valve structure. In *Coscinodiscus* numerous rimoportulae occur around the periphery. Although circular, this genus (like *Astrosyne* – Ashworth et al. 2012) is an araphid pennate not a centric diatom. The SEM image shows somes differences from the valves shown in Round et al. (1990), but the range of variation in this recently

erected monospecific genus is not clear. LM of a second species of *Psammodiscus* is shown by Hein et al. (2008), pl. 66, figs 10, 11, 13.

Ardissonea[3] *crystallina* (C. Agardh) Grunow Plate 15, Figs 1–3
Ref. illus.: Peragallo & Peragallo 1897–1908, pl. 79, figs 1–4; Hustedt 1931–1959, fig. 719; Navarro 1982b, figs 59, 60 (all as *Synedra crystallina*); Poulin et al. 1986, figs 28–30; Poulin et al. 1987, figs 1–11; Witkowski et al. 2000, pl. 31, fig. 12
Samples: **GU44I-1, GU44Y-13**
Dimensions: Length 220–350 µm, width 11–16 µm; striae 16–19 in 10 µm
Diagnostics: *A. crystallina* is nearly linear, slightly widened at the center, and has an evident bifacial annulus as well as the discontinuity along the midline. Internally, there is no additional plate as there is in *A. formosa*, and the transapical ribs are similar to those in *A. fulgens* (see below).
Comments: Peragallo & Peragallo (1897–1908: pls 78, 79) and Hustedt (1931–1959: figs 715–722) both gave excellent comparisons of the European *Ardissonea* species.

Ardissonea formosa Hantzsch ex Rabenhorst
Plate 15, Figs 4, 5; Plate 16, Figs 1, 2
Ref. illus.: Peragallo & Peragallo 1897–1908, pl. 78, fig. 6; Hustedt 1931–1959, fig. 720; Navarro 1982b, figs 61–63; Podzorski & Håkansson 1987, pl. 8, figs 1, 1a (all as *Synedra formosa*); Ricard 1987, figs 571, 572; Sullivan & Wear 1995, figs 1–8; Witkowski et al. 2000, pl. 30, figs 12; Hein et al. 2008, pl. 8, figs 3, 6
Samples: GU26A; **GU44I-2, GU44Z-15, GU44AA-5**
Dimensions: Length 240–300 µm, width 22–24 µm; striae 8–9 in 10 µm
Diagnostics: Strongly silicified, bright cells [like *Synedra bacillaris* (q.v.) but unlike other *Ardissonea* spp. here], apices slightly tapered; striae dissected by sternum and two lines of the bifacial annulus; striae sometimes appearing zigzag across sternum (Pl. 15, Fig. 5) because valve face is grooved.
Comments: We have included this species here, even though it was already reported for Guam by Navarro & Lobban (2009), because that paper did not illustrate it and we think it is useful now for contrast with the related species and genera.

Ardissonea fulgens (Greville) Grunow (var. *fulgens*) Plate 16, Figs 3–5
Ref. illus.: Peragallo & Peragallo (1897-1908), pl. 79, fig. 5; Hustedt 1931–1959, fig. 717a; Poulin et al. 1986, figs 31, 32 (all as *Synedra fulgens*); Witkowski et al. 2000, pl. 31, figs 9–11; Hein et al. 2008, pl. 8, figs 1, 2
Samples: GU7R; GU44N-A, **GU44Z-15,** GU44AC-3; GU52P-7; GU55B-4
Dimensions: Length 205–320 µm, width 9–15 µm except 11–20 µm at center and apices; striae 19 in 10 µm
Diagnostics: Distinguished from other *Ardisonnea* species by the lack of central rib and apparent lack of bifacial annulus, and by the narrow valves expanded slightly at center and apices, apices blunt.

[3]Although the genus name (with an *i*) goes back to *Ardissonia* De Notaris, and was spelled that way by Poulin et al. (1986) when they emended it, Round et al. (1990) used the spelling *Ardissonea* (with an *e*) as the basis for the new Order and Family; many subsequent authors and the California Academy of Sciences Catalog of Diatom Names and AlgaeBase follow this orthography, which commemorates Ardissone.

Comments: The nominate variety of *A. fulgens* forms colonies on short, branched stalks, with the cells separate except for a time after division. There is a break in the striae exactly along the valve face-mantle edge, visible in internal SEM views (Pl. 16, Fig. 3), which could be interpreted as a bifacial annulus.

Ardissonea fulgens var. *gigantea* (Lobarzewsky) De Toni
Plate 1, Figs 1, 2; Plate 16, Figs 6–8
Ref. illus.: Peragallo & Peragallo 1897-1908, pl. 79, fig. 6; Hustedt 1931–1959, fig. 717a (both as *Synedra fulgens* var. *gigantea*)
Samples: GU7L; **GU44J-2, GU44Z-15;** GU54B
Dimensions: Length 600–900 μm, width 9–12 μm at center, reducing to ca. 5 μm and expanding again at the poles to 7–10 μm; striae 18 in 10 μm
Diagnostics: The distinctive colonies (Pl. 1, Figs 1, 2), anchored by mucilage pads, appear curved but are actually flat, with the cells towards the outside becoming individually more flexed in the pervalvar axis until the fascicle splits. The cells are extremely long, distinctly swollen in the central area [as in *Toxarium hennedyanum* (Gregory) Pelletan (q.v.)] and with capitate apices. There is often a patch of disarrayed striae in the central inflation (Pl. 16, Fig. 8).

Toxarium hennedyanum (Gregory) Pelletan Plate 17, Figs 1–5
Ref. illus.: Peragallo & Peragallo 1897–1908, pl. 78, fig. 9; Hustedt 1931–1959, fig. 713 (both as *Synedra Hennedyana* Gregory); Witkowski et al. 2000, pl. 30, fig. 11, pl. 31 figs 5–7; Kooistra et al. 2003, figs 1, 2; Hein et al. 2008, pl. 15, fig. 2
Samples: **GU44I-2, GU44Y-13, GU44AC-4, GU44AR-1; GU52K-7, GU52Q-1;** GU55A-H
Dimensions: Length 340–560 μm, width 7–8 μm at center, narrowing to 3–4 μm along most of the cell and inflated to 5–6 μm at the apices.
Diagnostics: Extremely slender cells with inflated center; lines of puncta along the margins and uniformly scattered over the valve face. Cells sometimes curved.
Comments: Distinguished from *Ardissonea fulgens* var. *gigantea* by the pattern of pores vs. striae, and in life by colony structure (attached singly or in pairs to substrata). We have also observed the unnamed variety illustrated in Podzorski & Håkansson (1987, pl. 8, fig. 3) as "*Synedra* cf. *hennedyana* Greg." In these specimens the scattered puncta are absent (Pl. 17, Fig. 5), however there was a gradation (Pl. 17, Figs 3–5 vs Fig. 2) such that a separate variety is not warranted. Similar specimens with undulate margins were also recorded (not shown). Kooistra et al. (2003) suggested that this species may be conspecific with *T. undulatum* but the taxa remain separate at present. It should be noted, however, that there is significant genetic variation in the *T. hennedyanum* and *T. undulatum* isolates from Guam material used in the Theriot et al. (2010, 2011) molecular phylogenetic studies.

Toxarium undulatum Bailey ex Bailey Plate 17, Figs 6–8
Ref. illus.: Peragallo & Peragallo 1897–1908, pl. 78, fig. 7; Hustedt 1931–1959, fig. 714; Ricard 1987, figs 561–563 (all as *Synedra undulata* Bailey); Poulin et al.

1986, figs 34–36; Witkowski et al. 2000, pl. 30, fig. 11, pl. 31 figs 5–7; Kooistra et al. 2003, figs 1, 2; Hein et al. 2008, pl. 15, fig. 3
Samples: **GU44M-C, GU44Y-13, GU44Z-15, GU44AR-1;** GU52Q-10; GU54B-4
Dimensions: Length 270–400 µm; width 5–8.5 µm at center, narrowing to 4 µm along most of the cell and inflated to 6 µm at the apices; sometimes with only slight central inflation (Pl. 17, Fig. 8).
Diagnostics: Differing from *T. hennedyanum* in the undulate margin and narrower central inflation.

Rhabdonema adriaticum Kützing Plate 18, Figs 1–3
Ref. illus.: Navarro 1982a, figs. 47-50; Ricard 1987, figs 638–644; Güttinger 1989, series 3, 2.01.25-1; Witkowski et al. 2000, pl.13, figs 10–12
Samples: **GU44Z-15, GU44U-2, GU44AC-4**
Dimensions: Length 38–75 µm, width 7 µm; striae 14 in 10 µm
Diagnostics: Numerous coarsely areolate girdle bands in valve view, frustules often separated at the hyaline pleurae (Pl. 18, Fig. 1). Valve with large pore field and numerous irregular costae (Pl. 18, Figs 2, 3). In life forming robust ribbons.
Comments: The pattern of areolae, which appears as if there were two series of bars along the pervalvar axis (actually an illusion), distinguishes this from *R. arcuatum* (Witkowski et al. 2000, pl. 13, figs 2–4), which has a simple row of areolae along each girdle band and a much different valve view.

Florella pascuensis Navarro Plate 18, Figs 4, 5
Ref. illus.: Navarro 2002, figs. 12–15
Samples: GU7R; **GU52J-3;** ECT 3756
Dimensions: Length 64–70 µm, width 40–52 µm; striae 28 in 10 µm
Diagnostics: Broadly elliptical valve with an irregular sternum. Horseshoe-shaped series of slits at the apex (Pl. 18, Fig. 5) distinguish this species from *F. portoricensis* Navarro.

Hyalosira interrupta (Ehrenberg) Navarro Plate 1, Fig. 3, Plate 18, Figs 6, 7
Ref. illus.: Hustedt 1931–1959, fig. 562 (as *Striatella interrupta*); Hein et al. 2008, pl. 10, figs 3–8
Samples: GU3D; **GU44H, GU44Z-15, GU44AC-4; GU52K-7, GU52Q-3**
Dimensions: Length 14–25 µm, width 3.5 µm; striae 33 in 10 µm.
Diagnostics: In girdle view, the overlapping septa and unusual shape of the pigmented portion. Forming ribbons, in contrast to the zigzag chains of the much smaller *H. tropicalis* Navarro (also in our flora).
Comments: Ribbons of this species, commonly found in GU44 and GU52 samples, stand out in life because of the restriction of the plastids to an irregular area bounded by septa and lacking areolae on the copulae (Pl. 1, Fig. 3, Pl. 18, Fig. 6). Guam specimens in LM were illustrated in Lobban & Jordan (2010, fig. 5e). As far as we can determine, none of the SEM images in Round et al. (1990) (under the name *Microtabella*) is *H. interrupta*. Although Round et al. (1990) asserted that a sternum is absent or only slightly developed, *H. interrupta* has a distinct sternum

(Pl. 18, Fig. 7). There appears fairly consistently a rimoportula at each pole (Pl. 18, Fig. 7) but sometimes they are on the same side of the sternum, sometimes opposite. In contrast, *H. tropicalis* valves have sometimes one, sometimes none (Navarro & Williams 1991).

Grammatophora angulosa Ehenberg Pl. 19, Figs 1, 2
Ref. illus.: Hustedt 1931–1959, fig. 564; Navarro 1982b, fig 33; Witkowski et al. 2000, pl. 14, fig 17
Samples: **GU44AP-8**
Dimensions: Length 15 µm; striae 15–16 in 10 µm
Diagnostics: Very short cells (in our samples) with markedly hooklike septa.
Comments: Not yet observed in valve view. Distinguished from *G. hamulifera* Kützing (Hustedt 1927–1966, fig. 566; Witkowski et al. 2000, pl. 14, figs 14–16; López Fuerte et al. 2010, pl. 16, fig. 4) by the shape of the hook, which in the latter has a sharp fold or appears as a C joined by a short shelf to the apex.

Grammatophora macilenta W. Smith Plate 19, Figs 3–5
Syn.: *Grammatophora oceanica* var. *macilenta* (W. Smith) Grunow
Ref. illus.: Hustedt 1931–1959, fig. 574; Navarro 1982d, pl. 11, figs 6–8 [both as *G. oceanica* var. *macilenta* (Wm. Smith) Grunow]; Witkowski et al. 2000, pl. 15, figs 16–18
Samples: GU3D; **GU6D-1;** GU26A; **GU44Z-15, GU44AI-1; GU52P-2**
Dimensions: Length 66–72 µm, width 4–7 µm; striae 33 in 10 µm
Diagnostics: Distinctly swollen at apices and center, septa almost straight; more finely striated than the other two species reported and showing a quincunx pattern.
Comments: There is a slight heteropolarity: apical spines occur on one pole (on both valves at same pole) and that end appears slightly less inflated than the other pole (Pl. 19. Fig. 5). The synonymy follows Hendey (1964) and Witkowski et al. (2000), and the separation from *G. oceanica* seems to be supported by 3-gene phylogentic analysis (Ashworth in Lobban in press: fig. 68). Hustedt (1931–1959: 46, 49) notes a quincunx pattern in *G. oceanica* and *G. undulata*, but the coarser striae in these taxa in our samples of these two species appear predominantly transpical (compare Pl. 19, Fig. 4 with Pl. 19, Fig. 7 and Pl. 20, Fig. 3). The relationships of these three taxa warrant further study.

Grammatophora oceanica (Ehrenberg pro parte) Grunow var. *oceanica*
Plate 19, Figs 6–8
Ref. illus.: Hustedt 1931–1959, fig. 573; Witkowski et al. 2000, pl. 15, figs 13, 14, pl. 16, fig. 12, pl. 17, figs 3, 4
Samples: **GU44I-1, GU44AC-4, GU44AI-1; GU52P-5**
Dimensions: Length 32–50 µm, width 3–7 µm; striae 24 in 10 µm
Diagnostics: Parallel sides, apices not swollen. Septa straight except for distinct kink ca. 1/3 the way from the apex (Pl. 19, Fig. 6).
Comments: Hustedt (1931–1959) gives stria density as 15–20, rarely >22 in 10 µm for *G. marina* (Lyngbye) Kützing, versus 20–24 in 10 µm for *G. oceanica*, and *G.*

oceanica is narrower (4–8 vs. 8–15 µm). Sato et al. (2008a) presented a detailed account of *G. marina*.

Grammatophora undulata Ehrenberg
Plate 19, Fig. 3; Plate 20, Figs 1–3; Plate 44, Fig. 2
Ref. illus.: Hustedt 1931–1959, fig. 576; Ricard 1987, figs 660, 661; Güttinger 1989, series 2, 2.01.17-3; Witkowski et al. 2000, pl. 14, figs 8–11, pl. 15, fig. 1 and pl. 16, figs 5, 8.
Samples: GU3D; GU6C; **GU44V-3, GU44Z-15, GU44AC-4; GU52P-7**
Dimensions: Length 22–55 µm, width (central section) 5.5–6 µm; striae 20 in 10 µm.
Diagnostics: Undulate margin. Septa with slight wave near apices and near center (Pl. 19, Fig. 3).

Striatella unipunctata (Lyngbye) Agardh Plate 20, Figs 4, 5
Ref. illus.: Hustedt 1931–1959, fig. 560; Montgomery 1978, pl. 184A–E; Ricard 1987, figs 649–653; Round et al. 1990, pp. 432-433
Samples: GU7L; **GU44K-5, GU44Z-15, GU44AC-4;** GU46E; ECT 3648
Dimensions: Length 45–60 µm, width 14–23 µm; striae 32 in 10 µm
Diagnostics: Numerous septate girdle bands (Pl. 20, Fig. 4); prominent sternum with apically oriented rimoportula at each apex; apical pore field sunken in ocellulimbus (Pl. 20, Fig. 5).
Comments: The ocellulimbus gives the cell corner a truncated appearance, in contrast to the rounded corners of *Pseudostriatella oceanica* S. Sato, D.G. Mann & Medlin, which also has scattered rimoportulae (Sato et al. 2008d) (not yet recorded from Guam).

Lyrella hennedyi (W. Smith) Stickle & D.G. Mann Plate 20, Figs 6–8
Ref. illus.: Peragallo & Peragallo 1897–1908, pl. 25, figs 2–3; Hustedt 1961–1966, fig. 1516 (both as *Navicula hennedyi* Wm. Smith); Hendey 1964, pl. 33, fig. 14 (as *Navicula hennedyii*); Witkowski et al. 2000, pl. 95, fig. 3 and pl. 98, fig. 4
Samples: **GU44I-1, GU44J-2. GU44Z-15**
Dimensions: Length 60–65 µm; width 30 µm, 16 striae in 10 µm
Diagnostics: The diagnosis is difficult to define (see comments), but in general distinguished by the broad, lanceolate hyaline areas, of which the outer edges form a single curve and the inner edges are straight. Some specimens (Pl. 20, Fig. 6, 7) with granular texture to the hyaline areas (i.e., var. *granulosa* Grunow: Hustedt 1961–1966, figs 1518, 1519).
Comments: This species is very variable with many infraspecific taxa named (Hendey 1964: 213). It and its varieties appear in three groups within Hustedt's (1961–1966: 347–365) keys to *Navicula lyratae*, and he commented dryly, "Die außerordentliche Variabilität der Arten macht eine gewisse Unsicherheit bei der Aufstellung von dichotomen Bestimmungsschlüsseln leider unvermeidbar" [The extraordinary variability of the species makes a certain amount of uncertainty in the preparation of dichotomous identification keys, unfortunately, unavoidable]. *Lyrella* is generally considered to inhabit sediments and we have doubtless seen little of the variation in this species so far.

Petroneis granulata (Bailey) D.G. Mann Plate 21, Fig. 1
Ref. illus.: Hustedt 1961–1966, fig. 1696; Navarro 1982d, pl. 28, fig. 2; Ricard 1987, fig. 726 (all as *Navicula granulata* Bailey); Witkowski et al. 2000, pl. 97, figs 1, 2; Jones et al. 2005, fig 10 (Bailey's type)
Samples: GU4A, GU52N-7
Dimensions: Length 42–55 μm, width 23–27 μm; striae 12 in 10 μm.
Diagnostics: The differentiation of the valve face into two zones, the axial part with more widely and irregularly spaced pores in the striae, and the broader, less rounded central area in this species distinguish it from *P. marina* (Ralfs) D.G. Mann (Jones et al. 2005).
Comments: *P. plagiostoma* (Grunow) D.G. Mann (Hein et al. 2008, pl. 53, fig. 3) also has irregularly spaced pores but has a very large and asymmetrical hyaline expansion of the central area.

Olifantiella pilosella Riaux-Gobin Plate 21, Figs 2–7
Ref. illus.: Riaux-Gobin & Al-Handal 2012, figs 59–65
Samples: GU26A, **GU52P-2**
Dimensions: Length 7.8–13.2 μm, width 2.7–4.2 μm; striae 36–37 in 10 μm.
Diagnostics: Very small naviculoid cells, but the buciniportula is prominent and distinctive in LM (Pl. 21, Figs 2, 3). Striae consisting of single elongate areolae (macroareolae) interrupted along the margin. Two grooves run from the central area toward the external opening of buciniportula (Pl. 21, Figs 4, 5). Internally the buciniportula is a paired tubular process (Pl. 21, Figs 6, 7).
Comments: The assignment of these specimens relies entirely on the external morphology, since Riaux-Gobin & Al-Handal (2012) had only a few valves from Rodrigues (Mascarene Is.) and Moorea (Tahiti) and no interior views. The first-discovered buciniportula, in *Olifantiella mascarenica* Riaux-Gobin & Compère, was a straight tube but more recently several other species with different-shaped buciniportulae were described (Riaux-Gobin & Al-Handal 2012). That of *O. rodriguensis* Riaux-Gobin is paired, as our images suggest for *O. pilosella*. The systematic position of this genus has not been settled.

Gomphonemopsis littoralis (Hendey) Medlin Plate 22, Figs 1–3
Ref. illus.: Navarro 1982d, pl. 23, figs 2, 3 (as *Gomphonema littorale* Hendey); Medlin & Round 1986, figs 12, 52–54 ; Witkowski et al. 2000 pl. 61: 15, 16
Samples: GU26A; **GU44I-1, GU44O-F; GU52P-6**
Dimensions: Length 7.4–18.8 μm, width 1.8–2.8 μm; striae 25 in 10 μm.
Diagnostics: Small heteropolar valves with a fascia caused by areolae missing on valve face adjacent to central area. Single longitudinal lines of areolae on each side of raphe and on valve mantle.
Comments: Unlike *Gomphonema* (present in our freshwater streams and sometimes displaced into marine sediments) there is no pore field at the basal pole and the areolae are much different. *Gomphonemopsis exigua* (Kützing) Medlin (Witkowski et al. 2000 pl. 61, figs 1, 2) is similar but lacks the fascia.

Mastogloia achnanthioides Mann Plate 22, Figs 4, 5
Ref. illus.: Mann 1925, pl. 18, fig. 7; Hustedt 1931–1959, fig. 937; Ricard 1974, pl. 19, fig. 1; Ricard 1987, fig 772
Samples: **GU44R-2, GU44T-1, GU44AE-2; GU52J-3, GU52P-5, GU52P-9**
Hustedt's section: Rostellatae
Dimensions: Length 36–53 µm, width 18–22 µm; transapical striae 11–12 in 10 µm; partecta 12 in 10 µm, width 3 µm
Diagnostics: Distinctive valve outline, parallel or slightly constricted in the middle with cuneate apices; sinuous raphe with straight central endings; transapical striae consisting of quadrangular areolae. Partecta are transapically elongated and uniform in size and shape.

Mastogloia acutiuscula var. *elliptica* Hustedt Plate 22, Figs 6–8
Ref. illus.: Hustedt 1931–1959, fig. 947 c, d; Witkowski et al. 2000, pl. 81, figs 23, 24
Samples: **GU44Y-13**
Dimensions: Length 24 µm, width 10 µm; transapical striae 26 in 10 µm; partecta 6 in 10 µm, width 2 µm
Hustedt's section: Apiculatae.
Diagnostics: Valve elliptical with rostrate apices; raphe almost straight; fine transapical striae are radiate. The internal raphe-sternum is bordered by two thick, narrow and linear axial costae stopping just before the ends (Pl. 22, Fig. 8). Quadrangular partecta not reaching the apex, convex on the free margin and similar in size and shape except for the last one, which is smaller.
Comments: *M. acutiuscula* is very similar to *M. apiculata* W. Smith (q.v.), but the inner margins of the partecta are flat in that species rather than convex. The nominate variety (not seen) is longer and only weakly rostrate. The axial costae paralleling the raphe, called "gutters" by Paddock & Kemp (1990: 94), are characteristic of Hustedt's section Apiculatae, which in our flora includes also *M. citrus* Cleve, *M. robusta* Hustedt, and a species so far unidentified, akin to *M. apiculata*, but also occur in *M. tenuis* Hustedt, included in Hustedt's section Inaequales, and *M. paradoxa* Grunow (section Paradoxae). Hustedt (1931–1959) insisted that his sections were for the convenience of making keys, and characters used to create a group sometimes occur in species placed in other sections.

Mastogloia adriatica var. *linearis* Voigt Plate 22, Figs 9, 10
Ref. illus.: Voigt 1963, pl. 21, figs 4, 5
Samples: GU4A
Dimensions: Length 57 µm; width 20 µm, 18 striae in 10 µm, partecta 8 in 10 µm, width 2 µm
Hustedt's section: Apiculatae
Diagnostics: Valves linear-lanceolate to elliptical-lanceolate with subrostrate apices; raphe slightly sinuous; transapical striae parallel in the middle, weakly radiating at ends. Internally raphe-sternum is bordered by linear axial costae. Rectangular partecta flat in the inner margins and uniform in size and shape.

Comments: Our Guam specimen seems also to match Podzorski & Håkansson's (1987 pl. 25, figs 6, 7) marine specimen, identified as *M. recta* Hustedt, but does not match the *M. recta* description and figures in Witkowski et al. (2000: p. 260, pl. 74, fig. 2 and pl. 85, figs 5–7) or the figures of Hustedt's type in Simonsen (1987, pl. 403, figs 1–11), most strikingly because *M. recta* lacks the raphe gutter and its partecta stop much further from the apex. Voigt (1963) noted the differences between *M. adriatica* Voigt, *M. robusta* Hustedt (q.v.) and *M. recta*.

Mastogloia angulata Lewis Plate 23, Figs 1, 2
Ref. illus.: Hustedt, 1931–1959, fig. 885; Montgomery 1978 pl. 122A-F; Stephens & Gibson 1980b, figs 1–9; Foged 1987 (Fiji) pl. 11, figs 4–6; Navarro 1982d, pl. 25, figs 5, 6; Hein et al. 2008, pl. 34 figs 1, 2
Samples: GU21P, **GU52P-5**
Dimensions: Length 51 μm, width 27 μm; striae 12 in 10 μm; smaller partecta 5–6 in 10 μm, width 3 μm, central partecta width 5 μm
Hustedt's section: Inaequales.
Diagnostics: Valves elliptical to elliptical-lanceolate with subrostrate apices; raphe straight. Areolae irregular hexagonal, arranged in quincunx pattern (forming diagonal rows as well as transapical rows). Quadrangular partecta different in sizes, those in the middle distinctively larger than the others.

Mastogloia barbadensis (Greville) Cleve Plate 23, Fig. 3
Ref. illus.: Hustedt 1931–1959, fig. 891; Witkowski et al. 2000, pl. 75, fig. 10
Samples: GU55B-4
Dimensions: Length 21 μm; width 13 μm, 6 striae in 10 μm
Hustedt's section: Ellipticae.
Diagnostics: Valves elliptical; raphe slightly sinuous bordered by rows of the transapically elongated areolae. In outer zone areolae are irregular in shape and forming quincunx pattern. Two distinct longitudinal ribs are present near the first row of the areolae bordering the raphe-sternum (noted by Hustedt in LM as raphe appearing to be enclosed by two rows of short dashes). Partecta not observed but according to literature 2–4 in 10 μm, concave on inner margin, reaching the apices.
Comments: No SEM images present in literature until now. The outer pattern of striae is reminiscent of *M. lacrimata* Voigt (q.v.), but the oval valve outline is markedly different.

Mastogloia binotata (Grunow) Cleve Plate 23, Figs 4, 5
Ref. illus.: Hustedt 1931–1959, fig. 889; Montgomery 1978, pl. 118, figs C–H; Stephens & Gibson 1979b, figs 2-9; Podzorski & Håkansson 1987 pl. 53, fig. 4; Paddock & Kemp 1990 fig 112; Güttinger 1992, Series 6; Witkowski et al. 2000 pl. 75, figs 15-18; Lobban & Jordan 2010, fig. 5g
Samples: GU3D; GU32B; **GU44K-6 GU44W-10, GU44Y-13**
Dimensions: Length 22–28 μm, width 14–17 μm; transapical striae 16–18 in 10 μm; partecta width 2.5 μm
Hustedt's section: Ellipticae.

Diagnostics: Valves elliptical; raphe straight. Transapical striae parallel at center to curved and radiate near the poles, crossed by an oblique pattern more or less in quincunx; a narrow, tapered space between the central striae; areolae are circular. Distinguished by one long partectum for each side of the valve.
Comments: Consistently present in GU44 farmer fish turf samples. Valve fine structure reported by Stephens & Gibson (1979b), mucilage bubble and mucilage strands described by Stephens & Gibson (1979a) and Hein et al. (1993). *M. sigillata* Voigt (Voigt 1963, pl. 24, fig. 3; Ricard 1974, pl. 1, fig. 5)—perhaps synonymous with *M. pernotata* Mereschkowsky (Mereschkowsky 1900–1902, pl. 4, figs 1, 2)—has a very similar valve but there are 3–4 partecta on each side, together forming a similar shape.

Mastogloia borneensis Hustedt Plate 23, Figs 6–8
Ref. illus.: Hustedt 1931–1959, fig. 991; Simonsen 1987, pl. 187, figs 1–3; Witkowski et al. 2000, pl. 76: 28-29, Ricard 1977 pl. 1, fig. 14; Pennesi et al. 2011, figs 9–16
Samples: GU44T-1, GU44Y-13
Dimensions: Length 32 µm; width 11 µm; partecta 5 in 10 µm, width 1.1 µm
Hustedt's section: Sulcatae, Subgroup 1[4]
Diagnostics: Valves lanceolate with subrostrate apices; raphe slightly sinuous; transapical striae radiate and very fine; longitudinal ribs evident. Partecta apically elongated, convex inner margins.
Comments: Differences among several Sulcatae including this species, *M. neoborneensis* Pennesi & Totti, *M. hustedtii* Meister, and *M. umbra* Paddock & Kemp (all in our flora, see below) and other species are laid out by Pennesi et al. (2011). *M. borneensis* has a vestigial pseudoconopeum, whereas *M. neoborneensis* has a short, semi-elliptical pseudoconopeum (the latter shown in Pl. 33, Fig. 3).

Mastogloia cannii Kemp & Paddock Plate 24, Figs 1–3
Ref. illus.: Kemp & Paddock 1990, figs 59-64; Pennesi et al. 2012, figs 2A–H
Samples: **GU44T-1**
Dimensions: Length 23–32 µm, width 12–15 µm; transapical striae 26 in 10 µm; partecta 7 in 10 µm, width 1 µm
Hustedt's section: Sulcatae, Subgroup 2
Diagnostics: Valves elliptical with cuneate subrostrate apices; raphe sinuous. Two zones evident on the valve face, the inner one with transapically elongate areolae, the outer with apically elongated areolae; the former visible individually in LM, the latter only as striae, which are emphasized by internal costae. Transapical striae radiate. Partecta narrow, apically elongate.
Comments: Kemp and Paddock (1990) noted a similarity in the LM of this species and *M. apiculata*, but the latter has axial costae along the raphe.

[4]Pennesi et al. (2011, 2012) proposed a revision of the Hustedt's Sulcatae section by dividing it in two subgroups: (1) one with a median depressions on the external valve surface between the raphe-sternum and the margin, and variably developed siliceous outgrowths (i.e., conopeum and pseudoconopeum) covering the depressions to various degrees (Subgroup 1; Pennesi et al 2011) (2) the other lacking a developed conopeum or pseudoconopeum which covers the median depression (Subgroup 2; Pennesi et al. 2012).

Mastogloia capitata var. *lanceolata* (Wallich) Hustedt Plate 24, Figs 4–7
Ref. illus.: Wallich 1860, figs 7, 8 (as *Stigmaphora lanceolata*); Hustedt 1931–1959, fig. 1006; Kemp & Paddock 1988, figs 14–20 (as *Stigmaphora lanceolata*)
Samples: GU55B-4
Dimensions: Length 45 µm, width 7 µm; striae 32 in 10 µm; partecta width 2.5 µm
Hustedt's section: Lanceolatae.
Diagnostics: Valves lanceolate with subcapitate apices; raphe straight. Partectal ring more displaced interiorly toward the middle line of the valve by a siliceous flange. Two large partecta on each side at the central area, their inner walls convex. Partecta open externally throughout the apical ducts (arrow, Pl. 24, Fig. 6).
Comments: While Kemp & Paddock (1988) mention as synonymous only *Mastogloia woodiana* F.J.R. Taylor, Hustedt 1931–1959, fig. 1006 illustrated *Mastogloia capitata* (Brun) Cleve (based on *Stigmaphora capitata* Brun) and *M. capitata* var. *lanceolata* (Wallich) Hustedt, based on *Stigmaphora lanceolata* Wallich. Moreover, VanLandingham (1971) established a new combination for "*Stigmatophora lanceolata* Wallich," which was called *Mastogloia triconfusa* var. *lanceolata*. In LM an *S. lanceolata* valve without partectal ring might be mistaken for *Haslea howeana* (Hagelstein) Giffen (q.v.).

Mastogloia ciskeiensis Giffen Plate 25, Figs 1–3
Ref. illus.: Giffen 1966, figs 43–45; Kawamura & Hirano 1989, plate 8, figs A–F; Simonsen 1990, figs 35–46; Lobban & Navarro 2012a, figs 2, 15, 16
Samples: **GU44T-1**
Dimensions: Length 46-47 µm, width 9.4-12.5 µm; transapical striae 38 in 10 µm; partecta ca. 14–15 in 10 µm, width 1.3–1.4 µm except 0.9 µm in the middle and tapering at the apices
Section: Marginulatae Simonsen
Diagnostics: Valves narrowly elliptical, appearing hyaline in LM; raphe straight and bordered by ribs; central area asymmetrical. Internally, transapical interstriae are parallel. Partectal ring symmetrical, formed by partecta of different sizes.
Comments: Distinguished from *M. cuneata* (Meister) Simonsen and *M. inaequalis* Cleve (q.v.) (also members of Marginulatae), which have larger partecta at one pole, and from *Mastogloiopsis biseriata* Lobban & Navarro (2012, figs 5–29) by the presence of the partectal ring and the asymmetrical central area. A population of this species occurred in GU44T-1. Although it is clearly isopolar, unlike *M. cuneata* and *M. inaequalis* (see below), it was difficult to place in the taxa described by Simonsen (1990). We have classified it as *M. ciskeiensis* especially on the basis of width of the partecta. Striation is in the range for both *M. ciskeiensis* and *M. marginulata* Grunow; the partectal ring width in the range for *M. ciskeiensis* and too big for *M. marginulata*; neither is said to narrow in the middle; partecta count in the range of *M. marginulata* not *M. ciskeiensis*. All mucilage-duct openings are similar in size, curved slits (Lobban & Navarro 2012a, fig. 2). There is no evidence of polarity and we saw no mucilage stalks, but Kawamura & Hirano (1989) show a stalked specimen.

Mastogloia citrus Cleve Plate 25, Figs 4, 5
Ref. illus.: Hutstedt 1931–1959, fig. 952; Ricard 1974, pl. 19, fig. 4; Navarro et al. 1989, figs 50, 51; Witkowski et al. 2000, pl. 78, figs 3, 4, 13, 14; Hein et al. 2008, pl. 35, fig. 4
Samples: **GU44I-1, GU44Y-13**
Dimensions: Length 33–39 µm, width 21–23 µm; transapical striae 21 in 10 µm; partecta 11 in 10 µm, width 2.3 µm
Hustedt's section: Ellipticae.
Diagnostics: Valves broadly elliptical with rostrate apices, aptly named citrus. Striae strongly radiating. Raphe slightly sinuous within wide axial area, internally bordered by axial costae, proximal endings straight. Partecta transapically elongate, the ring tapering off short of the apex.

Mastogloia cocconeiformis Grunow Plate 25, Figs 6, 7
Ref. illus.: Hustedt 1931–1959, fig. 888, Güttinger 1998, Series 9; Hein et al. 1993, figs 1–4
Samples: **GU6D-3; GU44R-2; GU52K-7, GU52P-5**
Dimensions: Length 44–65 µm, width 37–55 µm; striae 13–14 in 10 µm; partecta 7 in 10 µm, width 4–5 µm
Hustedt's section: Ellipticae.
Valves broadly elliptical almost circular; raphe sinuous. Areolae hexagonal arranged in quincunx striae. Partectal ring form a complete circle. Transapically elongated partecta show a partial division wall at the center (Pl. 25, Fig. 7, arrows).
Comments: Distinguished from *M. composita* Voigt (Voigt 1952, pl. 3, fig. 27; Ricard 1975, pl. 1, fig. 3; Foged 1987, pl. 12, fig. 4), which has the valve similar to *M. cocconeiformis* but the partecta similar to *M. cribrosa*, i.e., square and lacking the half walls. Tube-forming habit described by John (1993) and Hein et al. (1993).

Mastogloia corsicana Grunow Plate 26, Figs 1–3
Ref. illus.: Hustedt 1931–1959, fig. 966; Yohn & Gibson 1981 figs 17–21; Navarro 1983a, figs 24–27; Witkowski et al. 2000, pl. 77, figs 15–18, Hein et al. 2008, pl. 34, figs 3, 4
Samples: **GU44I-2, GU44P-B, GU44Y-13;** GU54B-4
Dimensions: Length 26–30 µm, width 12–14 µm; striae 16–17 in 10 µm; partecta 8 in 10 µm, width 1.8 µm
Hustedt's section: Undulatae.
Diagnostics: Valves elliptical with protracted apices; raphe strongly sinuous. Ornamentation of the external valve face is highly silicified in transapically elongated areolae except for roundish ones near the valve margin. Partecta transapically rectangular, equal in size.
Comments: The number of longitudinal lines of small pores in the more distal part of the valve is often greater than in the specimens shown in Pl. 25, Fig. 3 and in Yohn & Gibson (1981). The flared proximal raphe endings of this group are also seen in *M. cyclops, M. erythraea, M. lineata, M. rhombica,* and *M. subaffirmata,* in our flora, among others.

Mastogloia cribrosa Grunow Plate 26, Figs 4, 5
Ref. illus.: Hustedt 1931–1959, fig. 887; Stephens & Gibson 1979b, figs 10–16; Navarro 1983a, figs 28, 29; Hein et al. 2008, pl. 36, figs 1–3
Samples: GU44AJ, **GU44AR-1**
Dimensions: Length 43–54 μm, width 35–38 μm; striae 10 in 10 μm, partecta 2 in 10 μm, width 2 μm
Hustedt's section's: Ellipticae.
Diagnostics: Valves broadly elliptical; raphe straight. Areolae hexagonal arranged in quincunx striae. Partecta are rectangular and equal in size, sligthly convex at the free margin.
Comments: The valve shape and quincunx pattern of areolae are similar to *M. fimbriata* (Brightwell) Cleve (q.v.), but striae do not become double at the margin, areolae are widely spaced and partecta are rectangular (not tapered toward the wall), apically elongate.

Mastogloia crucicula var. *crucicula* (Grunow) Cleve
Plate 26, Figs 6, 7; Plate 27, Fig. 1
Ref. illus.: Hustedt 1931–1959, fig. 894; Ricard 1974, pl. 3, fig. 11; Stephens & Gibson 1979b, figs 17-24; Navarro 1983a, figs 30, 31; Paddock and Kemp 1990 fig 111; Witkowski et al. 2000, pl. 75, fig. 3; Hein et al. 2008, pl. 36: 6–7
Samples: GU3D; **GU44I-2, GU44R-2, GU52Q-1,** GU52Q-10
Dimensions: Length 11–18 μm, width 6.5–9 μm; striae 23 in 10 μm; partecta width 0.8 μm
Hustedt's section: Ellipticae.
Diagnostics: Valves small elliptical; raphe straight. External valve shows a space between the two central striae forming a narrow fascia. Internally the areolae are roundish, externally crescents. Transapical striae are parallel at the center and radiate at apices. Partecta are apically elongate and slightly contracted in the middle.
Comments: The nominate variety has one partectum in each quadrant of the valvocopula (Pl. 26, Fig. 7). We have also seen specimens with partecta in two quadrants at the same end (Pl. 26, Fig. 6) and, commonly, var. *alternans* (see below). One of the most frequently encountered species in our samples.

Mastogloia crucicula var. *alternans* Zanon Pl. 26, Fig. 8
Ref. illus.: Ricard 1974, pl. 3, fig. 12; Witkowski et al. 2000, pl. 75, figs 4, 5; Hein et al. 2008, Pl. 36, fig. 5
Samples: **GU6D-2; GU44AR-2; GU52J-2, GU52Q-1,** GU52Q-10
Dimensions: Length 10–11 μm, width 7 μm; striae 24 in 10 μm; partecta width 0.9 μm
Diagnostics: Differs from the type variety in having two partecta in alternate quadrants, and generally smaller.

Mastogloia cuneata (Meister) Simonsen Plate 27, Figs 2, 3
Ref. illus.: Hustedt 1931–1959, fig. 1000; Ricard 1974, pl. 3, fig. 8; Stephens &

Gibson 1980b, figs 33-34 (all as *M. schmidtii* – see Simonsen 1990); Simonsen 1990, figs 76–111; Lobban & Navarro 2012a, figs 1, 3, 4
Samples: GU3D; GU56A-1; **GU52K-7; GU44U-2, GU44Y-13, GU44Z-15**
Dimensions: Length 13–37 µm, width 4–9 µm; striae (resolved in SEM) 38 in 10 µm; wider partecta (in apical half) width 1.3 µm, narrower partecta width 0.6 µm
Section: Marginulatae Simonsen.
Diagnostics: Stalked cells; valves narrow lanceolate; raphe sinuous, slightly deflected proximal endings; striae barely resolved in LM. Partecta wider at the apical pole, with large, oblique duct openings.
Comments: Distinguished from the very similar *M. inaequalis* (q.v.) by the narrowness of the partecta in the basal half, the abrupt transition in partecta width, and the valve width <10 µm. Distinguished from *M. ciskienesis* (q.v.) by the unequal partecta. Both *M. cuneata* and the similar *M. inaequalis* (q.v.) were observed in colonies, each cell on an individual stalk. Simonsen (1990) studied these taxa and others in a group he named Marginulatae, cleared up some misidentifications (including Hustedt's!), and described the differences between *M. inaequalis* and *M. cuneata*. He also noted the heteropolarity of the cells in both species, which results from the presence of oblique mucilage ducts draining the partecta at one end (shown ultrastructurally by Lobban & Navarro 2012a, fig. 1).

Mastogloia cyclops Voigt Plate 27, Figs 4, 5
Ref. illus.: Voigt 1942, pl. 2, fig. 8; Stephens & Gibson 1980a, figs 8-14; Paddock & Kemp 1990, fig. 14 (detail of isolated pore); Witkowski et al. 2000, pl. 77, figs 7, 8
Samples: GU3D; **GU44K-6**
Dimensions: Length 32–39 µm, width 15–18 µm; striae 21–24 in 10 µm; partecta 12 in 10 µm, width 1.8 µm
Hustedt's section: Undulatae (Stephens & Gibson 1980a).
Diagnostics: Valves lanceolate with apiculate apices; strongly sinuous raphe and flared proximal raphe endings. It distinguished by the single large stigma on one side of the central area. Quadrangular areolae consisting of slightly radiate transapical striae. Partecta transapically rectangular, inner margin convex, reaching almost to the apices.
Comments: Our specimens usually more rostrate that the type shown by Voigt (1942). As Podzorski & Håkansson (1987:74, pl. 29, figs 6, 7 and pl. 53, fig. 2) noted, the details of the pore in the specimens they designated as *M. undulata* Grunow (following Ricard 1974, pl. 22, fig. 6) appear identical to the pore in *M. cyclops* illustrated in Stephens & Gibson (1980a). It is not clear why Ricard and Podzorski & Håkansson identified their specimens as *M. undulata*, since in the older literature (e.g., Peragallo & Peragallo 1897–1908, pl. 6, fig. 13; Hustedt 1931–1959, fig. 961) there is no mention of a pore in *M. undulata* and the inner margin of the partecta is flat. Witkowski et al. (2000) showed *M. cyclops* and did not include *M. undulata*. Neither *M. undulata* nor *M. cyclops* is mentioned in Novarino's (1989) resemblance list.

Mastogloia decussata Grunow in Cleve Plate 27, Figs 6, 7
Ref. illus.: Hustedt 1931–1959, fig. 917; Ricard 1975, figs 23–25; Güttinger 1997, Series 8; Witkowski et al. 2000 pl. 78, figs 1, 2; Hein et al. 2008, pl. 38, fig. 6
Samples: GU4A; GU32B; GU39A; **GU44I-1**
Dimensions: Length 100–118 μm, width 30–35 μm; striae 31 in 10 μm; partecta 10 in 10 μm, width 4 μm
Hustedt's section: Decussatae.
Diagnostics: Valves large lanceolate; raphe slightly sinuous. Small roundish areolae arranged in transapical and decussate striae. Partecta are rectangular transapically elongated similar in size and shape.
Comments: Specimens resembling *M. dissimilis* are common in our Guam samples but appear to have a raphe gutter and wider partecta than that species (but still much narrower than those of *M. decussata*). Distinguished from *M. dissimilis* Hustedt (Hustedt 1931–1959, fig. 916; Simonsen 1987, pl. 224, figs 3–7), which has a more rostrate valve and a narrower band with ± square partecta.

Mastogloia dicephala Voigt Plate 27, Figs 8, 9
Ref. illus.: Voigt 1942, fig.7; Navarro 1982a, pl. 25, figs 9–10; Paddock & Kemp 1990, fig. 114
Samples: GU21Y
Dimensions: Length 20 μm, width 10 μm; striae 23 in 10 μm; partecta width 1.5 μm
Diagnostics: Valves elliptical with rostrate apices; raphe straight. Partecta similar in size and shape, strongly convex and restricted in the middle part of the valve.
Comments: Resembling *M. decipiens* Hustedt (Hustedt 1931–1959, fig. 929), but according to Voigt (1942) more coarsely striated, capitate, and the partecta larger and more convex. We have observed several taxa that are close to *M. decipiens*/*M. ignorata* Hustedt (both shown in Simonsen 1987, pl. 225) but we are not yet convinced of their identity and are studying them further.

Mastogloia erythraea Grunow Plate 27, Figs 10, 11; Plate 28, Figs 1–2
Ref. illus.: Hustedt 1931–1959, fig. 959; Voigt 1966, figs 5–8; Stephens & Gibson 1980b, figs 10–17; Güttinger 1989, Series 3; Navarro et al. 1989, figs 47, 48; Novarino & Muftah 1991, fig. 7; Witkowski et al. 2000, pl. 76, figs 2–7; Hein et al. 2008, pl. 39, figs 1, 2, 4
Samples: GU3D; **GU44I-1, GU44I-1, -2, GU44P-B, GU44Y-13;** GU55B-4
Dimensions: Length 23–40 μm, width 8–17 μm; striae 24–26 in 10 μm; larger partecta width 2.2–2.5 μm; smaller partecta width 1.5 μm
Hustedt's section: Inaequales.
Diagnostics: Valves lanceolate with protracted apices; sinuous raphe. Quadrangular areolae arranged in very slightly radiate transapical striae. The internal raphe-sternum is distinctively bordered by thin, linear and discontinuous axial costae (Pl. 28, fig. 1, arrow). Partecta different in size and shape, with the rectangular small ones disposed in an elliptical alignment on the margin and interrupted at mid-valve between center and poles by two groups of one to three large ones.

Comments: The type variety has 1–9 larger partecta symmetrically placed in each quarterband (Hustedt 1931–1959); var. *grunowii* (see below) has only one on each side, in opposite quarterbands; and we have also documented other asymmetrical combinations. The species is variable yet distinctive, the form in Pl. 28, Figs 1, 2 very common in our samples. Variety *biocellata*, with two inflated partecta on each side of the central area (not yet seen in our samples), was raised to species rank as *M. biocellata* (Grunow) Novarino & Muftah (1991).

Mastogloia erythraea var. *grunowii* Foged Plate 28, Fig. 3
Ref. illus.: Navarro et al. 1989, fig. 49; Witkowski et al. 2000, pl. 82, figs 7, 8
Samples: GU44P-B
Dimensions: Length 26 µm, width 10 µm; striae 26 in 10 µm; larger partecta width 2.4 µm; smaller partecta width 1 µm
Diagnostics: Differing from the nominate variety in having large chambers only in two diagonally opposite quarterbands.

Mastogloia exilis Hustedt Plate 28, Figs 6, 7
Ref. illus.: Hustedt 1931–1959, fig. 985; Simonsen 1987, pl. 233, figs 9–13; Witkowski et al. 2000, pl. 84, figs 12, 13; Pennesi et al. 2012, figs 4A–H
Samples: GU44R-2, **GU52P-1, GU52Q-1**
Dimensions: Length 26 µm, width 10 µm; 27 striae in 10 µm; partecta 3 in 10 µm, width 2 µm; Hustedt's section: Sulcatae, Subgroup 2
Diagnostics: Valves elliptical with rounded apices; raphe sinuous. Valve surface depressed in semilanceolate inner zone. Partecta restricted in the central part of the valve, which are different size and shape, with the central ones larger.

Mastogloia fimbriata (Brightwell) Cleve Plate 28, Figs 8–11
Ref. illus.: Hustedt 1931–1959, fig. 884; Stephens & Gibson 1979b, figs 25–32; Ricard 1987, figs 775–779; Navarro 1983b, figs 34–37; Witkowski et al. 2000, pl. 77, figs 1–4 and pl. 83, figs 1–4; Hein et al. 2008, pl. 38, figs 1, 3
Samples: GU3D; GU6D-3GU32B; **GU44P-B, GUGU44T-1, GU44W-5;** GU52J-3; GU55B-4
Dimensions: Length 37–61 µm, width 25–41 µm; striae 8 in 10 µm; partecta 1–2.5 in 10 µm, width 3.5–5 µm
Hustedt's section: Ellipticae.
Diagnostics: Valves elliptical; raphe straight. Roundish areolae arranged in quincunx patterns. Partecta are narrower at the base, more or less apically elongated; the number of partecta vary widely.
Comments: Reported by Navarro & Lobban (2009, figs 66–68) for Guam but with external SEM only; we provide here LM of this, one of our most common *Mastogloia* species.

Mastogloia gomphonemoides Hustedt Plate 28, Figs 4, 5
Ref. illus.: Hustedt 1931–1959, fig 1001; Simonsen 1987, pl. 234, figs 8–13; Simonsen 1990, figs 51–53, 60–63, 70–75

Samples: **GU44Y-13, GU44AR-2; GU52Q-1, -3**
Dimensions: Length 23–38 µm, width 6 µm; striae 40 in 10 µm; larger partecta width 1.4 µm; smaller partecta width 0.7 µm
Section: Marginulatae Simonsen
Diagnostics: Narrow, lanceolate valves with rounded apices; raphe sinuous. Partectal ring is formed by larger partecta at the head-pole, becoming much narrower in the opposite part of the valve.
Comments: It is similar to *M. inaequalis*, but tapered from one pole, thus valves heteropolar, whereas in other species in this group asymmetry is physiological or restricted to the partectal ring.

Mastogloia graciloides Hustedt Plate 28, Figs 12, 13
Ref. illus.: Hustedt 1931–1959, fig. 934; Simonsen 1987, pl. 225, figs 9, 10
Samples: GU56A-2
Dimensions: Length 29 µm, width 12 µm; striae 18 in 10 µm, partecta 7 in 10 µm, width 2 µm
Hustedt's section: Inaequales.
Diagnostics: Lanceolate valves, with rostrate apices. Valve face with transapically elongated areolae clearly visible in irregular longitudinal ribs, raphe straight, striae increasingly radial toward the apices. Partecta extend up to protracted apices, end partecta considerably longer than the rest, inner margins flat.
Comments: Although Hustedt also described *M. gracilis* (Hustedt 1931–1959, fig. 933), it is easily distinguished from *M. graciloides* by its lanceolate shape and uniform partecta with convex inner margins. No similar forms are listed by Novarino (1989).

Mastogloia horvathiana Grunow Plate 29, Figs 1, 2
Ref. illus.: Hustedt 1931–1959, fig. 890; Navarro 1983a, fig. 38; Witkowski et al. 2000, pl. 82, figs 15–16 and pl. 85, figs 1, 2; Hein et al. 2008, pl. 41, fig. 1
Samples: **GU44I-2, GU44Y-13**
Dimensions: Length 52–67 µm, width 35–42 µm; striae 12–14 in 10 µm; 5 partecta in 10 µm, width 4.3 µm
Hustedt's section: Ellipticae.
Diagnostics: Valves broad-elliptical; sinuous raphe branches. Surface of the valves with pattern of hexagonal areolae as seen in LM. Wide partectal ring, partecta narrowly rectangular, all the way to the apex.
Comments: Similar in size and form to *M. ovum-paschale* (A. Schmidt) A. Mann (q.v.) but that species has partecta square or nearly so, although both *Mastogloia horvathiana* and *M. ovum-paschale* have about 5 partecta in 10 µm. *M. ovata* Grunow (q.v.) is also generally similar but, like *M. ovum-paschale* has nearly square partecta.

Mastogloia hustedtii Meister Plate 29, Figs 3–5
Ref. illus.: Voigt 1942, pl. 2, fig. 13; Ricard 1974, pl. 3, fig. 6; Stephens & Gibson 1979a, figs 6, 13; Stephens & Gibson 1980c, figs 12–17; Navarro 1983a, figs

39-41; Paddock & Kemp 1990, figs 20a, 128; Pennesi et al. 2011, figs 17–26
Samples: GU26A; GU15C; GU55B-4; **GU44I-1**
Dimensions: Length 35–38 µm, width 17–19 µm; striae 24–25 in 10 µm; partecta 3.5 in 10 µm, partecta width 1.7–2.5 µm
Hustedt's section: Sulcatae, Subgroup 1
Diagnostics: Valves elliptical-lanceolate; raphe sinuous. Externally, longitudinal bands on either side of raphe mark the locations of the pseudoconopea. The partecta are ornamented by a cluster of pores on a slightly raised plaque, visible in LM as a point on the convex inner margin, but not as prominent as those of *M. mediterranea* Hustedt (q.v.), which are narrow-necked peduncles (Pennesi et al. 2011).
Comments: It has been inserted in the section Sulcatae Subgroup 1 by Pennesi et al. (2011). *M. hustedtii* is also distinguished from *M. mediterranea* by its sinuous raphe. As noted by Voigt (1942), the partecta in this species are stepped rather than gradually tapered, in contrast to *M. grunowi* A. Schmidt, which has a similar surface pattern.

Mastogloia inaequalis Cleve Plate 29, Figs 6–8
Ref. illus.: Hustedt 1931–1959, fig. 999b-c; Simonsen 1990, figs 47–50, 54–59, 64–69; Witkowski et al. 2000 pl. 81, figs 19, 20 and pl. 84, figs 5–8; Lobban & Navarro 2012a, figs 13, 14
Samples: GU3D; **GU44I-2,** GU44R, **GU44Y-13, GU44AR-2; GU52Q-3,** GU52Q-10
Dimensions: Length 42–44 µm, width 12 µm; striae 39–40 in 10 µm; partecta width in basal portion 1.0–1.1 µm; apical partecta width 1.4–1.6 µm
Section: Marginulatae Simonsen
Diagnostics: Cells attached by mucilage stalks from basal pole. Lanceolate valves; raphe sinuous and prominently thickened, proximal endings deflected in asymmetrical central area. Partecta gradually widening toward one pole.
Comments: Distinguished from *M. cuneata* (q.v.) by the width of the valve (>10 µm) and the width of the narrower part of the partectal ring (at least 1 µm) (Simonsen 1990).

Mastogloia jelinecki Grunow Plate 30, Figs 1–3
Ref. illus.: Hustedt 1931–1959, fig. 977; Navarro 1983b, figs 42, 43; Hein et al. 2008, pl. 41, figs 2, 3; Pennesi et al. 2012, figs 5A–F
Samples: GU6E-9, **GU44Y-13**
Dimensions: Length 51–62 µm, width 24 µm; striae 17–22 in 10 µm, partecta 4 in 10 µm, width 1.1–1.5 µm
Hustedt's section: Sulcatae, Subgroup 2
Diagnostics: Large lanceolate valve with four depressed areas in the valve face, the striae out of the focal plane of the central area and margins, partectal ring very narrow with rounded, apically elongate partecta reaching to the rostrate apices.
Comments: Similar to *M. strigilis* Hustedt (Hustedt 1931–1959, fig. 974; Hein et al. 2008, pl. 46, figs 1, 2), but that species has striae parallel, not radiate.

Mastogloia kjellmanii Cleve Plate 30, Figs 4, 5
Ref. illus.: Hustedt 1931–1959, fig. 915; Ricard 1974, pl. 2, fig. 11; Simonsen 1987, pl. 183, figs 4–7 (as *M. tropica* Hustedt); Navarro et al. 1989, figs 56, 57
Samples: **GU52P-3**
Dimensions: Length 40–50 µm, width 18–19 µm; striae 23–26 in 10 µm, partecta 4 in 10 µm, width 1.6 µm except apical ones 1.8–2.2 µm
Hustedt's section: Decussatae.
Diagnostics: Valves lanceolate with rostrate apices; raphe slightly bent. Areolae small but distinct, arranged in quincunx pattern, transapical striae radiate. Partecta apically elongate with convex inner margins, the last one before the apex notably larger than the rest.
Comments: Distinguished from *M. dissimilis* and *M. decussata* (q.v.) by the shape of the partecta, especially the inflated apical one. *M. rostellata* Grunow (Hustedt 1931–1959, fig. 907) has similar partecta but the cell shape and the areola pattern are markedly different. There is also some resemblance to *M. gracilis* Hustedt, especially as illustrated by Hein et al. (2008, pl. 39, fig. 5), but the areolae in that species are finer and arranged only in transapical striae, and the partecta are uniform. Hustedt (1931–1959: 491) noted the synonymy of his own *M. tropica*.

Mastogloia lacrimata Voigt Plate 30, Figs 6–8
Ref. illus.: Voigt 1963, pl. 24, fig. 6; Hein et al. 2008, pl. 41, fig. 4
Samples: **GU44T-1, GU52P-5**
Dimensions: Length 29 µm, width 15 µm; striae 11 in 10 µm, partecta 4 in 10 µm, width 1.7 µm
Diagnostics: Valves lanceolate; raphe sinuous. Quincunx pattern of tear-shaped areolae and the slightly concave inner wall of the partecta. Areolae more elongate along the raphe, and becoming circular along the margin. Partecta are quadrangular of same size and shape.
Comments: Distinguished from *M. peracuta* Janisch (Hustedt 1931–1959, fig. 906; Ricard 1974, pl. 4, fig. 12; Yohn & Gibson 1982a, figs 1–6; Hein et al. 2008, pl. 43, fig. 1) by the very different partecta (resembling those of *M. kjellmanii*), and from *M. pseudolacrimata* Yohn & Gibson (1982a, figs 7–12; Hein et al. 2008, pl. 43, figs 4, 6) by the unusual half divisions in the partecta (cf. *M. cocconeiformis*, Pl. 24, Fig. 8).

Mastogloia laterostrata Hustedt Plate 31, Fig. 3
Ref. illus.: Hustedt 1931–1959, fig. 948; Ricard 1974, pl. 3, fig. 9; Simonsen 1987, pl. 227, figs 11, 12
Samples: GU32B
Dimensions: Length 24 µm, width 9 µm; striae 24 in 10 µm; partecta 9 in 10 µm, width 1.5 µm
Hustedt's section: Apiculatae.
Diagnostics: Linear-elliptic valves with rostrate apices; raphe straight. Transapical striae are radiate. Quadrangular partecta not up to the apices. Raphe with axial costae (not obvious in our specimen).

Mastogloia lineata Cleve & Grove Plate 31, Figs 1, 2
Ref. illus.: Hustedt 1931–1959, fig. 971; Yohn & Gibson 1981, figs 9–16
Samples: GU55B-4
Dimensions: Length 81–93 µm, width 35–36 µm; striae 14 in 10 µm; partecta 6 in 10 µm, width 1.5 µm
Hustedt's section: Undulatae.
Diagnostics: Lanceolate valve with apiculate apices; raphe sinuous, proximal endings with flaps. Rounded areolae arranged in almost straight apical striae. Partecta narrow, uniform, square to apically elongate.
Comments: Hustedt (1931–1959, fig. 972) also showed *M. lineata* var. *albifrons* Hustedt but, while his drawings make it seem different, Yohn & Gibson (1981) concluded that there was insufficient difference to warrant a separate variety.

Mastogloia macdonaldii Greville Plate 31, Figs 4, 5
Ref. illus.: Hustedt 1931–1959, fig. 992 (as *M. macdonaldi*); Podzorski & Håkansson 1987, pl. 25, fig. 4; John 1994, figs 54–57; Witkowski et al. 2000, pl. 78, figs 7, 8 and pl. 79, figs 17, 18; Pennesi et al. 2012, figs 6A-I
Samples: **GU52J-3, GU52P-8**
Dimensions: Length 35 µm, width 18 µm; striae 24 in 10 µm; partecta 5 in 10 µm, width 2.5µm
Hustedt's section: Sulcatae, Subgroup 2
Diagnostics: Valve elliptical with subrostrate apices; raphe straight. Valve face with two zones: an inner zone with parallel striae in four panels extending from the stauroid central area, and an outer zone in which these striae continue radially to the margin. Partecta uniform, square, inner margins convex.
Comments: Differs from *M. foliolum* Brun (Hustedt 1931–1959, fig. 993) and *M. fallax* var. *biloculis* Foged (Hein et al. 2008, pl. 37, figs 5–7) in having uniform partecta. Hustedt asserts that the inner zone is completely featureless or shows but traces of the transapical ribs, but the image in Witkowski et al. (2000) clearly shows parallel striae there. The form described as *M. pisciculus* var. *staurophora* Ricard (Ricard 1975, pl. 3, fig. 36 = Ricard 1977, pl. 2, fig. 4), based on a specimen of *M. pisciculus* Cleve illustrated by Hustedt (Fig. 990, middle valve), may be *M. macdonaldii*.

Mastogloia manokwariensis Cholnoky Plate 32, Figs 1–3
Ref. illus.: Stephens & Gibson 1980b, figs. 18–23; Güttinger 1998, Series 9; Witkowski et al. 2000, pl. 80, fig. 11; Hein et al. 2008, pl. 38, fig. 2
Samples: GU32B; **GU44P-B;** GU55B-4
Dimensions: Length 12–13 µm, width 6 µm; striae 28 in 10 µm; partecta 4.5 in 10 µm, central partectum width 1.7 µm
Diagnostics: Valves elliptical-lanceolate with broad subrostrate apeices; raphe straight. Radiate striae, usually one large partectum with strongly convex inner margin and two tapering on each side (but reported with more).

Mastogloia mauritiana Brun Plate 32, Figs 4–10
Ref. illus.: Hustedt 1931–1959, fig. 995; Paddock & Kemp 1990, fig. 107; Witkowski et al. 2000, pl. 79, figs 7, 8; Hein et al. 2008, pl. 42, fig. 1.
Samples: GU3D; GU32B, **GU44AD-1;** Arai slide **Gab3C*; GU52Q-1;** GU52H
Dimensions: Length 29 μm, width 17 μm; striae 23 in 10 μm; larger partecta 4 in 10 μm, 1.8–2.5 μm wide, narrower partecta 8–9 in μm, width 1.1–2.0 μm
Hustedt's section: Sulcatae, Subgroup 2
Diagnostics: Valve lanceolate; raphe almost straight. Transapical striae are radiate. The inner zone near the raphe-sternum is depressed relative to the outer zone. The external valve face shows the series of lines paralleling the raphe branches, and the partectal ring with somewhat larger partecta between the middle and ends of the ring.
Comments: The differences between this species and *M. peragalli* Cleve (q.v.) are subtle but Hustedt (1931–1959: 563) relates how Brun lined up specimens of each to point out the differences when he named *M. mauritiana*. The partectal rings are very similar, but there are fewer chambers in 10 μm in *M. mauritiana*, 4 wider and 8 narrower, versus 6 and 12 in *M. peragalli*; another key difference is the extent of the valve occupied by the furrowed area, 1/3 or more in this species, vs. about 1/4–1/5 in *M. peragalli*. On these criteria it appears that all our specimens are *M. mauritiana*. Unidentified *Mastogloia* specimens shown by Montgomery (1978, pl. 128, figs E vs. C, D, F) may represent these two species, respectively. Similar longitudinal furrows are seen in *M. neomauritiana* Paddock & Kemp (1988, figs 26–36), but in this species the partectal ring is different, with the inflated partecta at the middle. Finally, *M. tautirensis* Ricard (q.v.) has a somewhat different pattern of longer and shorter partecta and has denser striae.

Mastogloia mediterranea Hustedt Plate 33, Figs 1, 2
Ref. illus.: Hustedt 1931–1959, fig. 1005; Simonsen 1987, pl. 234, figs 1–7; Pennesi et al. 2011 figs 27–33
Samples: **GU52P-5, GU52Q-1**
Dimensions: Length 21 μm, width 10 μm; striae not resolved (36–38 in 10 μm according to Pennesi et al. 2011); partecta 3 in 10 μm, width 2 μm
Hustedt's section: Sulcatae, Subgroup 1
Diagnostics: Lanceolate valves with protracted apices; raphe sinuous. On the valve face, prominent longitudinal lines mark the edges of the pseudoconopeum; 2–3 partecta on each side with prominent necked peduncles (arrowhead).
Comments: The peduncles (versus smaller plaques or nodules) distinguish this species from *M. hustedtii* (q.v.) and from *"M. baldjikiana"* sensu Pennesi et al. (2011, figs 1–6), which also differ in the number and shape of the partecta.

Mastogloia neoborneensis Pennesi & Totti Plate 33, Fig. 3
Ref. illus.: Pennesi et al. 2011, figs 45–54
Samples: GU55B-4, **GU52K-7, GU44Y-13**
Dimensions: Length 24 μm, width 8 μm; striae 34 in 10 μm; partecta 6 in 10 μm, width 1 μm

Hustedt's section: Sulcatae, Subgroup 1
Diagnostics: Valves elliptical-lanceolate with protracted apices; raphe sinuous. Transapical striae from slightly to strongly radiate from center to pole. Valve face shows irregular longitudinal ribs, semielliptical pseudoconopea and a thick marginal ridge. Areolae transapically elongated.
Comments: Identified so far only in SEM on the basis of the short pseudoconopea. Distinguished from *M. borneensis* (q.v.) by the larger pseudoconopea and protracted apices, from *M. umbra* (q.v.) which has a conopeum rather than a pseudoconopeum (compare Pl. 37, Fig 9 with Pl. 33, Fig. 3) and from other species studied by Pennesi et al. (2011) by the lack of structures on the inner margin of the partecta.

Mastogloia ovalis A. Schmidt Plate 33, Figs 4–6
Ref. illus.: Hustedt 1931–1959, fig. 893; Stephens & Gibson 1979b, figs 33-40; Paddock & Kemp 1990, fig 113 (mislabeled M. ovata); Witkowski et al. 2000, pl. 75, figs 11–13; Hein et al. 2008, pl. 40, fig. 6.
Samples: GU26A; **GU44P-B, GU44Y-13; GU52P-8, GU52Q-1**
Dimensions: Length 23 μm, width 13 μm; striae 23 in 10 μm; partecta 3.5–4 in 10 μm, width 1.2–1.5 μm
Hustedt's section: Ellipticae.
Diagnostics: Elliptical valves; raphe slightly sinuous. Face with radiate striae, partecta restricted to the middle, apically elongate with strongly concave inner margins. Areolae are more or less rounded, occluded by volae.
Comments: Several other small oval species with concave partecta have been distinguished, including *M. ovulum* Hustedt (q.v.), which is rather variable, *M. crucicula* (q.v.), *M. emarginata* Hustedt, and even *M. subaspera* Hustedt. *M. emarginata* (Hustedt 1931–1959, fig. 896) has elongate concave partecta distinguished by a distinct pore on the basal surface, *M. subaspera* (Hustedt 1931–1959, fig. 898) has a much different valve structure, which Hustedt compares with *M. ovum-paschale*.

Mastogloia ovata Grunow Plate 33, Figs 7, 8
Ref. illus.: Hustedt 1931–1959, fig. 895; Witkowski et al. 2000, pl. 82, fig. 1; Hein et al. 2008, pl. 38, fig. 5
Samples: **GU52P-7, GU6D-1**
Dimensions: Length 33 μm, width 23 μm; striae 15 in 10 μm; partecta 4 in 10 μm, width 2.5 μm
Hustedt's section: Ellipticae.
Diagnostics: Broadly elliptical valve with transapically elongate areolae in radiating rows, raphe stright or slightly sinuous, partecta nearly square, reaching the apices, inner margin flat to slightly concave.
Comments: Hein et al. (2008, pl. 40, fig. 3) show a slightly different specimen identified as *"Mastogloia* cf. *ovata." M. ovata* is smaller and proportionally broader than *M. ovum-paschale* (q.v.) and has more elongate areolae and a smaller central area.

Mastogloia ovulum Hustedt Plate 33, Figs 9, 10
Ref. illus.: Hustedt 1931–1959, fig. 892; Simonsen 1987, pl. 222, figs 1, 2, (3–5?), 6–11; Güttinger 1997, Series 8; Witkowski et al. 2000, pl. 75, fig. 14; Hein et al. 2008, pl. 40, fig. 7
Samples: **GU44K-6, GU44P-B, GU44Z-15**
Dimensions: Length 12–19 µm, width 8–11 µm; striae 20–24 in 10 µm; partecta 3 in 10 µm, width 1 µm
Hustedt's section: Ellipticae.
Diagnostics: Elliptical valves; raphe slightly sinuous. Striae are radiate, partecta reaching the apices, apically elongate with strongly concave inner margins.
Comments: While Hustedt (1931–1959) distinguished *M. ovalis* from *M. ovulum* partly on the basis of restriction of the chambers to the middle of the ring, the latter is rather variable as depicted in the references cited. In particular, Hustedt (1931–1959, fig. 892, upper right) shows a valve identified as *M. ovulum*, but with partecta amost identical to those of *M. crucicula*; a similar specimen is shown by Witkowski et al. (2000, pl. 75, figs 7–9), whereas Simonsen's (1987, pl. 222, figs 3–5) similar specimen from Hustedt's types seems to have a fascia and is scarcely distinguishable from *M. crucicula*. Witkowski et al. (2000, pl. 75, figs 7–9) show specimens close to *M. ovulum* but captioned "*Mastogloia* spec."

Mastogloia ovum-paschale (A. Schmidt) A. Mann Plate 34, Figs 1, 2
Ref. illus.: Hustedt 1931–1959, fig. 897; Ricard 1974, pl. 4, fig. 2; John 1994, figs 58, 59
Samples: **GU44I-2, GU44P-B, GU44Y-13, GU44AJ; GU52Q-2**
Dimensions: Length 65–71 µm, width 38–40 µm; striae 15 in 10 µm; partecta 4 in 10 µm, width 3 µm
Hustedt's section: Ellipticae.
Diagnostics: Large elliptical valves, sinuous raphe; partecta nearly square partecta with crenulate free ends.
Comments: See comments under *M. horvathiana*.

Mastogloia paradoxa Grunow Plate 34, Figs 3–5
Ref. illus.: Hustedt 1931–1959, fig. 953; Stephens & Gibson 1980a, figs 21–26; Paddock & Kemp 1990, fig 110; Hein et al. 2008, pl. 42, figs 3, 4
Samples: **GU44Y-13; GU52K-4, GU52P-5, GU52Q-1**
Hustedt's section: Paradoxae.
Dimensions: Length 35–36 µm, width 10–11 µm; striae 26–28 in 10 µm; larger partecta 4 in 10 µm, width 1.5 µm; smaller partecta 8 in 10 µm, width 1.0 µm
Diagnostics: Linear-elliptical valves with rostrate apices; sinuous raphe internally enclosed in axial costae. Transapical striae are parallel. Unequal partecta displaced internally from the valvocopula wall by siliceous flange, showing oblique ducts (Pl. 34, Fig. 5, arrow).
Comments: *M. similis* Hustedt (Hustedt 1931–1959, fig. 955) was distinguished on the basis of a completely straight raphe. Another similar species is *M. seychellensis* Grunow (Hustedt 1931–1959, fig. 958), which lacks the raphe gutter and has more uniform partecta.

Mastogloia pseudolatecostata Yohn & Gibson Plate 35, Figs 1, 2
Ref. illus.: Yohn & Gibson 1982a, figs 20-25; Witkowski et al. 2000, pl. 77, figs 5, 6; Hein et al. 2008, pl. 45, figs 1, 3
Samples: **GU44I-4, GU44T-1, GU44AJ**
Dimensions: Length 26–35 µm, width 16–26 µm; striae 21–25 in 10 µm; partecta 4–5 in 10 µm, width 2 µm
Hustedt's section: Ellipticae (Yohn & Gibson 1982a)
Diagnostics: Broadly elliptical valves; raphe straight. Transapically elongate areolae arranged neatly in both radiating transapical striae and undulate longitudinal rows. Partecta are rectangular and equal in size with concave margins.
Comments: Differing from *M. latecostata* Hustedt (Hustedt 1931–1959, fig. 969), which has half walls within the partecta and less regular longitudinal rows of areolae.

Mastogloia pulchella Cleve Plate 35, Figs 3, 4
Ref. illus.: Hustedt 1931–1959, fig. 968; Ricard 1974, pl. 4, fig. 5; Montgomery 1978, pl. 129 figs D–F
Samples: **GU44Y-13, GU44Z-15**
Dimensions: Length 41–51 µm, width 19–23 µm; striae 16–17 in 10 µm; partecta 10 in 10 µm, width 1.6–1.8 µm
Hustedt's section: Lanceolatae.
Diagnostics: Laneolate valves with protracted ends; raphe strongly sinuous. Striae strongly radiating, especially noticeable in the middle where short striae are inserted from the margins. Transapically elongate areolae in strong longitudinal rows that get narrower toward the margin. Partecta narrow, square to rectangular.
Comments: The valve pattern is similar to *M. beaufortiana* Hustedt (Hustedt 1955, pl. 6, fig. 11; Simonsen 1987, pl. 609, figs 16–19; Witkowski et al. 2000, pl. 84, figs 1, 2) but the partecta in that species are apically elongated.

Mastogloia punctatissima (Greville) Ricard Plate 35, Figs 7, 8
Ref. illus.: Hustedt 1931–1959, fig. 883; Stephens & Gibson 1979b, figs 41–46; Navarro 1983a, figs 64, 65; Witkowski et al. 2000, pl. 75, figs 1, 2 [all as *M. splendida* (Gregory) Cleve]; Ricard 1975, pl. 2, fig. 24 and pl. 4, figs 40, 41; Williams 1988, pl. 29, figs 13, 14; Hein et al. 2008, pl. 44, figs 1, 2
Samples: **GU44K-6, GU44I-2, GU44Y-13; ECT3569 = GU44J-2**
Dimensions: Length 50–55 µm, width 37 µm; striae 11 in 10 µm; partecta 7 in 10 µm, width 2 µm
Hustedt's section: Ellipticae.
Diagnostics: Large broadly elliptical to nearly circular valve; raphe slightly sinuous with distal ends of the branches swerving toward the same side just before the apices. Curving quincunx pattern of hexagonal areolae; striae biseriate at the margin.
Comments: The raphe hook serves to distinguish this species from all other large elliptical *Mastogloia* spp. Hein et al. (2008, p. 71) point out that this species, with hooked distal raphe endings has often been misidentified as *M. splendida* (Gregory) Cleve, which has a straight raphe. Ricard (1974:171) himself listed it as *M. splendida* before making the nomenclatural change.

Mastogloia rhombica Cleve Plate 35, Figs 5, 6
Ref. illus.: Hustedt 1931–1959, fig. 920; Yohn & Gibson 1982b, figs 44–50
Samples: **GU44I-2, GU44K-6, GU44Y-13, GU44Z-15; GU52K-7;** GU7V
Dimensions: Length 38–63 µm, width 20–27 µm; striae 11–12 in 10 µm; partecta 4–5 in 10 µm, width 1.7–1.9 µm
Hustedt's section: Undulatae.
Diagnostics: Valves rhombic-lanceolate; raphe strongly sinuous and the strongly deflected and distant central raphe endings (the latter standing 4–5 striae apart). Transapical triae are radiate and formed by relatively coarse areolae. Rectangular partecta are uniform in shape and size.

Mastogloia rimosa Cleve Plate 36, Figs 1, 2
Ref. illus.: Yohn & Gibson 1981, figs 24–30, Hein et al. 2008, pl. 46, figs 3, 5
Samples: **GU52P-5, GU52P-8**
Dimensions: Length 43 µm, width 18 µm, striae 11 in 10 µm; partecta 10 in 10 µm, width 3 µm
Hustedt's section: Undulatae (Yohn & Gibson 1981)
Diagnostics: Valves rhombic-lanceolate; raphe almost straight markedly deflected in the proximal endings. Areolae quadrangular arranged in radiate transapical striae. Partecta almost to the apices, transapically rectangular.
Comments: The valve structure is similar to *M. corsicana* (q.v.), but with many more longitudinal rows of areolae and that species also has nearly square partecta.

Mastogloia robusta Hustedt Plate 36, Figs 3–6
Ref. illus.: Hustedt 1931–1959, fig. 951; Simonsen 1987, pl. 228, figs 1–4; Witkowski et al. 2000, pl. 79, figs 3–6
Samples: **GU44Y-13;** GU56A-2
Dimensions: Length 31–39 µm, width 13–15 µm; striae 19–20 in 10 µm; partecta 6 in 10 µm, width 2 µm
Diagnostics: Linear-elliptical valves with rounded apices; raphe sinuous. Transapical striae are radiate. Internally, raphe-sternum is bordered by axial costae (Pl. 36, Figs 4, 6 arrows). Partecta transapically rectangular.
Comments: Distinguished from *M. adriatica* Voigt (Voigt 1963, pl. 21, figs 1–3; Witkowski et al. 2000, pl. 73, figs 14, 15 and pl. 79, figs 1, 2) in that the gutter is interrupted at the central area (and see *M. adriatica* var. *linearis* above); the transapical striae are coarser and much less radial, the puncta are closer than the striae (Voigt 1963: 112).

Mastogloia rostrata (Wallich) Hustedt Plate 36, Figs 9, 10
Ref. illus.: Wallich 1860, figs 5, 6 (as *Stigmaphora rostrata*); Hustedt 1931–1959, fig. 1007; Gibson & Stephens 1985, figs 1–11; Kemp & Paddock 1988, figs 1–13 (as *Stigmaphora rostrata* Wallich)
Samples: **GU44Z-15;** GU55B-4
Dimensions: Length 55–155 µm, width 11–16 µm; striae 27–29 in 10 µm; partecta width 3.5 µm

Hustedt's section: Rostellatae.
Diagnostics: Valves linear-lanceolate with long protracted apices; raphe straight. Partectal ring more displaced interiorly toward the middle line of the valve by a siliceous flange. Two partecta in the middle part of the valve for each side. In the apices there are the intercalary bands. Partectal ducts open about halfway between center and rostra (arrowhead on Pl. 36, Fig. 10).

Mastogloia sergensis Pennesi & Poulin Plate 36, Figs 7, 8; Plate 37, Figs 1, 2
Ref. illus.: Stephens & Gibson 1980c, figs 24–30 (as *M. omissa* Voigt); Pennesi et al. 2012, figs 9A–G
Samples: GU3D; GU26A, **GU44I-1, GU44P-B, GU44AN-6;** Arai slide **Gab3C***
Dimensions: Length 14–18 µm, width 8–9 µm; striae 30 in 10 µm; partecta 2.5–3 in 10 µm, width 1.5–1.8 µm
Hustedt's section: Sulcatae, Subgroup 2
Diagnostics: Valves elliptical-lanceolate with subrostrate apices; raphe sinuous. Lanceolate furrows along each side of the raphe, one (sometimes two) large partectum at the center, flanked by one tapering partectum on each side. Lanceolate depressed area crossed by single transapically elongate areolae.
Comments: Close to *M. exilis* Hustedt (Hustedt 1931–1959, fig. 985; Pennesi et al. 2012, figs 4A–H), but there are irregular rows of areolae across the furrow and correspondingly >1 longitudinal rows of pores, rather than one; and *M exilis* usually has two large partecta on each side. Other species with one partectum on each side include *M. manokwariensis* (q.v.) and *M. pusilla* var. *subcapitata* Hustedt (Hustedt 1931–1959, fig. 1002e, Ricard 1974, pl. 20, fig 8), a variety at the end of the range of *M. pusilla* Grunow, but the valve structure is different (Paddock and Kemp 1990, fig. 59). *M. lentiformis* Voigt (1942, fig. 33) has similar partecta but is a minute species with a straight raphe that also appears to lack a furrow. Overall it is similar to *Mastogloia* spec. 84/1 (Witkowski et al. 2000, pl. 84, figs 9–11).

Mastogloia tautirensis Ricard Plate 37, Figs 3–5
Ref. illus.: Ricard 1975, pl. 3, fig. 34, Ricard 1977, pl. 2, fig. 5
Samples: GU3D; **GU44I-1, GU44I-2, GU44Y-13; GU52Q-2**
Dimensions: Length 29 µm, width 12–13 µm; striae 26–28 in 10 µm; widest partecta 2.3 µm, central partest width 1.5 µm
Hustedt's section: Sulcatae
Diagnostics: Valves lanceolate with subrostrate apices; raphe straight. Transapical striae radiate. Apically elongated partecta are of different sizes, the largest lying between the middle and the ends.
Comments: Distinguished from *M. mauritiana* and *M. peragalli* by the pattern of large and small partecta, with the larger partecta followed apically by a tapering partectum. Ricard (1975) described two longitudinal *"areae depressae"* on the valve face; thus this species would be placed in Sulcatae, but it is not yet known whether there is a conopeum/pseudoconopeum or merely a depression.

Mastogloia tenuis Hustedt Plate 37, Figs 6–8
Ref. illus.: Hustedt 1931–1959, fig. 961; Simonsen 1987, pl. 234, figs 14–17; Kemp & Paddock 1988, figs 35–43
Samples: GU26A; **GU44Y-13**
Dimensions: Length 26–29 μm, width 7–9 μm; striae 30 in 10 μm; partecta width 2.5–3 μm
Hustedt's section: Inaequales.
Diagnostics: Valves small lanceolate with cuneate apices; raphe straight. Transapical striae slightly radiate. Internally, the raphe-sternum is bordered by axial costae. Two large central partecta plus two small ones tapering abruptly toward the apices.
Comments: As noted by Kemp & Paddock (1988), the ducts from the two partecta in each quadrant open as paired pores near the apices (Pl. 37, Fig. 8). Differing from *M. liatungensis* Voigt (Ricard 1974, pl. 2, fig. 1; Foged 1987, pl. 10, fig. 10) in the shapes of the partecta and the apices and in the lack of a gutter bordering the raphe.

Mastogloia umbra Paddock & Kemp Plate 37, Fig. 9
Ref. illus.: Paddock & Kemp 1988, figs 39–44; Pennesi et al. 2011, figs 34–44
Samples: **GU44Y-13, GU44AI-1; GU52P-1,** GU52Q-10
Dimensions: Length 16–19 μm; width 6–8 μm, striae 27–30 in 10 μm
Hustedt's Section: Sulcatae, Subgroup 1
Diagnostics: Valves elliptical with subrostrate apices; raphe sinuous. Transapical striae are radiate, formed by irregular areolae. The external valve face shows the conopeum that covers a median depression.
Comments: The small size and shape of the valve and the presence of conopea (vs. pseudoconopea) distinguish this from the similar species treated by Pennesi et al. (2012). Paddock & Kemp (1988) distinguished their species from *M. varians* Hustedt (Hustedt 1926–1996, fig. 909) and *M. delicatissima* Hustedt (Hustedt 1926–1996, fig. 903), which both apparently have no conopea.

Achnanthes brevipes C.A. Agardh (var.) Plate 38, Figs 1–4
Ref. illus.: Hustedt 1931–1959, fig. 877; Witkowski et al. 2000, pl. 45, figs 1–12; Toyoda et al. 2005, figs 1–3, 11–28; Cox 2006, figs 1, 3, 4, 6–9
Samples: GU15C; GU12A/B, GU12O; GU26A; GU39A; **GU44I-1, GU52K-7**
Dimensions: Length 15–53 μm, width 7–11 μm; striae 11 in 10 μm.
Diagnostics: Frustules flexed, heterovalvar; raphe valve (RV) with a stauros and median raphe, sternum valve (SV) with sternum along one margin, no stauros. Striae single rows of large areolae parallel throughout.
Comments: The lack of costae distinguishes this species from *A. longipes* (q.v.), and the parallel striae distinguish it from *A. javanica* Grunow. Valves in our samples linear-lanceolate with rounded apices. *A. brevipes* is very variable and many of our specimens do not agree with published illustrations, particularly in the extremely marginal sternum. Most of our specimens best agree with figures of *A. brevipes* var. *angustata* (Greville) Cleve shown in Foged (1987, pl. 9, figs 9–14) and with *A. brevipes* var. *intermedia* (Kützing) Cleve (Hustedt 1931–1959, fig 877d, e; Foged 1987, pl. 9, fig. 15).

Achnanthes citronella (Mann) Hustedt Plate 38, Figs 5, 6
Ref. illus.: Mann 1925, pl.13 figs 3–6 (as *Cocconeis citronella*); Hustedt in Schmidt et al. 1874–1959 pl. 415, fig 3–8; Montgomery 1987, pl. 72, figs E–G; Podzorski & Håkansson 1987, pl. 12, fig. 1 (RV); Riaux-Gobin et al. 2011b, pl. 1, fig. 6, pl. 8, figs 1–3 (SV)
Samples: **GU44I-1, GU44K-6, GU6D-4**
Dimensions: Length 28–30 µm, width 13 µm; striae of SV mostly parallel, 11–12 in 10 µm, of RV radiate, 26 in 10 µm
Diagnostics: The lemon-shaped outline, heterovalvy, and coarse areolae of the SV is a combination that separates these valves from similar shaped *Mastogloia* (cf. *M. citrus* Cleve) and from other *Achnanthes* spp. The RV has much finer areolae and a partial stauros (Pl. 38, Fig. 6).

Achnanthes cuneata (Grunow) Grunow Plate 38, Fig. 7
Ref. illus.: Mereschkowsky 1900–1902, pl. 4, figs 22, 23; Witkowski et al. 2000, pl. 44, figs 14, 15
Samples: GU26X, GU29G
Dimensions: Length 65 µm, width of wider half 10–12 µm; striae 10–11 in 10 µm
Diagnostics: Distinguished from *A. brevipes* by the wider valve in one half.
Comments: Witkowski et al. (2000: 87) give stria density of 8–10 in 10 µm for the RV. Rarely seen and our specimens possibly just a variant (or deviant) *A. brevipes*.

Achnanthes longipes C.A. Agardh Plate 39, Figs 1–3
Ref. illus.: Hustedt 1931–1959, fig. 878; Navarro 1982c, figs 3, 4; Witkowski et al. 2000 pl. 45:13–14
Samples: GU4A, GU15C, GU011, **GU44I-1**
Dimensions: Length 23–57 µm, width 8–10 µm; striae 13–14 in 10 µm.
Diagnostics: Frustules flexed (Pl. 39, Fig. 2); transapical costae separating pairs of striae on both valves. Sternum medial.
Comments: The girdle view (Pl. 39, Fig. 2) is bi/triseriate on both valves and therefore indeed *A. longipes* and not the newly recognized *A. pseudolongipes* Toyoda & Nagumo, in which the RV has uniseriate striae (like *A. brevipes*) but the SV has 2 (or 3) rows of striae (like *A. longipes*) (Toyoda et al. 2010). Their paper casts doubt on the identity of acid-cleaned raphe valves with uniseriate striae (e.g., our Pl. 38, Figs. 1, 4). *A. pseudolongipes* has numerous plastids, like *A. longipes* but unusual for *Achnanthes* (Toyoda et al. 2010).

Planothidium campechianum (Hustedt) Witkowski, Lange-Bertalot and Metzeltin Plate 39, Fig. 4
Ref. illus.: Witkowski et al. 2000, pl. 48, figs 3–9
Samples: GU26A; **GU44L-C**
Dimensions: Length 10–12 µm, width 4–5 µm; striae 17–18 in 10 µm
Diagnostics: Very small cells with acute apices, biseriate striae with very coarse areolae.

Comments: Specimens in SEM identified on the basis of the SEM in Witkowski et al. (2000). Only SV identified.
Comments: There are numerous species of *Planothidium* and *Achnanthidium*, mostly resolvable only with SEM (see Riaux-Gobin et al. 2011b).

Anorthoneis vortex Sterrenburg Plate 39, Fig. 5
Ref. illus.: Sterrenburg 1988, figs 5, 7–15; Witkowski et al. 2000, pl. 42, fig 23–25; Riaux-Gobin et al. 2011b, pl. 1, figs 4, 5 and pl. 26, figs 1–6
Samples: **GU44L-E,** GU44T-4, **GU44W-5**
Dimensions: Length 17–18 μm, width 13–15 μm; striae 18–19 in 10 μm
Diagnostics: Broadly elliptical to nearly circular valve, sternum displaced from apical axis, asymmetric central area on the wide side of the sternum.
Comments: Distinguished from *A. excentrica* (Donkin) Grunow and *A. pulex* Sterrenburg by the size and the stria count; in addition, the former has no hyaline area to one side of the raphe or sternum. Species in this genus may have hyaline areas on both valves or only the SV; *A. vortex* has one on each valve (Sterrenburg 1988); we have not seen the RV.

Cocconeis coronatoides Riaux-Gobin & Romero Plate 39, Fig. 6
Ref. illus.: Riaux-Gobin et al. 2010, figs 1–3; Riaux-Gobin et al. 2011b, plates 34–36
Samples: GU55B-4; GU56A-1
Dimensions: Length 21–22 μm, width 12–13 μm; striae 20 in 10 μm
Diagnostics: Prominent submarginal ridge and numerous spines around the areolae of the SV.
Comments: The submarginal ridge and the spines distinguish this species from *C. scutellum* (q.v.) and *C. alucitae* Riaux-Gobin & Compère, but Riaux-Gobin et al. (2011b) note that the spines can be absent. RV (not seen) markedly different from those two species, with unique submarginal depressed hyaline rim separating the outermost three rows of areolae. Riaux-Gobin et al. (2011a) provided the legitimate name.

Cocconeis dirupta Gregory Plate 40, Figs 1–5
Ref. illus.: Hustedt 1931–1959, fig. 809a–c; Kobayasi & Nagumo 1985, pl. 2, figs 15–27; Witkowski et al. 2000, pl. 39, figs 1–5
Samples: GU7R; **GU44I-1, GU44R-2, GU44Z-15**
Dimensions: Length 16–17 μm, width 9–11 μm; striae (RV and SV, respectively) 26 and 20 in 10 μm
Diagnostics: Raphe sigmoid, often with small fascia, RV finely striated; SV more coarsely striated, sternum narrow to broadly lanceolate, sometimes constricted in the middle. The SV is fairly distinct because of the shape of the sternum in combination with the coarse striae.
Comments: There are a few other *Cocconeis* species with a fascia on the RV, among them *C. molesta* var *crucifera* Grunow (Witkowski et al. 2000, pl. 33, figs 8, 9 and pl. 37, figs 9–13), C. *pseudodiruptoides* Foged (Witkowski et al. 2000, pl. 39, figs 11–18), and *Cocconeis subdirupta* Cholnoky (Cholnoky 1959, figs 102–

104). Finally, Riaux-Gobin et al. (2011b, p. 26, pl. 4, figs 1, 2 and pl. 41, figs 1–6) describe "*Cocconeis* sp. aff. *dirupta*" that has a straight raphe but symmetrical fascia, distinguishing it from both *C. dirupta* and *C. subdirupta*; such specimens have also been seen in the Guam samples (Pl. 40, Fig. 3). Riaux-Gobin et al. (2011b: 10) comment, "The characteristic features of the smaller taxa are hardly discernible on specimens preserved in permanent preparations with a refractive mounting media used for LM observations. The SEM was essential to fully clarify their morphology." This certainly applies to many small *Cocconeis* seen in Guam samples, and the level of detail requires a full-size SEM.

Cocconeis dirupta var. *flexella* (Janisch & Rabenhorst) Grunow Pl. 40, Figs 4, 5
Ref. illus.: Witkowski et al. 2000: 105, pl. 39, figs 1–5, Riaux-Gobin et al. 2011b, pl. 42
Samples: **GU44I-1**
Dimensions: Length 11–16 µm, width 7–10 µm; (RV) striae 28 in 10 µm; (SV) striae 26 in 10 µm
Diagnostics: Differing from the nominate variety in the sigmoid sternum and raphe.
Comments: Striae counts on SV and RV in these specimens are similar, in contrast to finer striae on RV of the nominate variety. Moreover, Riaux-Gobin et al. (2011b) reported stria density of SV as 27–35 in 10 µm, much finer than our specimens or to SV of the nominate variety (they did not find the RV of var. *flexella*, nor any var. *dirupta*). This taxon needs further study.

Cocconeis distans Gregory Plate 41, Figs 4, 5
Ref. illus.: Hustedt 1931–1959, fig. 797; Witkowski et al. 2000, pl. 38, figs 12, 13; Riaux-Gobin et al. 2011b, pl. 4, fig. 3, pls 46, 47.
Samples: GU12Z
Dimensions: Length 35 µm, width 21 µm; striae (SV) 5 in 10 µm; parts of striae just visible at valve edge (Pl. 40, Fig. 5, arrow) suggest RV striae 16 in 10 µm
Diagnostics: Very widely spaced areolae on SV.
Comments: Similar to *C. guttata* Hustedt in Aleem & Hustedt in LM (Witkowski et al. 2000, pl. 40, figs 13-18) and both have much finer striae on the RV. Stria density and valve size of this specimen more closely match *C. distans* (Witkowski et al. 2000, pp 106 vs. 108), whereas *C. guttata* is smaller and has finer striae, 8–9 in 10 µm. Indeed, Riaux-Gobin et al. (2011b: 28) suggest that the images of *C. guttata* in Sar et al. (2003, figs 16–21) may be *C. distans*.

Cocconeis heteroidea Hantzsch Plaate 40, Figs 6, 7; Plate 41, Figs 1–3
Ref. illus.: Hustedt 1931–1959, fig. 811; Ricard 1987, figs 1158, 1159; Foged 1987, pl. 8, figs 10, 11; Witkowski et al. 2000, pl. 35, figs 4, 5; Suzuki et al. 2001a, figs 1–28
Samples: **GU44Y-13, GU44T-1, GU44U-1A, GU44AE-2**
Dimensions: Length 37–60 µm, width 29–50 µm; RV striae 19 in 10 µm at the margin near the center, SV striae 30 in 10 µm
Diagnostics: Large *Cocconeis*, raphe and sternum strongly sigmoid, with prominent sigmoid ridges along each side of the raphe/sternum (both valves).

Comments: *C. heteroidea* is one of several species in the genus that have complex valve structure on the SV, as well illustrated for this species by Suzuki et al. (2001a, figs 15–18). The outer face of the SV has axial lines of long slits that virtually cover the valve surface whereas the inner face has several isolated axial rows of pores [we have not yet identified such a view for this species but see *C. convexa* (Sar et al. 2003, fig. 5; Navarro & Lobban 2009, fig. 75)]. Suzuki et al. (2001a, b) used and recommend a bleach process (Nagumo & Kobayasi 1990) as particularly effective for clarifying the taxonomy of *Cocconeis*, given the heterovalvy and the differences in internal and external views of the SV.

Cocconeis scutellum Ehrenberg Plate 41, Figs 6, 7
Ref. illus.: Mizuno 1987, figs 6A–F; Kawamura & Hirano 1989, pl. 4, figs E-H; Witkowski et al. 2000, pl. 38, fig. 10 and pl. 42, figs 17–19; De Stefano et al. 2008, figs 19–35; Riaux-Gobin et al. 2011b, pl. 5, figs 12–17, pl. 66, figs 1–8
Samples: GU56A-1; **GU44AC-4**
Dimensions: Length 17–23 μm, width 10–14 μm; striae (SV) 12–17 in 10 μm
Diagnostics: Striae of large areolae, uniseriate on the valve face becoming bi- or triseriate on the mantle.
Comments: Numerous varieties have been described and considered by Mizuno (1982, 1987), Romero (1996) and De Stefano et al. (2008).

Cocconeis scutellum var. *ornata* Grunow Plate 42, Figs 1–3
Ref. illus.: Riaux-Gobin et al. 2011b, pl. 68, figs 1–8
Samples: GU52P-9
Dimensions: Length 17–23 μm, width 10–14 μm; striae (SV) 12–17 in 10 μm
Diagnostics: Differing from the nominate variety in the quadrate areolae.

Climaconeis coxii Reid & Williams Plate 42, Figs 4, 5
Ref. illus.: Reid & Williams 2002, figs 19–30
Samples: **GU6D-2; GU44L-A, GU44AN-6;** Arai 2010 (as *Climaconeis* sp. 2)
Dimensions: Length 140–160 μm, width 11 μm; striae 15–17 in 10 μm
Diagnostics: A straight species with craticular bars; straight proximal raphe endings. Striae weakly radiating near the center becoming weakly convergent at the apices; in some specimens appearing virtually parallel throughout.
Comments: Straight proximal raphe endings distinguish it from *C. lorenzii* Grunow (Lobban et al. 2010, figs 33, 34), which has deflected endings. The stria density is appropriate for *C. coxii*. Our specimens are longer than the size range given for *C. coxii* and approach the range of *C. lorenzii* (indeed, one is virtually the same length as the Yap specimens of *C. lorenzii* shown by Lobban et al. 2010, figs 33, 34). However, the size range of *C. coxii* is known only from the Abu Dhabi population. The number of plastids is supposedly fewer in *C. coxii*, but that is probably just a function of length; exceedingly long *C. lorenzii* had a correspondingly higher number of plastids (Prasad et al. 2000). The putative Guam record of *C. lorenzii* mentioned in Lobban et al. 2010 cannot be included in the flora at this time, given this finding of *C. coxii* and Arai's (2010, pl. 35, fig. 7) figure of a valve that is also clearly *C. coxii*.

Parlibellus hamulifer (Grunow) De Toni Plate 42, Fig. 6
Ref. illus.: Navarro 1987, figs 1–22; Navarro et al. 1989, fig. 77
Samples: GU26A, **GU44I-2, GU44Z-15**
Dimensions: Length 37–80 µm, width 8–20 µm; striae 22–23 in 10 µm
Diagnostics: Broadly lanceolate valves with apices slightly deflected in the same direction. Distal raphe endings are far from the apex and strongly deflected (Pl. 42, Fig. 6, arrow). Numerous girdle bands. Plate-like plastids on the girdle faces, strongly lobed along the valvar edges.
Comments: A tube dwelling species but commonly encountered outside of tubes. The relatively large size and slightly deflected apices of this species distinguish it from most other species of *Parlibellus*, as do the plastids, but the size range is considerable and smaller individuals are less distinct.

Diploneis bombus Ehrenberg Plate 43, Figs. 1–4
Ref. illus.: Hustedt 1931–1959, fig. 1086, esp. 1086c; Witkowski et al. 2000, pl. 86, fig.s 1, 2, pl. 92, figs 1–3.
Samples: GU7N
Dimensions: Length 22 µm, width 10–11 µm at widest, 6–7 µm at constriction; striae 14–16 in 10 µm
Diagnostics: The small specimens in our samples distinguished from the more common *D. weissflogii* (A. Schmidt) Cleve (q.v) by the wide raphe sternum and the more distinct longitudinal canal; markedly different valve structure in SEM (Pl. 43, Figs 3, 4 vs. Pl. 47, Figs 6, 7). External stria openings slits, internal three rows of large pores; longitudinal canal opening to single biarcuate rows of pores externally, internally without openings.
Comments: "The structure of *Diploneis* valves is complex," (Droop 1996a: 411), and the internal and external views in SEM are frequently different and difficult to match. The wall is hollow with different patterns of openings on the external and internal surfaces. Moreover, the valve surface is curved, so that in any given focal plane in LM one is looking partly at the exterior, partly at the interior (see Droop 1996a, fig. 1). In this case we are confident LM and SEM views are of the same species because this was the only *Diploneis* in GU7N. One half of the cell sometimes a little larger than the other, as for *D. weissflogii*, though Hustedt (1931–1959) does not mention the asymmetry for either species.

Diploneis chersonensis (Grunow) Cleve Plate 44, Figs 1–4
Ref. illus.: Peragallo & Peragallo 1897–1908, pl. 19, fig. 9; Hustedt 1931–1959, fig. 1088; Hendey 1964, pl. 32, figs 7, 8; Navarro 1982c, fig. 49; Witkowski et al. 2000, pl. 86, fig. 10
Samples: **GU44I-2, GU44R-2, GU44Z-15**
Dimensions: Length 60–90 µm, width 20-27 µm; striae 12–13 in 10 µm
Diagnostics: True longitudinal ribs paralleling the outer margin of the straight longitudinal canals rather than the valve margin and the relative closeness of the transapical ribs suggest that this is *D. chersonensis* rather than *D. bomboides* (A. Schmidt) Cleve [in Hustedt 1931–1959, fig. 1089 as *D. splendida* (Gregory)

Cleve; see Droop 1996 a, b for revision and comments and Droop 1996a for terminology].
Comments: On the basis of species present in GU44Z-15 and GU44R-2, we believe that the SEMs in Pl. 44, Figs 2–4 represent the same species. The central area appears square in LM, with four chambers bordering each side. In SEM these chambers are hidden by the coverings of the longitudinal canals; the distal two are shorter than the central two and externally have distinctive curled slits (in Pl. 44, Fig. 3). External stria openings slits, internal openings straie of transapically elongate slits with a hymen; internal and external openings aligned. Longitudinal canal cover with single line of small pores externally and internally.

Diploneis crabro Ehrenberg Plate 44, Fig. 5; Plate 45, Figs 1, 2
Ref. illus.: Hustedt 1931–1959, figs 1028, 1032, 1034; Ricard 1987, figs 744–751; Navarro 1982c, figs 50–52; Witkowski et al. 2000 pl. 93, figs 18–21; Hein et al. 2008, pl. 28, fig. 1
Samples: GU7F; **GU44I-1**; GU54B
Dimensions: Length 104–107 µm, width 36 µm; striae 4 in 10 µm
Diagnostics: Large constricted valves with double rows of areolae in the outer parts of the striae. External openings of longitudinal canals also multiporate (Pl. 45, Figs 1, 2).
Comments: The biseriate outer striae distinguish *D. crabro* from other large, constricted *Diploneis*, e.g., *D. bomboides* (A. Schmidt) Cleve and *D. rex* S.J.M. Droop (see Droop 1996a, b).

Diploneis smithii (de Brébisson) Cleve Plate 45, Figs 3–6; Plate 46, Fig. 1
Ref. illus.: Hustedt 1931–1959, fig. 1051; Hendey 1964, pl. 32, fig. 10; Droop 1994a, figs 1–38; Witkowski et al. 2000, pl. 90, figs 7, 15, pl. 91, figs 1, 2; Hein et al. 2008, pl. 27, fig. 2
Samples: **GU44I-1, GU44AK-1; GU52N-7**
Dimensions: Length 33–43 µm, width 21–22 µm; striae 8–10 in 10 µm
Diagnostics: Moderately large oval cells with differing pattern over the longitudinal canals.
Comments: Classically in *D. smithii* the striae are undivided internally and consist of double rows of alternating pores; in contrast, in *D. fusca* there are longitudinal ribs dividing the striae. In SEM the external surfaces is seen to be covered by a thin membrane that is finely perforated (Pl. 45, Fig. 4), and the LM structure is more easily seen if this membrane is absent (Pl. 45, Fig. 6, Pl. 46, Fig. 1). Supposedly distinguished from *D. nitescens* (Gregory) Cleve (Hustedt 1931–1959, fig. 1047 and keys pp. 582–593; Witkowski et al. 2000, p. 189 and 193, pl. 90, figs 1–3, pl. 94, fig. 1) by narrower longitudinal canals (up to one-third rather than half or more of the valve width)—but the various figures in Witkowski et al. (2000, pl. 90) do not seem to fit this criterion. Droop (1994a, b) exposed a complex of 11 morphotypes in a complex encompassing *D. smithii* and *D. fusca* (Gregory) Cleve and showed (a) that the classic difference does not hold, (b) that such populations are not restricted to a single location. Several varieties are shown by Witkowski

et al. (2000). The cells shown here appear to meet the classical criterion, but we have seen other cells that differ subtly, suggesting that similar complexity can be expected in our flora.

Diploneis suborbicularis (Gregory) Cleve Plate 46, Figs 2–4
Ref. illus.: Schmidt et al. 1874–1959, pl. 8, figs 2, 3, 5, 6; Hustedt 1931–1959, fig. 1026; Gerloff & Natour 1982, pl. 12, fig. 4; Witkowski et al. 2000, pl. 93, figs 9, 10; Hein et al. 2008, pl. 26, fig. 5 and pl. 27, fig. 5.
Samples: **GU52N-7,** GU52Q-10
Dimensions: Length 32–36 µm, width 22–24 µm; striae 8 in 10 µm
Diagnostics: The striking feature of these cells is the almond-shape of each half of the raphe sternum and the oval valve outline. Central area is quadrangular.
Comments: *D. suborbicularis* is similar to *D. coffaeiformis*, but the central area of the latter is markedly elongate, according to Hustedt (1931–1959), and on this character we have made the determination. Drawings and photographs in the literature show considerable variation in both *D. suborbicularis* and *D. coffaeiformis*; the stria densities are higher in the latter, but there is overlap and our specimens are in the overlapping range. The drawing to which our specimens are closest is Hustedt's fig. 1026b and the photographs in Hein et al. (2008). Some of the figures of *D. coffaeiformis* in Witkowski et al. (2000) are nearer than their *D. suborbicularis*. Both of these *Diploneis* species are superficially similar to several *Fallacia* species (although generally larger), e.g., *F. forcipata* (Greville) Stickle & D.G. Mann (Witkowski et al. 2000, pl. 72, figs 2–9), and all were formerly in *Navicula*. However, *Fallacia* spp. have very narrow raphe sterna with the striae interrupted by lyre-shaped hyaline areas, thus the "almond" shape around the raphe has striae in it, whereas these *Diploneis* spp. do not.

Diploneis weissflogii (A. Schmidt) Cleve Plate 46, Figs 5–7
Ref. illus.: Hustedt 1931–1959, fig. 1085; Ricard 1987, figs 737–742 (as *D. bombus*); Witkowski et al. 2000, pl. 92, figs 4-5, pl. 94, figs 12-13
Samples: **GU44R-2, GU44Y-13, GU44Z-15**
Dimensions: Length 32–33 µm, width 15–17 µm; striae 10 in 10 µm
Diagnostics: Longitudinal canal narrow and poorly separated from the striated part of the valve because of the similar openings on both sides of the valve; "asterisk" pattern of six pores around the central area often distinct.
Comments: Similar to *D. bombus* (q.v.). One half of the cell sometimes a little larger than the other. Internal and external patterns correspond.

Chamaepinnularia clamans (Hustedt) Witkowski, Lange-Bertalot & Metzeltin Plate 46, Figs 8, 9
Ref. illus.: Hustedt 1961–1966, fig. 1313; Navarro 1982 ,pl. 27, fig. 7; Simonsen 1987 pl. 379, figs. 20-22 (all as *Navicula clamans*); Witkowski et al. 2000, pl. 69, fig. 12
Samples: GU4A; GU44AF-5; GU52N-7
Dimensions: Length 17–20 µm, width 8 µm; striae 20–22 in 10 µm

Diagnostics: Apices truncated; striae interrupted by longitudinal line near the margin, axial and central areas forming broad lanceolate area.

Cymatoneis sulcata (Greville) Cleve Plate 47, Fig. 1
Ref. illus.: Schmidt et al. 1874–1959, pl. 212, figs 41–47 (as *Navicula sulcata* Greville); Peragallo & Peragallo 1897–1908, pl. 13, fig. 29; Ricard 1977, pl. 4, fig. 12; Ricard 1987, fig. 785; Navarro & Lobban 2009, figs 84–89 (from Yap)
Samples: GU55B-4
Dimensions: Length 33 µm, width ca. 17 µm; striae 12 in 10 µm
Diagnostics: The undulate outline, quadrangular pattern of areolae, and the raphe raised on a keel along with several other parallel ridges on the folded valve face are distinctive.
Comments: So far observed only rarely and in SEM. Witkowski et al. (2000, pl. 109, fig. 17) show an SEM image of *C. margarita* Witkowski, with similar ridges along the raphe. Although Round et al. (1990: 578–579) do not identify any species in their generic treatment, it is apparent that they illustrated *C. sulcata* for *Cymatoneis*.

Haslea howeana (Hagelstein) Giffen Plate 47, Figs 6, 7
Ref. illus.: Hagelstein 1939, pl. 7, fig. 1; Podzorski & Håkansson 1987, pl. 30, fig. 6 (both as *Navicula howeana*); Giffen 1980, fig. 20; Witkowski et al. 2000, pl. 148, figs 12, 13; Hein et al. 2008, pl. 31, fig. 6
Samples: GU13AC; GU26A; **GU44J-2, GU44Z-15, GU44AB-8; GU52P-4,** GU52Q-10
Dimensions: Length 30–62 µm, width 7–10 µm; striae 17–18 in 10 µm
Diagnostics: Linear-lanceolate valve with equally spaced apical and transapical striae, transapical striae weakly radiating, those more distal parallel; central and axial areas absent.
Comments: *H. nautica* (Cholnoky) Giffen (Giffen 1980, fig. 21, Witkowski et al. 2000, pl. 148, figs 9–11) is very similar but smaller (45–60 x 9–12 µm vs "(50)75–85" µm x "(8)11–12 µm" (Witkowski et al. 2000: 224–224), regularly lanceolate valves with rounded, not tapered ends (Giffen 1980: 146). The stria density is slightly higher here than reported elsewhere (18 vs. 15) and the size range includes some below the range of *H. nautica*. The differences in shape are subtle. As further material of both species is studied, the distinction between them may disappear.

Navicula cancellata Donkin Plate 47, Figs 2–5
Ref. illus.: Van Heurck 1896, pl. 3, fig. 128; Hendey 1964, p. 203, pl. 30, figs. 18–20; Witkowski et al. 2000, pl. 144, figs 1–7
Samples: GU6E-9
Dimensions: Length 38–46 µm, width 10 µm; striae 7–8 in 10 µm
Diagnostics: The angled raphe and depressed valve surface.
Comments: The raphe is strikingly asymmetrical along the sternum.

Navicula consors A. Schmidt Plate 47, Fig. 8
Ref. illus.: Ricard 1977, pl. 4, fig 10 and pl. 10, fig 15; Foged 1987, pl. 19, figs 1–3; Podzorski & Håkansson 1987, pl. 34, fig. 4 (as *Navicula pugio* Mann); Navarro et al. 2000, pl. 19, figs 7–9
Samples: **GU44I-1, GU44R-2, GU44Y-13**
Dimensions: Length 60–78 µm, width 17–20 µm; striae 7 in 10 µm
Diagnostics: Radiating striae of linear areolae separated into macroareolae by irregular longitudinal ribs (essentially vimines), except those nearest the apices.

Navicula mannii Hagelstein Plate 47, Fig. 9
Ref. illus.: Hagelstein 1939, pl. 7, figs 7, 8; Navarro 1983a, figs 102, 103; Navarro et al. 1989, fig. 74
Samples: GU44Y-13
Dimensions: Length 34 µm, width 10 µm; striae 8 in 10 µm
Diagnostics: Unusually shaped for a *Navicula*, with coarse striae, linear areolae clearly visible.

Navicula plicatula Grunow Plate 48, Figs 1–3
Ref. illus.: Peragallo & Peragallo 1897–1908, pl. 8, fig. 17; Mann 1925, pl. 24, figs 8, 9
Samples: GU6E-9; GU44U-1A, GU44AS-4; GU55B-4
Dimensions: Length 49–64 µm, width 15–18 µm; striae 15–24 in 10 µm
Diagnostics: The sinuous, raised external raphe is unique.

Trachyneis aspera (Ehrenberg) Cleve Plate 48, Figs 4–9
Ref. illus.: Schmidt et al. 1874–1959, pl. 48, figs 2–6 (as *Navicula aspera* Ehr.); Navarro 1982c, fig. 114; Cardinal et al. 1984, figs 99–100; Ricard 1987, figs 834–839; Witkowski et al. 2000, pl. 159, figs 1–6, 9; Hein et al. 2008, pl. 55, fig. 3.
Samples: GU15C; **GU44I-1, GU44I-2, GU44U, GU44Z-15**
Dimensions: Length 42–100 µm, width 12–21 µm; striae 17 in 10 µm
Diagnostics: Readily recognized by the broad "bow tie" fascia and the interrupted striae (caused by partitions within the wall structure along the striae—compare internal and external SEM views, Pl. 47, Fig. 10, Pl. 48, Fig. 1).
Comments: Similar to *T. velata* Schmidt (see below), which has only a small central area. The platelike plastids along each girdle face have markedly lobed margins (Pl. 47, Figs 7, 8). Internal SEM view (Pl. 48, Fig. 1) matches images in Navarro (1982c) and Round et al. (1990: 568–569, apparently *T. aspera*), but not those in Cardinal et al. (1984).

Trachyneis velata A. Schmidt Plate 49, Figs 1, 2
Ref. illus.: Schmidt et al. 1874–1959, pl. 48, figs 33–34; Witkowski et al. 2000, pl. 159, figs. 7, 8; Stidolph et al. 2012, pl. 35, figs 32, 33
Samples: **GU44R-2, GU52Q-1a**
Dimensions: Length 50–100 µm, width 15–35 µm; striae 16 in 10 µm

Diagnostics: Similar to the common *Trachyneis* aspera but with a small, rounded central area.
Comments: Differs from *T. velatoides* Ricard (Ricard 1975, pl. 1, fig. 12; Ricard 1977, pl. 4, figs 8, 9) in having almost parallel striae around the central area, rather than distinctly radiating, and having a decussate arrangement of areaolae (Ricard 1975: 218).

Caloneis egena (A. Schmidt) Cleve Plate 49, Figs 3, 4
Ref. illus.: Podzorski & Håkansson 1987, pl. 18, fig. 7, pl. 52, figs 2–4; Witkowski et al. 2000, pl. 160, figs. 13-14
Samples: **GU6D-4; GU44I-2, GU44AF-5**
Dimensions: Length 19 μm; width 4 μm; striae ca. 26–34 in 10 μm (on apical portions of valve)
Diagnostics: Valves doubly constricted, all three portions equal in width. Striae absent from central portion.
Comments: The smaller size of the cell, the relative width of the central portion, and the absence of striae in the central portion, distinguish this from *C. lewisii* Patrick (cf. Witkowski et al. 2000, pl. 153, fig. 7). Witkowski et al. (2000: 164) give a stria density of only 11 in 10 μm for *C. egena*, but this seems unlikely as they cannot be resolved in their LMs.

Caloneis liber (W. Smith) Cleve Plate 49, Figs 5, 6; Plate 50, Figs 1–3
Ref. illus.: Schmidt et al. 1874–1959, pl. 50, figs 38, 40; Peragallo & Peragallo 1897–1908, pl. 9, figs 5, 6 (as *Navicula liber*); Witkowski et al. 2000, pl. 152, fig. 9; Hein et al. 2008, pl. 25, figs 2, 3.
Samples: **GU6E-4; GU44I-1, GU44I-2; GU55B-4**
Dimensions: Length 65–166 μm, width 14–20 μm; striae 22–27 in 10 μm
Diagnostics: Valves linear to linear-elliptical with rounded apices, striae parallel throughout, crossed by a longitudinal line (the internal pores) about half way between the raphe valve margin. Central area ± symmetrical, proximal raphe endings scarcely deflected.
Comments: As noted by Peragallo & Peragallo (1897–1908: 71), among others, this is a very variable species, with numerous named varieties. Our specimens have finer striae (vs. 13–20 in Peragallo & Peragallo, 18 in Witkowski et al.) and are rather broader than most illustrated. Some (Pl. 49, Fig. 6) approach *C. excentrica* (Grunow) Boyer (Hein & Winsborough 2001, figs 31–33) in shape but without the strongly deflected proximal raphe endings and asymmtrical central area. Hein & Winsborough (2001) compared *C. excentrica* with *Oestrupia* and noted that if each stria is composed of two alveoli (suggested in their specimens by a hyaline line along the valve margin—not present in our specimens, Pl. 50, Fig. 2), then *C. excentrica* should be transferred to *Oestrupia*. *Caloneis* has undivided alveoli (Pl. 50, Fig. 2 vs. Fig. 4) and a single row of pores on each side of the raphe (Pl. 50, Fig. 3).

"Oestrupia 4" sensu Hein et al. 2008 Plate 50, Fig. 4
Ref. illus.: Hein et al. 2008, p. 101, pl. 67, fig. 15.

Samples: **GU52P-5**
Dimensions: Length 44 μm, width 19 μm; striae 36 in 10 μm
Diagnostics: Shape similar to *Oestrupia grandis* Hein & Winsborough, but smaller and differing from that and *"Oestrupia 3" sensu* Hein et al. (2008, pl. 72, figs 1–3) by the simple deflected proximal raphe endings (rather than hooked). The presence of divided areolae is shown by the break in the striae near the margin (Pl. 50, Fig. 4, arrow).

Donkinia minuta (Donkin) Ralfs Plate 50 Figs 5, 6; Plate 51, Fig. 1
Ref. illus.: Cox 1983, figs 2–4
Samples: **GU44H-15;** GU42—ECT3739
Dimensions: Length 46–58 μm, width 10 μm; striae not resolved (>35 in 10 μm)
Diagnostics: The unequal keeling and the cell size identify this species (Cox 1983).

Pleurosigma intermedium Wm. Smith Plate 51, Figs 2–4
Ref. illus.: Van Heurck 1896, pl. 6, fig. 267; Peragallo & Peragallo 1897–1908, pl. 32, fig. 21; Cardinal et al. 1986, fig. 58–60
Samples: GU26A; **GU44Z-15, GU44AR-1; GU52J-3, GU52P-9**
Dimensions: Length 110–133 μm, width 13–14 μm; striae 26 in 10 μm
Diagnostics: Cell and raphe both straight. Oblique striae crossing at ~60°.
Comments: Although the character states in our specimens (central bars =1; hyaline area = 1; striae = 2) appear not to match *P. intermedium* as defined by Cardinal et al. (1989), for which they give a stria state of 3 (their table 1) (biseriate striae), their text states that they saw state 3 only in *P. clevei*. In all other respects our specimens correspond to illustrations for this species; possibly there is a typographic error in their table. Hustedt (1955: pl. 10, fig. 12) illustrated *P. intermedium* var. *mauritiana* Grunow, which is narrower (14 μm) than the nominate variety (20–22 / 17–18 μm—Peragallo & Peragallo 1897–1908 / Hendey 1964) and 136 μm long. This more closely fits our specimens but in Hustedt's opinion this taxon is a form rather than a variety; in our opinion such a slight difference calls for a search for intermediate sizes.

Plagiotropis lepidoptera (Gregory) Kuntze Plate 51, Figs 5–8
Ref. illus.: Ricard 1987, figs 843–851; Paddock 1988, pl. 13, figs 1–11; Witkowski et al. 2000, pl. 174, figs 1, 2; Hein et al. 2008, pl. 54, figs 1, 2
Samples: **GU44R-2; GU52J-3, GU52Q-1,** GU52Q-10
Dimensions: Length 67–141 μm, width 18 μm; striae 20–23 in 10 μm
Diagnostics: Raphe ridge extends well above valve face; low lying longitudinal fold on the valve face. Distinctive and prominent helictoglossa in this genus (Pl. 50, Figs 7, 8).
Comments: The species is larger, has a higher raphe ridge, and less prominent folds on the valve face than a second, so far unidentified species of *Plagiotropis* common in our samples.

Staurotropis seychellensis (Giffen) Paddock Plate 52, Figs 1–3
Ref. illus.: Giffen 1980, figs 42–44 (as *Tropidoneis seychellensis*); Paddock 1988, pl. 34, figs 1–12
Samples: ECT 3721 (from GU44)
Dimensions: Length 61 μm; striae 32 in 10 μm
Diagnostics: Raphe raised on arched raphe ridges, as in *Plagiotropis* and *Donkinia* but distinguished by the presence of a true (thickened) stauros (Pl. 52, Fig. 2) and striate girdle bands (Pl. 52, Fig. 3), and the absence of the prominent helictoglossae characteristic of *Plagiotropis* (q.v.).

Stauroneis retrostauron (Mann) Meister Pl. 52, Figs 4, 5
Ref. illus.: Mann 1925 pl. 25, fig. 5 and pl. 26, figs 1, 2 (as *Navicula retrostauros*); Meister 1937, p. 272, pl. 12 figs 2, 3
Samples: **GU44J-2,** GU44S-3, GU44X-7, **GU44Z-15**
Dimensions: Length 48–51 μm, width 13 μm; striae 31–32 in 10 μm
Diagnostics: Frustules square in girdle view from numerous copulae; valves elliptical, finely but distinctly striate; narrow, strongly defined stauros reaching the valve margin and not interrupting the striae.
Comments: Smaller and more rounded than *S. polynesiae* (Brun) Hustedt (Hustedt 1931–1959, fig. 1179); similar to *S. biblos* Cleve (Hustedt 1931–1959, fig. 1178) but apparently somewhat coarser. It differs in several ways from *Stauropsis membranacea* (Cleve) Meunier [= *Stauroneis membranacea* (Cleve) Hustedt] (Hustedt 1931–1959, fig. 1176; Hendey 1964, pl. 21, fig. 3; Navarro 1982c, figs 106, 107?; Paddock 1986, figs 1–14): the plastids of *S. retrostauron* are lenticular rather than contorted ribbons, the cells do not occur in chains in our observations of live cells, there is no large pore at the apices, and the valve is evidently much more robust.

Proschkinia complanatoides (Hustedt) Karayeva
Plate 1, Figs 4–6; Plate 52, Fig. 6; Plate 53, Figs 1–4
Ref. illus.: Hustedt 1961–1966, fig. 1451; Brogan & Rosowski 1988, figs 1–8, 12; Kawamura & Hirano 1989, pl. 9, figs A–D (all as *Navicula complanatoides*)
Samples: **GU44Z-15;** GU62A-7
Dimensions: Length 32–48 μm, width 6–8 μm; striae 30–32 in 10 μm
Diagnostics: The presence of a stigma distinguishes this genus from other naviculoids; long stigma with several pores. Numerous girdle bands.
Comments: The stigma distinguishes this species from *P. complanata* Grunow and *P. complanatula* Hustedt, which both clearly have single pores. Central striae barely further apart but the ribs are thicker. Brogan & Rosowski (1988) characterized their specimens as "putative *Navicula complanatoides*" and apparently did not examine Hustedt's type material, but the Guam materials clearly are the same as theirs, as seen in live features of the plastid (Pl. 1, Figs 4–6) as well as structure of the valve. The stigma, which they describe as a pore, shows several openings in both their figure 12 and our Pl. 53, Fig 2, but no internal openings are visible in Round et al. (1990, p. 597, fig. h), perhaps the same species. Illustrations in Hustedt (1961–1966) do not clearly show the stigma, but in our experience it was

readily apparent in acid-cleaned valves (Pl. 51, Fig. 6, Pl. 52, Fig. 1) and even in live specimens (Pl. 1, Fig. 4, arrow). *P. complanata* and *P. complanatula* are very similar to *P. complanatoides* (Hustedt 1961–1966, figs 1449, 1450; Cox 1988, figs 57–61; Witkowski et al. 2000, pl. 60, figs 29–32 and pl. 147, figs 8–11) except for the single pores in their stigmata. The plastid of *P. complanata* is much simpler than that of *P. complanatoides* (cf. Cox 1988, figs 12–14).

Amphora arcuata A. Schmidt Plate 53, Fig. 5
Ref. illus.: Schmidt et al. 1874–1959, pl. 26, figs 27–29; Peragallo & Peragallo 1897–1908, pl. 49, figs 27, 28; Ricard 1977, pl. 6, fig. 22; Montgomery 1978, pl. 8, figs A-F; Wachnicka & Gaiser 2007, fig. 81; Hein et al. 2008, pl. 18, fig. 9 [all as *A. acuta* var. *arcuata* (A. Schmidt) Cleve]; Levkov 2009, pl. 80, figs. 9, 10.
Samples: **GU6E-4**
Dimensions: Length 41 µm, width 13 µm; (dorsal) striae 16 in 10 µm.
Diagnostics: Broad valve with acute, slightly recurved apices; evident areolae; a fascia; ventral striae not resolved in LM.
Comments: Differs from *A. aspera* Petit (Peragallo & Peragallo 1897–1908, pl. 50, fig. 1) in having a fascia and from *A. acuta* var. *parva* Wachnicka & Gaiser in lacking ventral striae and having recurved apices. Our specimen is small compared with dimensions in the literature. Hein et al. 2008, pl. 67, fig. 12 show a rather similar cell as "*Amphora* 8," which has ventral striae much finer striae than its dorsal striae.

Amphora arenaria Donkin Plate 53, Figs 5, 6; Plate 54, Figs 1, 2
Ref. illus.: Peragallo & Peragallo 1897–1908, pl. 48, figs 15, 17, 18; Li 1978 pl. 12, fig. 3; Schoeman & Archibald 1986, figs 1–20; Witkowski et al. 2000, pl. 168, fig. 14; Wachnicka & Gaiser 2007, fig. 188; Levkov 2009, pl. 115, figs 1–3 and pl. 116, figs 1–6
Samples: **GU44I-2, GU44R-2, GU44AP-2**
Dimensions: Length 86–92 µm, width 14–20 µm; striae 28 in 10 µm (dorsal) / 33 in 10 µm (ventral).
Diagnostics: Broad ventral area, smaller dorsal area, raphe branches arcing strongly from proximal endings set back from ventral margin over to dorsal margin.
Comments: Distinguished with difficulty from *A. obtusa* Gregory (q.v.) by the slightly denser striae, which are less obviously punctate in LM. While *A. arenaria* is very close to *A. obtusa* the two species belong different subgenera (*A. arenaria* to *Psammamphora, A. obtusa* to *Ambylamphora*). According to Peragallo & Peragallo (1897–1908: 214) the difference between these groups rests on the girdle bands [narrow in *A. arenaria* (but see Hein et al. 2008, pl. 19, figs 1, 2], complex in *A. obtusa*), such that, "il est souvent impossible de décider si une valve détachée appartient à l'*A. obtusa* ou à l'*A. arenaria*." Navarro (1982c) showed a specimen labeled *A. obtusa* for which the stria count was 17–18 striae in 10 µm, but morphological measurements in Wachnicka & Gaiser (2007: table 1 and p. 435) for *A. arenaria* and several varieties of *A. obtusa* show broadly overlapping ranges of 21–28 striae in 10 µm for both dorsal and ventral, except for *A. obtusa* var.

oceanica (Castracane) Cleve with 18–22 striae in 10 µm. An additional character cited as distinguishing is a slightly sinuous straight ventral margin (Wachnicka & Gaiser 2007: 435), and on the basis of this, the stria counts, and the girdle bands (Pl. 53, Fig. 1) we have assigned our specimens to *A. arenaria*. But even that difference is unclear in images of type materials published by Schoeman & Archibald (1986, 1987). Levkov (2009) keys the difference as "Striae hard to resolve, finely punctate…*A. arenaria* / Striae coarse and distinctly punctate… *A. obtusa*."

Amphora decussata Grunow Plate 1, Figs 7–9; Plate 54, Fig. 5; Plate 55, Figs 1–3
Ref. illus.: Peragallo & Peragallo 1897–1908, pl. 49, fig. 24; Gerloff & Natour 1982, pl. 11, fig. 5; Stidolph et al. 2012, pl. 24, fig. 69
Samples: **GU44Z-15, GU44AK-6,** GU65A-3, GU65A-1A, GU43C
Dimensions: Length 55–83 µm, width 15–17 µm; dorsal striae 21 in 10 µm, ventral striae 16 in 10 µm
Diagnostics: Dorsal striae distinctively oblique relative to both raphe and fascia, internally and in LM appearing as rectangular areolae (Pl. 54, Fig. 5; Pl. 55, Fig. 1), externally in SEM as parallel slits (Pl. 55, Fig. 2). Two rows of quadrangular areolae in the ventral striae. Distinctive short conopea over the proximal raphe endings on both sides (Pl. 1, Fig. 8; Pl. 55, Figs 1, 2). A single stria of quadrangular areolae, externally a slit, runs along the dorsal margin. Externally, the copulae have a similar pattern of slits (Pl. 55, Fig. 2); not determined how many copulae there are.
Comments: This species is very distinctive and widespread, yet not well illustrated in recent floras.

Amphora immarginata Nagumo Plate 56, Figs 1–4
Ref. illus.: Nagumo 2003, pl. 38–42; Witkowski et al. 2000, pl. 162, fig. 20; Wachnicka & Gaiser 2007, figs 161, 162
Samples: **GU44I-1, GU44Z-15,** GU54B-4
Dimensions: Length 29–45 µm, width 7–11 µm; striae radiating, dorsal striae 21 in 10 µm, ventral striae 17 in 10 µm
Diagnostics: Ventral margin straight, dorsal margin convex, apices broadly rounded. Raphe biarcuate. Dorsal striae distinctly areolate, the pattern resulting from the internal valve face, externally seen as continuous slits (Pl. 56, Figs 3, 4). A raphe ledge extends over the ends of the striae, obscuring them in SEM (Pl. 56, Fig. 3) but they show through as "ghost striae" in LM (Pl. 56, Fig. 2). Ventral striae coarser, single areolae except near apices radial at the center becoming strongly convergent toward the apices.

Amphora obtusa Gregory Plate 54, Figs 3, 4
Ref. illus.: Peragallo & Peragallo 1897–1908, pl. 48, figs 9, 10; Navarro 1982c, figs 25–30; Schoeman & Archibald 1987, figs 1–12; Wachnicka & Gaiser 2007, fig. 186; Levkov 2009, pl. 115, figs 5, 6 and pl. 250, figs 1, 2, 4
Samples: **GU44Z-15, GU44AK-6**
Dimensions: Length 87 µm, width 15 µm; striae 25 in 10 µm (dorsal and apical) / 22 in 10 µm (ventral central).

Diagnostics: Broad ventral area, smaller dorsal area, raphe branches arcing strongly from proximal endings set back from ventral margin over to dorsal margin.
Comments: Distinguished with difficulty from *A. arenaria* (q.v.) by the slightly less dense striae, which are obviously punctate. Navarro (1982c) shows specimens with wider striae spacing at the center suggestive of a fascia, as well as the transition from radiate to convergent striae seen in our specimen (Pl. 54, Fig. 4) (also present in *A. arenaria*). See also comments under *A. arenaria*.

Amphora ostrearia Brébisson var. *vitrea* (Cleve) Cleve Plate 56, Figs 5, 6
Ref. illus.: Peragallo & Peragallo (1897-1908) pl. 49, figs 14–15; Levkov 2009, pl. 80, fig. 7
Samples: **GU44I-1, GU44K-6, GU44Z-15**
Dimensions: Length 50–60 µm; width 10–18 µm, dorsal and ventral striae 13–14 in 10 µm
Diagnostics: Very wide cells with prominent stauros, ventral margin convex, raphe angled away from ventral margin, reaching the edge of the valve on the dorsal side of the apex.
Comments: We have based our identification on Cleve (1895: 129), Peragallo & Peragallo (1897–1908) and Levkov (2009), which indicate dorsal and ventral striae have the same density (9–11 in in 10 µm). Our specimens have slightly denser striae. Specimens in Wachnicka & Gaiser (2007: 411, figs 82, 83) and Hein et al. (2008: 45, pl. 21, figs 2, 7 and pl. 22, fig. 1) show valves that appear to be substantially narrower than ours and in particular that have only a very narrow band of ventral striae, twice as dense as the dorsal striae.

Amphora vaughanii Giffen Pl. 56, Figs 7–9
Ref. illus.: Giffen 1980, figs 9,10
Samples: **GU44Z-15, GU52J-3,** GU43C
Dimensions: Length 66 µm, width 17 µm; striae 20 in 10 µm
Diagnostics: Ventral margin straight, dorsal margin semi-orbicular, as in *A. hyalina* Kützing (Witkowski et al. 2000, pl. 163, fig. 22), but differing from that species and *A. pseudohyalina* Simonsen (Witkowski et al. 2000, pl. 163, figs 20, 21) in that the dorsal striae stop short of the dorsal margin, and the latter also has 28–30 striae in 10 µm.
Comments: As seen in SEM (Pl. 56, Figs 9, 10), the raphe is very close to the ventral margin, very slightly biarcuate, and there is only a small nodule in the central area (Pl. 56, Fig. 10) [in contrast to the specimens in Navarro & Lobban (2009, figs 97, 98) identified as *A. hyalina*]. There are no ventral striae (note that there is an intercalary band lying on top of the valve near the raphe in Pl. 56, Figs 9, 10, arrowheads). The striae consist of two rows or fine pores between the interstriae, and the hyaline border in fact has exceedingly fine striae, ca. 52 in 10 µm (Pl. 56, Fig. 9).

Undatella lineata (Greville) Paddock & Sims Plate 57, Figs 1, 2
Ref. illus.: Paddock & Sims 1980, figs 15–34

Samples: **GU44I-1**
Dimensions: Length 167 μm
Diagnostics: Distinctive very narrow biundulate valve with fibulae distributed along the entire raphe, in contrast to *U. quadrata* (q..v.).

Undatella quadrata (Brébisson ex Kützing) Paddock & Sims Plate 57, Figs 3–6
Ref. illus.: Paddock & Sims 1980, figs 35–46
Samples: ECT 3729; **GU44I-1**
Dimensions: Length 73 μm, width 10 μm
Diagnostics: Fibulae limited to the distal half of the raphe (Pl. 57, Figs 5, 6).

Thalassiophysa hyalina Paddock & Sims Plate 2, Figs 1–8; Plate 58, Fig. 1
Ref. illus.: Paddock & Sims 1980, figs 51–62 (as *Proboscidea insecta*; see Paddock & Sims 1981); Round et al. 1990, pp. 606–607; Hein et al. 2008, pl. 60, fig. 6 and pl. 61, fig. 1
Samples: GU7R, GU7S; **GU44I-2**
Dimensions: Length 105 μm
Diagnostics: Hemispherical cells with extremely delicate walls. Deeply indented raphe, exceedingly fine striae, barely resolvable in our desktop SEM (Pl. 58, Fig. 1).
Comments: These cells have a complex shape (Pl. 2, Figs 3–8) but the delicate frustules flatten in both whole mounts and acid-cleaned material. Paddock & Sims (1980) describe the valves as "canoe shaped" with the raphe arcing along one face only—the other face designated the mantle face, and the whole frustule as hemispherical with the mantle faces of the two valves adjacent. On the flat side the two raphe faces are separated by the girdle bands—thus forming the ventral surface—and the single flat, bilobed plastid lies along this side (Pl. 2, Figs 1, 2). Paddock & Sims (1980) did not observe living cells but cite two 19th century illustrations. Our sequence of images of a cell moving around a seaweed filament (Pl. 2, Figs 3–8) confirm this and also show a network of fine "veins" on the dorsal side (especially Pl. 2, Figs 4, 5).

"Bacillaria Group B" sensu Schmid Plate 58, Figs 2–6, Plate 59, Figs 1, 2
Ref. illus.: Navarro 1983b, figs 9–11; Witkowski et al. 2000, pl. 212, figs 9–12; Schmid 2007, figs 8d, 8e, 8f, 11
Samples: GU7N; GU21A; **GU44I-1, GU44I-2, GU44J, GU44Z-15, GU44AC**
Dimensions: Length 25–150 μm, width 6–7 μm; striae 23–25 in 10 μm; fibulae 11 in 10 μm
Diagnostics: Living colonies very actively sliding back and forth along interlocked raphe flanges. Frustules nitzschioid with the raphe displaced slightly from the apical axis, in contrast to *Nitzschia socialis* Gregory, which has it on the axis. The external transapical ribs distinguish this from the freshwater and brackish species, which Jahn & Schmid (2007) redefined as *Bacillaria sensu stricto*. In *Bacillaria sensu stricto* faults in the striae on the wider side are readily seen, but absent in the marine Group B. The expanded distal raphe endings (Pl. 59, Fig. 1) appear to be diagnostic at the SEM level, separating them from both *Bacillaria* and *Nitzschia*.

Comments: Schmid (2007) identified three forms of *B. paxillifer*, with our material agreeing with the marine benthic forms of Group B. However, Jahn & Schmid (2007) then lectoptypified the species (correcting the name to *paxillifera*) from near the original collection site and restricted *Bacillaria* to the freshwater/brackish forms, naming 3 new taxa, but leaving the marine forms orphaned without a genus. To date, their work on these forms is still in progress (R. Jahn, pers. comm., Aug. 2012). We have observed two widely different plastid forms (Pl. 58, Figs 2, 3) and cell sizes (Pl. 58, Figs 4–6); all our specimens are from fully marine, benthic situations. Schmid (2007) mentions literature records of samples with multiple plastids but did not observe them herself.

Nitzschia angularis W. Smith Plate 59, Figs 3–5
Ref. illus.: Peragallo & Peragallo 1897–1908, pl. 73 figs 6-7; Lobban & Mann 1987, figs 14, 15; Poulin et al. 1990, figs 16–22; Witkowski et al. 2000, pl. 199, fig. 7
Samples: **GU44I-1, GU44K-6**
Dimensions: Length 168 µm, width 10 µm; striae 28 in 10 µm; fibulae 6 in 10 µm
Diagnostics: conopeum and the fine, decussate striae are distinctive.
Comments: It is noteworthy that the small Section Spathulatae is represented in our flora by at least four species, including also *N. dissipata, N. martiana*, and an unnamed species shown in Navarro Ramas (2009, p. 52).

Nitzschia constricta (Gregory) Grunow (*non* Kützing) Plate 59, Figs 6–8
Basionym: *Tryblionella constricta* Gregory
Synonym: *Psammodictyon constrictum* (Gregory) D.G. Mann
Ref. illus.: Navarro 1983b, figs 16-19, Witkowski et al. 2000, pl. 187, figs 8–12
Samples: **GU44J-2, GU44Z-15**
Dimensions: Length 12 µm, width 6 µm; striae 22 in 10 µm
Diagnostics: Panduriform, generally small *Nitzschia* species; one fibula aligned with each interstria. See comments.
Comments: Our identification of this species from Guam is based on SEM, particularly Pl. 59, Fig. 7 with reference to Navarro's (1983b) fig.18; we have also documented the larger more constricted form he showed in figs 16, 17, 19. Several species appear very similar in LM (Pl. 59, Fig. 6), while in GU44Z-15 and other samples we distinguished several taxa in SEM with this shape and general pattern. Such species are common in our samples. Witkowski et al. (2000, pl. 183, 185) show LMs of several similar specimens unassigned to species and refer to *N. ruda* Cholnoky, which is illustrated by Hein et al. (2008, pl. 58, fig. 15), again in LM. Witkowski et al. (2000) distinguish *N. constricta* from *N. coarctata* Grunow in which the stria density is only 8–10 in 10 µm. Witkowski et al. (2000) note for both species that the striae are interrupted by a longitudinal fold, but there is no actual break in the striae as there is in *Psammodictyon* (q.v.).

Nitzschia dissipata (Kützing) Grunow Plate 60, Figs 1–3
Ref. illus.: Poulin et al. 1990, figs 28, 29
Samples: GU26A; **GU44I-1, GU44Z-15**

Dimensions: Length 35–52 μm, width 5 μm; striae 52 in 10 μm; fibulae 5–6 in 10 μm
Diagnostics: Conopeum (visible in LM as two thin lines paralleling the keel) and extremely fine striae (not resolvable in LM). On the basis of size and stria density this is *N. dissipata* rather than *N. distans* (cf. Poulin et al. 1990, figs 38–41).
Comments: The conopeum distinguishes this from several otherwise similar common hyaline *Nitzschia* species with narrow, widely-spaced fibulae. However, *N. dissipata* is commonly regarded as a freshwater species, and as such is described by Hoffman et al. (2011: 441, pl. 109, figs 8–13) and Kelly et al. (2005), but their figures do not correspond well with our material or that of Poulin et al. (1990), especially the eccentric raphe-keel.

Nitzschia granulata Grunow Plate 60, Fig. 4
Syn.: *Tryblionella granulata* (Grunow) D.G. Mann
Ref. illus.: Witkowski et al. 2000, pl. 189, figs 1–5, Ohtsuka 2005, figs 48, 49
Samples: GU4A; GU26A
Dimensions: Length 26–27 μm, width 10–13 μm; striae 7–8 in 10 μm
Diagnostics: Oval valve with rounded apices and very coarse areolae sometimes becoming biseriate on the margin (cf. Witkowski et al. 2000, pl. 189, figs 1, 2).
Comments: Although Mann (in Round et al. 1990) separated sections of *Nitzschia* into *Psammodictyon* and *Tryblionella*, many species remain too poorly studied to be sure which species definition they fit, and we have followed Witkowski et al. (2000) in retaining all these in *Nitzschia*, except for *Psammodictyon panduriforme* (q.v.), which is the generitype.

Nitzschia lanceola (Grunow in Cleve) Grunow in Cleve & Grunow
Plate 60, Figs 5–8
Syn.: *Trybionella lanceola* Grunow in Cleve
Ref. illus.: Grunow in Cleve 1878, p. 14, pl. 4, fig. 25; Navarro 1982d, pl. 35, figs 1, 2 (as "*Nitzschia lanceolata* W. Smith"); Foged 1987, pl. 29, figs 8, 9; Güttinger 1998, Series 9; Witkowski et al. 2000, pl. 212, figs 13–17
Samples: GU12G, GU55B-4
Dimensions: Length 23–32 μm, width 9 μm; striae 12–13 in 10 μm
Diagnostics: Lanceolate cells with longitudinal fold, striae coarse, incomplete; a ridged but nonperforated area adjacent to the keel (Pl. 60, Figs 6, 8).
Comments: The shape and density of the areolae and the shape of the fibulae in SEM differ somewhat from the specimen shown in Güttinger (1998), who gives 9–10 striae in 10 μm. Navarro (1982d) referenced Foged (1975), who apparently made the easy typographical confusion of *N. lanceola* with *N. lanceolata*; the latter, shown in Witkowski et al. (2000, pl. 194, figs 1–5) is entirely different.

Nitzschia longissima (Brébisson ex Kützing) Ralfs
Plate 60, Fig. 9; Plate 61, Fig. 1
Ref. illus.: Witkowski et al. 2000, pl. 207, fig. 6, 7; Hein et al. 2008, pl. 59, fig. 1
Samples: **GU44Z-15; GU52I;** GU54B-4

Dimensions: Length ca. 180–250 µm, width of central portion 8 µm; striae 40 in 10 µm.
Diagnostics: Lanceolate valve with extremely long, slender, rostrate ends, the keel eccentric, central nodule present; striae not resolvable in LM.
Comments: Distinguished from *N. ventricosa* (q.v.) by the lack of costae (Pl. 61, Fig. 1). *Ceratoneis* Ehrenberg (*Cylindrotheca* Rabenhorst) species (see Jahn & Kusber 2005) are common in our samples but have weakly silicified frustules and thin, curved, very flexible rostra; in acid cleaned material their only recognizable feature is the row of fibulae along the raphe-keel. In contrast the raphe-keel and central nodule are very apparent in *N. longissima* (Pl. 60, Fig. 9). At low magnifications, the shape is similar to *Psammosynedra closterioides* (Grunow) Round (Hein et al. 2008, pl. 11, fig. 6, pl. 12, figs 8, 9); the latter has not yet been found around Guam.

Nitzschia marginulata Grunow var. *didyma* Grunow Plate 61, Figs 2, 3
Syn.: *Trybionella marginulata* Grunow var. *didyma* (Grunow) D.G. Mann
Ref. illus.: Podzorski & Håkansson 1987, pl. 43, fig. 6 and pl. 53, fig. 6 (f. *parva*); Navarro et al. 1989, fig. 94; Witkowski et al. 2000, pl. 183, figs 4, 5); López Fuerte et al. 2010, pl. 38, fig. 11
Samples: **GU44I-2, GU44J-2, GU44Z-15**
Dimensions: Length 27–41 µm, width 9–10 µm; striae 31 in 10 µm
Diagnostics: Panduriform valve with one half covered by a hyaline area where there are tracings of the striae but perforations do not go through the valve. Valve surface undulate.
Comments: Witkowski et al. (2000) show both *N. marginulata* var. *didyma* (pl. 183, figs 4, 5) and *N. carnicobarica* Desikachary & Prema (pl. 183, figs 9, 10) and describe striae in the former interrupted by broad, hyaline long fold, in the latter by distinct longitudinal hyaline area. The former is also illustrated by Li (1978, pl. 13, fig. 2). Specimens labeled "*Nitzschia* cf. *carnicobarica*" are shown by Hein et al. (2008), pl. 58 figs 9–11. The distinction between these species is not very clear and the identity proposed here for our specimens is based especially on the internal SEM view in Podzorski & Håkansson (1987) (compare to our Pl. 61, Fig. 3).

Nitzschia sigma var. *intercedens* Grunow Plate 2, Figs 9, 10; Plate 61, Fig. 4
Ref. illus.: Grunow in Van Heurck 1880–1885, pl. 66, fig. 1; Van Heurck 1896, pl. 16, fig. 532; Peragallo & Peragallo 1897–1908, pl. 74, fig. 7 (as *N. intercedens* Grunow); Jin et al. 1985, pl. 59, fig. 725
Samples: **GU44AN-6, GU44AR-2**
Dimensions: Length 159–271 µm; striae ~ 30 in 10 µm; fibulae uniform, 8–9 in 10 µm.
Diagnostics: Distinguished by the fact that girdle view is sigmoid, while the valve view is straight; in this large variety the curves are very pronounced and the valve very narrow, so that living cells move primarily on their girdle faces. The frustule is more strongly sigmoid and more finely striated than the nominate variety.
Comments: The sigmoid girdle view distinguishes it from *N. lorenziana* Grunow

(Van Heurck 1896, pl. 17, fig. 572), *N. insignis* Gregory (Witkowski et al. 2000, pl. 202, fig. 5), *N. scabra* Cleve (Witkowski et al. 2000, pl. 195, figs 13, 14), etc., although *N. lorenziana* var. *subtilis* Grunow as shown by Peragallo & Peragallo (1897–1908, pl. 74, fig. 24) is remarkably similar, but the stria density is only 17–20 in 10 μm—whereas Van Heurck (1896) gives 27–28 for *N. sigma* var. *intercedens*—and the fibulae are much closer (20 in 10 μm). Two other varieties of *N. sigma* are shown by Hein et al. (2008, pl. 60, figs 3–5). Peragallo & Peragallo (1897–1908: 290) proposed raising this variety to species rank but this suggestion was not adopted by subsequent authors.

Nitzschia ventricosa Kitton Plate 62, Figs 1, 2
Ref. illus.: Giffen 1970, fig. 84; Ricard 1977, pl. 4, fig. 15; Witkowski et al. 2000, pl. 204, fig. 8
Samples: GU6C; **GU44Z-15**
Dimensions: Length 150 μm, width 10 μm; striae 34 in 10 μm; fibulae and ribs in central section 7–10 in 10 μm
Diagnostics: Lanceolate valve with extremely long, slender, rostrate ends, the keel very eccentric, central nodule present; striae not resolvable in LM, but valve crossed by numerous irregular costae, which distinguish it from *N. longissima* (q.v.).

Psammodicyton panduriforme (Gregory) D.G. Mann Plate 62, Figs 3, 4
Ref. illus.: Podzorski & Håkansson 1987, pl. 43, fig. 11; Witkowski et al. 2000, pl. 184, figs 13, 14 and pl. 186, figs 1, 2 (both as *Nitzschia panduriformis*); Round et al. 1990, pp. 612–613; Navarro & Lobban 2009, figs 105, 106 (Yap)
Samples: GU6C; GU21Y; GU44S, **GU44Z-15**
Dimensions: Length 59–80 μm, width 18–42 μm; striae 17–20 in 10 μm
Diagnostics: Panduriform valves with marginal keel, undulate surface and distinct hyaline stripe in which there are no puncta.
Comments: In nitzschioids with undulate valve surfaces it is possible to get the impression of a hyaline stripe, depending on the focal plane. Some of the images in Witkowski et al. (2000: pl. 184, fig. 13, pl. 186, fig. 3) do not convincingly display areas without puncta.

Auricula complexa (Gregory) Cleve Plate 63, Figs 1, 2
Ref. illus.: Peragallo & Peragallo 1897–1908, pl. 42, figs 14, 15; Ricard 1977, pl. 8, fig. 1; Navarro 1983b, figs 1–5
Samples: **GU44J-2, GU44Z-15**
Dimensions: Length 25–38 μm, width 20 μm, striae 26–28 in 10 μm
Diagnostics: Small, biarcuate valve with the keel along the dorsal edge, more finely striated than *A. intermedia* (q.v.).

Auricula intermedia (Lewis) Cleve Plate 63, Figs 3, 4
Ref. illus.: Peragallo & Peragallo 1897–1908, pl. 42, figs 12, 13; Ricard 1977, pl. 8, fig. 3
Samples: GU55B-4; **GU44I-2**

Dimensions: Length 62–63 μm, width 25 μm; striae 14–16 in 10 μm
Diagnostics: Larger valve with the raphe following a biarcuate curve away from the convex/straight dorsal margin, more coarsely striated than *A. complexa*.

Campylodiscus ambiguus Greville Plate 63, Figs 5–7; Plate 64, Fig. 1
Ref. illus.: Schmidt 1874–1959, pl. 18, figs 23–26; Williams 1988, pl. 26, figs 1, 2; Ruck & Kociolek 2004, pl. 36–38
Samples: **GU44I-2, GU44R-2, GU44Y-13, GU44AN-7**
Dimensions: Diameter 77–110 μm
Diagnostics: Valve surface warty, infundibula (approx. 2 in 10 μm) extending from the raphe keel toward a broad lanceolate central area that has a raised peak. Infundibula on raised areas of valve externally, with pore fields along the sides externally (Pl. 63, Fig. 6) and corresponding porate depressions internally (Pl. 64, Fig. 1). Mantle uniformly divided into porate segments by costae ca. 5 in 10 μm.
Comments: Ruck & Kociolek (2004) note the synonymy with *C. latus* Shadboldt (proposed in VanLandingham 1968 and Williams 1988) but in the absence of examination of Shadboldt's type treated *C. ambiguus* as separate.

Campylodiscus brightwellii Grunow Plate 64, Figs 2–4
Ref. illus.: Schmidt 1874–1959, pl. 18, fig. 11; Navarro 1983b, fig. 50, 51; Navarro & Lobban 2009, figs 125, 126 (Yap)
Samples: GU6C-2; **GU44J-2, GU44Y-13, GU44AN-7**
Dimensions: Diameter 50–70 μm
Diagnostics: Singular tubes (3 in 10 μm) connect the interior cell to canal raphe. Externally, flat, spiny flaps of silica lie atop the tubes and extend from the canal raphe toward the central area. External valve surface finely papillate with a central area divided by two parallel sets of costae (Pl. 64, Figs 3, 5), 4 in 10 μm. Between these central costae are short, paired striae (visible internally, Pl. 64, Fig. 4). Costae on valve mantle corresponding to the tubes leading to the canal raphe (Pl. 64, Fig. 5).

Campylodiscus decorus Brébisson Plate 64, Figs 5, 6
Ref. illus.: Peragallo & Peragallo 1897–1908, pl. 56, figs 2, 3; Witkowski et al. 2000, pl. 214 fig. 15
Samples: **GU44U-1A, GU44AN-7, GU44AR-3; GU52P-4**
Dimensions: Diameter 28 μm
Diagnostics: Infundibula absent, single tubes connect the interior cell to the canal raphe (as in *C. brightwellii*). Fenestral openings have 1 or 2 fenestral bars each. Narrow ribs extending from keel to very narrow lanceolate sternum (sometimes just a line). The pores in this species are resolvable in LM, in contrast to the similar species *C. ralfsii* Smith (Navarro & Lobban 2009, figs 128, 129).
Comments: Peragallo & Peragallo (1897–1908) give the differences between this species and *C. ralfsii* as the central area reduced to a simple line, and smaller size, but the presence of *C. decorus* var. *pinnatus* with a similar central area raises questions about this distinction.

Campylodiscus decorus var. *pinnatus* Peragallo Plate 65, Figs 1, 2
Ref. illus.: Peragallo & Peragallo 1897–1908, pl. 56, figs 5, 6; Ricard 1987, figs 974, 975
Samples: **GU44I-1, GU44R-2, GU44AR-2**
Dimensions: Diameter 33–41 μm
Diagnostics: Differing from the nominate variety in the numerous thin spines.

Campylodiscus humilis Greville Plate 65, Figs 3–6
Syn: *Campylodiscus socialis* Witt
Ref. illus.: Schmidt et al. 1874–1959, pl. 14, figs 7–9 (as C. socialis); Williams 1988, pl. 26, fig. 10
Samples: **GU44I-1, -2, GU44J-2, GU44Y-13, GU44AN-7**
Dimensions: Diam. 18–28 μm
Diagnostics: Valve face with numerous costae extending to a central area that is pyriform towards each apex, the central area papillate but the pores in the outer ridged area not resolved in LM. Externally the whole surface of the valve excluding the central area as well as the mantle is finely punctate (Pl. 65, Fig. 6), whereas internally the valve is completely smooth with one large oval portula at each apex and a few small, irregularly placed portulae irregularly spaced along the margin (Pl. 65, Fig. 5).

Hydrosilicon mitra Brun Plate 66, Fig. 1
Ref. illus.: Van Heurck 1896, fig. 118; Foged 1987, pl. 33, fig. 3; Gerloff & Natour 1982, pl. 18, fig. 8; Ricard 1987, figs 989-995; Round et al. 1990, pp. 636-637
Samples: See Comments
Dimensions: Not recorded; Foged (1987) gives 144 x 34–52 μm.
Diagnostics: Highly distinctive valve with two biarcuate margins, a sternum across the constriction as well as apically, the latter forked at both distal ends. However, Van Heurck (1896: 366) refers to another species in the genus and VanLandingham (1971) also lists *H. rimosa* (O'Meara) Brun, which differs in central sternum morphology were the apical sternum has a set of additional branches before the forked distal ends.
Comments: Single valve from plankton tow across Sella Bay observed and photographed by E. Ruck. No voucher specimen.

Petrodictyon patrimonii (Sterrenburg) Sterrenburg Plate 66, Figs 2, 3
Ref. illus.: Sterrenburg in Lange-Bertalot & Krammer 1987, fig. 57: 1, 4, 5; Sterrenburg 2001, fig. 1
Samples: GU13J; GU16P; ECT 3681
Dimensions: Length 62 μm, width 25–28 μm
Diagnostics: Oval valves with straight/zigzag longitudinal costa from apex to apex, and lateral, slightly radiating costae all connecting to it between several rows of striae. In *P. patrimonii* the striae are barely or not at all resolved in LM but those of the simulacrum species *P. gemma* (Ehrenberg) D.G. Mann are visible (see Sterrenburg 2001).

Plagiodiscus martensianus Grunow & Eulenstein Plate 67, Fig. 1
Ref. illus.: Ricard 1977, pl. 14, figs 1–11 [as *Surirella martensiana* (Grunow) Peragallo]; Ricard 1987, figs 980–988; Paddock 1978, Plate 1A–E, Plate 2A–C, Plate 3A–D; Montgomery 1978, pl. 177, figs A, B; Podzorski & Håkansson 1987, pl. 48, fig. 2 [as *Surirella nervata* (Grunow) Mereschkowsky]; Ruck & Kociolek 2004, pl. 51
Samples: **GU52P-5.**
Dimensions: Length 70 µm, width 43 µm, striae 13 in 10 µm
Diagnostics: Large reniform valve that lacks the central axis costae compared to *P. nervatus*.
Comments: Observed only in this sample, whereas *P. nervatus* was commonly encountered. The unusual flat sacs (palmulae), illustrated in Round et al. (1990: 641, figs e, g) are not present in this specimen but we have seen them in specimens from Chuuk, FSM. They do not occur in *P. nervatus*.

Plagiodiscus nervatus Grunow emend Paddock Plate 66, Figs 4, 5
Ref. illus.: Peragallo & Peragallo 1897–1908, pl. 65, fig. 5, Paddock 1978 pl. 2D, E, 3E, 4F, G
Samples: GU55B-4; GU52H, **GU52P-5**
Dimensions: Length 27–41 µm, width 13–18 µm; striae ca. 20 in 10 µm
Diagnostics: Reniform valve with costa running along the apical axis. Internally, short fibulae alternate with larger transverse costae that extend from the margin and most often reach the longitudinal costa. Several biseriate striae between each costa. Internally, the raphe fissures are continuous and traverse a conspicuous spur-like process located at the center of the more constricted side of the valve (Pl. 66, Fig. 4, arrow). This spur is almost always visible in the LM.

Surirella fastuosa (Ehrenberg) Kützing Plate 67, Figs 2, 3; Plate 68, Figs 1–3
Ref. illus.: Peragallo & Peragallo 1897–1908, pl. 58, figs 5–7; Ricard 1977, pl. 7, fig. 3; Ricard 1987, figs 951–961; Navarro 1983b, figs 69–71; Witkowski et al. 2000, pl. 215, figs 1–3; Hein et al. 2008, pl. 62, figs 2, 3 and pl. 64, fig. 1
Samples: **GU44K-6, GU44W-10;** GU55B-4
Dimensions: Length 36–68 µm, width 24–52 µm
Diagnostics: Oval-lanceolate valves with infundibula extending to curved, striated ridges enclosing a lanceolate central area often called the circlet. The central area may be broad or narrow but is crossed by costae extending from the infundibula. There is much variation in the species and many named varieties, but other species differ in lacking the striated ridges, except *P. pahoensis* Ricard (Ricard 1977, pl. 7, fig. 6), which has a different pattern of costae and infundubula.
Comments: Present in almost all farmer fish turf samples. Plate 67, Figs 2, 3 show that the valve pattern can be different on the two valves: the width of the central area is markedly narrower on one side in this case. Plastid as described by Round et al. (1990:644).

Surirella scalaris Giffen Plate 68, Figs 4–6, Pl. 69, Figs 1, 2
Ref. illus.: Navarro 1983b, fig. 68 (as *S. comis* Schmidt); Podzorski & Håkansson 1987, pl. 46, fig. 6 (as *Surirella ovata* Kützing); Witkowski et al. 2000, pl. 215, figs 4–6; Hein et al. 2008, pl. 64, fig. 4
Samples: **GU44J-2, GU44Z-15; GU52P-9,** GU52Q-10
Dimensions: Length 10–13 μm, width 10 μm
Diagnostics: Small round valve with the appearance of a walnut shell, 3–5 infundibula along each side; two parallel series of striated ridges down the apical axis.
Comments: *Campylodiscus fastuosus* Ehrenberg (= *C. thuretii* Brébisson) (Ruck & Kociolek 2004, pl. 39–41) appears to be similar, but larger. We are not convinced that any of our specimens, all rather spiny, conform to that species, partly because we have not encountered any complete frustules. Valves in *Campylodiscus* are oriented at right angles to one another (cf. Pl. 64, Figs 5, 6), whereas those in *Surirella* (and all other pennate diatoms) are oriented parallel to one another. The complete frustules we have observed (e.g., Pl. 68, Figs. 5, 6) belong to *Surirella*.

Discussion

Progress with the flora. The 179 taxa reported here for the first time plus those already reported bring the total for Guam to 237 (Appendix 1) and comprise less than a third of the taxa we have documented in the samples analyzed to date. However, this paper is only a beginning toward a description of the flora. We are discovering new taxa at a rapid pace. We have recently described several new species in the established genera of *Climaconeis, Cyclophora, Licmosphenia,* etc. (Lobban et al. 2010, Ashworth et al. 2012, Lobban in press). We have described four new genera: *Astrosyne, Gato, Mastogloiopsis,* and *Perideraion* (Ashworth et al. 2012, Lobban & Navarro 2012, in press, Lobban et al. 2011b). There are several habitats either not sampled or under-sampled. Our samples were largely from epiphytic communities, especially those associated with farmer-fish territories, yet we have by no means exhausted this habitat as new records and new species continue to turn up. Several major habitats remain to be studied, although a few species documented here originate from them: mangroves, sediments (both fine grained such as deeper sediments protected from waves and currents and coarse grained such as coral rubble), river estuaries, and the phytoplankton. Riaux Gobin et al. (2011b) have noted the richness of diatoms in sediments and associated algal turf in the borders of lagoons. Moreover, it is already clear from comparison with Konno's (2006) study of epiphytic diatoms in Palau that we can expect differences in the flora from island to island within the broad geographic expanse of Micronesia and probably depending on the particular circumstances of the island (high, volcanic vs. low, carbonate islands; extent of mangroves and lagoons, presence of marine lakes, and so forth). It is humbling to note that Hustedt (1955) identified 388 taxa—including 93 new to science—from just two samples of mud from Beaufort, N.C.

Progress with farmer-fish diatom assesmblages. Of the 237 marine species identified to date, at least 193 appear to inhabit farmer-fish territories (Appendix 1).

Analysis is incomplete and uncommon species continue to be found in samples from farmer-fish territories. This number excludes 6 known marine planktonic species (e.g., *Asterolampra marylandica*) and known freshwater/ brackish species (not listed), but it may nevertheless include a number of other redeposited taxa. It is clear from the net collections of Navarro (1981a, b, 1982a–c, 1983a, b) and Ricard (1974, 1975, 1977) that many benthic taxa become entrained in the tychoplankton, and these may then be redeposited elsewhere. Although we routinely observe the live collections, most taxa are not seen until after acid cleaning, so a list of species actually observed *living* in farmer-fish territories would be much shorter. For this reason, and because the samples frequently contained naturally trapped sediment and coral surface material scraped off during harvesting in the laboratory, we cannot in many cases determine the precise substrate of the taxa. Moreover, we are wary of declaring habitats of species, having observed both *Climaconeis undulata* and *Licmophora flucticulata* in particular habitats and then found them in markedly different situations (Lobban et al. 2010, 2011a). More broadly, much work remains before we can determine whether the diatom assemblage of farmer fish turfs is different from that of epiphytic communities in general. We do, however, feel that the documentation to date goes a long way toward meeting the needs of ecologists interested in the diets of farmer fish, and should make it possible to examine whether different fish species are associated with different diatom assemblages, or whether *Plectroglyphydodon* turf assemblages differ in deep, open-coast territories versus the shallow-water territories in the harbor.

Geographical comparison. In the alphabetical list of Guam records (Appendix 1), we have also listed those species that were also reported for several other tropical island areas. The list for the Society Islands (Pacific Ocean), compiled from Ricard (1977) is based on his own collections. Giffen's (1970) list for Mahé (Indian Ocean) includes earlier records but is primarily the results of his own observations. For the Caribbean/Atlantic we compiled two lists for Puerto Rico—(a) from Hagelstein (1939) and (b) from Navarro (1981a, b, 1982a–c, 1983a) plus Navarro et al. (1989)—and used Hein et al.'s (2008) records for The Bahamas. In addition we used Navarro & Hernández-Becerril's (1997) list for the Caribbean Sea, which includes Puerto Rico and the continental coasts in Central and South America as well as the Caribbean Islands. Some of these works and older literature they incorporate were not fully illustrated, including Giffen's (1970) and Ricard's (1977); they must be used with the caveat that they cannot be completely verified for possible synonymies and misidentifications. We alluded to this problem already under *Petrodictyon patrimonii*, i.e, where new species were distinguished that are similar to older ones, or where interpretation has changed, as in *Mastogloia cyclops* and *M. punctatissima*. In the latter case, for example, we can see from Navarro's (1983a) illustration of *M. splendida* that he had *M. punctatissima* and we have listed it as such in Appendix 1. Ricard (1974) listed *M. splendida* without illustration but he later (Ricard 1975) made the taxonomic change and the species appears in his Society Islands list (Ricard 1977) as *M. punctatissima*. Moreover, there was confusion about *Climacosphenia moniligera* vs. *C. elongata* until Round's (1982) study,

and finally, we have observed *Licmophora* aff. *ehrenbergii* which differs especially in ultratructural features from *L. ehrenbergii* (Lobban in press), but would be classified as such in an LM survey. Further, as noted in the introduction, sampling by Ricard and Navarro was largely by net, thus a mixture of phytoplankton and tychoplantkton, rather than direct benthic sampling. In particular, farmer fish turfs appear not to have been particularly noticed in other studies, although seaweed substrata have been frequently collected. Most especially, however, the absence of species from these lists is not evidence of their absence from that region. Even with these caveats comparison is instructive.

These lists have surprisingly small overlap (28–41% of our species on other "local" lists, Appendix 1), suggesting that either there are major regional differences in floras and/or those studies sampled only a fraction of the biodiversity. Even taking the entire Caribbean Sea list (55% overlap), 104 of our taxa are absent, of which only about 36 were described more recently than that list was compiled. Comparing the frequency with which our taxa appear on all local lists, 71 taxa are on 4 or 5 out of 5 (Table 4). These include all our *Diploneis* species identified to date, 17 of the 55 *Mastogloia* species, and many of the taxa in *Ardissonea* and *Toxarium*. These are clearly at least pan-tropical, and many are known to be globally distributed. Conversely 64 taxa (27%) appear only on our list, including 17 (7%) that we described very recently from Guam. The remaining 47 (20%) include several rarely recorded taxa, such as *Falcula paracelsianus, Ardissonea fulgens* var. *gigantea* and *Triceratium pulchellum*; 12 of the 55 *Mastogloia* species; and of course several species described by other authors since the various lists were published (1977–2008) (e.g., *Mastogloia neoborneensis, Olifantiella pilosella, Psammoneis japonica*). For now, the presence of long-known species only in our locality out of these five must be attributed to accidents of sampling. Overall, we see no evidence yet of real regional differences.

Mastogloia deserves special mention, since Witkowski et al. (2000:12–13) noted that "taxa belonging to this genus are usually found in hot spots or 'oases'," mostly in the tropics, and they cited the studies of John (1990) and Hein et al. (2008) that both emphasized stromatolites. John reported 36 taxa and Hein et al. 75 taxa (62 identified to species or below). We count 48 taxa in Hein et al. (2008) that were recorded from stromatolites. For Guam, we have so far identified 55 taxa, including representatives of all Hustedt's sections except Constrictae, with >40 more still to be determined; 48 of the 55 occurred in farmer-fish territories, almost all of which were collected in Apra Harbor. Hustedt (1931–1959:443) noted 60 species of *Mastogloia* in a single mud sample from Borneo and considered the Indo-Malaysian islands to be the center of distribution of the genus. While this biogeographic assertion may not yet be well supported by evidence, it is evident that Guam farmer-fish territories are *Mastogloia* 'oases.'

On the other hand, a few large and obvious species common in some other floras have not yet been recorded for Guam, among them *Gephyria media* Arnott (shown as a common epiphyte on seaweed in Hawaii, Huisman et al. 2007: 246), and *Licmophora normanniana* (Greville) Wahrer, sometimes abundant in Bahamas (Hein et al. 2009) and also collected by M.A. in Texas (unpublished). Conversely,

Table 4. Guam taxa occurring in 4 or 5 of the five localities [Guam, Society Islands, Mahé, Puerto Rico (Hagelstein & Navarro combined), The Bahamas] in Appendix 1.

In all 5 localities	In 4 of 5 localities
Amphora ostrearia var. *vitrea*	*Achnanthes longipes*
Biddulphia biddulphiana	*Achnanthes brevipes*
Caloneis liber	*Amphora arenaria*
Climacosphenia moniligera	*Amphora bigibba*
Cocconeis dirupta (var. *dirupta)*	*Amphora obtusa*
Diploneis crabro	*Ardissonea formosa*
Diploneis smithii	*Ardissonea fulgens (*var. *fulgens)*
Diploneis suborbicularis	*Auricula complexa*
Hyalosira interrupta	*Berkeleya rutilans*
Mastogloia cocconeiformis	*Campylodiscus brightwellii*
Mastogloia corsicana	*Chaetoceros peruvianus*
Mastogloia crucicula	*Cocconeis convexa*
*Mastogloia erythraea (*var. *erythraea)*	*Cocconeis dirupta* var. *flexella*
Mastogloia fimbriata	*Cocconeis heteroidea*
Mastogloia horvathiana	*Cocconeis scutellum*
Mastogloia ovalis	*Diploneis bombus*
Mastogloia ovulum	*Diploneis chersonensis*
Nitzschia longissima	*Diploneis weissflogii*
Plagiodiscus nervatus	*Grammatophora marina*
Plagiotropis lepidoptera	*Grammatophora undulata*
Podocystis adriatica	*Hyalosynedra laevigata*
Rhaphoneis amphiceros	*Licmophora remulus*
Striatella unipunctata	*Lyrella lyra*
Surirella fastuosa	*Mastogloia acutiuscula* var. *elliptica*
Toxarium hennedyanum	*Mastogloia angulata*
Toxarium undulatum	*Mastogloia binotata*
Trachyneis aspera	*Mastogloia citrus*
	Mastogloia cribrosa
	Mastogloia decussata
	Mastogloia jelinecki
	Mastogloia manokwariensis
	Mastogloia punctatissima
	Mastoneis biformis
	Navicula cancellata
	Nitzschia angularis
	Nitzschia ventricosa
	Nitzschia vidovichii
	Perissonoë cruciata
	Plagiogramma staurophorum
	Podocystis spathulata
	Podosira hormoides
	Psammodicyton panduriforme
	Psammodiscus nitidus
	Triceratium dubium

some large/distinctive and abundant taxa in our flora have not been widely recorded at the other localities, e.g., *Ardissonea fulgens* var. *gigantea*. *Stictocyclus stictodiscus* has not been reported from the Caribbean/Atlantic [but that was also the case for *Chrysanthemodiscus floriatus* until Gibson & Navarro (1981) found it off Florida]. *Biddulphiopsis membranacea* is absent from the other local lists but is on the Caribbean Sea list. *Licmophora flabellata* is also an interesting case: while very common in Guam, easily distinguished from congeners, and known to be very widespread, it is only on the lists for Mahé and the Caribbean.

Many taxa (especially in genera *Actinocyclus, Amphora, Cocconeis, Campylodiscus, Diploneis, Licmophora, Navicula, Nitzschia, Plagiotropis,* and *Rhopalodia*) will require further study before we are sufficiently confident of their identities. Some taxa are made more difficult by complications arising from recent studies showing that (1) some broadly conceived taxa may contain many morphotypes (e.g., in *Diploneis*, Droop 1996a, b), or (2) some taxa contain simulacrum species, hidden by the current definition of the species but distinguishable on the basis of additional LM characters (Sterrenburg 1995, 2001). We also note Stoermer's (1967) report of two supposedly different *Mastogloia* taxa combined in the same frustule (Janus cells – McBride & Edgar 1998), and the new species *Achnanthes pseudolongipes* (Toyoda et al. 2010), which consistently has a raphe valve like that of *A. brevipes* and a sternum valve like that of *A. longipes*! Nevertheless, it is clear from our studies of *Climaconeis, Cyclophora, Perideraion,* etc. that there are plenty of novel species and opportunities to resolve further taxa, and work is underway on *Licmophora* and *Mastogloia* among others and on additional new genera as we continue to gather and analyze samples.

Acknowledgements

The microscopes used at U. Guam were funded by NIGMS RISE award GM063682 and US Dept. Education MSEIP award P120A040092. Funding for the Theriot laboratory was through NSF AToL award EF-0629410 and the Jane and Roland Blumberg Centennial Professorship in Molecular Evolution. R.W.J.'s research was partially funded by a Grant-in-Aid from the Ministry of Education, Science and Culture of Japan (18405015) awarded to Professor H. Tamate (Dept. of Biology, Yamagata University), of which R.W.J. was a co-recipient. C.S.L. and M.S. thank COMNAVMAR for access to the main study site on Naval Base Guam. Nelson Navarro kindly applied his extensive knowledge of tropical diatoms to a review of an early "manuscript atlas" of images in presentation slides, suggesting identities for several taxa and correcting our names for others, and we also thank Zlatko Levkov and Catherine Riaux-Gobin for advice on some difficult identities. We thank Robert Edgar and Genevieve Lewis-Gentry for loan of Van Heurck slide 545 from the Farlow Herbarium, Harvard University. We appreciate the suggestions for improvement in the manuscript from Michel Poulin, Michael Sullivan and two anonymous reviewers. Finally, C.S.L. thanks students who have assisted the work: Lydell Lopez, Michael Natuel, Isumechraard Ngirairikl, Anjelica Perez, Jennifer Renguul, Kalani Reyes, Linda Song, and the Biodiversity course students

of 2010. Linda Song was supported by an apprenticeship from the Agricultural Development in the American Pacific (ADAP) project under the U.S. Department of Agriculture.

References

Alverson, A.J. & L. Kolnick. 2005. Intragenomic nucleotide polymorphism among small subunit (18S) rDNA paralogs in the diatom genus *Skeletonema* (Bacillariophyta). Journal of Phycology 41: 1248–1257.

Andresen, N.A. 1995. A taxonomic investigation of a little known species of *Isthmia*. *In* J.P. Kociolek & M.J. Sullivan (eds), A Century of Diatom Research in North America: A Tribute to the Distinguished Careers of Charles W. Reimer and Ruth Patrick, pp. 103–110. Koeltz Scientific Books, Koenigstein, Germany.

Arai, Y. 2010. Attached diatoms communities in farmer-fish territories. M.S. Thesis, Dept. of Earth and Environmental Sciences, Yamagata University, Japan.

Ashworth, M., E.C. Ruck, C.S. Lobban, D.K. Romanovicz & E.C. Theriot. 2012. A revision of the genus *Cyclophora* and description of *Astrosyne* gen. nov. (Bacillariophyta), two genera with the pyrenoids contained within pseudosepta. *Phycologia* 51: 684–699.

Bérard-Therriault, L., A. Cardinal & M. Poulin. 1986. Les diatomées (Bacillariophyceae) benthiques de substrats durs des eaux marines et saumâtres du Québec. 6. Naviculales: Cymbellaceae et Gomphonemataceae. Naturaliste Canadien 113: 405–429.

Bérard-Therriault, L., A. Cardinal & M. Poulin. 1987. Les diatomées (Bacillariophyceae) benthiques de substrats durs des eaux marines et saumâtres du Québec. 8. Centrales. Naturaliste Canadien 114: 81–103.

Boyer, C.S. 1927. Synopsis of North American Diatomaceae. Part 1. Coscinodiscatae, Rhizosolenatae, Biddulphiatae, Fragilariatae. Proceedings of the National Academy of Sciences of Philadelphia 78 (Supplement): 1–228.

Brogan, M.W. & J.R. Rosowski. 1988. Frustular morphology and taxonomic affinities of *Navicula complanatoides* (Bacillariophyceae). Journal of Phycology 24: 262–273.

Cardinal, A., M. Poulin & L. Bérard-Therriault. 1984. Les diatomées benthiques de substrats durs des eaux marines et saumâtres du Québec. 5. Naviculales, Naviculaceae; les genres *Donkinia, Gyrosigma* et *Pleurosigma*. Naturaliste Canadien 113: 167–190.

Cardinal, A., M. Poulin & L. Bérard-Therriault. 1986. Les diatomées benthiques de substrats durs des eaux marines et saumâtres du Québec. 4. Naviculaceae (à l'exclusion des genres *Navicula, Donkinia, Gyrosigma* et *Pleurosigma*). Naturaliste Canadien 111: 369–394.

Cardinal, A., M. Poulin & L. Bérard-Therriault. 1989. New criteria for species characterization in the genera *Donkinia, Gyrosigma* and *Pleurosigma* (Naviculaceae, Bacillariophyceae). Phycologia 28: 15–27.

Ceccarelli, D.M. 2007. Modification of benthic communities by territorial damselfish: a multi-species comparison. Coral Reefs 26: 853–866.

Ceccarelli, D.M., G.P. Jones & L.J. McCook. 2001. Territorial damselfishes as determinants of the structure of benthic communities on coral reefs. Oceanography and Marine Biology Annual Review 39: 355–389.

Cholnoky, B.J. 1959. Neue und seltene Diatomeen aus Afrika. IV. Diatomeen aus der Kaap-Provinz. Österreichische Botanische Zeitschrift 106: 1-69.

Cleve, P.T. 1878. Diatoms from the West Indian Archipelago. Bihang till Kongliga Svenska Vetenskaps-Akademiens Handlingar 5(8): 1-22, 5pls.

Cleve, P.T. 1895. Synopsis of the naviculoid diatoms. Kongliga Svenska Vetenscaps-Academiens Handlingar 26: 1–264.

Cox, E.J. 1983. Observations on the diatom genus *Donkinia* Ralfs in Pritchard. III. Taxonomy. Botanica Marina 26: 567–580.

Cox, E.J. 1988. Taxonomic studies on the diatom genus *Navicula* V. The establishment of *Parlibellus* gen. nov. for some members of *Navicula* Sect. *Microstigmaticae*. Diatom Research 3: 9–38.

Cox, E.J. 2006. *Achnanthes* sensu stricto belongs with genera of the Mastogloiales rather than with other monoraphid diatoms European Journal of Phycology 41: 67–81.

Desikachary, T.V. 1987. Atlas of Diatoms. Vol. 1. Marine Fossil Diatoms from India and Indian Ocean Region. Madras Science Foundation, Madras.

Desikachary, T.V. & P.M. Sreelatha. 1989. Oamaru Diatoms. Bibliotheca Diatomologica 19: 3-330, pls 1-145.

De Stefano, M., O.E. Romero & C. Totti. 2008. A comparative study of *Cocconeis scutellum* Ehrenberg and its varieties (Bacillariophyta). Botanica Marina 51: 506–536.

Droop, S.J.M. 1994a. Morphological variation in *Diploneis smithii* and *D. fusca* (Bacillariophyceae). Archiv für Protistenkunde 144: 249–270.

Droop, S.J.M. 1994b. A morphological and geographical analysis of two races of *Diploneis smithii* / *D. fusca* (Bacillariophyceae) in Britain. *In* D. Marino & M. Montresor (eds), Proceedings of the Thirteenth International Diatom Symposium, pp. 347–369. BioPress, Bristol, U.K.

Droop, S.J.M. 1996a. The identity of *Diploneis splendida* (Bacillariophyceae) and some related species. Phycologia 35: 404–420.

Droop, S.J.M. 1996b. Correction: *Diploneis splendida* is an illegitimate name. Diatom Research 11: 381–382.

Droop, S.J.M. 1998. *Diploneis sejuncta* (Bacillariophyta) and some new species form an ancient lineage. Phycologia 37: 340–356.

Edgar, S.M. & E.C. Theriot. 2003. Heritability of mantle areolar characters in *Aulacoseira subarctica* (Bacillariophyta). Journal of Phycology 39: 1057–1066.

Edgar, S.M. & E.C. Theriot. 2004. Phylogeny of *Aulacoseira* (Bacillariophyta) based on morphology and molecules. Journal of Phycology 40: 772–788.

Foged, N. 1975 Some littoral diatoms from the coast of Tanzania. Bibliotheca Phycologica 16: 1–127.

Foged, N. 1984. Freshwater and littoral diatoms from Cuba. Bibliotheca Diatomologica 5: 1–243.

Foged, N. 1987. Diatoms from Viti Levu, Fiji Islands. Bibliotheca Diatomologica 14: 1–195.
Franz, S.M. & A.-M.M. Schmid. 1994. Cell-cycle and phenotypes of *Biddulphiopsis titiana* in culture. Diatom Research 9: 265–288.
Gallagher, J.C. 1980. Population genetics of *Skeletonema costatum* (Bacillariophyceae) in Narragansett Bay. Journal of Phycology 16: 464–474.
Gaul, U., U. Geissler, M. Henderson, R. Mahoney & C.W. Reimer. 1993. Bibliography on the fine structure of diatom frustules (Bacillariphyceae). Proceedings of the Academy of Natural Sciences Philadelphia 144: 69–238.
Geissler, U. & J. Gerloff. 1963. Elektronenmikroscopischen beitrage zur phylogeny der Diatomeen raphe. Nova Hedwigia 6: 339–352.
Gerloff, J. & R.M. Natour. 1982. Diatoms from Jordan II. Nova Hedwigia Beihefte 73: 157–209 + 19 pl.
Gibson, R. A. & J.N. Navarro. 1981. *Chrysanthemodiscus floriatus* Mann (Bacillariophyceae), a new record for the Atlantic Ocean with comments on its structure. Phycologia 20: 338–341.
Gibson, R. A. & F. C. Stephens. 1985. Valve structure in *Mastogloia rostrata* with a comparison of intercalary band internal construction in two dissimilar diatom species. Cryptogamie: Algologie 6: 13–24.
Giffen, M.H. 1966. Contributions to the diatom flora of South Africa. III. Nova Hedwigia 13: 245–292.
Giffen, M.H. 1970. Contributions to the diatom flora of South Africa. IV. The marine littoral diatoms of the estuary of the Kowie River, Port Alfred, Cape Province. *In* J. Gerloff & J.B. Cholnoky (eds) Diatomaceae II. Nova Hedwigia Beihefte 31: 259–312, 5 pls.
Giffen, M.H. 1980. A checklist of marine littoral diatoms from Mahé, Seychelles Islands. Bacillaria 3: 129–159.
Greville, R.K. 1866. Descriptions of new and rare diatoms. Series XX. Transactions of the Microscopical Society, New Series, London 14:77-86, pls VIII & IX.
Güttinger, W. 1989. Collection of SEM-micrographs of Diatoms. Series 1–3. 150 plates. (Available from Koeltz Scientific Books, Koenigstein)
Güttinger, W. 1992. Collection of SEM-micrographs of Diatoms. Series 6. 50 plates. (Available from Koeltz Scientific Books, Koenigstein)
Güttinger, W. 1994. Collection of SEM-micrographs of Diatoms. Series 7. 50 plates. (Available from Koeltz Scientific Books, Koenigstein)
Güttinger, W. 1996. Collection of SEM-micrographs of Diatoms. Series 8. 50 plates. (Available from Koeltz Scientific Books, Koenigstein)
Güttinger, W. 1998. Collection of SEM-micrographs of Diatoms. Series 9. 50 plates. (Available from Koeltz Scientific Books, Koenigstein)
Hagelstein, R. 1939. Botany of Porto Rico and the Virgin Islands. Diatomaceae. New York Academy of Sciences, Scientific Survey of Porto Rico and the Virgin Islands, 8(3): 313–450.
Hein, M.K. & B.M. Winsborough. 2001. *Oestrupia grandis* sp. nov., a new benthic marine diatom from the Bahamas. Diatom Research 16: 325–341.

Hein, M.K., B.M. Winsborough, J.S. Davis & S. Golubic. 1993. Extracellular structures produced by marine species of *Mastogloia*. Diatom Research 8: 73–88.

Hein, M.K., B.M. Winsborough & M.J. Sullivan. 2008. Bacillariophyta (diatoms) of the Bahamas. Iconographia Diatomologica 19. Gantner Verlag, Ruggell, Germany.

Henderson, M.V. & C.W. Reimer. 2003. Bibliography on the Fine Structure of Diatom Frustules (Bacillariphyceae). II. A.R.G. Gantner Verlag, Ruggell, Germany. 372 pp.

Hendey, N.I. 1964. An Introductory Account of the Smaller Algae of British Coastal Waters. Part V. Bacillariophyceae (Diatoms). Her Majesty's Stationery Office, London.

Hernández-Becerril, D.U. 1995. Planktonic diatoms from the Gulf of California and coasts off Baja California: genera *Rhizosolenia, Proboscia, Pseudosolenia*, and former *Rhizosolenia* species. Diatom Research 10: 251–267.

Hernández-Becerril, D.U. & [J.] N. Navarro. 1998. Observations on the diatom *Roundia cardiophora* from the Caribbean Sea. Nova Hedwigia 66: 481–487.

Hixon M.A. & W.N. Brostoff. 1983. Damselfish as keystone species in reverse: intermediate disturbance and diversity of reef algae. Science 230: 511–513.

Hoban, M.A. 2008. Biddulphioid diatoms III: morphology and taxonomy of *Odontella aurita* and *Odontella longicruris* (Bacillariophyta, Bacillariophytina, Mediophyceae) with comments on the sexual reproduction of the latter. Nova Hedwigia 133: 47–65.

Hofmann, G., M. Wermun & H. Lange-Bertalot. 2011. Diatomeen in Süßwasser-Benthos von Mitteleuropa. A.R.G. Gantner Verlag/ Koeltz Scientific Books, Königstein, Germany.

Honeywill C. 1998. A study of British *Licmophora* species and a discussion of its morphological features. Diatom Research 13: 221–271.

Huisman, J.M., I.A.Abbott & C.M. Smith. 2007. Hawaiian Reef Plants. University of Hawaii Sea Grant College Program, Honolulu, HI.

Hustedt, F. 1927–1930. Die Kieselalgen Deutschlands, Österreichs und der Schweiz. *In* Rabenhorst's Kryptogamenflora, Band 7, Teil 1. Johnson Reprint, New York.

Hustedt, F. 1931–1959. Die Kieselalgen Deutschlands, Österreichs und der Schweiz. *In* Rabenhorst's Kryptogamenflora, Band 7, Teil 2. Johnson Reprint, New York.

Hustedt, F. 1961–1966. Die Kieselalgen Deutschlands, Österreichs und der Schweiz. *In* Rabenhorst's Kryptogamenflora, Band 7, Teil 3. Johnson Reprint, New York.

Hustedt, F. 1955. Marine Littoral Diatoms of Beaufort, North Carolina. Duke University Press. Durham, North Carolina. 67 pp.

Jahn, R. & W.-H. Kusber. 2005. Reinstatement of the genus *Ceratoneis* Ehrenberg and lectotypification of its type specimen: *C. closterium* Ehrenberg. Diatom Research 20: 295–304.

Jahn, R. & A.-M.M. Schmid. 2007. Revision of the brackish-freshwater diatom genus *Bacillaria* Gmelin (Bacillariophyta) with the description of a new variety and two new species. European Journal of Phycology 42: 295–312.

Jin, D. (T.G. Chin), Z. Cheng, J. Lin & S Liu. 1985. The Marine Benthic Diatoms in China. Vol. I. China Ocean Press, Beijing / Springer-Verlag, Berlin. 313 pp.

John, J. 1993. Morphology and ultrastructure of the tubes of *Mastogloia cocconeiformis* (Bacillariophyta) from Shark Bay, Western Australia. Phycologia 32: 388–394.

John, J. 1994. *Mastogloia* species associated with active stromatolites in Shark Bay, west coast of Australia. *In*: J.P. Kociolek (ed.) Proceedings of the 11th International Diatom Symposium, pp. 189–209. California Academy of Sciences, San Francisco.

Jones, H.M., G.E. Simpson, A.J. Stickle & D.G. Mann. 2005. Life history and systematics of *Petroneis* (Bacillariophyta) with special reference to British waters. European Journal of Phycology 40: 61–87.

Jones, G.P., L. Santana, L.J. McCook & M.I. McCormick. 2006. Resource use and impact of three herbivorous damselfishes on coral reef communities. Marine Ecology Progress Series 328: 215–224.

Jordan, R.W. & R. Ligowski. 2004. New observations on *Proboscia* auxospores and validation of the family Proboscideae fam. nov. Vie et Milieu 54: 91–103.

Jordan, R.W., R. Ligowski, E.-M. Nöthig & J. Priddle. 1991. The diatom genus *Proboscia* in Antarctic waters. Diatom Research 6: 63–78.

Jordan, R.W., C.S. Lobban & E.C. Theriot. 2009–2012. Western Pacific diatoms project. ProtistCentral. http://www.protistcentral.org/Project/get/project_id/17, accessed 1 Nov. 2012.

Kaczmarska, I., J.M. Ehrman, M.B.J. Moniz & N. Davidovich. 2009. Phenotypic and genetic structure of interbreeding populations of the diatom *Tabularia fasciculata* (Bacillariophyta). Phycologia 48: 391–403.

Kawamura, T. & R. Hirano. 1989. Notes on attached diatoms in Aburatsubo Bay, Kanagawa Prefecture, Japan. Bulletin of the Tohoku Regional Fisheries Research Laboratory 51: 41–73.

Kelly, M.G., H. Bennion, E.J. Cox, B. Goldsmith, J. Jamieson, S. Juggins, D.G. Mann & R.J. Telford (2005). River diatoms: a multiacess key. http://craticula.ncl.ac.uk/EADiatomKey/html/taxon13540370.html, accessed 1 Dec. 2012.

Kemp, K.-D. & T. B. B. Paddock. 1988. Observations on the diatom genus *Stigmaphora* G. C. Wallich and two species of *Mastogloia* Thwaites ex Wm. Smith. *In* F. E. Round (ed.), Proceedings of the 9th International Diatom Symposium, Bristol, August 24–30, 1986. Biopress, Bristol, U.K., pp. 405–416.

Kemp, K.-D. & T.B.B. Paddock. 1990. A description of two new species of the diatom genus *Mastogloia* with further observations on *M. amoyensis* and *M. gieskesii*. Diatom Research 5: 311–323.

Kobayasi, H. & T. Nagumo. 1985. Observations on the valve structure of marine species of the diatom genus *Cocconeis* Ehr. Hydrobiologia 127: 97–103.

Konno, S. 2006. Epiphytic Diatoms in Palauan Marine Lakes. M.S. Thesis, Dept. of Earth and Environmental Sciences, Yamagata University, Japan.

Konno, S. & R.W. Jordan. 2008. *Paralia longispina* sp. nov., an extant species from Palau and Haha-jima, western North Pacific. In: Likhoshway, Y. (ed.), Proceedings of the Nineteenth International Diatom Symposium. Biopress, Bristol, U.K. pp. 55–69.

Konno, S., N. Inoue, D.U. Hernández-Becerril & R.W. Jordan. 2010. *Chaetoceros affinis* blooms in Palauan meromictic marine lakes. Vie et Milieu 60: 257–264.

Kooistra, W.H.C.F., M. De Stefano, D.G. Mann, N. Salma & L.M. Medlin. 2003. Phylogenetic position of *Toxarium*, a pennate-like lineage within centric diatoms (Bacillariophyceae). Journal of Phycology 39: 185–197.

Kooistra, W.H.C.F., D. Sarno, D.U. Hernández-Becerril, P. Assmy, C. Di Prisco & M. Montresor. 2010. Comparative molecular and morphological phylogenetic analyses of taxa in the Chaetocerotaceae (Bacillariophyta). Phycologia 49: 471–500.

Kuriyama, K., H. Suzuki, T. Nagumo & J. Tanaka. 2010. Morphology and taxonomy of marine benthic diatom (1), *Tabularia* (Fragilariaceae, Fragilariales). Journal of Japanese Botany 85: 79–89.

Lange-Bertalot, H. and K. Krammer. 1987. Bacillariaceae, Epithemiaceae, Surirellaceae. Bibliotheca Diatomologica 15: 1–289.

Leuduger-Fortmorel, G. 1898. Diatomées marines de la côte occidentale d'Afrique. *Mémoires de la Société Emulation des Côtes-du-Nord*. St. Brieuc. 1–41, pl. 1–8.

Levkov, Z. 2009. *Amphora* sensu lato. In H. Lange-Bertalot (ed.), Diatoms of Europe. A.R.G. Gantner Verlag, Ruggell, Liechtenstein / Koeltz Scientific Books, Königstein, Germany.

Li, C.-W. 1978 . Notes on marine littoral diatoms of Taiwan. I. Some diatoms of Pescadora. Nova Hedwigia 29: 787–812.

Lobban, C.S. The marine araphid diatom genus *Licmosphenia* in comparison to *Licmophora*, with the description of three new species. Diatom Research (in press).

Lobban, C.S. & Jordan R.W. 2010. Diatoms on coral reefs and in tropical marine lakes. *In* J.P. Smol & E.F. Stoermer (eds), The Diatoms: Applications for the Environmental and Earth Sciences (2nd ed.). Cambridge University Press, Cambridge, U.K., pp. 346–356.

Lobban, C.S. & D.G. Mann. 1987. The systematics of the tube-dwelling diatom *Nitzschia martiana* and *Nitzschia* section *Spathulatae*. Canadian Journal of Botany 65: 2396–2402.

Lobban C.S. & J.N. Navarro. 2012. *Mastogloiopsis biseriata*, gen. et sp. nov., a diatom without partecta, is very similar to the Marginulatae group of *Mastogloia*. Nova Hedwigia 94: 251–263.

Lobban, C.S. & J.N. Navarro. *Gato hyalinus*, gen. et sp. nov., an unusual araphid tube-dwelling diatom from Western Pacific and Caribbean islands. 21st International Diatom Symposium, St. Paul, MN, 2010. Phytotaxa (in press).

Lobban, C.S. & M. Schefter. 2012. Blooms of a benthic ciliate, *Maristentor dinoferus* (Heterotrichea: Maristentoridae), on coral reefs of Guam, Mariana Islands. Micronesica 43: 114–127.

Lobban, C.S. & R.T. Tsuda. 2003. Revised checklist of benthic marine macroalgae and seagrasses of Guam and Micronesia. Micronesica 35-36: 54–99.

Lobban, C.S., M.P. Ashworth & E.C. Theriot. 2010. *Climaconeis* species (Bacillariophyceae: Berkeleyaceae) from western Pacific islands, including *C.*

petersonii sp. nov. and *C. guamensis* sp. nov., with emphasis on the plastids. European Journal of Phycology 45: 293–307.

Lobban, C.S., M. Schefter & E.C. Ruck. 2011a. *Licmophora flucticulata* sp. nov. (Licmophoraceae, Bacillariophyceae), an unusual flabellate species from Guam and Palau. Phycologia 50: 11–22.

Lobban, C.S., M. P. Ashworth, Y. Arai, R.W. Jordan & E.C. Theriot. 2011b. Marine necklace-chain Fragilariaceae (Bacillariophyceae) from Guam, including descriptions of *Koernerella* and *Perideraion*, genera nova. Phycological Research 59: 175–193.

López Fuerte, F.O., D.A. Siqueiros Beltrones & J.N. Navarro. 2010. Benthic Diatoms Associated with Mangrove Environments in the Northwest Region of México. CONABIO, Gobierno Federal Méxicano, Mexico City. ISBN 978-607-7607-30-4.

Mann, A. 1925. Marine Diatoms of the Philippine Islands. Smithsonian Institution Bulletin 100, 6(1): 1–182 + 39 pl.

McBride, S.A. & R.K. Edgar. 1998. Janus cells unveiled: frustular morphometric variability in *Gomphonema angustatum*. Diatom Research 13: 293–310.

MacGillivary, M.L. & I. Kaczmarska. 2012. Genetic differentiation within the *Paralia longispina* (Bacillariophyta) complex. Botany 90: 205–222.

Medlin, L.K. & F.E. Round. 1986. Taxonomic studies of marine gomphonemoid diatoms. Diatom Research 1: 205–225.

Medlin, L.K. G.A. Fryxell & E.R. Cox. 1985. Successional sequences of microbial colonization on three species of rhodophycean macroalgae. Annals of Botany 56: 399–413.

Medlin, L.K., S. Sato, D.G. Mann & W.H.C.F. Kooistra. 2008. Molecular evidence confirms sister relationship of *Ardissonea, Climacosphenia* and *Toxarium* within the bipolar centric diatoms (Bacillariophyta, Mediophyceae), and cladistic analyses confirm that extremely elongated shape has arisen twice in diatoms. Journal of Phycology 44: 1340–1348.

Meister, F. 1937. Seltene und neue Kieselalgen. II. Berichte der Schweizerischen Botanischen Gesellschaft 47: 258-276, pls. 3-13.

Mereschkowsky, C. 1900–1902. On Polynesian diatoms. Botanicheskiia Zapiski (Leningrad University) 18: 137–164 + pl. 4–6.

Mizuno, M. 1982. Change in straiation density and systematics of *Cocconeis scutellum* var. *ornata* (Bacillariophyceae). Botanical Magazine, Tokyo 95: 547–553.

Mizuno, M. 1987. Morphological variation of the attached diatom *Cocconeis scutellum* var. *scutellum* (Bacillariophyceae). Journal of Phycology 23: 591–597.

Montgomery, R.T. 1978. Environmental and Ecological Studies of the Diatom Communities Associated with the Coral Reefs of the Florida Keys. Volumes I and II. Ph.D. Dissertation, Florida State University, Tallahassee.

Moreno, J.L., S. Licea & H. Santoyo. 1996. Diatomeas del Golfo de California. Universidad Autonoma de Baja California Sur.

Nagumo, T. 2003. Taxonomic studies of the subgenus *Amphora* Cleve of the genus *Amphora* (Bacillariophyceae) in Japan. Bibliotheca Diatomologica 49: 1–265.
Nagumo, T. & H. Kobayasi. 1990. The bleaching method for gently loosening and cleaning a single diatom frustule. Diatom 5: 45–50.
Navarro, J.N. 1981a. A survey of the marine diatoms of Puerto Rico. I. Suborders Coscinodiscineae and Rhizosoleniineae. Botanica Marina 24: 427–439.
Navarro, J.N. 1981b. A survey of the marine diatoms of Puerto Rico. II. Suborder Biddulphineae: Families Biddulphiaceae, Lithodesmiaceae and Eupodiscaceae. Botanica Marina 24: 615–630.
Navarro, J.N. 1982a. A survey of the marine diatoms of Puerto Rico. III. Suborder Biddulphiineae: Family Chaetoceraceae. Botanica Marina 25: 305–319.
Navarro, J.N. 1982b. A survey of the marine diatoms of Puerto Rico. IV. Suborder Araphidinae: Families Diatomaceae and Protoraphidaceae. Botanica Marina 25: 247–263.
Navarro, J.N. 1982c. A survey of the marine diatoms of Puerto Rico. V. Suborder Raphidineae: Families Achnanthaceae and Naviculaceae (excluding *Navicula* and *Mastogloia*). Botanica Marina 25: 321–338.
Navarro, J.N. 1982d. Marine diatoms associated with mangrove prop roots in the Indian River, Florida, U.S.A. Bibliotheca Phycologica 61: 1–151.
Navarro, J.N. 1983a. A survey of the marine diatoms of Puerto Rico. VI. Suborder Raphidineae: Family Naviculaceae (genera *Haslea, Mastogloia* and *Navicula*). Botanica Marina 26: 119–136.
Navarro, J.N. 1983b. A survey of the marine diatoms of Puerto Rico. VII. Suborder Raphidineae: Families Auriculaceae, Epithemiaceae, Nitzschiaceae and Surirellaceae. Botanica Marina 26: 393–408.
Navarro, J.N. 1987. Observations of a tube-dwelling diatom: *Navicula hamulifera* (Bacillariophyceae). Journal of Phycology 23: 164–170.
Navarro, J.N. 2002. *Florella pascuensis* sp. nov., a new marine diatom species from Easter Island (Isla de Pascua), Chile. Diatom Research 17: 283-289.
Navarro J.N. & C.S. Lobban. 2009. Freshwater and marine diatoms from the western Pacific islands of Yap and Guam, with notes on some diatoms in damselfish territories. Diatom Research 24: 123–157.
Navarro, J.N. & D.U. Hernández-Becerril. 1997. Checklist of Marine Diatoms from the Caribbean Sea. 1997. Listados Floristicos De Mexico Lfg. 15. 48 p.
Navarro, J.N. & D.M. Williams. 1991. Description of *Hyalosira tropicalis* sp. nov. (Bacillariophyta) with notes on the status of *Hyalosira* Kützing and *Microtabella* Round. Diatom Research 6: 327–336.
Navarro, J.N., C. Pérez, N. Arce & B. Arroyo. 1989. Benthic marine diatoms of Caja de Muertos Island, Puerto Rico. Nova Hedwigia 49: 333–367.
Navarro, J.N., C.J. Micheli & A.O. Navarro. 2000. Benthic diatoms of Mona Island (Isla de Mona), Puerto Rico. Acta Cientifica 14: 103-143.
Navarro Ramas, N. 2009. Glosario Diatomológico Ilustrado. Lulu.com. ISBN 978-0-557-04258-6.
Novarino, G. 1989. An update on the taxa of the genus *Mastogloia*, with a 'resemblance list' for the more recently described ones. Diatom Research 4: 319-343.

Novarino, G. & A.R. Muftah. 1991. A description of *Mastogloia biocellata* stat. nov. from Qatari coastal waters. Diatom Research 6: 337–344.

Ohtsuka, T. 2005. Epipelic diatoms blooming in Isahaya Tidal Flat in the Ariake Sea, Japan, before the drainage following the Isahaya-Bay Reclamation Project. Phycological Research 53:138–148

Paddock, T.B.B. 1978. Observations on the valve structures of diatoms of the genus *Plagiodiscus* and on some associated species of *Surirella*. Botanical Journal of the Linnean Society 76: 1–25.

Paddock, T.B.B. 1986. Observations on the genus *Stauropsis* Meunier and related species. Diatom Research 1: 89–98.

Paddock, T.B.B. 1988. *Plagiotropis* Pfitzer and *Tropidoneis* Cleve, a summary account. Bibliotheca Diatomologica 16:1–152 + 38 pls.

Paddock, T.B.B. & K.D. Kemp. 1988. A description of some new species of the genus *Mastogloia* with further observations on *M. elegans* and *M. goessii*. Diatom Research 3: 109–121.

Paddock, T.B.B. & K.D. Kemp. 1990. An illustrated survey of the morphological features of the diatom genus *Mastogloia*. Diatom Research 5: 73–103.

Paddock, T. B. B. & P. A. Sims. 1980. Observations on the marine diatom genus *Auricula* and two new genera, *Undatella* and *Proboscidea*. Bacillaria 3: 161–196.

Paddock, T.B.B. & P.A. Sims. 1981. A morphological study of keels of various raphe-bearing diatoms. Bacillaria 4: 177–222.

Pandolfi, J.M., R.H. Bradbury, E. Sala, T.P. Hughes, K.A. Bjorndal, R.G. Cooke, D. McArdle, L. McClenachan, M.J.H. Newman, G. Paredes, R.R. Warner & J.B.C. Jackson. 2003. Global trajectories of long-term decline of coral reef ecosystems. Science 301: 955–958.

Paulay, G. (ed.) 2003. Marine biodiversity of Guam and the Marianas. Micronesica 35-36: 1–682.

Pennesi, C., M. Poulin, M. De Stefano, T. Romagnoli & C. Totti C. 2011. New insights to the ultrastructure of some marine *Mastogloia* species section Sulcatae (Bacillariophyceae), including *M. neoborneensis* sp. nov. Phycologia 50: 548–562.

Pennesi, C., M. Poulin, M. De Stefano, T. Romagnoli & C. Totti C. 2012. Morphological studies of some marine *Mastogloia* (Bacillariophyceae) belonging to section Sulcatae, including the description of new species. Journal of Phycology 48: 1248–1264.

Peragallo H. & M. Peragallo 1897–1908. Diatomées Marines de France et des Districts Maritimes Voisins. M.J. Tempère, Grez-sur-Loing, France, pp. 491 + 137 pl.

Podzorski, A.C. & H. Håkansson. 1987. Freshwater and marine diatoms from Palawan (a Philippine island). Bibliotheca Diatomologica 13: 1–245. J. Cramer, Berlin.

Polunin, N.V.C. 1988. Efficient uptake of algal production by a single resident herbivorous fish on the reef. Journal of Experimental Marine Biology and Ecology 123: 61–76.

Poulin M., L. Bérard-Therriault & A. Cardinal. 1986. *Fragilaria* and *Synedra* (Bacillariophyceae): a morphological and ultrastructural approach. Diatom Research 1: 99–112.

Poulin M., L. Bérard-Therriault & A. Cardinal. 1987. *Ardissonia crystallina* (Bacillariophyceae): une etude en microscopie électronique à balayage des elements structuraux des valves. Canadian Journal of Botany 65: 2686–2689.

Poulin M., L. Bérard-Therriault, A. Cardinal & P.B. Hamilton. 1990. Les diatomées (Bacillariophyta) benthiques de substrats durs des eaux marines et saumâtres du Québec. 9. Bacillariaceae. Naturaliste Canadien 117: 73–101.

Prasad, A.K.S.K., R.J. Livingston & G.L. Ray. 1989. The marine epizoic diatom *Falcula hyalina* from Choctawhatchee Bay, the northeastern Gulf of Mexico: frustule morphology and ecology. Diatom Research 4: 119–129.

Prasad, A.K.S.K., K.A. Riddle & J.A. Nienow. 2000. Marine diatom genus *Climaconeis* (Berkeleyaceae, Bacillariophyta): two new species, *Climaconeis koenigii* and *C. colemaniae*, from Florida Bay, U.S.A. Phycologia 39: 199–211.

Proshkina-Lavrenko, A.I. 1955. Plankton Diatoms of the Black Sea. Moscow. USSR AS. 222 p. (in Russian) [Figure 66 accessed online 12 June 2012 at http://phyto.bss.ibss.org.ua/wiki/Images/a/a1/Hemiaulus_hauckii.jpg]

Rattray, J. 1888. A revision of the genus *Aulacodiscus* Ehrenberg. Journal of the Royal Microscopical Society 8: 337-382.

Reid, G. and D.M. Williams. 2002. The marine diatom genus *Climaconeis* (Berkeleyaceae, Bacillariophyta): two new species from Abu Dhabi, United Arab Emirates. Diatom Research 17: 309–318.

Riaux-Gobin, C. & A.Y. Al-Handal. 2012. New species in the marine diatom genus *Olifantiella* (Bacillariophyta, Biraphidineae) from Rodrigues Island (Western Indian Ocean). Fottea, Olomouc 12: 199–217.

Riaux-Gobin, C. & P. Compère. 2009 *Olifantiella mascarenica* gen. & sp. nov., a new genus of pennate diatom from Réunion Island, exhibiting a remarkable internal process. Phycological Research 57: 178–185.

Riaux-Gobin, C., O.E. Romero, A.Y. Al-Handal & P. Compère. 2010. Two new *Cocconeis* taxa (Bacillariophyceae) from coral sands off the Mascarenes (Western Indian Ocean) and some related unidentified taxa. European Journal of Phycology 45: 278-292.

Riaux-Gobin, C., O.E. Romero, A.Y. Al-Handal & P. Compère. 2011a. Corrigendum. European Journal of Phycology 46: 88.

Riaux-Gobin, C., O.O. Romero, P. Compère & A.Y. Al-Handel. 2011b. Small-sized Achnanthales (Bacillariophyta) from coral sands off Mascarenes (Western Indian Ocean). Bibliotheca Diatomologica 57: 1–234 pp.

Ricard, M. 1974. Etude taxonomique des diatomées marines du lagon de Vairao (Tahiti) 1. Le genre *Mastogloia*. Revue Algologique, nouvelle série 11: 161–177.

Ricard, M. 1975. Quelques diatomées nouvelles de Tahiti décrites en microscopie photonique et électronique à balayage. Bulletin du Musée National d'Histoire Naturelle, 3^{e} serie, 326: 201–229.

Ricard, M. 1977. Les peuplements de diatomeés des lagons de l'Archipel de la Société (Polynésie Française). Revue Algologique, nouvelle série 12: 137–336.

Ricard, M. 1979. *Podocystis perrinensis* et *Podocystis guadalupensis*: deux espèces nouvelles du genre *Podocystis* récoltées en Guadaloupe. Revue Algologique 14: 33–38.

Ricard, M. 1987. Atlas du Phytoplancton Marin. Vol. 2. Diatomées. Editions du CNRS, Paris.

Ross, R. & P.A. Sims. 1971. Generic limits in the Biddulphiaceae as indicated by the scanning electron microscope. In: V. H . Heywood (ed.) Scanning Electron Microscopy. Systematic and Evolutionary Applications, pp. 155-177. Academic Press, London and New York

Ross, R., Sims, P. & G.R. Hasle. 1977. Observations on some species of the Hemiauloidea. Beiheft zur Nova Hedwigia 54: 179-213.

Ross, R., E.J. Cox, N.I. Karayeva, D.G. Mann, T.B.B. Paddock, R. Simonsen & P.A. Sims. 1979. An amended terminology for the siliceous components of the diatom cell. Nova Hedwigia Beih. 64: 513–533.

Round, F.E. 1982. The diatom genus *Climacosphenia* Ehr. Botanica Marina 25: 510–527.

Round, F.E. 1984. Structure of the cells, cell division and colony formation in the diatoms *Isthmia enervis* Ehr. and *I. nervosa* Kütz. Annals of Botany 53: 457–468.

Round, F.E. 1988. A new species of *Thalassiosira, T. cardiophora*. Diatom Research 3: 123–127.

Round, F.E., R.M. Crawford & D.G. Mann. 1990. The Diatoms: Biology and Morphology of the Genera. Cambridge University Press, Cambridge, U.K., 747 pp.

Ruck, E.C. 2010. Phylogenetic systematics of the canal bearing orders Surirellales and Rhopalodiales (Bacillariophyta). Ph.D. dissertation, The University of Texas at Austin.

Ruck, E.C. & J.P. Kociolek. 2004. Preliminary phylogeny of the family Surirellaceae (Bacillariophyta). Bibliotheca Diatomologica 50: 1–236.

Sar, E.A., O. Romero & I. Sunesen. 2003. *Cocconeis* Ehrenberg and *Psammococconeis* Garcia (Bacillariophyta) from the Gulf of San Matías, Patagonia, Argentina. Diatom Research 18: 79–106.

Sar, E.A., I. Suneson, R. Jahn, W-H. Kusber & A.S. Lavigne. 2007. Revision of *Odontella atlantica* (Frenguelli) Sar comb. et stat. nov. with comparison to two related species, *O. rhombus* (Ehrenb.) Kütz. and *O. rhomboides* R. Jahn et Kusber. Diatom Research 22: 341–353.

Sarno, D., W. Kooistra, L.K. Medlin, I. Percopo & A. Zingone. 2005. Diversity in the genus *Skeletonema* (Bacillariophyceae). II. An assessment of the taxonomy of *S. costatum*-like species with the description of four new species. Journal of Phycology 41: 151–176.

Sasaki, A. 2010. Observations on diatom assemblages attached to seaweeds and seagrasses in Guam. Undergraduate Thesis, Dept. of Earth and Environmental Sciences, Yamagata University, Japan.

Sato, S., D.G.Mann, T. Nagumo, J. Tanaka, T. Tadano & L.K. Medlin. 2008a. Auxospore fine structure and variation in modes of cell size changes in *Grammatophora marina* (Bacillariophyta). Phycologia 47: 12–27.

Sato, S., W.H.C.F. Kooistra, T. Watanabe, S. Matsumoto and L.K. Medlin. 2008b. A new araphid diatom genus *Psammoneis* gen. nov. (Plagiogrammaceae, Bacillariophyta) with three species based on SSU and LSU rDNA sequence data and morphology. Phycologia 47: 510–528.

Sato, S., T. Watanabe, R.M. Crawford, W.H.C.F. Kooistra & L.K. Medlin. 2008c. Morphology of four plagiogrammaceaen diatoms; *Dimeregramma minor* var. *nana, Neofragilaria nicobarica, Plagiogramma atomus* and *Psammogramma vigoensis* gen. et sp. nov., and their phylogenetic relationship inferred from partial large subunit rDNA. Phycological Research 56: 255–268.

Sato, S., D.G. Mann, S. Matsumoto & L.K. Medlin. 2008d. *Pseudostriatella* (Bacillariophyta): a description of a new araphid diatom genus based on observations of frustule and auxospore structure and 18S rDNA phylogeny. Phycologia 47: 371–391.

Sato, S., T. Watanabe, T. Nagumo & J. Tanaka. 2011. Valve morphogenesis in an araphid diatom *Rhaphoneis amphiceros* (Rhaphoneidaceae, Bacillariophyta). Phycological Research 59: 236–243.

Sawai, Y., T. Nagumo & K. Toyoda. 2005. Three extant species of *Paralia* (Bacillariophyceae) along the coast of Japan. Phycologia 44: 517–529.

Schmid, A-M.M. 2007. The "paradox" diatom *Bacillaria paxillifer* (Bacillariophyta) revisited. Journal of Phycology 43: 139–155.

Schmidt, A. et al. 1874–1959. Atlas der Diatomaceen-Kunde. Series I–X. R. Reisland, Leipzig. (Reprint 1974 Koeltz, Koenigstein.)

Schoeman, F.R. & R.E.M. Archibald. 1986. Observations on *Amphora* species (Bacillariophyceae) in the British Museum (Natural History). II. Some species from the subgenus *Psammamphora* Cleve. Nova Hedwigia 43: 473–484.

Schoeman, F.R. & R.E.M. Archibald. 1987. Observations on *Amphora* species (Bacillariophyceae) in the British Museum (Natural History). III. Two species from the subgenus *Amblyamphora* Cleve. Nova Hedwigia 44: 125–135.

Shevchenko, O.G., Orlova, T.Y. & Hernández-Becerril, D.U. 2006. The genus *Chaetoceros* (Bacillariophyta) from Peter the Great Bay, Sea of Japan. Botanica Marina 49: 236–258.

Simonsen, R. 1987. Atlas and Catalogue of the Diatoms Types of Friedrich Hustedt. 3 vols. J. Cramer, Berlin.

Simonsen, R. 1990. On some diatoms of the genus *Mastogloia*. Nova Hedwigia Beihefte 100: 121–142.

Sims, P.A. & R. Ross. 1990. *Triceratium pulvinar* and *T. unguiculatum*, two confused species. Diatom Research 5: 155–169.

Smol, J.P. & E.F. Stoermer (eds). 2010. The Diatoms: Applications for the Environmental and Earth Sciences (2nd ed.). Cambridge University Press, Cambridge, U.K.

Snoeijs, P. 1992. Studies in the *Tabularia fasciculata* complex. Diatom Research 7: 313–344.

Stephens, F. C. & R. A. Gibson. 1979a. Observations of loculi and associated extracellular material in several *Mastogloia* (Bacillariophyceae) species. Revue Algologique, nouvelle série 14: 21–32.

Stephens, F. C. & R. A. Gibson. 1979b. Ultrastructural studies on some *Mastogloia* (Bacillariophyceae) species belonging to the group Ellipticae. Botanica Marina 22: 499–509.

Stephens, F. C. & R. A. Gibson. 1980a. Ultrastructural studies of some *Mastogloia* (Bacillariophyceae) species belonging to the groups Undulatae, Apiculatae, Lanceolatae and Paradoxae. Phycologia 19: 143–152.

Stephens, F. C. & R. A. Gibson. 1980b. Ultrastructure studies on some *Mastogloia* species of the group Inaequales (Bacillariophyceae). Journal of Phycology 16: 354-363.

Stephens, F. C. & R. A. Gibson. 1980c. Ultrastructural studies on some *Mastogloia* (Bacillariophyceae) species belonging to the group Sulcatae. Nova Hedwigia 33: 219–248

Sterrenburg, F.A.S. 1988. Observations on the genus *Anorthoneis* Grunow. Nova Hedwigia 47: 363–376.

Sterrenburg, F.A.S. 1995. Studies on the genera *Gyrosigma* and *Pleurosigma* (Bacillariophyceae). *Gyrosigma balticum* (Ehrenberg) Rabenhorst, *G. pensacolae* sp. n. and simulacrum species. Botanica Marina 38: 401–408.

Sterrenburg, F.A.S. 2001. Transfer of *Surirella patrimonii* Sterrenburg to the genus *Petrodictyon*. Diatom Research 16: 109–111.

Stidolph, S.R., F.A.S. Sterrenburg, K.E.L. Smith & A. Kraberg. 2012. Stuart R. Stidolph Diatom Atlas. U.S. Geological Survey Open-File Report 2012-1163. http://pubs.usgs.gov/of/2012/1163/

Stoermer, E.F. 1967. Polymorphism in *Mastogloia*. Journal of Phycology 3: 73–77.

Sullivan, M.J. & D.J. Wear. 1995. A morphological study of the giant diatoms *Ardissonea formosa* and *Synedra bacillaris*. Diatom Research 10: 179–190.

Sundström, B.G. 1986. The marine diatom genus *Rhizosolenia* (A new approach to the taxonomy). Ph.D. dissertation, Lund University, Sweden.

Suzuki, H., T. Nagumo & J. Tanaka. 2001a. Morphology of the marine epiphytic diatom *Cocconeis heteroidea* (Bacillariophyceae). Phycological Research 49: 129–136.

Suzuki, H., J. Tanaka & T. Nagumo. 2001b. Morphology of the marine diatom *Cocconeis pseudomarginata* Gregory var. *intermedia* Grunow. Diatom Research 16: 93–102.

Takahashi, K., R.[W.] Jordan & J. Priddle. 1994. The diatom genus *Proboscia* in Subarctic waters. Diatom Research 9: 411–428.

Tanako, H. 1983. New and rare diatoms from Japanese marine waters. XI. Three new species epizoic on copepods. Bulletin of the Tokai Regional Fisheries Research Laboratory 111: 23–35.

Theriot, E. 1987. Principal component analysis and taxonomic interpretation of environmentally related variation in silicification in *Stephanodiscus* (Bacillariophyceae). British Phycological Journal 22: 359–374.

Theriot, E.C. 1992. Clusters, species concepts, and morphological evolution of diatoms. Systematic Biology 41: 141–157.

Theriot, E. & T.B. Ladewski. 1986. Morphometric analysis of shape of specimens from the neotype of *Tabellaria flocculosa* (Bacillariophyceae). American Journal of Botany 73: 224–229.

Theriot, E. & E.F. Stoermer. 1981. Some aspects of morphological variation in *Stephanodiscus niagarae* (Bacillariophyceae). Journal of Phycology 17: 64–72.

Theriot, E.C. & E.F. Stoermer. 1984. Principal component analysis of variation in *Stephanodiscus rotula* and *S. niagarae* (Bacillariophyceae). Systematic Botany 9: 53–59.

Theriot, E., H. Håkansson & E.F. Stoermer. 1988. Morphometric analysis of *Stephanodiscus alpinus* (Bacillariophyceae) and its morphology as an indicator of lake trophic status. Phycologia 27: 485–493.

Theriot, E.C., M. Ashworth, E. Ruck, T. Nakov & R.K. Jansen. 2010. A preliminary multigene phylogeny of the diatoms (Bacillariophyta): challenges for future research. Plant Ecology and Evolution 143: 278–296.

Theriot E.C., E. Ruck, M. Ashworth, T. Nakov & R.K. Jansen. 2011. Status of the pursuit of the diatom phylogeny: are traditional views and new molecular paradigms really that different? *In* J. Seckbach & J.P. Kociolek (eds) The Diatom World, pp 119–142. Springer Science+Business Media.

Toyoda, K., E.J. Cox, P.A. Sims & D.M. Williams. 2005. The typification of *Achnanthes* Bory based on *Echinella stipitata* Lyngbye, with an account of the morphology and fine structure of Lyngbye's species. Diatom Research 20: 375–386.

Toyoda, K., T. Nagumo & D.M. Williams. 2010. New marine monoraphid species, *Achnanthes pseudolongipes*, sp. nov., from Miyagi, Japan. Diatom Research 25: 185–193.

Tyler, P.A. 1996. Endemism in freshwater algae, with special reference to the Australian region. Hydrobiologia 336: 127–135.

Van Heurck, H. 1880–1885. Synopsis des Diatomées de Belgique. Ducaju & Co., Anvers, Belgium. [A digitial edition compiled by John Jeffrey Dodd, 2005 is online at http://sdrc.lib.uiowa.edu/algae/vanheurck/vanheurck1/about.htm]

Van Heurck, H. 1880–1887. Types de Synopsis de Belgique. Series I–XXII. 550 slides; text by A. Grunow.

Van Heurck, H. 1896. A Treatise on the Diatomaceae. William Wesley, London.

VanLandingham, S.L. 1968. Catalogue of the Fossil and Recent Genera and Species of Diatoms and their Synonyms. Part II. *Bacteriastrum* through *Coscinodiscus*. J. Cramer, Lehre.

VanLandingham, S.L. 1971. Catalogue of the Fossil and Recent Genera and Species of Diatoms and their Synonyms. Part IV. *Fragiliaria* through *Naunema*. J. Cramer, Lehre.

Vanormelingen, P., E. Verleyen & W. Vyverman. 2008. The diversity and distribution of diatoms: from cosmoplitanism to narrow endemism. Biodiversity and Conservation 17: 393–405.

Voigt, M. 1942. Contribution to the knowledge of the diatom genus *Mastogloia*. Journal of the Royal Microscopical Society 62(3): 1–20.

Voigt, M. 1952. A further contribution to the knowledge of the diatom genus *Mastogloia*. Journal of the Royal Microscopical Society 71: 440–449.

Voigt, M. 1960. *Falcula*, un nouveau genre de diatomées de la Méditerrannée Revue Algologique, nouvelle série 5: 85–88 + pl. 10–11.
Voigt, M. 1961. Sur le genre *Falcula*. Revue Algologique, nouvelle série 6: 53–56 + pl. 7.
Voigt, M. 1963. Some new and interesting *Mastogloia* from the Mediterranean area and the Far East. Journal of the Royal Microscopical Society 82: 111–121.
Voigt, M. 1966. La nervure apicale de la valve naviculoïde. Revue Algologique, nouvelle série 8: 82–88 + pl. 8.
Von Stosch, H.A. 1987. Some marine diatoms from the Australian region, especially from Port Phillip Bay and tropical North-eastern Australia. II. Survey of the genus *Palmeria* and of the family *Lithodesmiaceae* including the new genus Lithodesmioides. Brunonia 9: 29-87.
Von Stosch, H.A. & R. Simonsen. 1984. *Biddulphiopsis*, a new genus of the Biddulphiaceae. Bacillaria 7: 9–36.
Wachnicka, A. & E. E. Gaiser. 2007. Morphological characterization of *Amphora* and *Seminavis* (Bacillariophyceae) from South Florida, U.S.A. Diatom Research 22: 387–455.
Watkins, T.P. & G.A. Fryxell. 1986. Generic characterization of *Actinocyclus*: consideration in light of three new species. Diatom Research 1: 291–312.
Williams. D.M. 1988. An illustrated catalogue of the type specimens in the Greville diatom herbarium. Bulletin of the British Museum (Natural History), Botany 18: 1–148.
Williams, D.M. & F.E. Round. 1986. Revision of the genus *Synedra* Ehrenb. Diatom Research 1: 313–339.
Witkowski A., Lange-Bertalot H. & Metzeltin D. 2000. Diatom Flora of Marine Coasts, I. A.R.G. Gantner Verlag, Ruggell, Germany.
Wolfe, A.P. & P.A. Siver. 2009. Three extant genera of freshwater thalassiosiroid diatoms from Middle Eocene sediments in northern Canada. American Journal of Botany 96: 487–497.
Yohn, T. A. & R. A. Gibson. 1981. Marine diatoms of the Bahamas. I. *Mastogloia* Thw. ex Wm. Sm. species of the groups Lanceolatae and Undulatae. Botanica Marina 24: 641–655.
Yohn, T. A. & R. A. Gibson. 1982a. Marine diatoms of the Bahamas. II. *Mastogloia* Thw. ex Wm. Sm. species of the groups Decussatae and Ellipticae. Botanica Marina 25: 41–53.
Yohn, T. A. & R. A. Gibson. 1982b. Marine diatoms of the Bahamas. III. *Mastogloia* Thw. ex Wm. Sm. species of the groups Inaequales, Lanceolatae, Sulcatae and Undulatae. Botanica Marina 25: 277–288.
Zingone, A., I. Percopo, P.A. Sims & D. Sarno. 2005. Diversity in the genus *Skeletonema* (Bacillariophyceae). I. A reexamination of the type material of *S. costatum* with the description of *S. grevillei* sp nov. Journal of Phycology 41: 140–150.
Zolan, W. J. 1980. Periphytic diatom assemblages on a windward fringing reef flat in Guam. Unpublished M.S. thesis, University of Guam.

Received 20 Oct. 2012, accepted 1 Dec.

Appendix 1. Checklist and alphabetical index of marine diatoms documented for Guam, with a column for taxa recorded in farmer-fish territories (Guam FFTs) and comparison of records of these taxa in other tropical diatom lists[a]: Society Islands (French Polynesia Pacific Ocean), Mahé (Indian Ocean), Puerto Rico (Caribbean Sea), Bahamas (Atlantic Ocean), and a list for the entire Caribbean sea including continental coasts. Boldface flags the 17 new species reported from Guam to date.

Taxon	**Guam Index: Reference[b] or page + figures in this paper**	**Guam FFTs[c]**	**Society Islands**	**Mahé**	**Puerto Rico [H]**	**Puerto Rico [NN]**	**The Bahamas**	**Caribbean Sea**
Achnanthes brevipes C.A. Agardh	p. 284; Pl. 38:1–4	X	X	X	X			X
Achnanthes citronella (Mann) Hustedt	p. 285; Pl. 38:5,6	X	X					X
Achnanthes cuneata (Grunow) Grunow	p. 285; Pl.38:7							
Achnanthes longipes C.A. Agardh	p. 285; Pl. 39:1–3	X	X		X	X	X	X
Actinocyclus tenuissimus Cleve	p. 249; Pl. 5:1,2	X				X		X
Amphora arcuata A. Schmidt	p. 297; Pl 53:5	X		X				X
Amphora arenaria Donkin	p. 297; Pl. 53:5,6. 54:1,2	X	X	X			X	X
Amphora bigibba Grunow	2	X	X	X	X	X		X
Amphora decussata Grunow	p. 298; Pl. 1:7–9, 54:5, 55:1–3	X		X	X	X		X
Amphora immarginata Nagumo	p. 298; Pl. 56:2–5	X						
Amphora obtusa Gregory	p. 298; Pl. 54:3,4	X	X	X	X	X		X
Amphora ostrearia Brébisson var. *vitrea* (Cleve) Cleve	p. 299; Pl. 56:5,6	X	X	X	X	X	X	X
Amphora vaughanii Giffen	p. 299; Pl. 56:8–10	X						
Anorthoneis vortex Sterrenburg	p. 286; Pl. 39:5	X						
Ardissonea crystallina (C. Agardh) Grunow	p. 259; Pl.15:1–4	X		X		X		X
Ardissonea formosa (Hantzsch) Grunow	2 & p. 259; Pl.15:4,5, 16:1,2	X		X	X	X	X	X
Ardissonea fulgens (Greville) Grunow	p. 259; Pl. 16:3–5	X		X	X	X	X	X

Taxon	Guam Index: Reference[b] or page + figures in this paper	Guam FFTs[c]	Society Islands	Mahé	Puerto Rico [H]	Puerto Rico [NN]	The Bahamas	Caribbean Sea
Ardissonea fulgens var. *gigantea* (Lobarzewsky) De Toni	p. 260; Pl. 1:1,2; 16:6–8	X			X			
Asterolampra marylandica Ehrenberg	p. 249; Pl. 5:6		X				X	X
Astrosyne radiata Ashworth & Lobban	9	X						
Aulacodiscus orientalis Greville	p. 249; Pl. 5:3–5		X					
Auricula complexa (Gregory) Cleve	p. 304; Pl. 63:1,2	X	X	X		X		X
Auricula intermedia (Lewis) Cleve	p. 304; Pl. 63:3,4	X	X					X
"*Bacillaria* Group B" *sensu* Schmid	p. 300; Pl. 58:2–6, 59:1,2	X	X			X		X
Berkeleya rutilans (Trentepohl) Grunow	2	X		X		X	X	X
Biddulphia biddulphiana (J.E. Smith) Boyer	2	X	X	X	X	X	X	X
Biddulphiopsis membranacea (Cleve) von Stosch & Simonsen	2	X						X
Biddulphiopsis titiana (Grunow) von Stosch & Simonsen	p. 251; Pl. 7:3	X			X	?		X
Bleakeleya notata (Grunow in Van Heurck) F.E. Round	6	X		X	X	X		X
Caloneis egena (A. Schmidt) Cleve	p. 294; Pl. 49:3,4	X					X	X
Caloneis liber (W. Smith) Cleve	p. 294; Pl. 49:5,6, 50:1–3	X	X	X	X		X	X
Campylodiscus ambiguus Greville	p. 305; Pl. 63:5,6, 64:1	X						
Campylodiscus brightwellii Grunow	p. 305; Pl. 64:2–4	X	X	X		X		X
Campylodiscus decorus Brébisson var. *decorus*	p. 305; Pl. 64:5, 6	X	X					

Taxon	Guam Index: Reference[b] or page + figures in this paper	Guam FFTs[c]	Society Islands	Mahé	Puerto Rico [H]	Puerto Rico [NN]	The Bahamas	Caribbean Sea
Campylodiscus decorus var. *pinnatus* Peragallo	p. 306; Pl. 65:1,2	X	X					
Campylodiscus humilis Greville	p. 306; Pl. 66:1–4	X						
Chaetoceros atlanticus var. *skeleton* (Schütt) Hustedt	p. 253; Pl. 9:3							
Chaetoceros peruvianus Brightwell	p. 254; Pl. 9:4,5		X			X	X	X
Chamaepinnularia clamans (Hustedt) Witkowski, Lange-Bertalot & Metzeltin	p. 291; Pl. 46:8,9	X		X				
Chrysanthemodiscus floriatus A. Mann	2	X	X			X		X
Climaconeis coxii Reid & Williams	p. 288; Pl. 42:4,5	X						
Climaconeis guamensis Lobban, Ashworth & Theriot	4	X						
Climaconeis inflexa (Brébisson) Cox	4			X				
Climaconeis petersonii Lobban, Ashworth & Theriot	4							
Climaconeis riddleae A.K.S.K. Prasad	4	X						
Climaconeis silvae A.K.S.K. Prasad	4	X						
Climaconeis undulata (Meister) Lobban, Ashworth & Theriot	4							
Climacosphenia elongata Bailey	2	X	X		X			X
Climacosphenia moniligera Ehrenberg	2	X	X	X	X	X	X	X
Cocconeis convexa Giffen	2	X		X		X	X	X
Cocconeis coronatoides Riaux-Gobin & Romero	p. 286; Pl. 39:6							

Taxon	Guam Index: Reference[b] or page + figures in this paper	Guam FFTs[c]	Society Islands	Mahé	Puerto Rico [H]	Puerto Rico [NN]	The Bahamas	Caribbean Sea
Cocconeis dirupta Gregory	p. 286; Pl. 40:1, 2	X	X	X	X		X	X
Cocconeis sp. aff. *dirupta* (sensu Riaux-Gobin et al. 2011b)	p. 287; Pl. 40:3	X						
Cocconeis dirupta var. *flexella* (Janisch & Rabenhorst) Grunow	p. 287; Pl. 40:4,5	X	X	X	X			X
Cocconeis distans Gregory	p. 287; Pl. 41:4,5		X	X				X
Cocconeis heteroidea Hantzsch	p. 287; Pl. 40:6,7, 41:1–3	X	X	X	X	X		X
Cocconeis scutellum Ehrenberg	p. 288; Pl. 41:6,7	X	X	X	X	X		X
Cocconeis scutellum var *ornata* Grunow	p. 288; Pl. 42:1–3	X						
Cyclophora tenuis Castracane	2	X		X		X		X
Cyclophora castracanei Ashworth & Lobban	9	X						
Cylophora minor Ashworth & Lobban	9	X						
Cyclophora taballariformis Ashworth & Lobban	9	X						
Cymatoneis sulcata (Greville) Cleve	p. 292; Pl. 47:1		X	X				X
Diploneis bombus Ehrenberg	p. 289; Pl. 43:2–5		X	X	X	X		X
Diploneis chersonensis (Grunow) Cleve	p. 289; Pl. 44:1–4	X	X		X	X	X	X
Diploneis crabro Ehrenberg	p. 290; Pl. 44:5, 45:1,2	X	X	X	X	X	X	X
Diploneis smithii (de Brébisson) Cleve	p. 290; Pl. 45:3–6, 46:1	X	X	X	X	X	X	X
Diploneis suborbicularis (Gregory) Cleve	p. 291; Pl. 46:2–4	X	X	X	X	X	X	X
Diploneis weissflogii (A. Schmidt) Cleve	p. 291; Pl. 46:5–7	X		X	X	X	X	X

Taxon	Guam Index: Reference[b] or page + figures in this paper	Guam FFTs[c]	Society Islands	Mahé	Puerto Rico [H]	Puerto Rico [NN]	The Bahamas	Caribbean Sea
Donkinia minuta (Donkin) Ralfs in Pritchard	p. 295; Pl. 50:5,6, 51:1	X						
Entomoneis corrugata (Giffen) Witkowski, Lange-Bertalot & Metzeltin	2							
Falcula parcelsiana Voigt	p. 255; Pl. 11:1–6	X						
Florella pascuensis Navarro	p. 261; Pl. 18:4,5	X						
Gato hyalinus Lobban & Navarro	7	X						
Gomphonemopsis littoralis (Hendey) Medlin	p. 264; Pl. 22:1–3	X						
Grammatophora angulosa Ehenberg	p. 262; Pl. 19:1,2	X				X		X
Grammatophora macilenta Wm. Smith	p. 262; Pl. 19:3–5	X	X	X	X			X
Grammatophora oceanica (Ehrenberg pro parte) Grunow (var. *oceanica*)	p. 262; Pl. 19:6–8	X	X	X	X			X
Grammatophora undulata Ehrenberg	p. 263; Pl. 19:3, 20:1–3, 43:2	X	X	X		X		X
Haslea howeana (Hagelstein) Giffen	p. 291; Pl. 47:6, 7	X		X			X	X
Hemiaulus hauckii Grunow in Van Heurck	p. 252; Pl. 8:4		X			X		X
Hyalosira interrupta (Ehrenberg) Navarro	p. 261; Pl. 1:3, Pl. 18:6,7	X	X	X		X	X	X
Hyalosira tropicalis Navarro	2	X				X		X
Hyalosynedra laevigata (Grunow) Williams & Round	2	X	X		X		X	X
Hydrosilicon mitra Brun	p. 306; Pl. 66:5							
Isthmia minima Harvey & Bailey	p. 251; Pl. 7:4–6	X	X			X	X	X

Taxon	Guam Index: Reference[b] or page + figures in this paper	Guam FFTs[c]	Society Islands	Mahé	Puerto Rico [H]	Puerto Rico [NN]	The Bahamas	Caribbean Sea
Koernerella recticostata (Körner) Ashworth, Lobban & Theriot	6	X						
Lampriscus orbiculatus (Shadbolt) Peragallo & Peragallo	2	X				X		X
Lampriscus shadboltianus var. *crenulatus* (Grunow) Navarro	2	X				X		X
Licmophora abbreviata Agardh	10			X		X		X
Licmophora aff. *ehrenbergii* (Kützing) Grunow	10							
Licmophora flabellata (Carmichael ex Greville) C. Agardh	5	X		X	X			X
Licmophora flucticulata Lobban, Schefter & Ruck	5	X						
Licmophora remulus Grunow	2, 5	X		X	X	X	X	X
Licmosphenia albertmannii Lobban	10	X						
Licmosphenia leuduger-fortmorelii Lobban	10	X						
Licmosphenia peragallioides Lobban	10	X						
Lithodesmioides polymorpha von Stosch	p. 252; Pl. 8:5,6							
Lyrella hennedyi (W. Smith) Stickle & D.G. Mann	p. 263; Pl. 20:6	X			X	X		X
Lyrella hennedyi var. *granulosa* Grunow	p. 263; Pl. 20:7,8	X	X					
Lyrella lyra (Ehrenberg) Karayeva	2	X	X	X	X	X		X
Mastogloia achnanthioides Mann	p. 265; Pl. 22:4,5	X	X					

Taxon	Guam Index: Reference[b] or page + figures in this paper	Guam FFTs[c]	Society Islands	Mahé	Puerto Rico [H]	Puerto Rico [NN]	The Bahamas	Caribbean Sea
Mastogloia acutiuscula var. *elliptica* Hustedt	p. 265; Pl. 22:6–8	X	X	X		X		X
Mastogloia adriatica var. *linearis* Voigt	p. 265; Pl. 22:9,10							
Mastogloia angulata Lewis	p. 266; Pl. 23:1,2	X	X			X	X	X
Mastogloia barbadensis (Greville) Cleve	p. 266; Pl. 43:3							X
Mastogloia binotata (Grunow) Cleve	p. 266; Pl. 23:4,5	X	X	X	X	X		X
Mastogloia borneensis Hustedt	p. 267; Pl. 23:6–8	X	X					
Mastogloia cannii Kemp & Paddock	p. 267; Pl. 24:1–3	X						
Mastogloia capitata var. *lanceolata* (Wallich) Hustedt	p. 268; Pl. 24:4–7	X	X					
Mastogloia ciskeiensis Giffen	7 & p. 268; Pl. 25:1–3	X		X				
Mastogloia citrus Cleve	p. 269; Pl. 25:4,5	X	X		X	X	X	X
Mastogloia cocconeiformis Grunow	p. 269; Pl. 25:6,7	X	X	X		X	X	X
Mastogloia corsicana Grunow	p. 269; Pl. 26:1–3	X	X	X		X	X	X
Mastogloia cribrosa Grunow	p. 270; Pl. 26:4,5	X		X		X	X	X
Mastogloia crucicula (Grunow) Cleve	p. 270; Pl. 26:6,7, 27:1	X	X	X	X	X	X	X
Mastogloia crucicula var. *alternans* Zanon	p. 270; Pl. 26:8	X					X	
Mastogloia cuneata (Meister) Simonsen	7 & p. 271; Pl. 27:2,3	X					X	
Mastogloia cyclops Voigt	p. 271; Pl. 27:4,5	X	X					
Mastogloia decussata Grunow	p. 272; Pl. 27:6,7	X	X	X			X	X
Mastogloia dicephala Voigt	p. 272; Pl. 27:8,9							

Taxon	Guam Index: Reference[b] or page + figures in this paper	Guam FFTs[c]	Society Islands	Mahé	Puerto Rico [H]	Puerto Rico [NN]	The Bahamas	Caribbean Sea
Mastogloia erythraea Grunow var. *erythraea*	p. 272; Pl. 27:10,11, 28:1,2	X	X	X	X	X	X	X
Mastogloia erythraea var. *grunowi* Foged	p. 273; Pl. 28:3	X				X	X	X
Mastogloia exilis Hustedt	p. 273; Pl. 28:6,7	X	X					
Mastogloia fimbriata (Brightwell) Cleve	2 & p. 273; Pl. 28:8–11	X	X	X	X	X	X	X
Mastogloia gomphonemoides Hustedt	p. 273; Pl. 28:4,5	X		X				
Mastogloia graciloides Hustedt	p. 274; Pl. 28:12,13			X				X
Mastogloia horvathiana Grunow	p. 274; Pl. 29:1,2	X	X	X	X	X	X	X
Mastogloia hustedtii Meister	p. 274; Pl. 29:3–5	X	X			X		X
Mastogloia inaequalis Cleve	p. 275; Pl. 29:6–8	X	X	X	X			X
Mastogloia jelinecki Grunow	p. 275; Pl. 30:1–3	X		X	X	X	X	
Mastogloia kjellmanii Cleve	p. 276; Pl. 30:4,5	X	X			X		X
Mastogloia lacrimata Voigt	p. 276; Pl. 30:6–8	X					X	
Mastogloia laterostrata Hustedt	p. 276; Pl. 31:3							
Mastogloia lineata Cleve and Grove	p. 277; Pl. 31:1,2			X			X	
Mastogloia lyra Lobban & Pennesi	11							
Mastogloia macdonaldii Greville	p. 277; Pl. 31:4,5	X						
Mastogloia manokwariensis Cholnoky	p. 277; Pl. 32:1–3	X	X			X	X	X
Mastogloia mauritiana Brun	p. 278; Pl. 32:4–10	X	X				X	X
Mastogloia mediterranea Hustedt	p. 278; Pl. 33:1,2	X						

Taxon	Guam Index: Reference[b] or page + figures in this paper	Guam FFTs[c]	Society Islands	Mahé	Puerto Rico [H]	Puerto Rico [NN]	The Bahamas	Caribbean Sea
Mastogloia neoborneensis Pennesi & Totti	p. 278; Pl. 33:3	X						
Mastogloia ovalis A. Schmidt	p. 279; Pl. 33:4–6	X	X	X		X	X	X
Mastogloia ovata Grunow	p. 279, Pl. 33:7,8	X			X		X	X
Mastogloia ovulum Hustedt	p. 280; Pl. 33:9,10	X	X	X		X	X	X
Mastogloia ovum-paschale (A. Schmidt) A. Mann	p. 280; Pl. 34:1,2	X	X					X
Mastogloia paradoxa Grunow	p. 280; Pl. 34:3–5	X				X	X	X
Mastogloia parlibellioides Lobban & Pennesi	11	X						
Mastogloia pseudolatecostata Yohn & Gibson	p. 281; Pl. 35:1,2	X					X	
Mastogloia pulchella Cleve	p. 281; Pl. 35:3,4	X	X	X				
Mastogloia punctatissima (Greville) Ricard	p. 281; Pl. 35:7,8	X	X			X	X	X
Mastogloia rhombica Cleve	p. 282; Pl. 35:5,6	X	X			X		X
Mastogloia rimosa Cleve	p. 282: Pl. 36:1,2	X					X	
Mastogloia robusta Hustedt	p. 282; Pl. 36:3–6	X		X				
Mastogloia rostrata (Wallich) Hustedt	p. 282; Pl. 36:9,10	X	X					X
Mastogloia sergensis Pennesi & Poulin	p. 283; Pl. 36:7,8, 38:1,2	X						
Mastogloia tautirensis Ricard	p. 283; Pl. 37:3–5	X	X					
Mastogloia tenuis Hustedt	p. 284; Pl. 37:6–8	X	X	X				
Mastogloia umbra Paddock & Kemp	p. 284; Pl. 37:9	X						
Mastogloiopsis biseriata Lobban & Navarro	7							
Mastoneis biformis (Grunow) Cleve	7			X		X	X	

Taxon	Guam Index: Reference[b] or page + figures in this paper	Guam FFTs[c]	Society Islands	Mahé	Puerto Rico [H]	Puerto Rico [NN]	The Bahamas	Caribbean Sea
Melosira nummuloides C.A. Agardh	2			X	X			X
Nanofrustulum shiloi (Lee, Reimer & McEnery) Round, Hallsteinsen & Paasche	2						X	
Navicula cancellata Donkin	p. 292; Pl. 47:2–5		X	X	X	X		?
Navicula consors A. Schmidt	p. 293; Pl. 47:8	X	X					X
Navicula mannii Hagelstein	p. 293; Pl. 47:9	X			X	X		X
Navicula plicatula Grunow	p. 293; Pl. 48:1–3		X					X
Neofragilaria nicobarica Desikachary, Prasad & Prema	p. 254; Pl. 10:1,2	X					X	
Neosynedra provincialis (Grunow) Williams & Round	2	X		X	X			X
Neosynedra tortosa (Grunow) Williams & Round	p. 255; Pl. 12:1	X		?	X			X
Nitzschia angularis W. Smith	p. 301; Pl. 59:3–5	X	X	X	X	X		X
Nitzschia constricta (Gregory) Grunow	p. 301; Pl. 59:6–8	X		X	X	X		X
Nitzschia dissipata (Kützing) Grunow	p. 301; Pl. 60:1–3	X		X	X			X
Nitzschia granulata Grunow	p. 302; Pl. 60:4				X			X
Nitzschia lanceola Grunow	p. 302; Pl. 60:5–8				X			X
Nitzschia longissima (Brébisson ex Kützing) Ralfs in Prichard	p. 302; Pl. 60:9, 61:1	X	X	X	X	X	X	X
Nitzschia marginulata var. *didyma* Grunow	p. 303; Pl. 61:2,3	X			X	X		
Nitzschia martiana (C.A. Agardh) van Heurck	1	X						X
Nitzschia sigma var. *intercedens* Grunow	p. 303; Pl. 2:9,10; 61:4	X			X			X

Taxon	Guam Index: Reference[b] or page + figures in this paper	Guam FFTs[c]	Society Islands	Mahé	Puerto Rico [H]	Puerto Rico [NN]	The Bahamas	Caribbean Sea
Nitzschia ventricosa Kitton	p. 304; Pl. 62:1,2	X	X	X	X	X		X
Nitzschia vidovichii Grunow	2	X	X	X	X	X		X
Odontella aurita (Lyngbye) C.A. Agardh	p. 250; Pl. 6:1,2					X	X	X
"Oestrupia 4" *sensu* Hein et al. 2008	p. 294; Pl. 50:4	X					X	
Olifantiella pilosella Riaux-Gobin	p. 264; Pl. 21:2–7	X						
Paralia longispina Konno & Jordan	p. 249; Pl. 4:5–7	X						
Parlibellus berkeleyi (Kützing) Cox	2							
Parlibellus hamulifer (Grunow) De Toni	p. 289; Pl. 42:6	X		X	X	X		X
Perideraion decipiens Lobban	6	X						
Perideraion elongatum Jordan, Arai et Lobban	6	X						
Perideraion montgomeryi Lobban, Jordan & Ashworth	6	X						
Perissonoë cruciata (Janisch & Rabenhorst) Andrews & Stoelzel	p. 258; Pl. 14:1,2	X	X		X	X	X	X
Petrodictyon patrimonii (Sterrenburg) Sterrenburg	p. 306; Pl. 66:2,3	X						
Petroneis granulata (Bailey) D.G. Mann	p. 264; Pl. 21:1	X	X		X			X
Plagiodiscus martensianus Grunow & Eulenstein	p. 307; Pl. 67:1	X	X					
Plagiodiscus nervatus Grunow emend Paddock	p. 307; Pl. 66:4,5	X	X	X		X	X	
Plagiogramma staurophorum (Gregory) Heiberg	p. 254; Pl. 10:3–5		X	X	X			X
Plagiotropis lepidoptera (Gregory) Kuntze	p. 295; Pl. 51:5–8	X	X	X	X	X	X	X

Taxon	Guam Index: Reference[b] or page + figures in this paper	Guam FFTs[c]	Society Islands	Mahé	Puerto Rico [H]	Puerto Rico [NN]	The Bahamas	Caribbean Sea
Planothidium campechianum (Hustedt) Witkowski, Lange-Berthalot & Metzeltin	p. 285; Pl. 39:4	X						
Pleurosigma intermedium Wm. Smith	p. 295; Pl. 51:2–4	X		X	X	X		X
Podocystis adriatica Kützing	p. 256; Pl. 12:2,3	X	X	X	X	X	X	X
Podocystis spathulata (Shadbolt) Grunow	p. 256; Pl. 12:4–6	X	X	X		X		X
Podosira baldjickiana Grunow	p. 247; Pl. 3:3–6	X						
Podosira hormoides (Montagne) Kützing	p. 248; Pl. 4:1,2	X	X	X	X			X
Podosira montagnei Kützing	p. 248; Pl. 4:3,4	X			X			X
Proboscia alata (Brightwell) Sundström	p. 253; Pl. 9:1,2		X			X		X
Proschkinia complanatoides (Hustedt) Karayeva	p. 296; Pl. 1:4–6, 52:6, 53:1–4	X						
Psammodicyton panduriforme (Gregory) D.G. Mann	p. 304; Pl. 62:3,4	X	X	X	X	X		X
Psammodiscus nitidus (Gregory) Round and Mann	p. 258; Pl. 14:6,7	X	X		X	X	X	X
Psammoneis japonica S. Sato, Kooistra & Medlin	p. 254; Pl. 10:6,7							
Rhabdonema adriaticum Kützing	p. 261; Pl. 18:1–3	X	X		X	X		X
Rhaphoneis amphiceros (Ehrenberg) Ehrenberg	p. 258; Pl. 14:3,4	X	X	X	X		X	X
Rhaphoneis castracanii Grunow	p. 258; Pl. 14:5							
Rhopalodia guettingeri Krammer	3	X					X	
Rhopalodia musculus (Kützing) Müller	2	X	X	X				

Taxon	Guam Index: Reference[b] or page + figures in this paper	Guam FFTs[c]	Society Islands	Mahé	Puerto Rico [H]	Puerto Rico [NN]	The Bahamas	Caribbean Sea
Roundia cardiophora (Round) Makarova	p. 247; Pl. 3:1,2	X						
Stauroneis retrostauron (Mann) Meister	p. 296; Pl. 52:4,5	X						
Staurotropis seychellensis (Giffen) Paddock	p. 296; Pl. 52:1–3			X				
Stictocyclus stictodiscus (Grunow) Ross	2	X						
Striatella unipunctata (Lyngbye) Agardh	p. 263; Pl. 20:4,5	X	X	X	X	X	X	X
Surirella fastuosa (Ehrenberg) Kützing	p. 307; Pl. 67:2,3, 68:1–3	X	X	X	X	X	X	X
Surirella scalaris Giffen	p. 308; Pl. 68:4–6, 69:1,2	X					X	
Synedra bacillaris (Grunow) Hustedt	p. 256; Pl. 13:1,2	X	X				X	X
Synedra lata (Giffen) Witkowski	p. 257; Pl. 13:3,4	X		X				
Tabularia fasciculata (C.A. Agardh) Williams & Round	p. 257; Pl. 13:5	X				X		X
Tabularia parva (Kützing) Williams & Round	p. 257; Pl. 13:6,7	X				X		X
Thalassiophysa hyalina Paddock & Sims	p. 300; Pl. 2:1–8, 58:1	X					X	
Toxarium hennedyanum (Gregory) Pelletan	p. 260; Pl. 17:1–5	X	X	X	X	X	X	X
Toxarium undulatum Bailey ex Bailey	p. 260; Pl. 17:6–8	X	X	X	X	X	X	X
Trachyneis aspera (Ehrenberg) Cleve	p. 293; Pl. 48:4–9	X	X	X	X	X	X	X
Trachyneis velata A. Schmidt	p. 293; Pl. 49:1,2	X		X	X			X
Triceratium dictyotum (Roper) Ross & Sims	p. 250; Pl. 6:3,4					X		X
Triceratium dubium Brightwell	2	X	X	X	X	X		X

Taxon	Guam Index: Reference[b] or page + figures in this paper	Guam FFTs[c]	Society Islands	Mahé	Puerto Rico [H]	Puerto Rico [NN]	The Bahamas	Caribbean Sea
Triceratium pulchellum (Grunow) Grunow	p. 250; Pl. 6:5–7, 7:1,2							
Trigonium diaphanum A. Mann	p. 252; Pl. 8:1–2	X				X		X
Trigonium formosum f. *pentagonale* Hustedt	2	X				X		X
Trigonium formosum f. *quadrangularis* (Greville) Desikachary & Sreelatha	p. 252; Pl. 8:3	X	X			X		X
Undatella lineata (Greville) Paddock & Sims	p. 299; Pl. 57:1,2	X						
Undatella quadrata (Brébisson ex Kützing) Paddock & Sims	p. 300; Pl. 57:3–6	X						X
Totals	**237**	**193**	**101**	**92**	**76**	**95**	**69**	**135**
Percent of our records in these lists			**41**	**38**	**31**	**39**	**28**	**55**

[a] References to other studies: Tahiti (Ricard 1974, 1975, 1977), Mahé (Seychelles) (Giffen 1980), Puerto Rico [H] (Hagelsetin 1939, Puerto Rico records only), Puerto Rico [NN] (Navarro 1981a, b, 1982a–c, 1983a, b, 1987; Navarro & Williams 1991; Navarro et al. 1989), The Bahamas (Hein et al. 2008), and the Caribbean Sea (Navarro & Hernández-Becerril 1997).

[b] References to previous Guam records: 1. Lobban and Tsuda (2003); 2. Navarro & Lobban (2009); 3. Lobban & Jordan 2010; 4. Lobban et al. (2010); 5. Lobban et al. (2011a); 6. Lobban et al. (2011b); 7. Lobban & Navarro (2012a); 8. Lobban & Navarro (in press); 9. Ashworth et al. (2012); 10. Lobban (in press); 11. Lobban & Pennesi (submitted)

[c] Species recorded in samples from farmer-fish territories, excluding planktonic taxa presumably deposited allochthonously.

Plate 1.
Color photomicrographs of live cells.
Figs 1, 2. Colonies of *Ardissonea fulgens* var. *gigantea*, DIC and darkfield (GU44J-3, GU44Q-4 resp.).
Fig. 3. *Hyalosira interrupta*. Living cell in chain, showing confinement of plastids to irregular section between septa (GU44H).
Figs 4–6. Cells of *Proschkinia complanatoides* at various angles, showing plastid and stigma (arrow on Fig. 4), DIC (GU62A-7).
Figs. 7–9. Cell of *Amphora decussata* at three focal planes showing plastid and valve structure (GU44AK-6). Arrow on Fig. 8 indicates the conopeum.
Scale bars: Figs 1, 2 = 250 μm, Fig. 3 = 20 μm, Figs 4–9 = 10 μm.

Plate 1

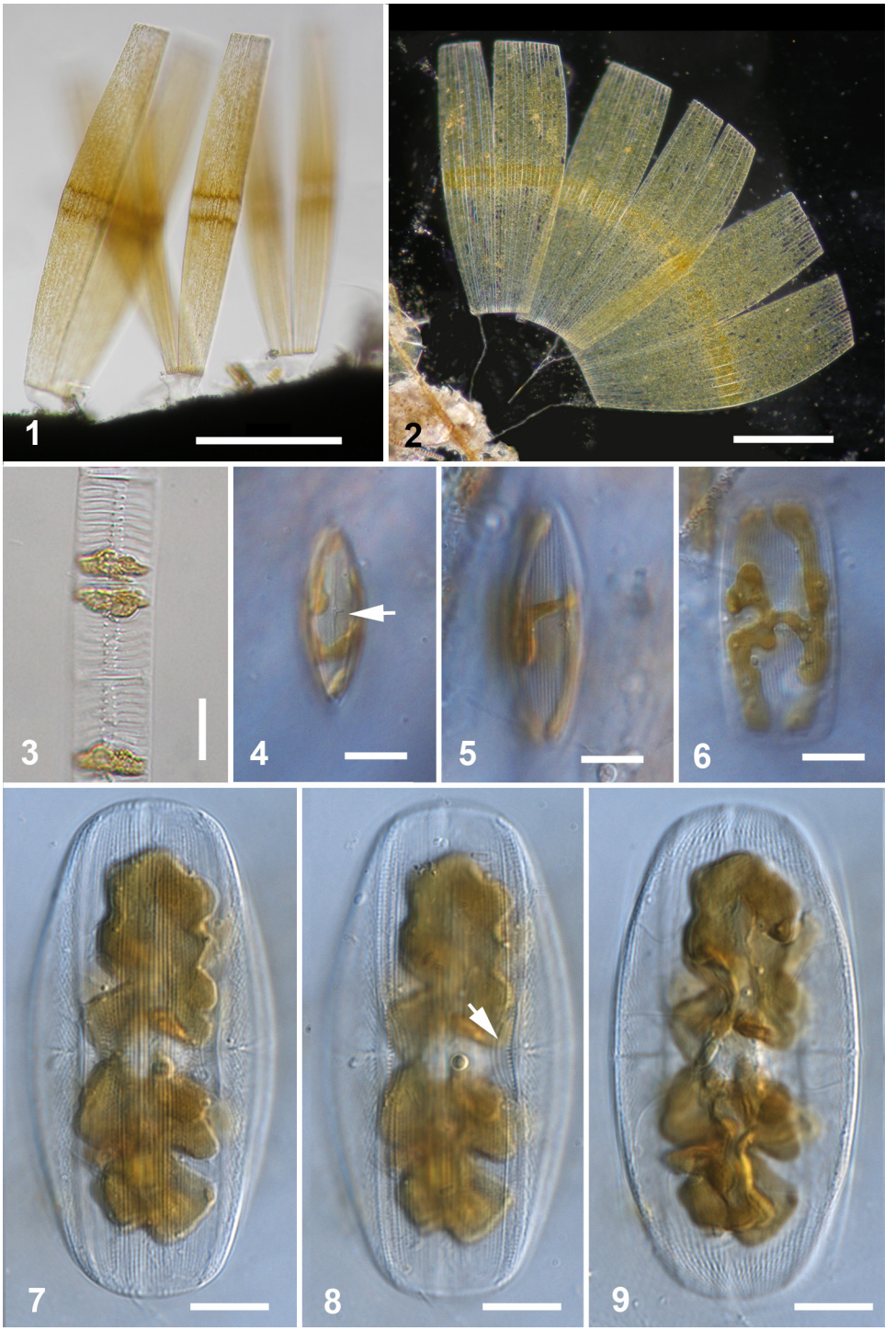

Plate 2.
Color photomicrographs of live cells, DIC.
Figs 1–8. *Thalassiophysa hyalina* (GU7S).
Figs 1, 2. Valve in ventral view at two focal planes.
Figs 3–8. Single live cell in various positions on a seaweed filament.
Figs. 9, 10. *Nitzschia sigma* var. *intercedens* pair of cells full length and enlarged to show plastids (GU44AR-2).
Scale bars: Figs 1–8 = *ca*. 50 μm (bar on Fig. 2 applies to Figs 1, 2; bar on Fig. 3 applies to Figs 3–8), Fig. 9 = 50 μm, Fig. 10 = 20 μm.

Plate 2

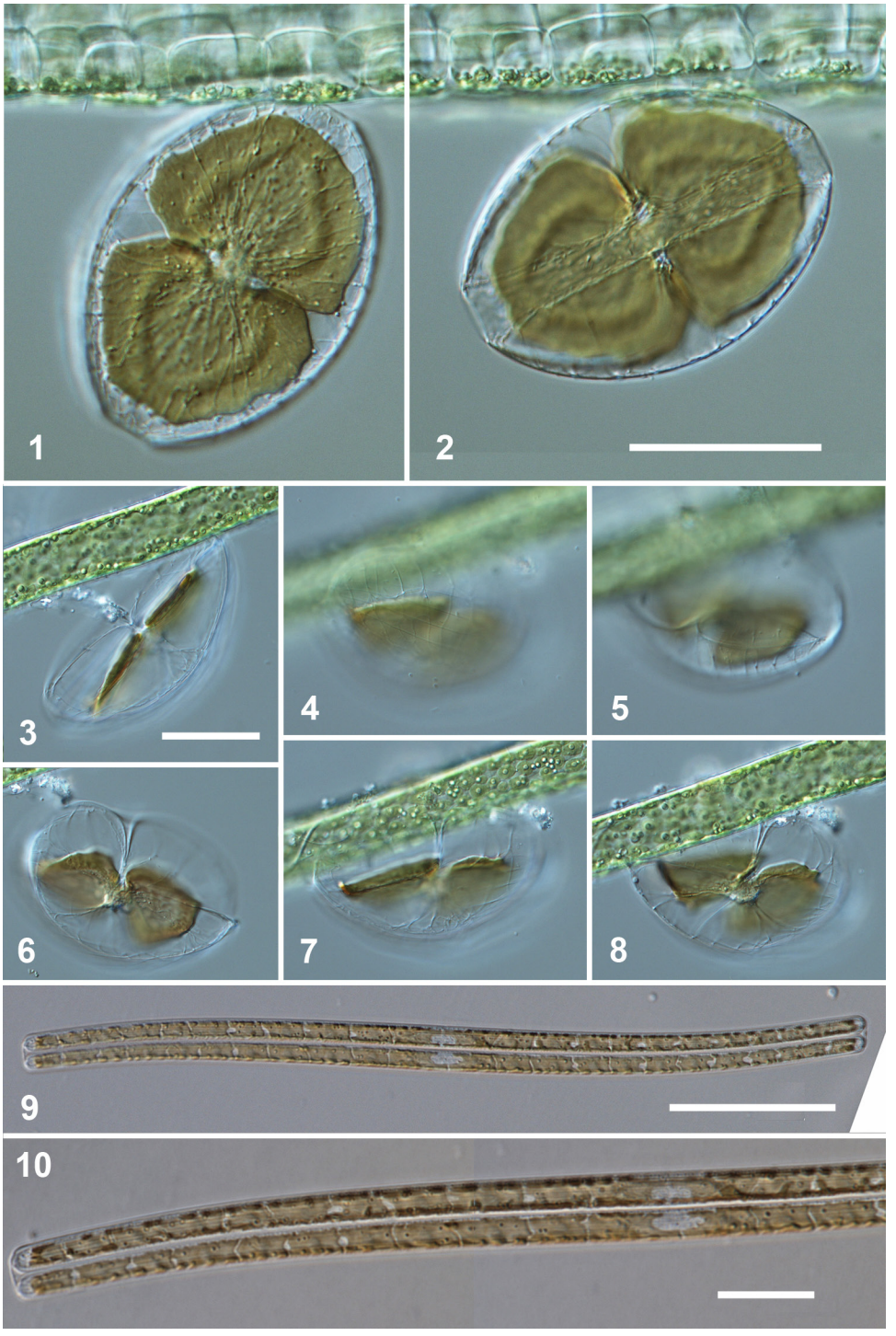

Plate 3.

Figs 1, 2. *Roundia cardiophora*, LM.

Fig. 1. Live cell in girdle view (ECT 3681).

Fig. 2. Acid-cleaned valve showing the fused fultoportulae (arrow) (GU44Z-15).

Figs 3–7. *Podosira baldjickiana*.

Figs 3, 4. Intact frustule at two focal planes, DIC (GU44AE-2).

Fig. 5. Valve with outer membrane eroded away showing rimoportulae (arrow), SEM (GU44I-2).

Figs 6, 7. Frustule on Van Heurck *Types* slide 545 matching the type drawing of *P. baldjickiana*, two focal planes, DIC.

Fig. 8. Frustule on Van Heurck *Types* slide 545 with similar shape to *P. baldjickiana* but markedly coarser and more irregular pattern, DIC.

Figs 6–8 taken and published with permission of Farlow Herbarium of Harvard University, Cambridge, Massachussetts.

Scale bars: Figs 1–4, 6–8 = 10 μm, Fig. 5 = 5 μm

Plate 3

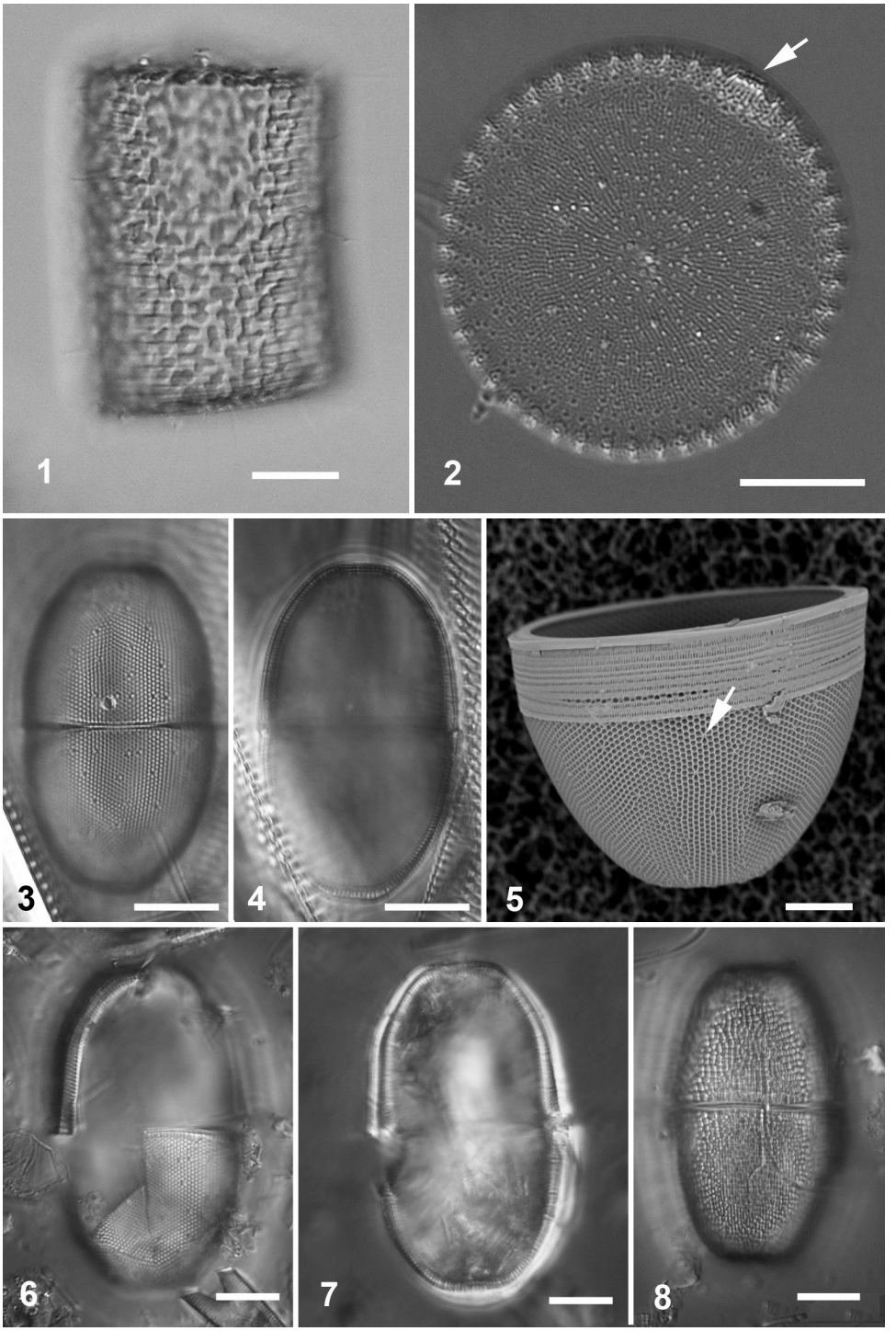

Plate 4.

Figs 1, 2. *Podosira hormoides*.

Fig. 1. Internal oblique view, SEM (GU44I-1).

Fig. 2. Pair of live cells showing plastids, DIC (sample).

Figs 3–5. *Podosira montagnei* whole frustules, DIC (GU44Z-15), SEM (GU44AC-4), and live (two focal planes stacked in Photoshop) (GU66A-4).

Figs 6–8. *Paralia longispina,* DIC at two focal planes (GU44I-1) and SEM (GU55B-4).

Scale bars: Figs 1–5 = 10 μm, Figs 6–8 = 5 μm.

Plate 4

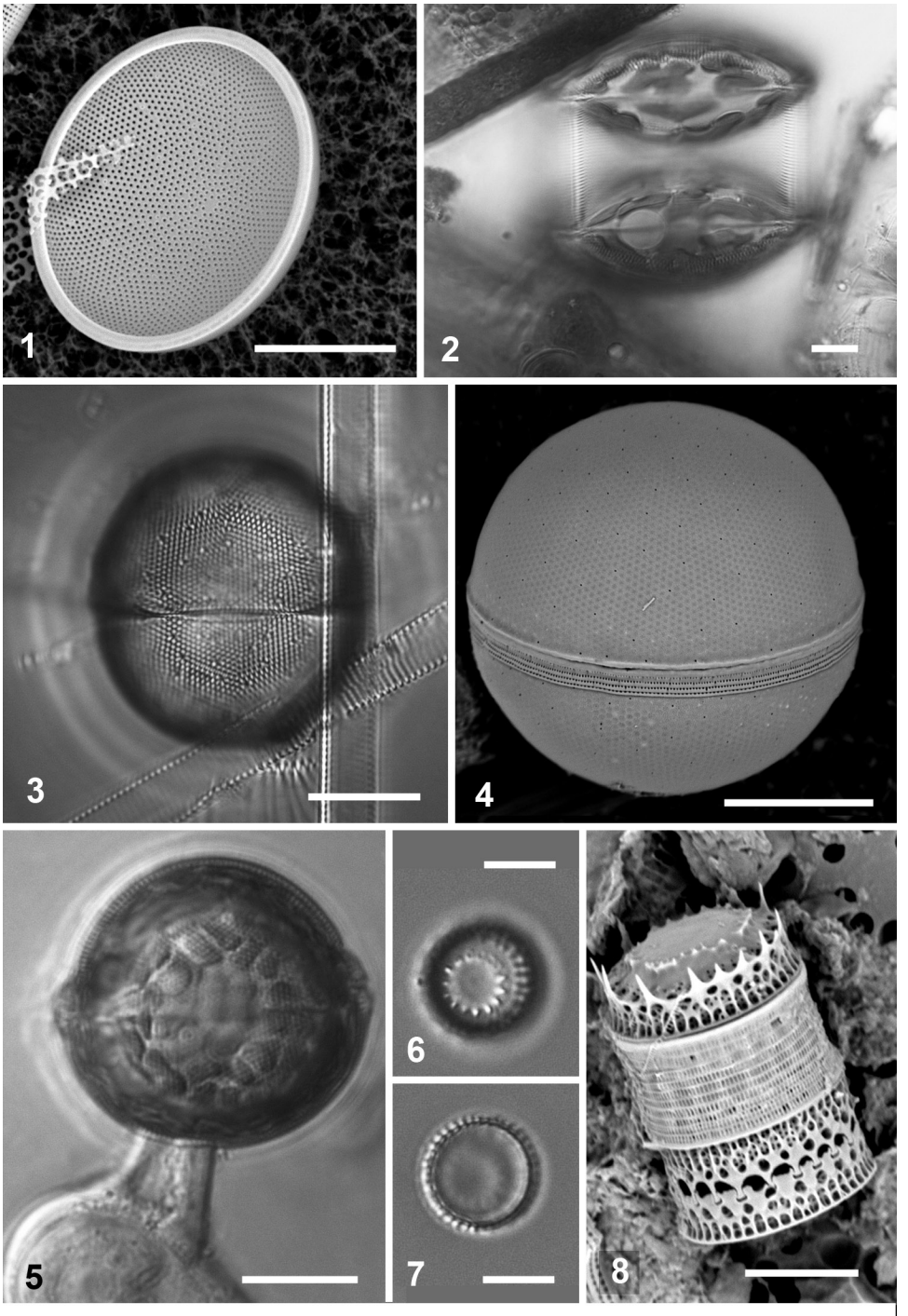

Plate 5.

Figs 1, 2. *Actinocyclus tenuissimus,* LM at two focal planes showing valve surface and rimoportulae (GU44Z-15). Arrow in Fig. 1 indicates the pseudonodulus.

Figs 3–5. *Aulacodiscus orientalis* SEM (ECT3746).

Fig. 3. Valve, slightly tilted, brightfield.

Fig. 4. External valve view.

Fig. 5. Frustule in girdle view, SEM.

Fig. 6. *Asterolampra marylandica*, internal view, SEM (ECT3754).

Scale bars: Figs 1, 2, 6 = 10 μm, Figs 3–5 = 20 μm.

Plate 5

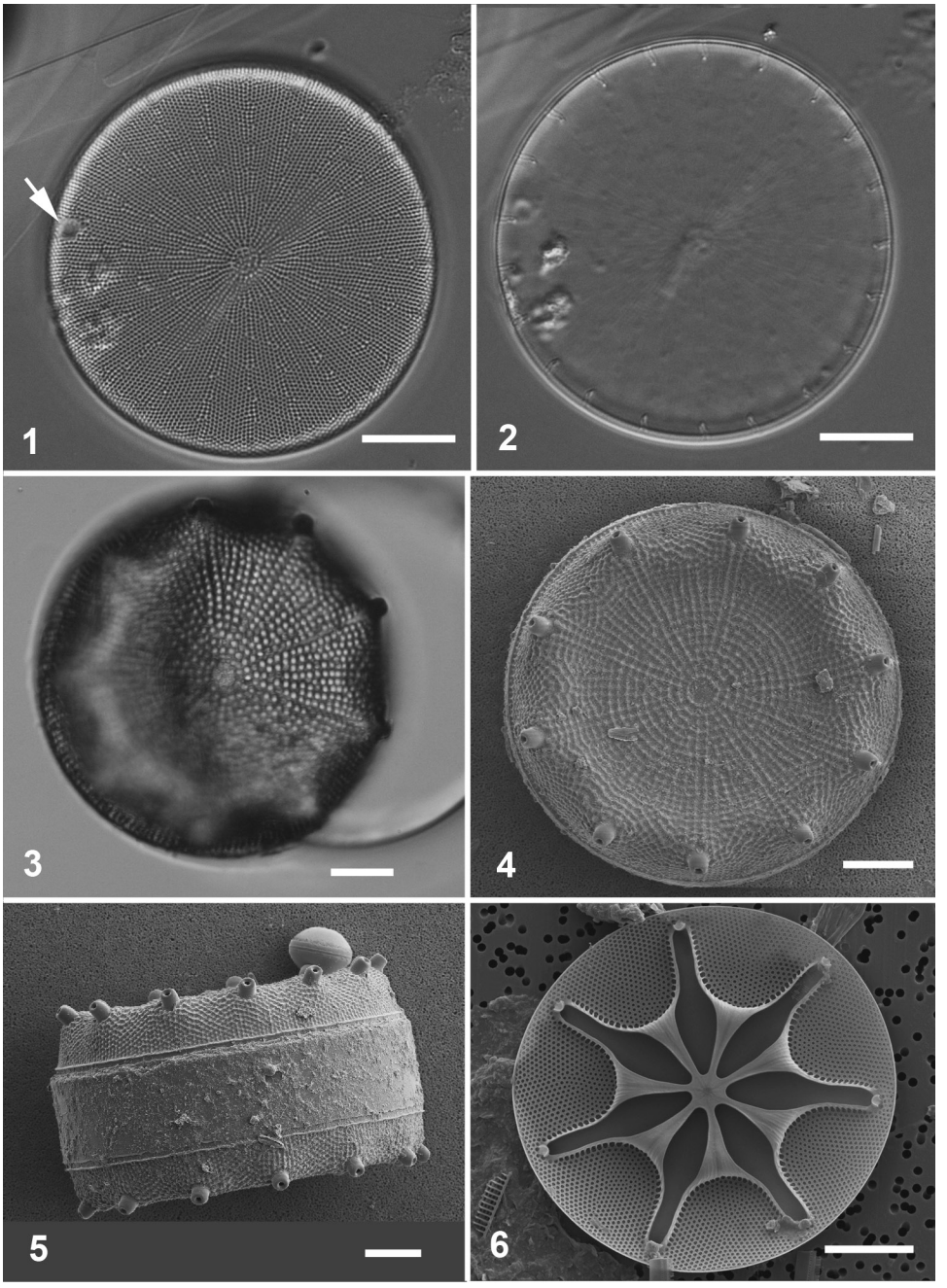

Plate 6.
Figs 1, 2. *Odontella aurita,* valve view, DIC (GU6D-2) and girdle view showing rimoportula (arrow), SEM (23vi08-1A).
Figs 3, 4. *Triceratium dictyotum* valve views in DIC and SEM; arrow points to rimoportula (GU32B).
Figs 5–7. *Triceratium pulchellum*, cell at three focal planes, showing rimoportulae (arrow) in highest focus, valve surface and valve margin. DIC (GU7N).
Scale bars: Figs 1, 2, 5–7 = 10 μm (bar on Fig. 5 applies to Figs 5–7), Figs 3, 4 = 20 μm.

Plate 6

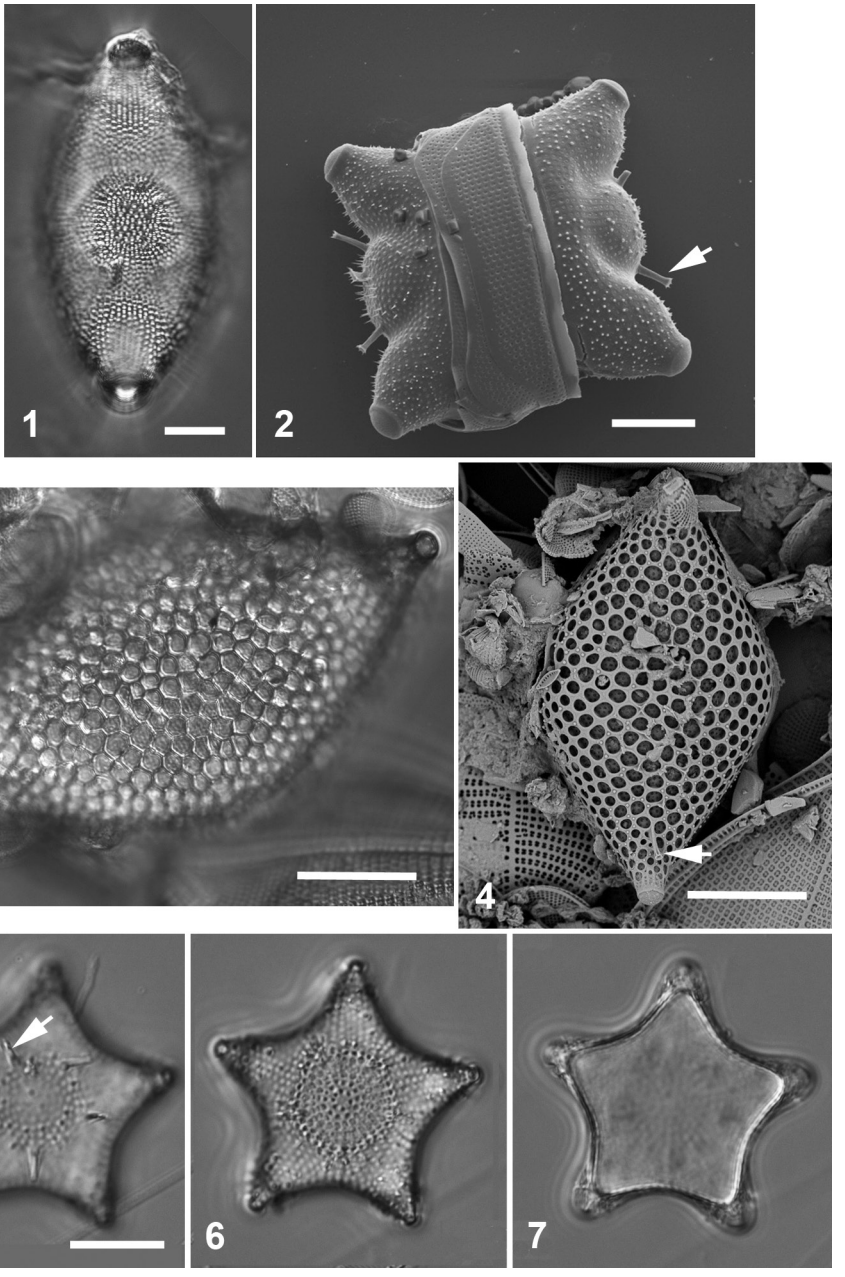

Plate 7.

Figs 1, 2. *Triceratium pulchellum*, exterior and interior views, SEM (GU7N).

Fig. 3. *Biddulphiopsis titiana,* cleaned valve, DIC (GU44I-2).

Figs 4–6. *Isthmia minima*.

Fig. 4. Whole acid cleaned frustule (wet mount, 3-dimensional shape retained), DIC (GU44Y-8).

Fig. 5. Detail of flattened epivalve showing the invaginated cribra (arrows), DIC (GU44Y-8).

Fig. 6. SEM (Marshall Is. specimen from sample M-2) showing detail of invaginated cribra (arrow) and rimoportulae (arrowhead).

Scale bars: Figs 1, 2, 5, 6 = 10 μm, Fig. 3 = 20 μm, Fig. 4 = 50 μm.

Plate 7

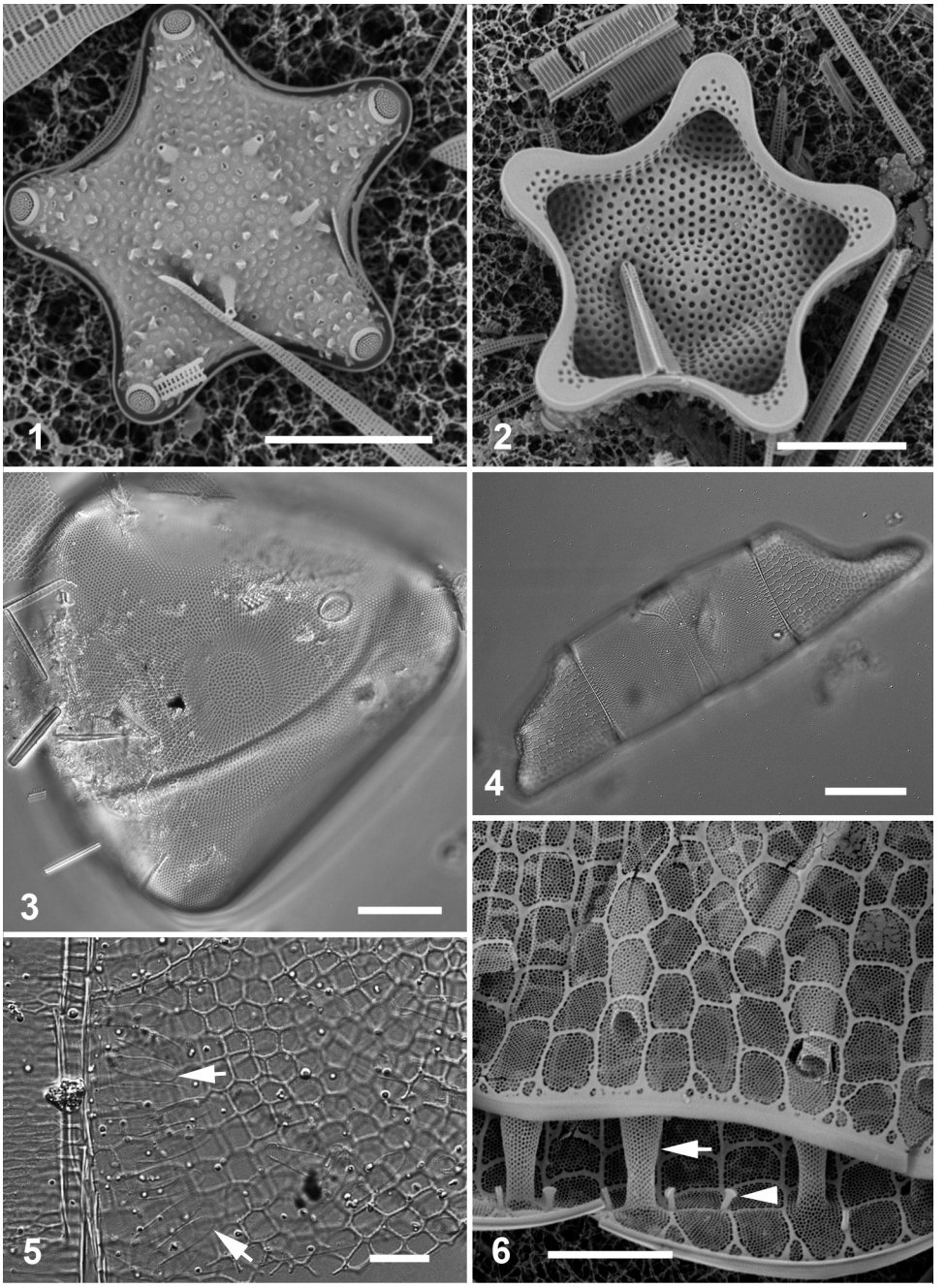

Plate 8. Figs 1, 2. *Trigonium diaphanum*.
Fig. 1. Valve in DIC (GU44I-1).
Fig. 2. Detail of valve surface showing transition in areolae (arrow; pole to upper right), SEM (GU44I-2).
Fig. 3. *Trigonium formosum* var. *quadrangularis*, voucher specimen from DNA preparation, showing uniform areolae, SEM (ECT 3671).
Fig. 4. *Hemiaulus hauckii*, valve, SEM (ECT 3753).
Figs 5, 6. *Lithodesmioides polymorpha*, valve and detail of center of valve showing external tube of rimoportula, SEM (ECT 3772).
Scale bars: Figs 1, 3–5 = 10 μm, Fig. 2 = 5 μm, Fig. 6 = 2 μm.

Plate 8

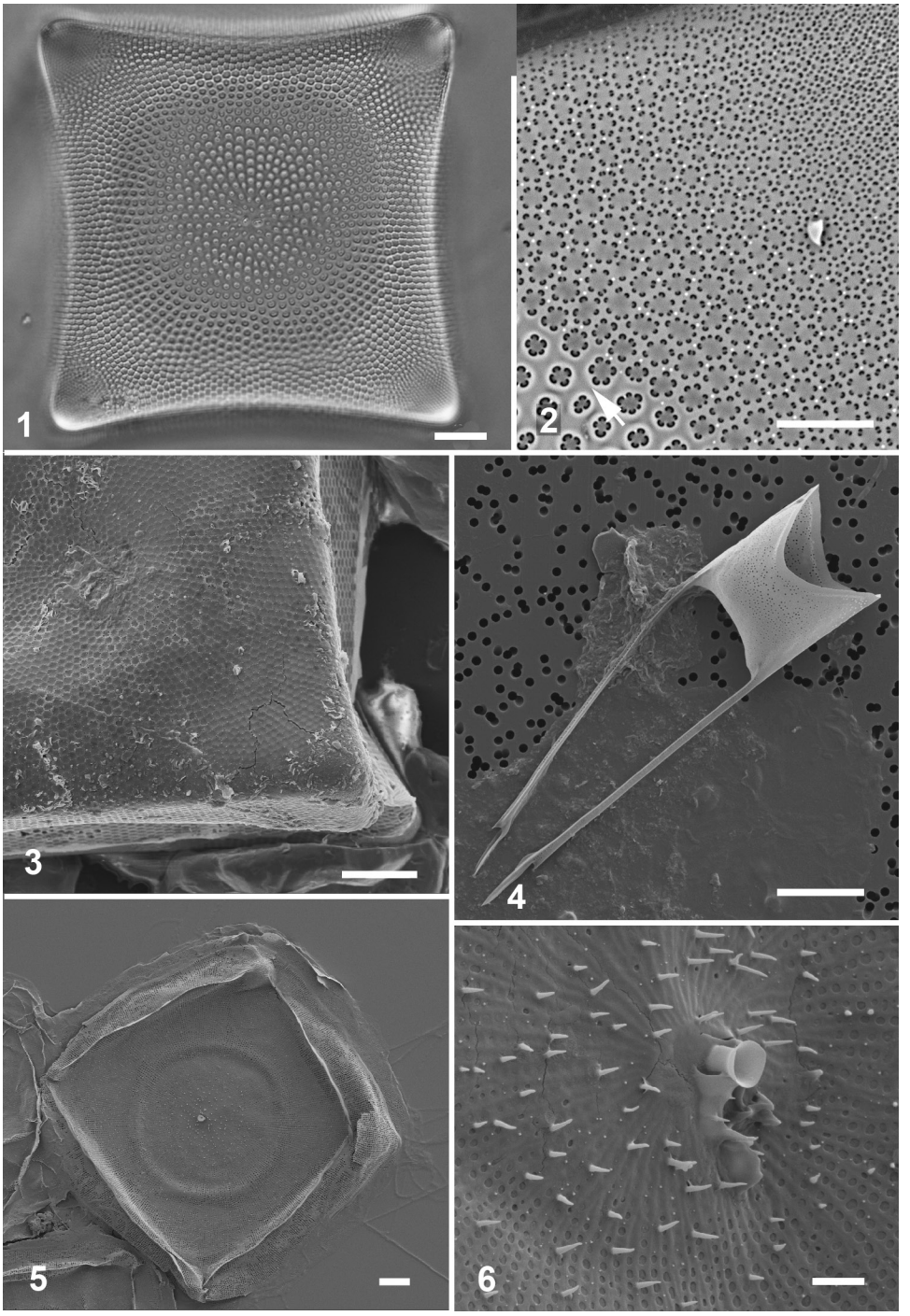

Plate 9.

Figs 1, 2. *Proboscia alata* (GU52J-3).

Fig. 1, Valve with some copulae, DIC.

Fig. 2, View of valve showing claspers, and a frustule of *Perideraion elongatum*, SEM.

Fig. 3. *Chaetoceros atlanticus* var. *skeleton*, two valves joined by the setae, SEM (GU55B-4).

Figs. 4, 5. *Chaetoceros peruvianus,* SEM (GU52J-3).

Fig. 4. Interlocked anterior (below) and posterior valves and portions of the setae.

Fig. 5. Anterior valve showing rimoportula (arrow).

Scale bars: Figs 1–3, 5 = 10 μm, Fig. 4 = 20 μm.

Plate 9

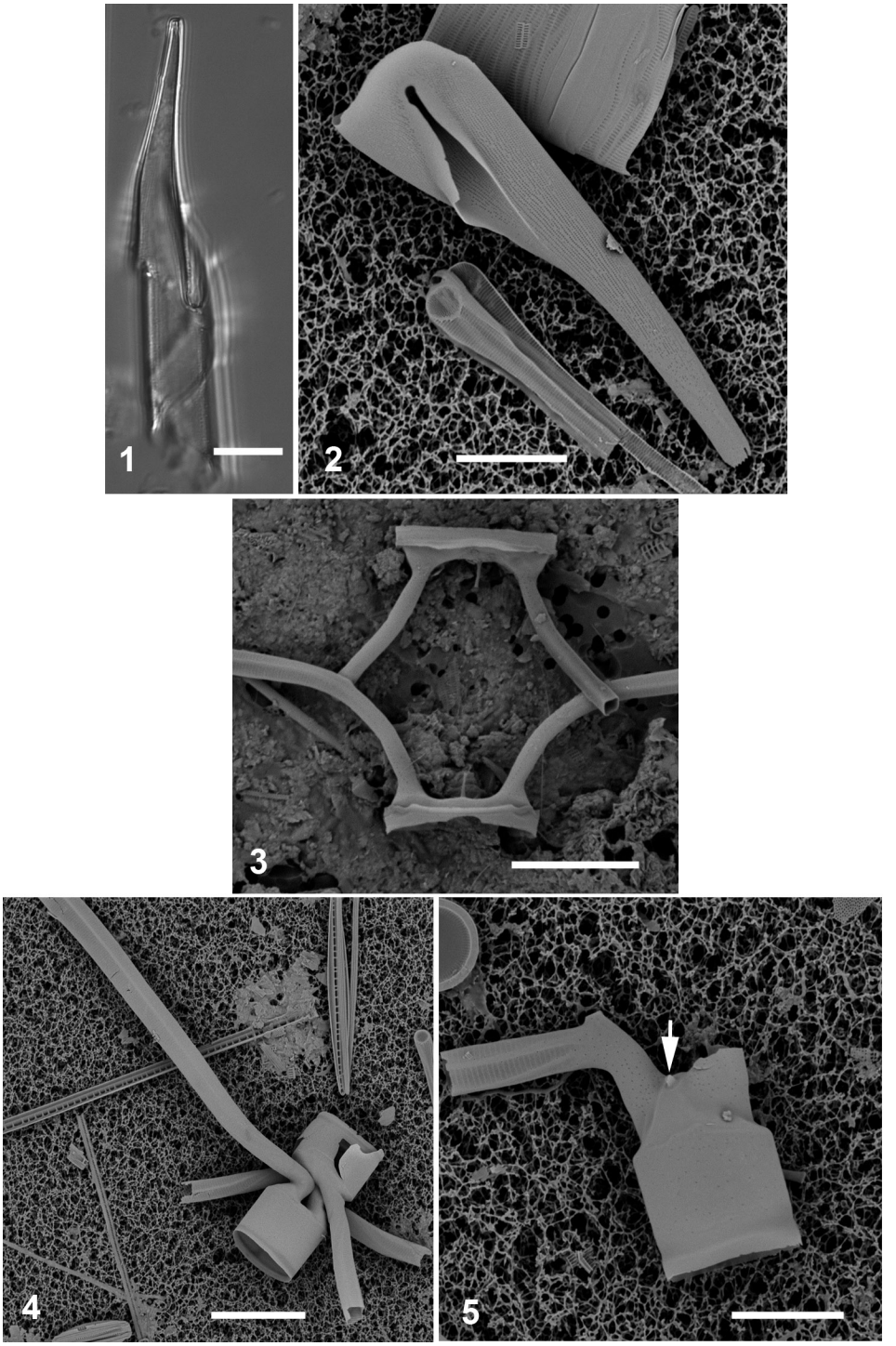

Plate 10.

Figs 1, 2. *Neofragilaria nicobarica* DIC (GU44AF-5) and SEM (GU44AK-1).

Figs 3–5. *Plagiogramma staurophorum,* LM.

Figs. 3, 4. Live and cleaned valve from culture (ECT 3776).

Fig. 5. Specimen in field material (GU26A).

Figs 6, 7. *Psammoneis japonica,* wild specimen (GU26A) and cultured specimen (GU52O), SEM.

Scale bars: Figs 1, 2, 4, 5 = 10 μm, Fig. 3 = 20 μm, Figs 6, 7 = 2 μm.

Plate 10

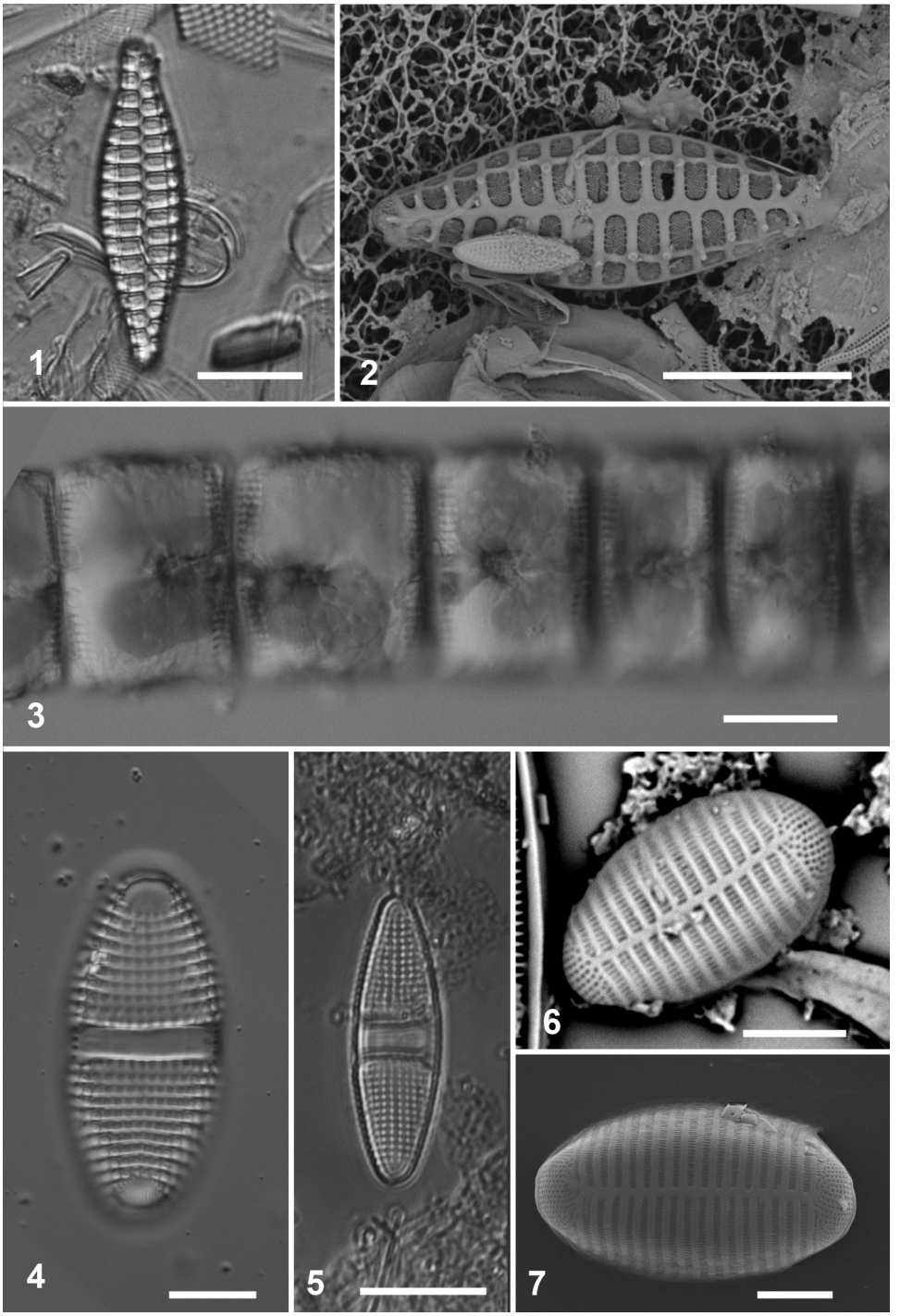

Plate 11.

Figs 1–6. *Falcula paracelsiana*.

Fig. 1. Live cell showing plastids, DIC (GU52K-4).

Fig. 2. Acid cleaned valve, DIC (GU14P).

Figs 3–6. Whole mounts in SEM (GU52K-4).

Fig. 3. Apices with slit fields.

Fig. 4. Detail of apex showing areolae, sternum (between two slightly offset lines of areolae, double-headed arrow), rimoportula (arrowhead), and apical slits.

Fig. 5. Apex showing internal aspect of rimoportula (arrowhead).

Fig. 6. Internal structure with inner silica membrane partially eroded.

Scale bars: Figs 1, 2 = 10 μm, Fig. 3 = 5 μm, Figs 4, 5 = 1 μm.

Plate 11

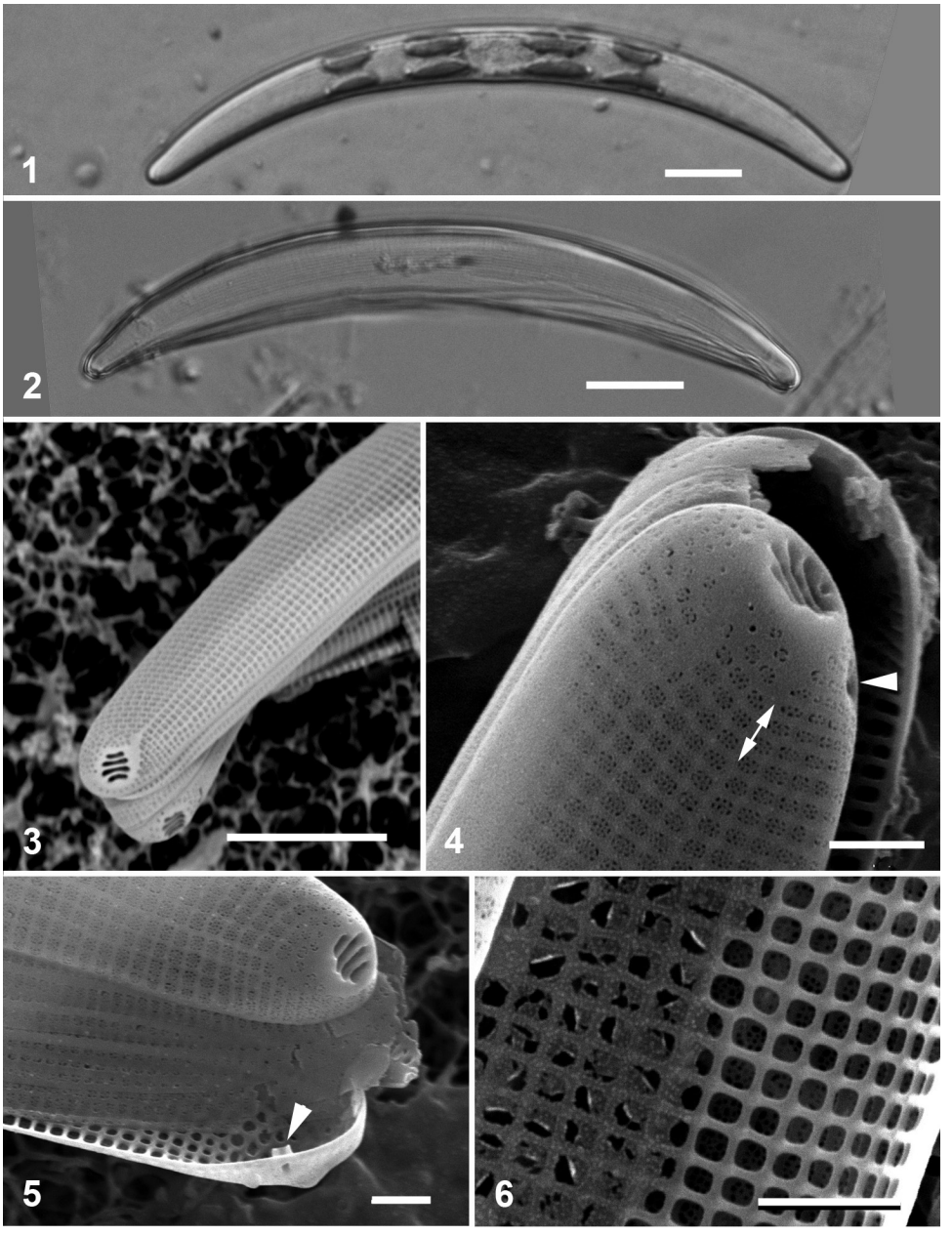

Plate 12.

Fig. 1. *Neosynedra tortosa*, frustule, DIC (GU52J-3).

Figs 2, 3. *Podocystis americana*, LM (GU6C) and external, SEM (GU44Y-13).

Figs 4–6. *Podocystis spathulata*.

Fig. 4. Internal view of whole valve showing rimoportulae on foot pole and head pole (arrows) and isolated pore (arrowhead) (GU44O-F).

Figs 5, 6. Details of foot poles with (arrow) and without rimoportula, SEM.

Scale bars: Figs 1–3, 5, 6 = 10 μm, Fig. 4 = 20 μm.

Plate 12

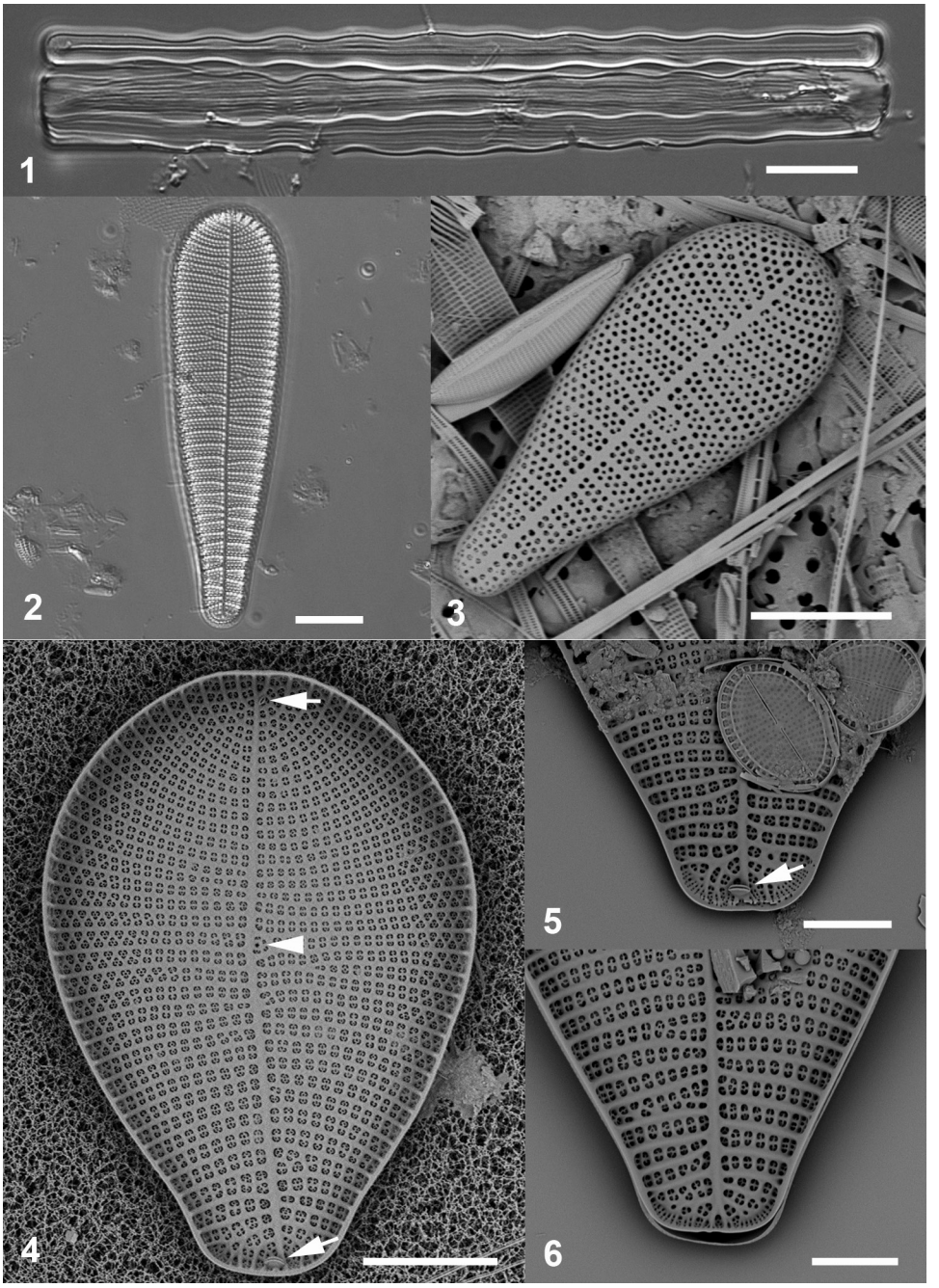

Plate 13.

Figs 1, 2. *Synedra bacillaris,* cleaned frustule in valve view, DIC (composite image) (GU44Z-15), and internal apex detail, SEM (GU44L-C).

Figs 3, 4. *Synedra lata* valves in DIC (GU44AK-1).

Fig. 5. *Tabularia fasciculata* apex, external, SEM (GU26A).

Figs 6, 7. *Tabularia parva* (GU44Z-15).

Fig. 6. External view of apex, SEM.

Fig. 7. Cleaned valve, LM.

Scale bars: Figs 1, 3, 4, 7 = 10 μm, Figs 2, 5, 6 = 5 μm.

Plate 13

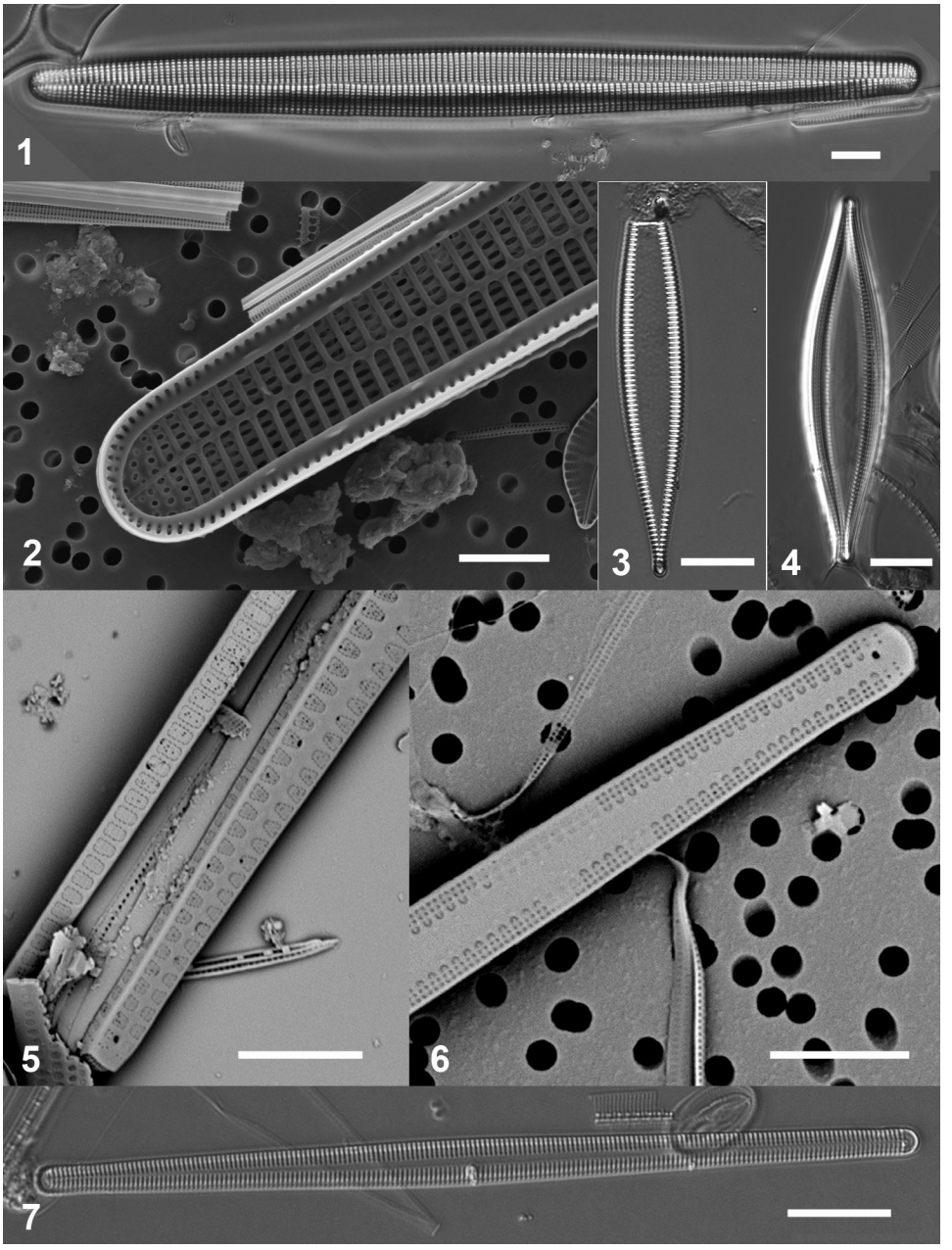

Plate 14.
Figs 1, 2. *Perissonoë cruciata,* DIC (GU44Y-13) and external SEM (GU14P).
Figs 3, 4. *Rhaphoneis amphiceros,* DIC (GU44X-2) and internal SEM (GU44K-6).
Fig. 5. *Rhaphoneis castracanii,* DIC (GU14P).
Figs 6, 7. *Psammodiscus nitidus,* DIC (GU56A-2), and external SEM showing areolae closed by rotae (GU52K-4).
Scale bars: Figs 1, 3, 5, 6 = 10 μm, Figs 2, 4, 7 = 5 μm.

Plate 14

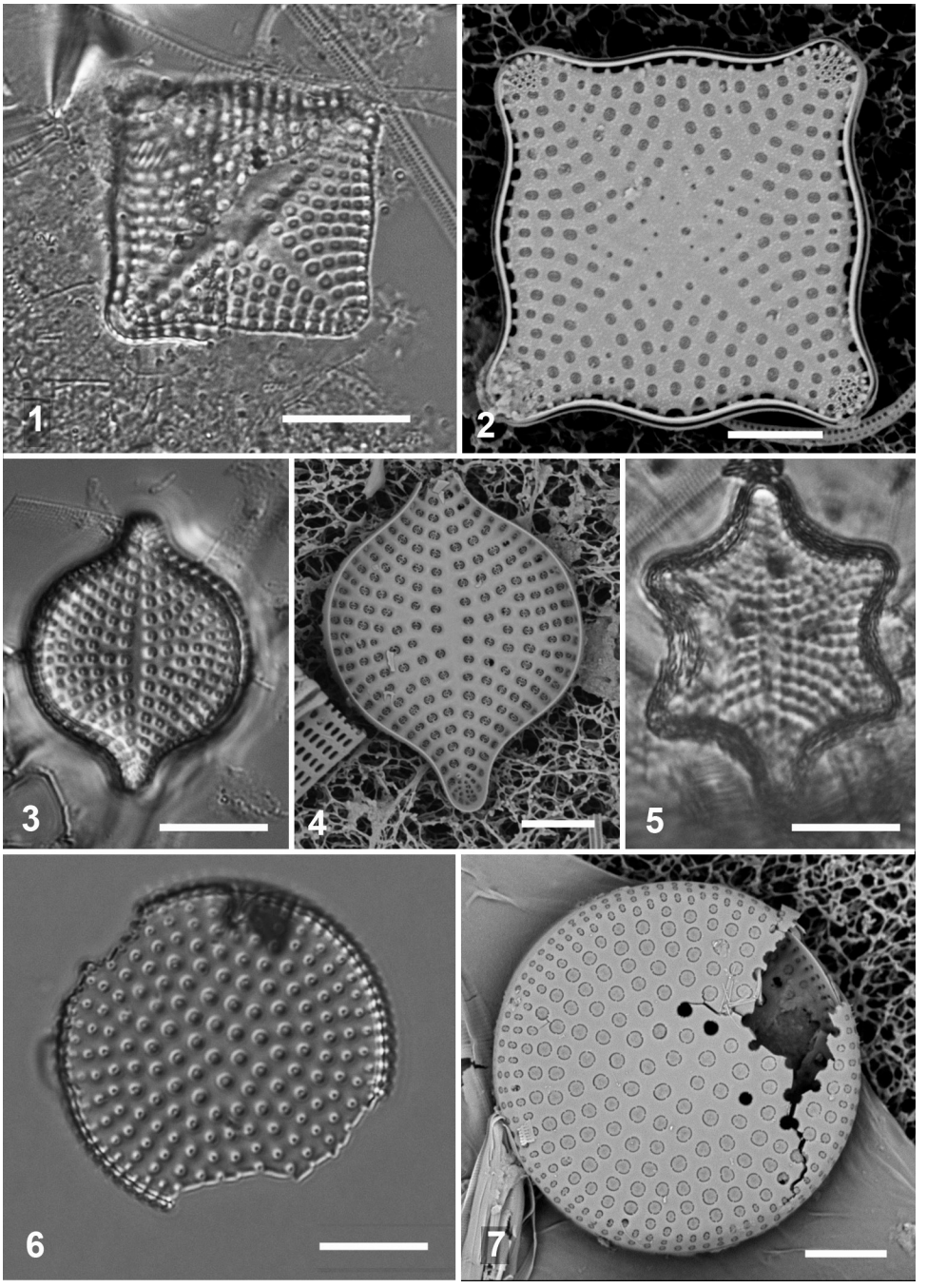

Plate 15.

Figs 1–3. *Ardissonea crystallina*.

Figs 1–2. Whole cell and details of center and apex, DIC (GU44Y-13).

Fig. 3. Internal detail of apex, SEM (GU56A-2).

Figs 4, 5. *Ardissonea formosa*, whole valve and detail of apex indicating the central furrow, DIC (GU44I-2).

Scale bars = 10 μm.

Plate 15

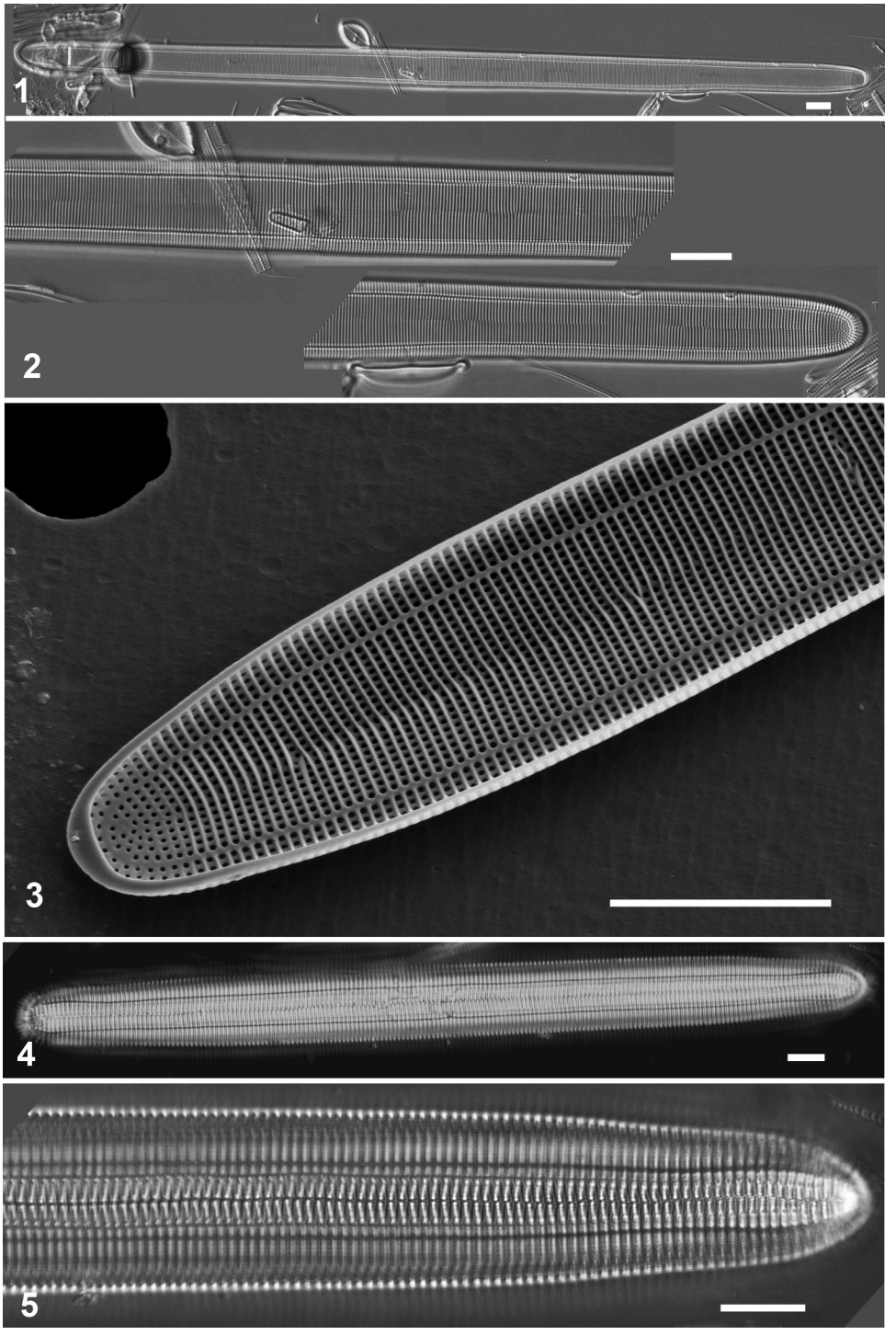

Plate 16.

Figs 1, 2. *Ardissonea formosa*.

Fig. 1. External girdle view of valve apex and girdle bands, showing central furrow on valve and lack of pores on girdle bands, SEM (GU44AA-5).

Fig. 2. Internal detail of apex showing the internal silica membrane, SEM (GU44Z-15).

Figs 3–5. *Ardissonea fulgens* var. *fulgens*.

Fig. 3. Internal detail of central area showing longitudinal ribs at the valve margin, SEM (GU44N-A).

Figs 4, 5. Whole cell and details of center and apex, DIC (GU44Y-13).

Figs 6–8. *Ardissonea fulgens* var. *gigantea*.

Figs 6, 7. Portions of cell to indicate length and details of center and apex, DIC (GU44Y-13).

Fig. 8. Internal detail of central area showing disoriented striae and absence of longitudinal ribs at the valve margin, SEM (GU44Z-15).

Scale bars: Figs 1, 2, 4–7 = 10 μm, Figs 3, 8 = 2 μm.

Plate 16

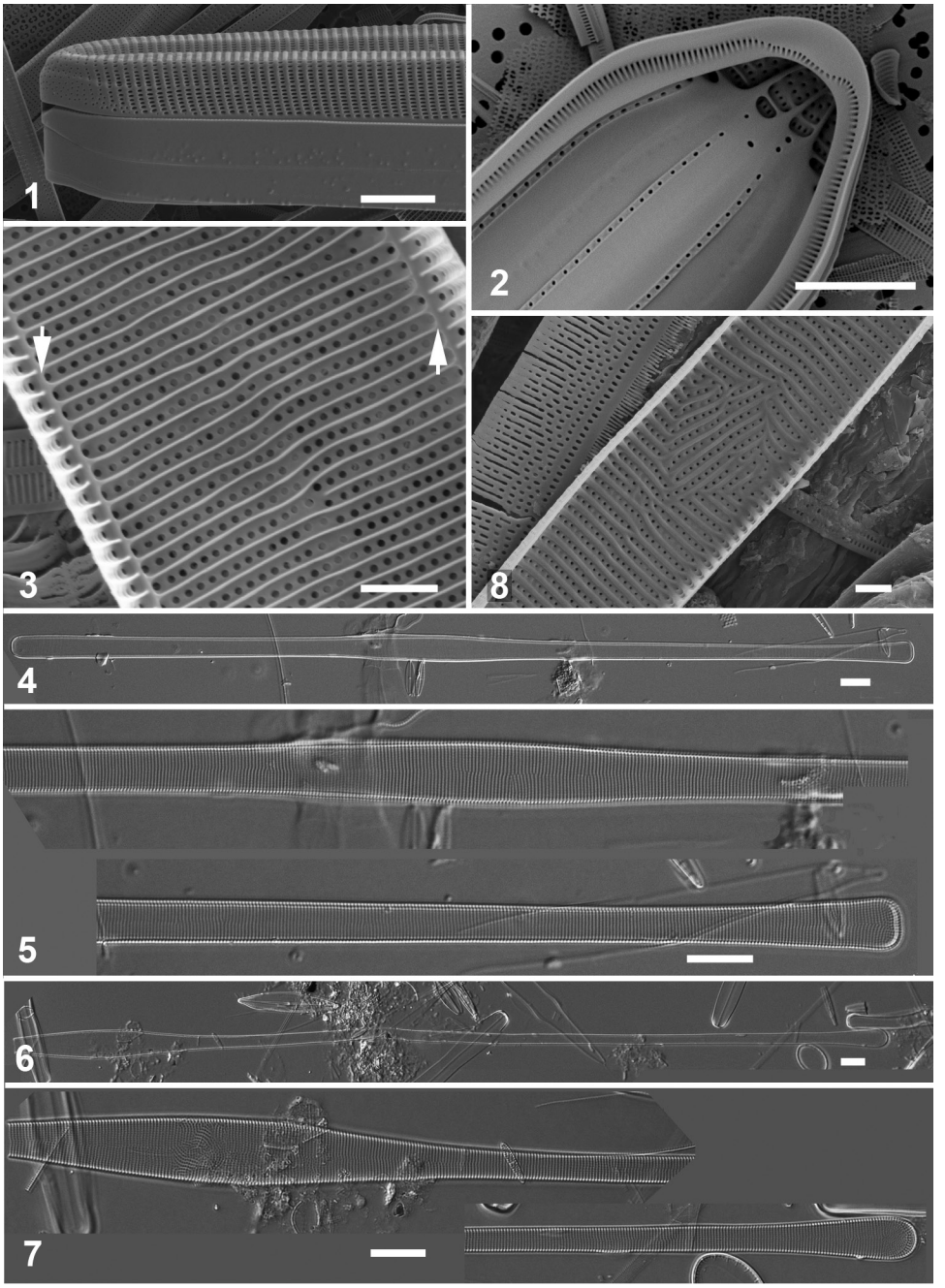

Plate 17.

Figs 1–5. *Toxarium hennedyanum,* DIC.

Figs 1, 2. Portion of cell to indicate length and details of center and apex, DIC (GU44I-2).

Figs 3–5. Central areas of series of cells with more scattered pores, very few pores, and only marginal rows of pores on the valve face (GU44Y-13).

Figs 6–8. *Toxarium undulatum*, DIC.

Figs 6, 7. Portion of typical cell and detail of center, DIC (GU44Y-13).

Fig. 8. Cell with no inflation in the middle (GU44AF-5).

Scale bars = 10 μm.

Plate 17

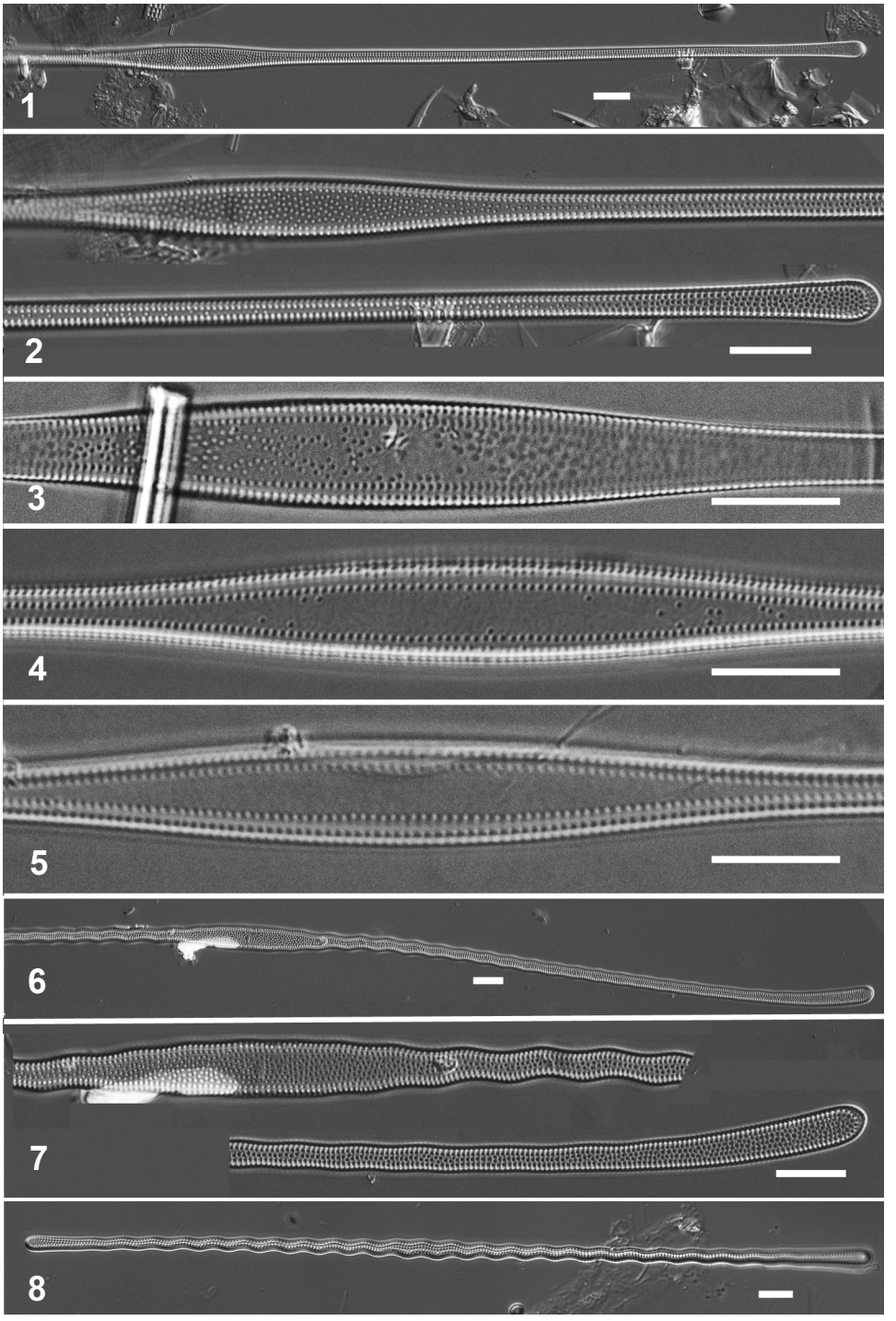

Plate 18.

Figs 1–3. *Rhabdonema adriaticum*.

Figs 1, 2. Girdle and valve views; arrow indicates the hyaline pleurae, DIC (GU44Z-15).

Fig. 3. Corner of frustule showing apical pore field and copulae, SEM (GU44U-2).

Figs 4, 5. *Florella pascuensis*, valve and detail of apex showing U-shaped series of slits (arrow), SEM (GU52J).

Figs 6, 7. *Hyalosira interrupta*.

Fig. 6. Single complete frustule; the plastids lie behind the bands without areolae (arrow) (GU44AC-4).

Fig. 7. Internal view of valve, showing rimoportulae at both apices (arrows), SEM (GU44Z-15).

Scale bars: Figs 1, 2 = 10 μm, Fig. 3 = 2 μm, Fig. 4 = 20 μm, Figs 5–7 = 5 μm.

Plate 18

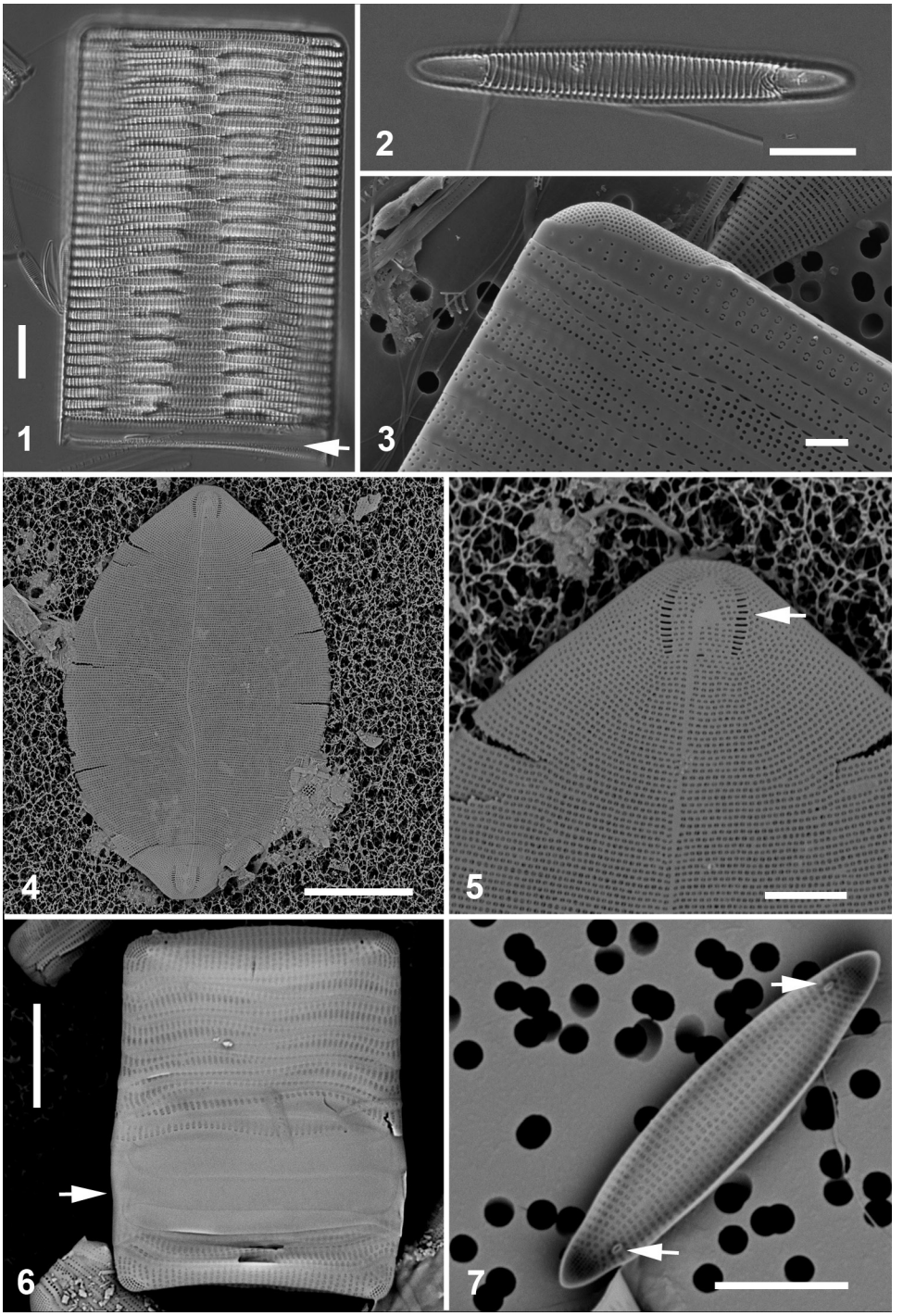

Plate 19.

Figs 1, 2. *Grammatophora angulosa,* frustule at two focal planes showing profile of septa, DIC (GU44AP-8).

Fig. 3. *Grammatophora macilenta* (lower left) and *G. undulata* girdle views (GU44Z-15).

Figs 4, 5. *Grammatophora macilenta* (GU44Z-15).

Fig. 4. Valve with underlying septum, DIC.

Fig. 5. External view of valve showing spines at one end, SEM.

Figs 6–8. *Grammatophora oceanica*.

Fig. 6. Living colonies, girdle view, DIC (GU44AC-4).

Fig. 7. Valve, DIC (GU44I-1).

Fig. 8. Whole mount showing mucilage attached over apical pore field but not generally over the apical slits in the valvocopula, SEM (GU44AC-4).

Scale bars: Figs 1–6, 8 = 10 μm, Fig. 7 = 5 μm.

Plate 19

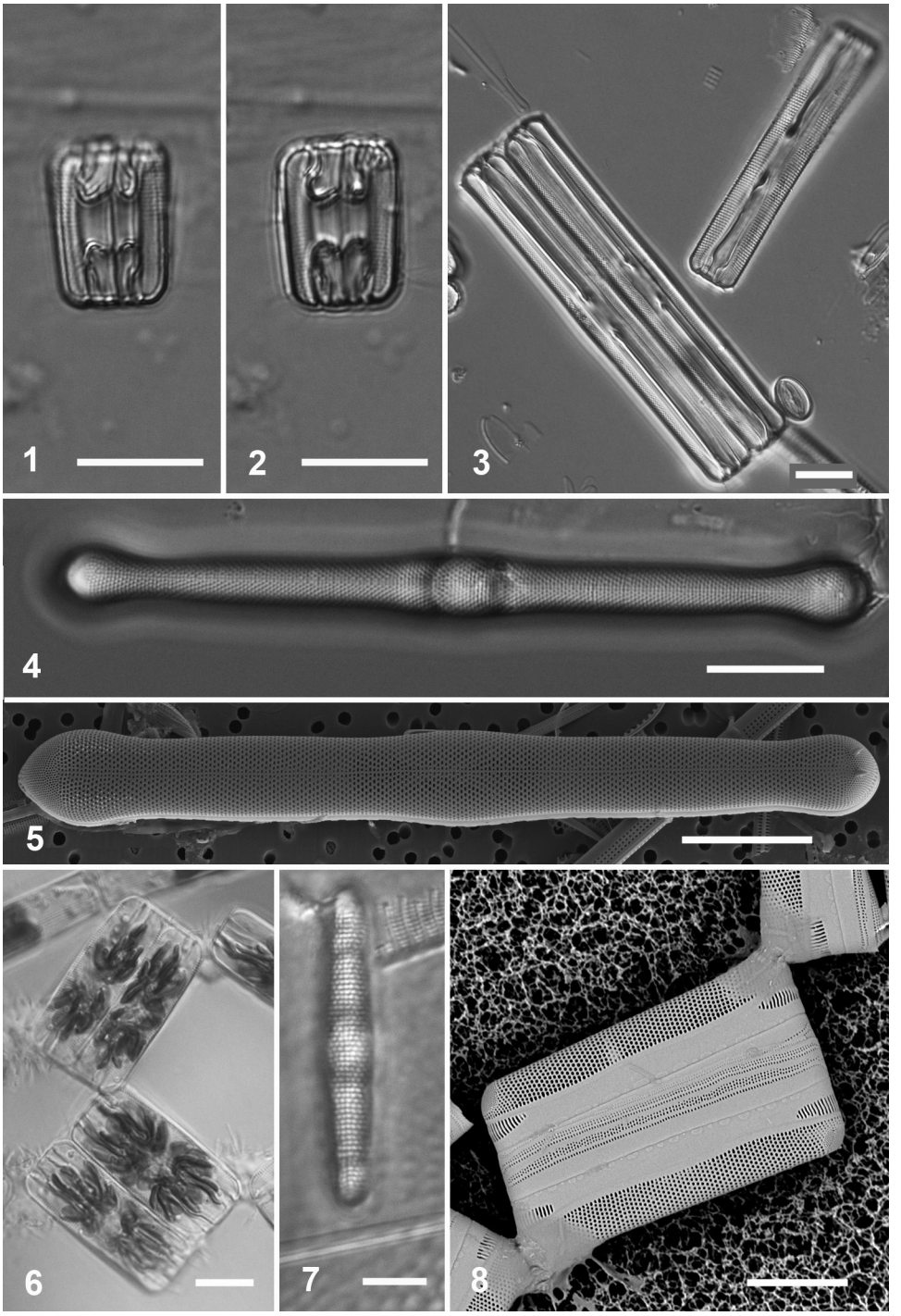

Plate 20.

Figs 1–3. *Grammatophora undulata*.

Fig. 1. Whole mount of chains, cells in oblique view, SEM (GU44AC-4).

Figs. 2, 3. Valve views, DIC (GU44Z-15).

Figs 4, 5. *Striatella unipunctata*.

Fig. 4. Valve (arrow) and girdle bands in typical DIC preparation (GU44Z-15).

Fig. 5. Detail of apex with ocellulimbus and rimoportula opening (arrow), cultured cell, SEM (ECT 3648).

Fig. 6. *Lyrella hennedyi* valve in DIC (GU44I-1)

Figs 7, 8. *Lyrella hennedyi* var. *granulosa* valves in DIC (GU44AE-2) and SEM (GU44Z-15).

Scale bars: Figs 1–4, 6–8 = 10 μm, Fig. 5 = 5 μm.

Plate 20

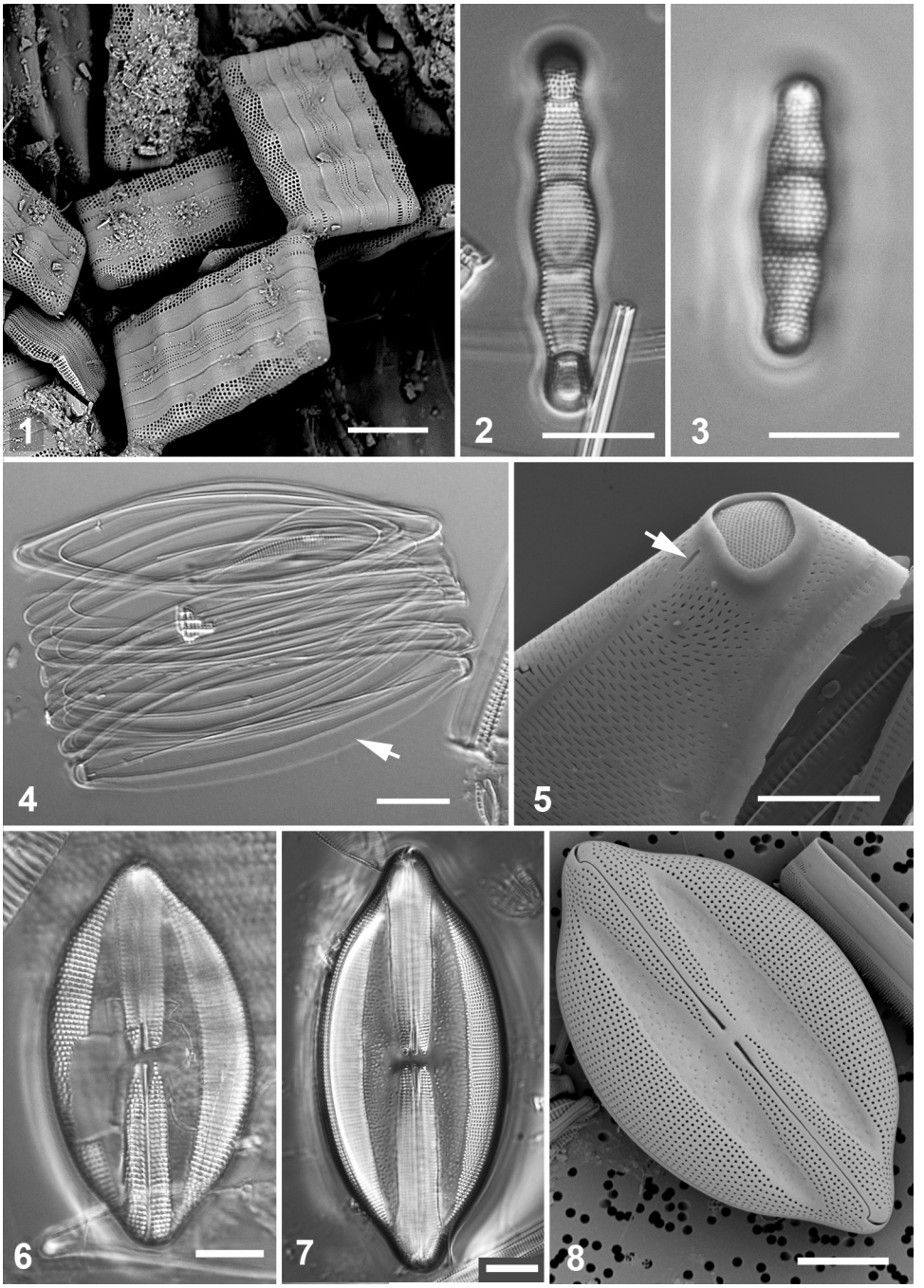

Plate 21.

Fig. 1. *Petroneis granulata*, DIC (GU4A).

Figs 2–7. *Olifantiella pilosella* (GU26A).

Figs 2, 3. Valves in DIC, showing the buciniportula (arrow).

Figs 4, 5. External view of whole valve and detail of central area showing deflected proximal raphe endings and opening of buciniportula (arrow).

Figs 6, 7. Internal view of whole valve and detail of paired tubular process of the buciniportula, SEM.

Scale bars: Figs 1–3 = 10 μm, Fig. 4 = 5 μm, Fig. 6 = 2 μm, Figs 5, 7 = 0.5 μm.

Plate 21

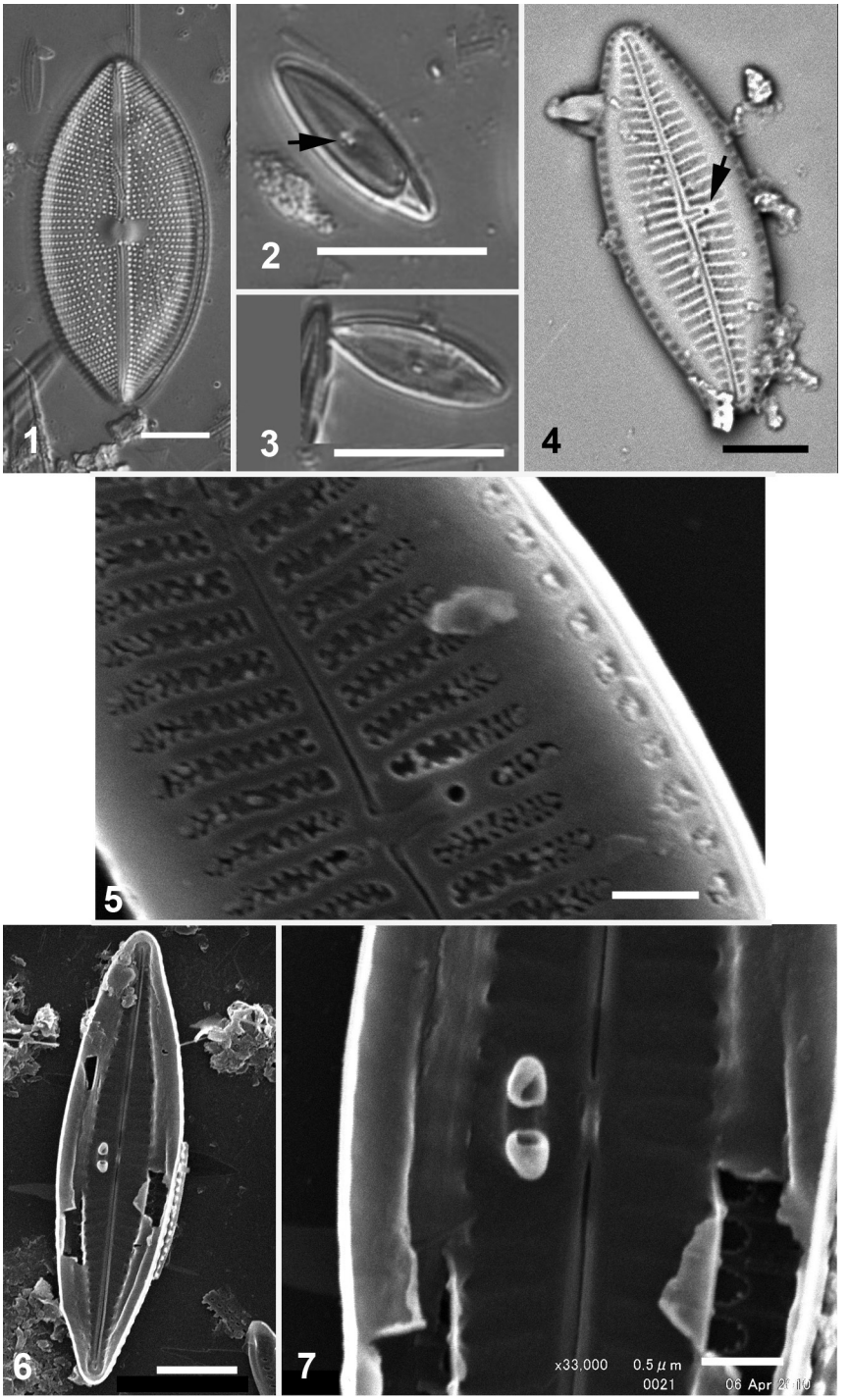

Plate 22.

Figs 1–3. *Gomphonemopsis littoralis*.

Fig. 1. Valves in DIC (GU44I-1).

Fig. 2. Valve in SEM (GU26A).

Fig. 3. Frustule in girdle view and valve interior view, SEM (GU26A).

Figs 4, 5. *Mastogloia achnanthioides*. Valve with attached valvocopula at two focal planes showing valve structure and partectal ring, DIC (GU44R-2).

Figs 6–8. *Mastogloia acutiuscula* var. *elliptica*.

Figs 6, 7. Valve at two focal planes, DIC (GU44Y-13).

Fig. 8. Internal view, SEM showing axial costae (arrow) and partectal ring (GU55B-4).

Figs 9, 10. *Mastogloia adriatica* var. *linearis* valve at two focal planes, DIC (GU4A).

Scale bars: Figs 1–3, 8 = 5 μm, Figs 4–7, 9, 10 = 10 μm.

Plate 22

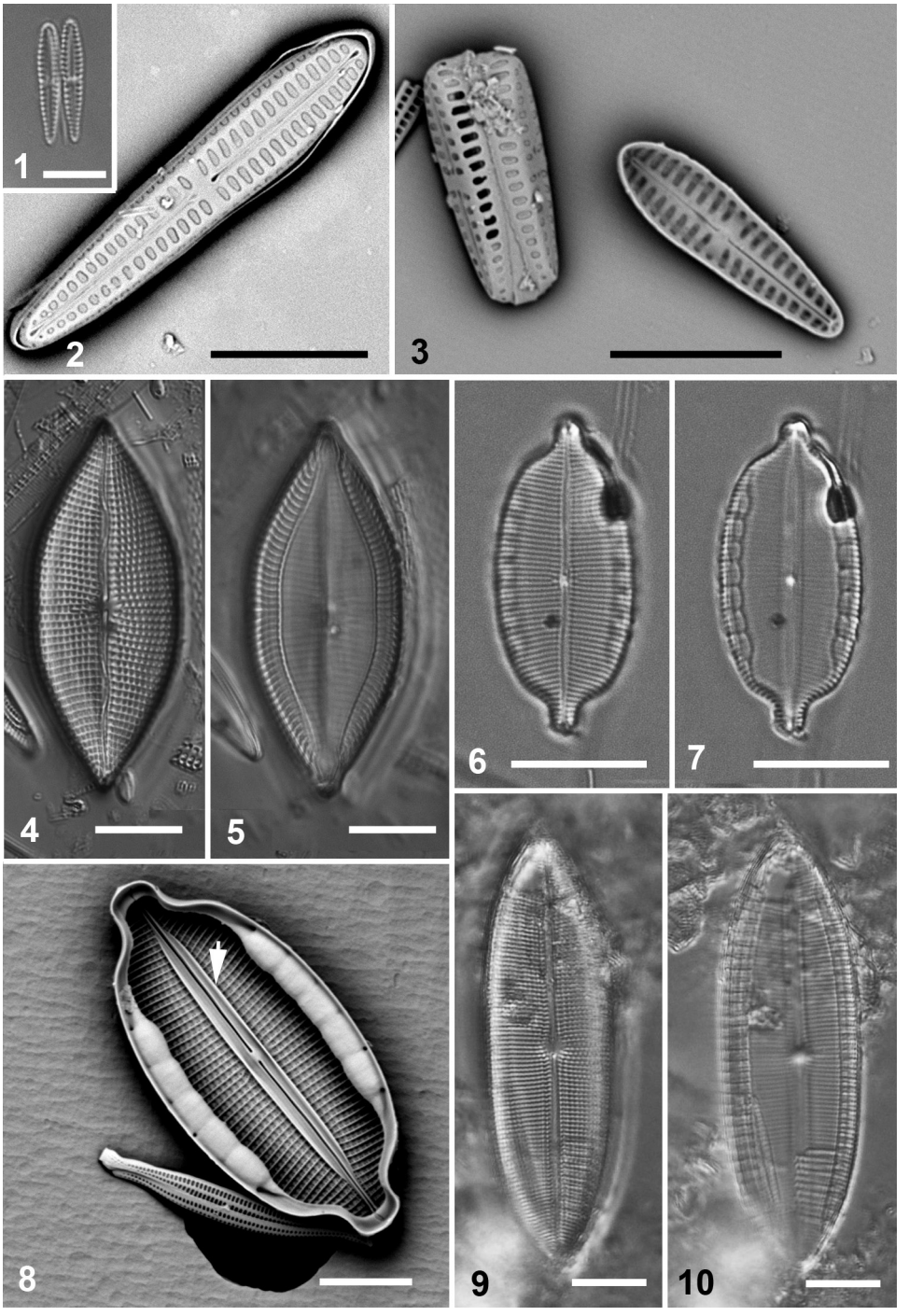

Plate 23.

Figs 1, 2. *Mastogloia angulata* valve at two focal planes, DIC (GU52P-5).

Fig. 3. *Mastogloia barbadensis* valve external view, SEM (GU55B-4).

Figs 4, 5. *Mastogloia binotata*.

Fig. 4. Several valves with valvocopulae, DIC (GU32B).

Fig. 5. Internal view of valve with partecta, also showing the single pore (arrow), SEM (GU55B-4).

Figs 6–8. *Mastogloia borneensis*.

Figs 6, 7. Valve at two focal planes, DIC (GU44Y-13).

Fig. 8. Internal view, SEM (GU44H-7).

Scale bars: Figs 1, 2, 4, 8 = 10 μm, Figs 3, 5–7 = 5 μm.

Plate 23

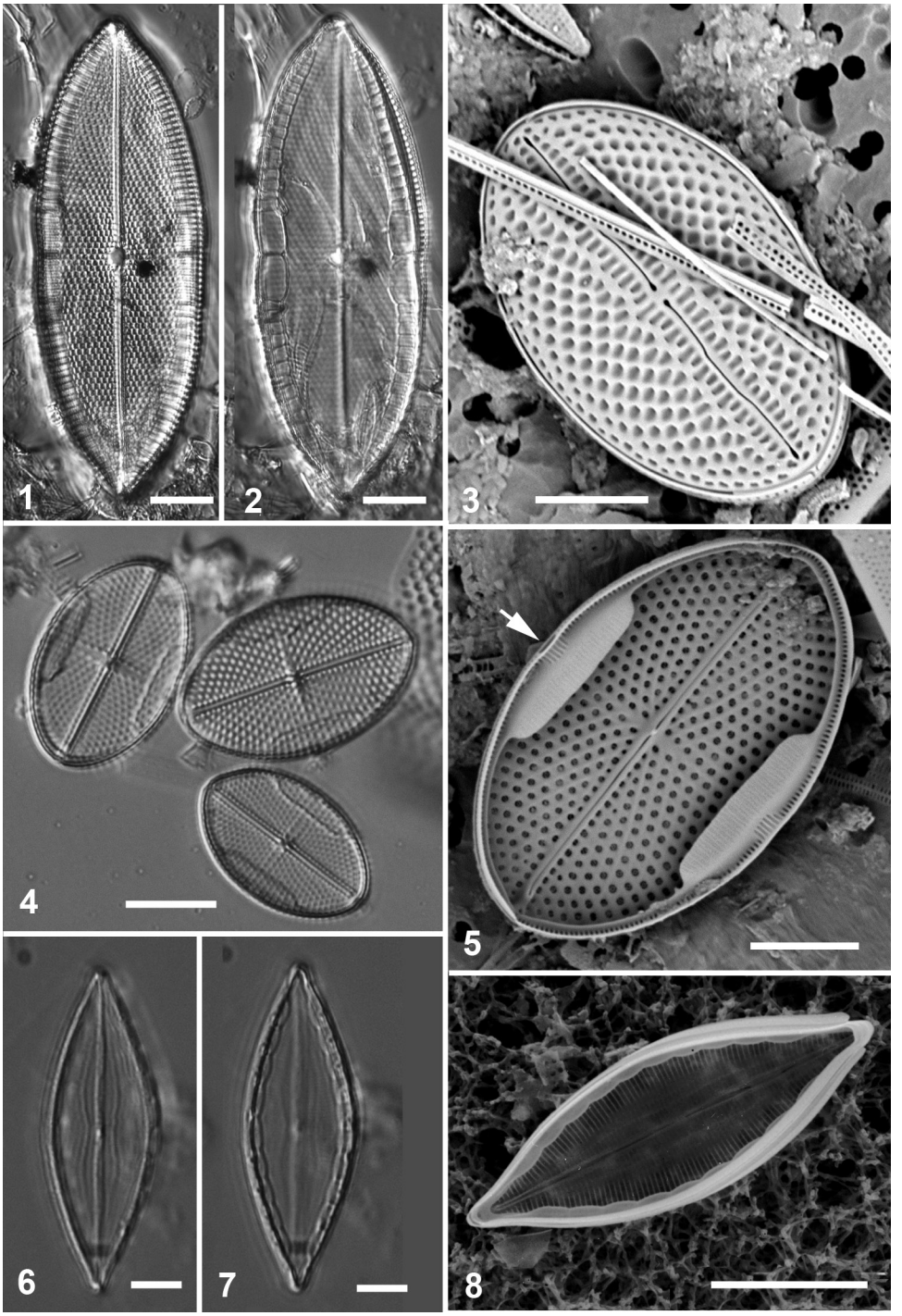

Plate 24.

Figs. 1–3. *Mastogloia cannii* (GU44T-1).

Figs 1, 2. Valve at two focal planes, DIC.

Fig. 3. External valve surface, SEM.

Figs 4–7. *Mastogloia capitata* var. *lanceolata* (GU55B-4).

Fig. 4. Valve and partecta, DIC.

Figs 5, 6. Internal view of whole valve and partecta and detail of partecta showing duct opening (arrow), SEM.

Fig. 7. Detail of external central area, SEM.

Scale bars: Figs 1, 2, 4, 5 = 10 μm, Figs 3, 6, 7 = 5 μm.

Plate 24

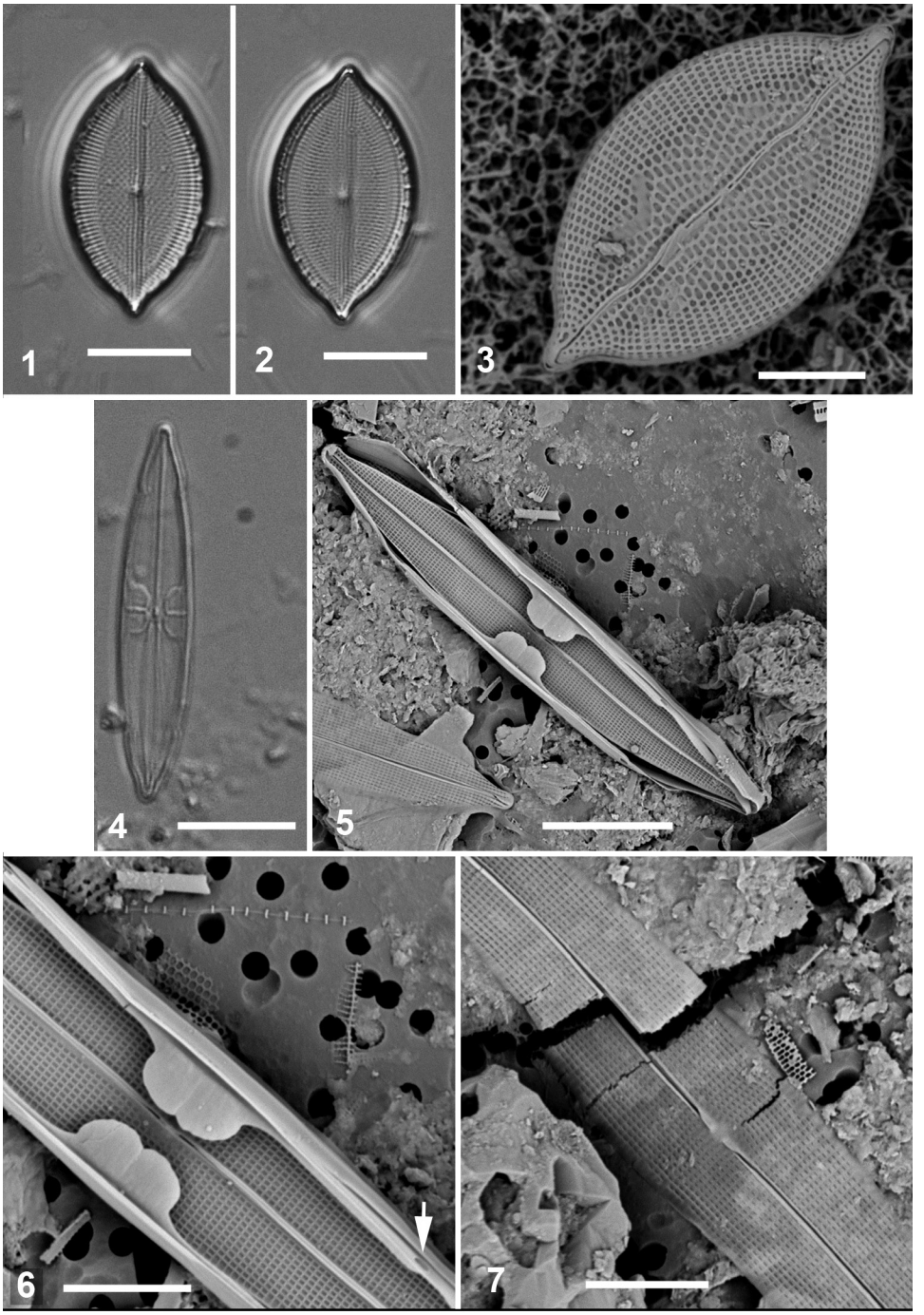

Plate 25.
Figs 1–3. *Mastogloia ciskeiensis* (GU44T-1).
Figs 1, 2. Valve at two focal planes, DIC.
Fig. 3. Valve internal view showing partectal band width, SEM.
Figs 4, 5. *Mastogloia citrus* valve at two focal planes, DIC (GU44I-1).
Figs 6, 7. *Mastogloia cocconeiformis* valve at two focal planes, in the lower focus showing the half walls within the partecta (arrows), DIC (GU44R-2).
Scale bars: all = 10 μm.

Plate 25

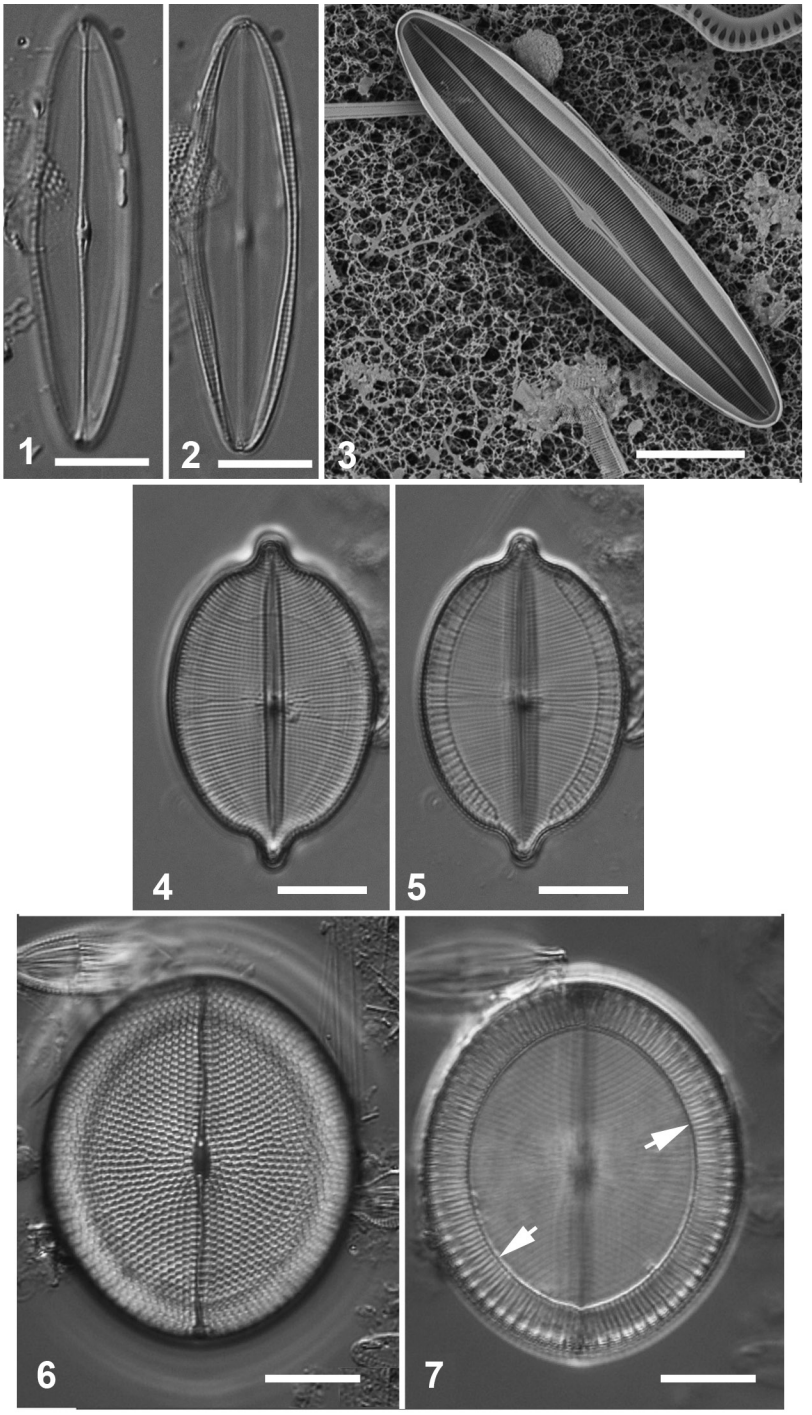

Plate 26.

Figs 1–3. *Mastogloia corsicana*.

Fig. 1, 2. Valve at two focal planes, DIC (GU44Y-13).

Fig. 3. External valve view, SEM (GU55B-4).

Figs 4, 5. *Mastogloia cribrosa* valve at two focal planes, DIC (GU44AJ).

Figs 6–8. *Mastogloia crucicula*.

Fig. 6. Valve with partecta in two quarters of the frustule, DIC (GU44Z-15).

Fig. 7. Valve of the nominate variety, internal SEM (GU44I-2).

Fig. 8. SEM of cell with partecta in opposite quarters (var. *alternans*) (GU44Z-15).

Scale bars: Figs 1, 2, 4–6 = 10 μm, Figs 3, 7 = 5 μm, Fig. 8 = 2 μm.

Plate 26

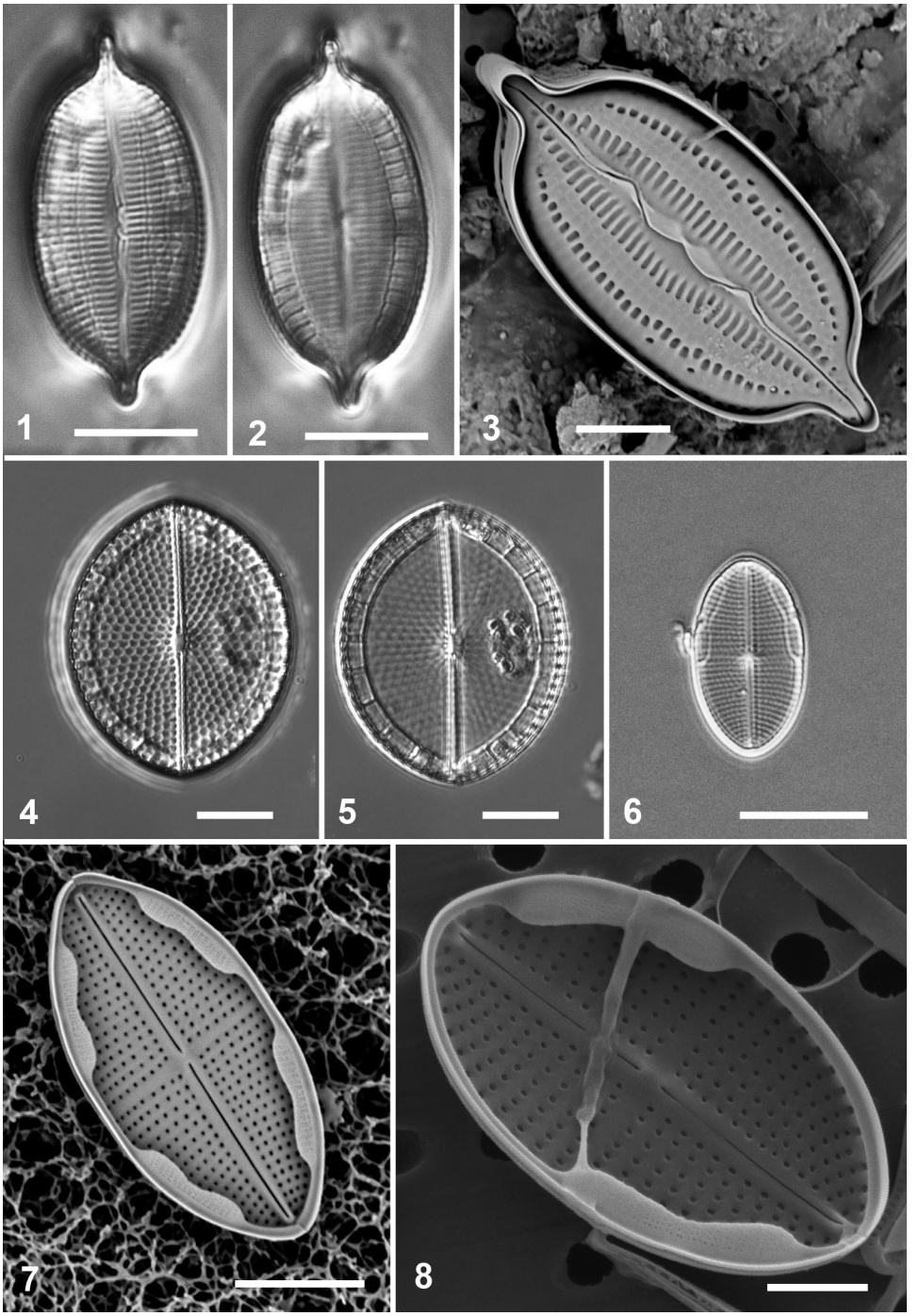

Plate 27.
Fig. 1. *Mastogloia crucicula* external view, SEM (GU26A).
Figs 2, 3. *Mastogloia cuneata* valve at two focal planes, DIC (GU44Y-13).
Figs 4,5. *Mastogloia cyclops* valve at two focal planes, showing stigma (arrow), DIC (GU44Y-13).
Figs 6, 7. *Mastogloia decussata* valve at two focal planes, DIC (GU44I-4).
Figs 8, 9. *Mastogloia dicephala* valve at two focal planes, DIC (GU21Y).
Figs 10, 11. *Mastogloia erythraea* valve at two focal planes showing two large partecta in each quarter, DIC (GU44I-1).
Scale bars: Figs 1–3, 8, 9 = 5 μm, Figs 4–7, 10, 11 = 10 μm.

Plate 27

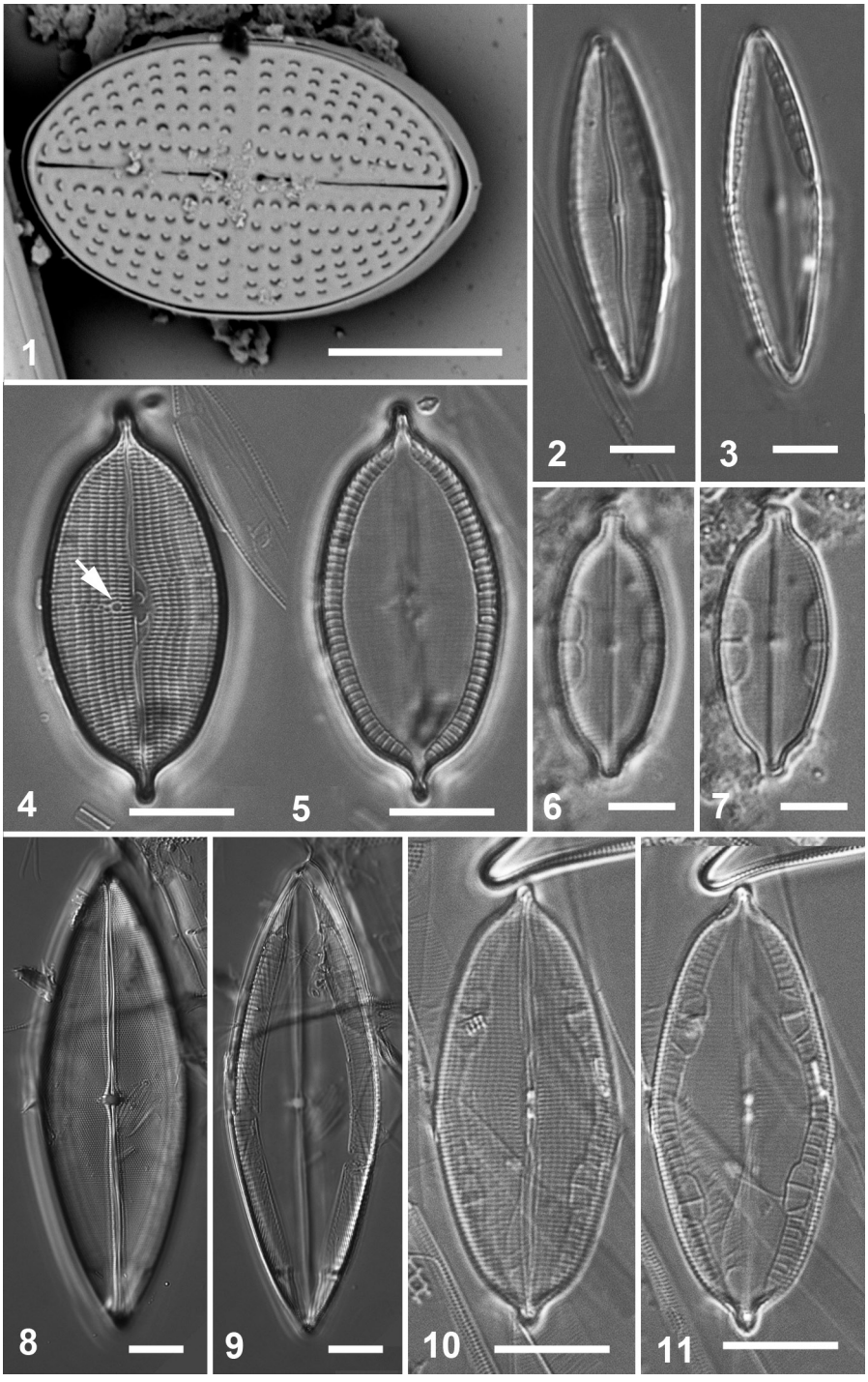

Plate 28.
Figs 1, 2. *Mastogloia erythraea* valve at two focal planes showing one large chamber in 3 of 4 quarters and the partial gutter along the raphe branches (arrow) (GU44I-2).
Fig. 3. *Mastogloia erythraea* var. *grunowii*, valve with valvocopulae, showing one large partectum in two opposite quadrants; the short ribs bordering the raphe can be seen on the internal face (arrow), SEM (GU44P-B).
Figs 4, 5. *Mastogloia gomphonemoides*, valve at two focal planes, DIC (GU44Y-13).
Fig. 6, 7. *Mastogloia exilis*, valve at two focal planes, DIC (GU44R-2).
Figs 8–11. *Mastogloia fimbriata,* two valves at two focal planes, showing range in partecta shape and size, DIC (GU44T-1).
Figs 12, 13. *Mastogloia graciloides* valve at two focal planes DIC (GU56A-2).
Scale bars: Figs 1–7, 12, 13 = 5 μm, Figs 8–11 = 10 μm.

Plate 28

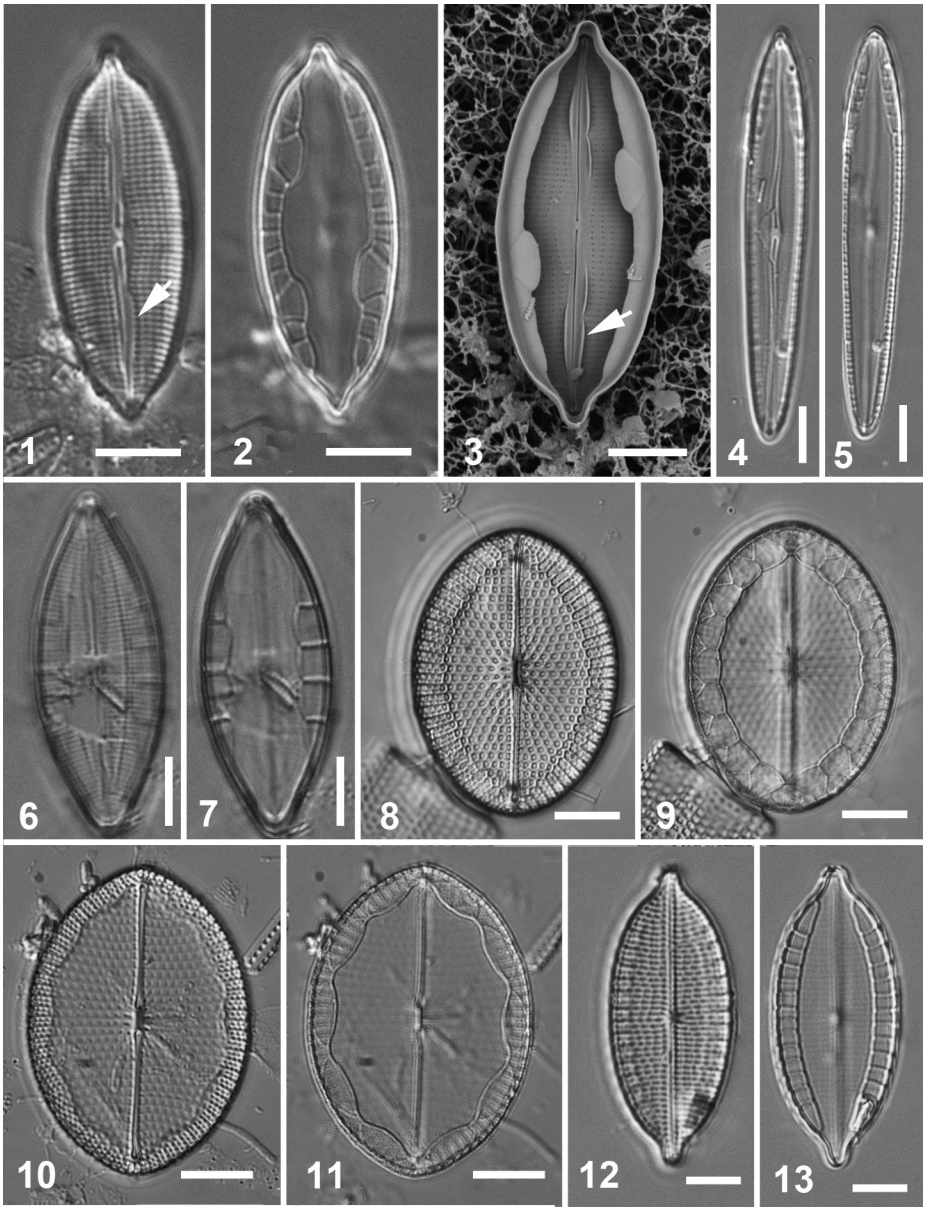

Plate 29.

Figs 1, 2. *Mastogloia horvathiana*, DIC (GU44Y-13).

Figs 3–5. *Mastogloia hustedtii* (GU55B-4).

Figs 3, 4. Valve at two focal planes, arrowhead indicates plaque on the partecta, DIC.

Fig. 5. Internal view showing compact plaques on the partectae (arrowhead), SEM.

Figs 6–8. *Mastogloia inaequalis*.

Fig. 6. Live cells in girdle, valve and oblique views showing stalks, DIC (GU44R).

Figs 7, 8. Valve at two focal planes, DIC (GU44I-2).

Scale bars: Figs 1, 2, 5, 7, 8 = 10 μm, Figs 3, 4 = 5 μm, Fig. 6 = 20 μm.

Plate 29

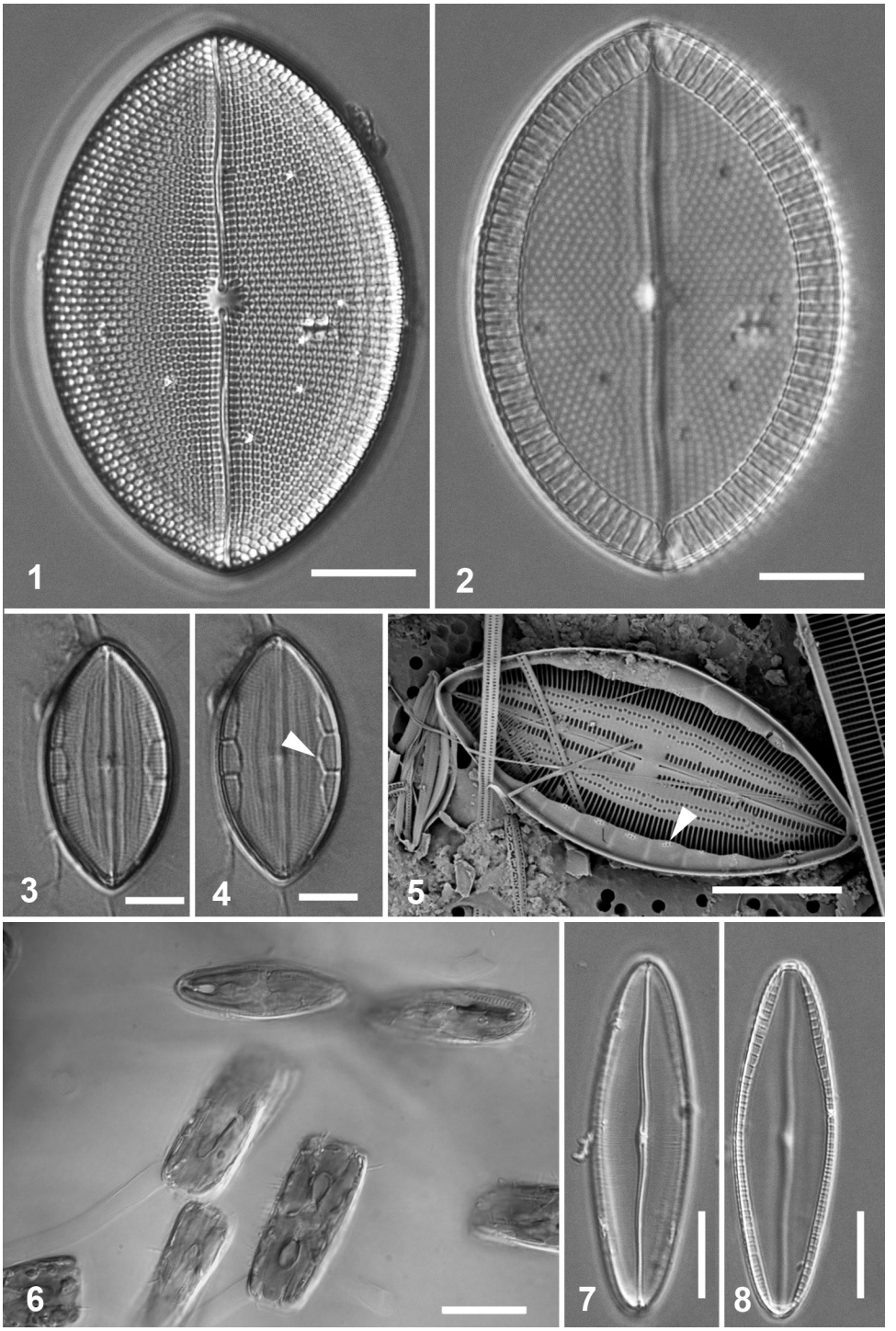

Plate 30.

Figs 1–3. *Mastogloia jelinecki* valve at three focal planes, DIC (GU6E-9).

Figs 4, 5. *Mastogloia kjellmanii* valve at two focal planes, arrow indicating the larger apical partectum, DIC (GU52P-5).

Figs 6–8. *Mastogloia lacrimata* (GU44T-1).

Figs 6, 7. Valve at two focal planes, DIC.

Fig. 8. External view of broken valve showing partecta beneath, SEM.

Scale bars: Figs 1–5, 8 = 10 μm, Figs 6, 7 = 5 μm.

Plate 30

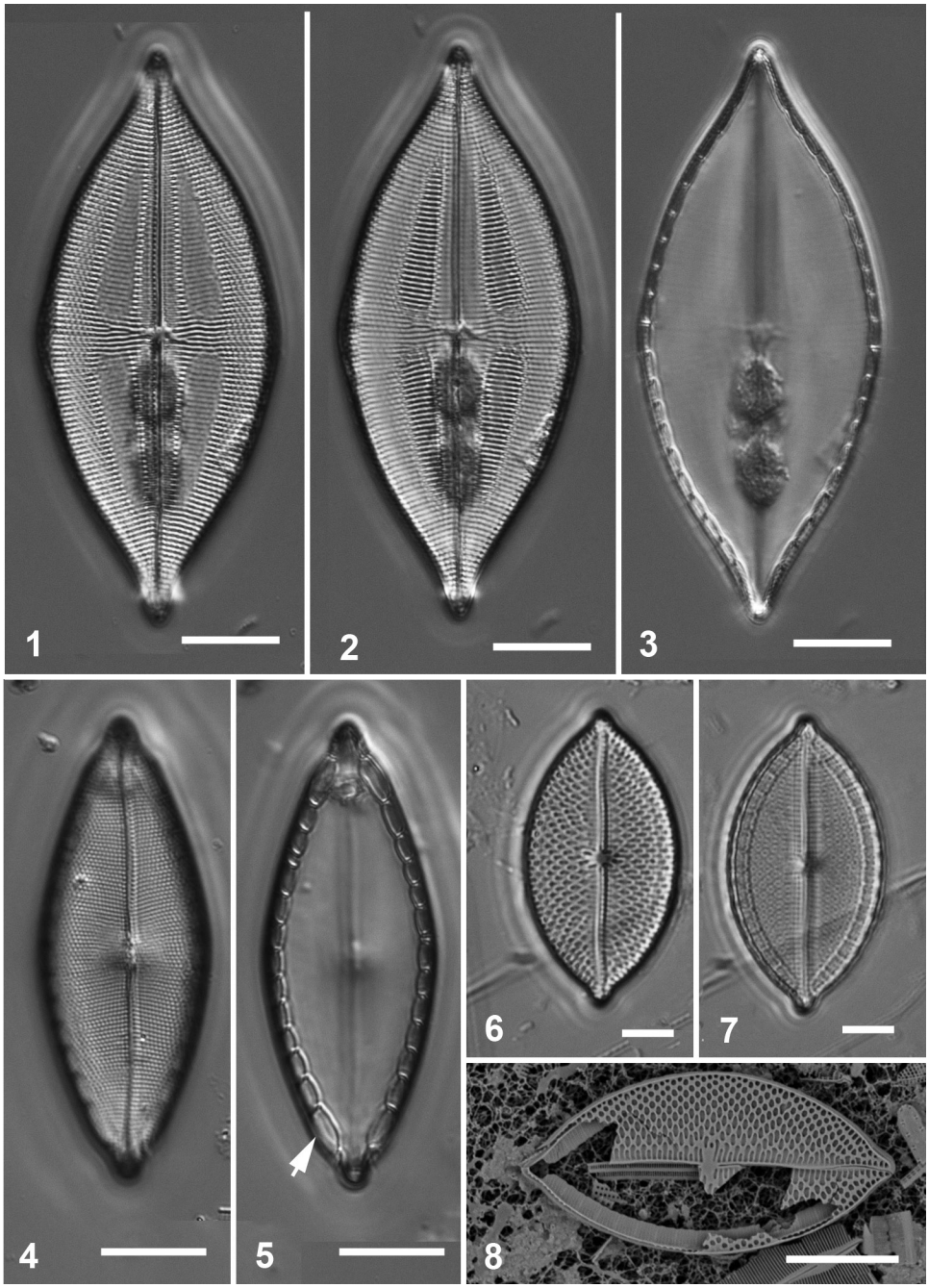

Plate 31.
Figs 1, 2. *Mastogloia lineata* valve at two focal planes, DIC (GU55B-4).
Fig. 3. *Mastogloia laterostrata*, DIC (GU32B).
Figs 4, 5. *Mastogloia macdonaldii* valve at two focal planes, DIC (GU52P-8).
Scale bars = 10 μm.

Plate 31

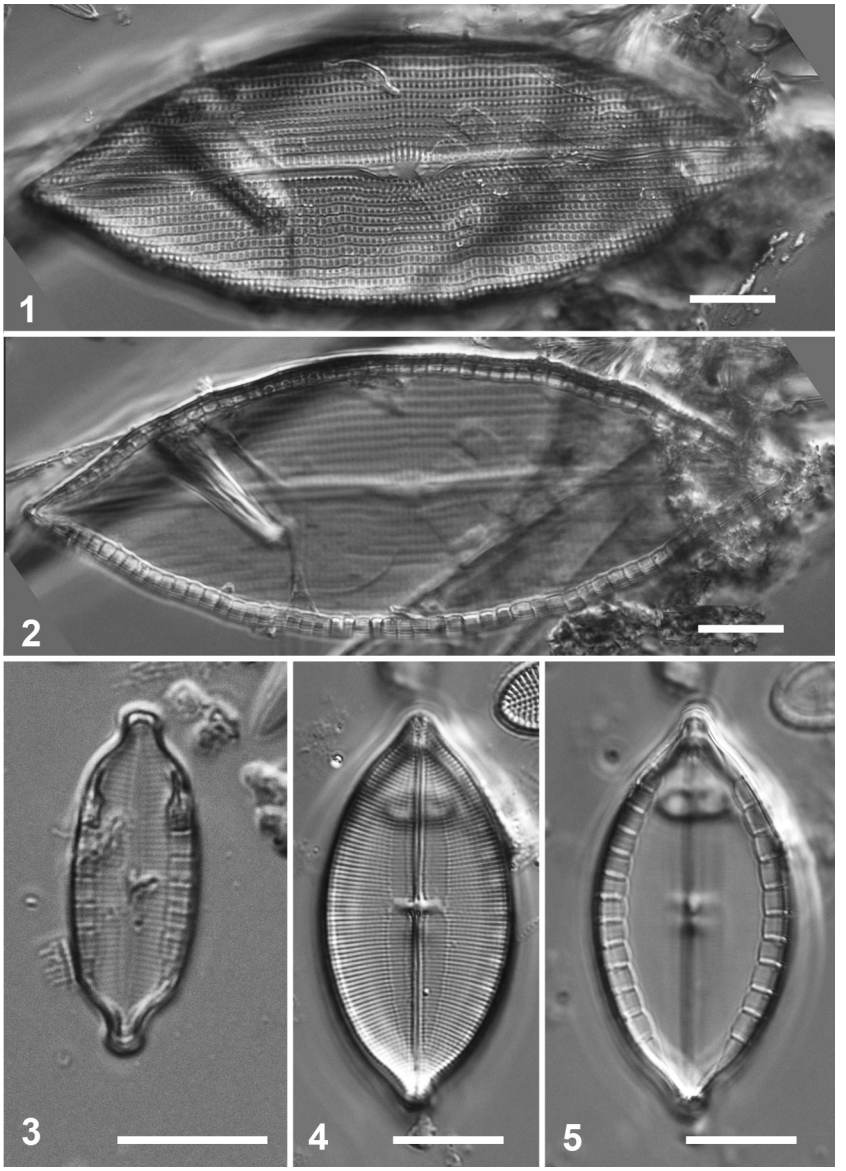

Plate 32.

Figs 1–3. *Mastogloia manokwariensis* (GU55B-4).
Figs. 1, 2. Valve at two focal planes, DIC.
Fig. 3. Internal view, SEM.
Figs 4–10. *Mastogloia mauritiana,* DIC.
Figs 4–6. Valve at three focal planes (GU32B).
Figs. 7–10. Valves at two focal planes (GU52Q-2 and Gab3C*, respectively).
Scale bars: Figs 1–3, 9, 10 = 5 μm, Figs 4–8 = 10 μm.

Plate 32

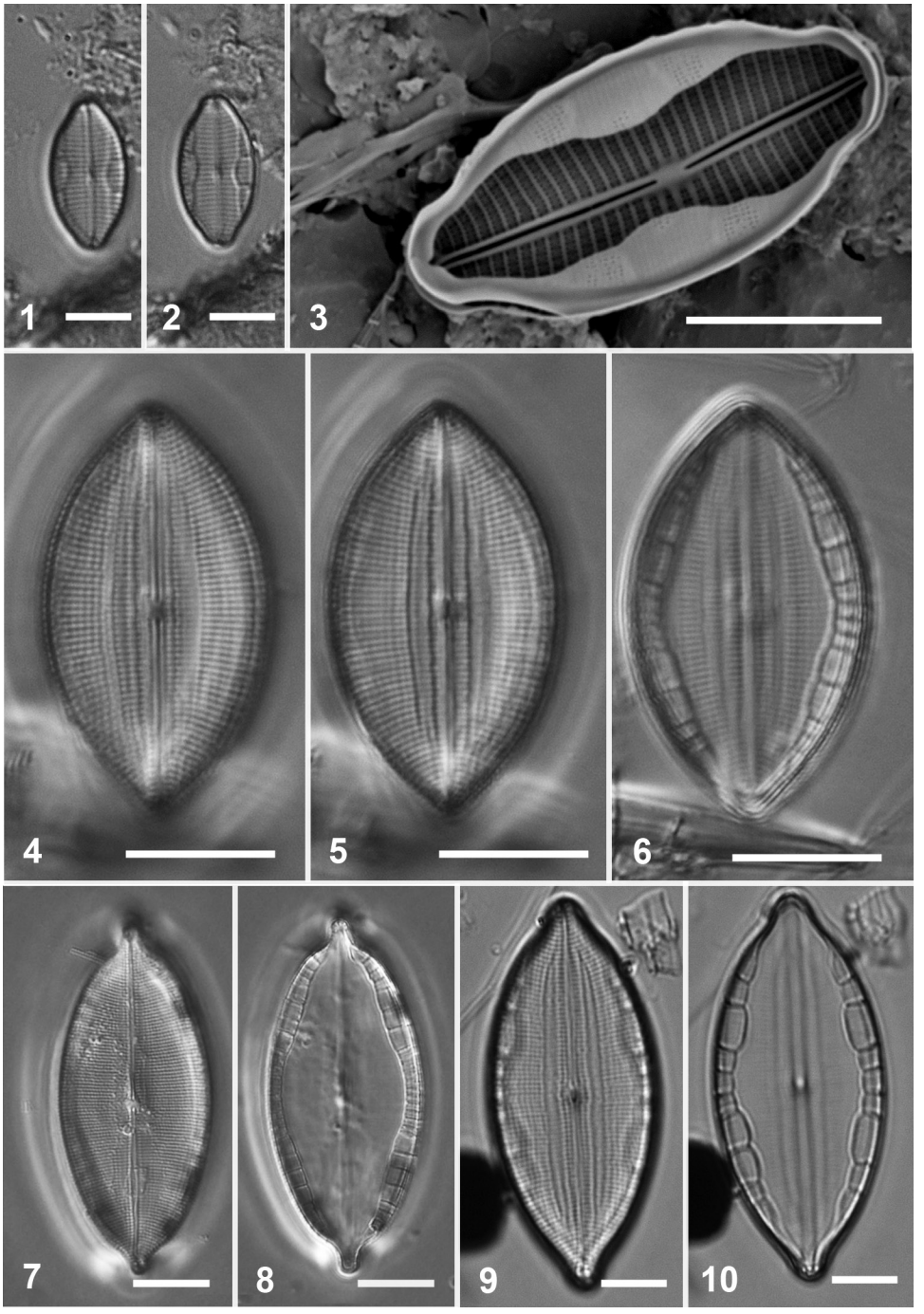

Plate 33.

Figs 1, 2. *Mastogloia mediterranea* valve at two focal planes, showing peduncles (arrowhead), DIC (GU52Q-1).

Fig. 3. *Mastogloia neoborneensis* external SEM showing pseudoconopeum (arrow) (GU52K-7).

Figs. 4–6. *Mastogloia ovalis,* DIC.

Figs 4, 5. Valve at two focal planes, DIC (GU26A).

Fig. 6. Valve (GU52Q-1).

Figs 7, 8. *Mastogloia ovata* valve at two focal planes, DIC (GU52P-7).

Figs 9, 10. *Mastogloia ovulum* valve at two focal planes (GU44R-2).

Scale bars: Figs 1–6, 9, 10 = 5 μm, Figs 7, 8 = 10 μm.

Plate 33

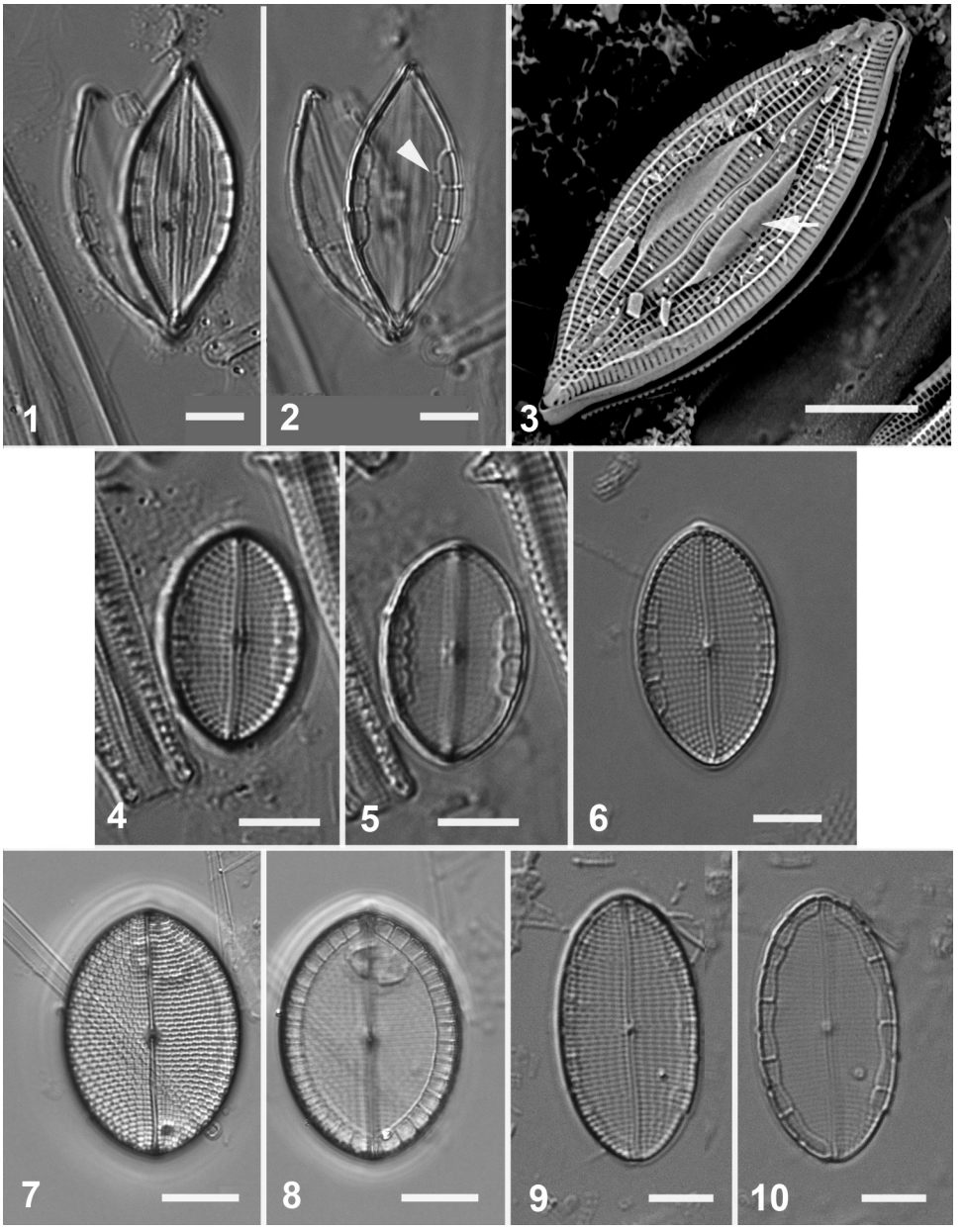

Plate 34.
Figs 1, 2. *Mastogloia ovum-paschale* valve at two focal planes, DIC (GU52Q-2).
Figs 3–5. *Mastogloia paradoxa* valve with focus on (left to right) valve face and sinuous raphe, internal longitudinal silica ribs, and partectal ring with oblique partectal ducts (arrow), DIC (GU44Y-13).
Scale bars = 10 μm.

Plate 34

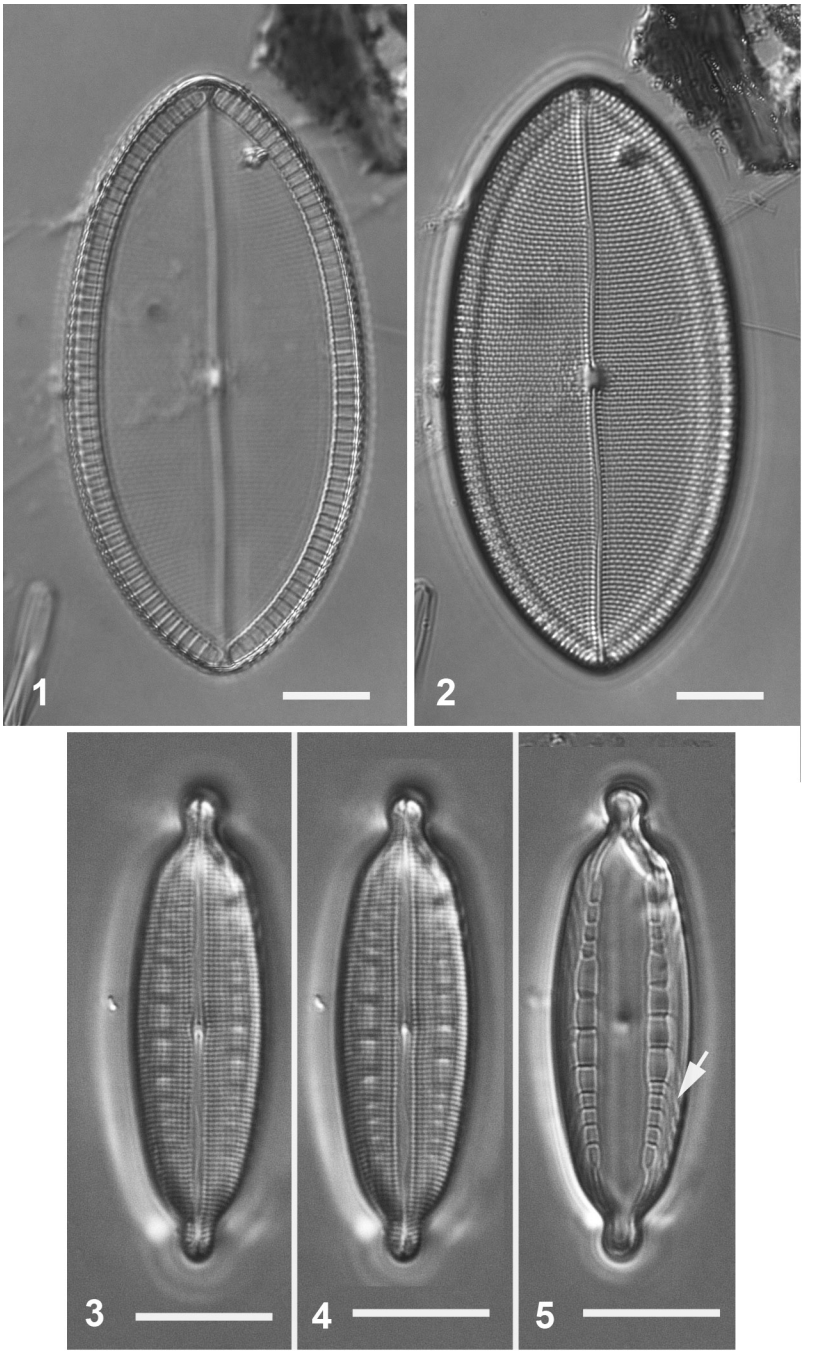

Plate 35.
Figs 1, 2. *Mastogloia pseudolatecostata* valve at two focal planes, DIC (GU44AJ).
Figs 3, 4. *Mastogloia pulchella* valve at two focal planes, DIC (GU44Y-13).
Figs 5, 6. *Mastogloia rhombica* valve at two focal planes, DIC (GU44Z-15).
Figs 7, 8. *Mastogloia punctatissima* valve at two focal planes, showing the strongly hooked distal raphe endings (arrow), DIC (GU44I-2).
Scale bars = 10 μm.

Plate 35

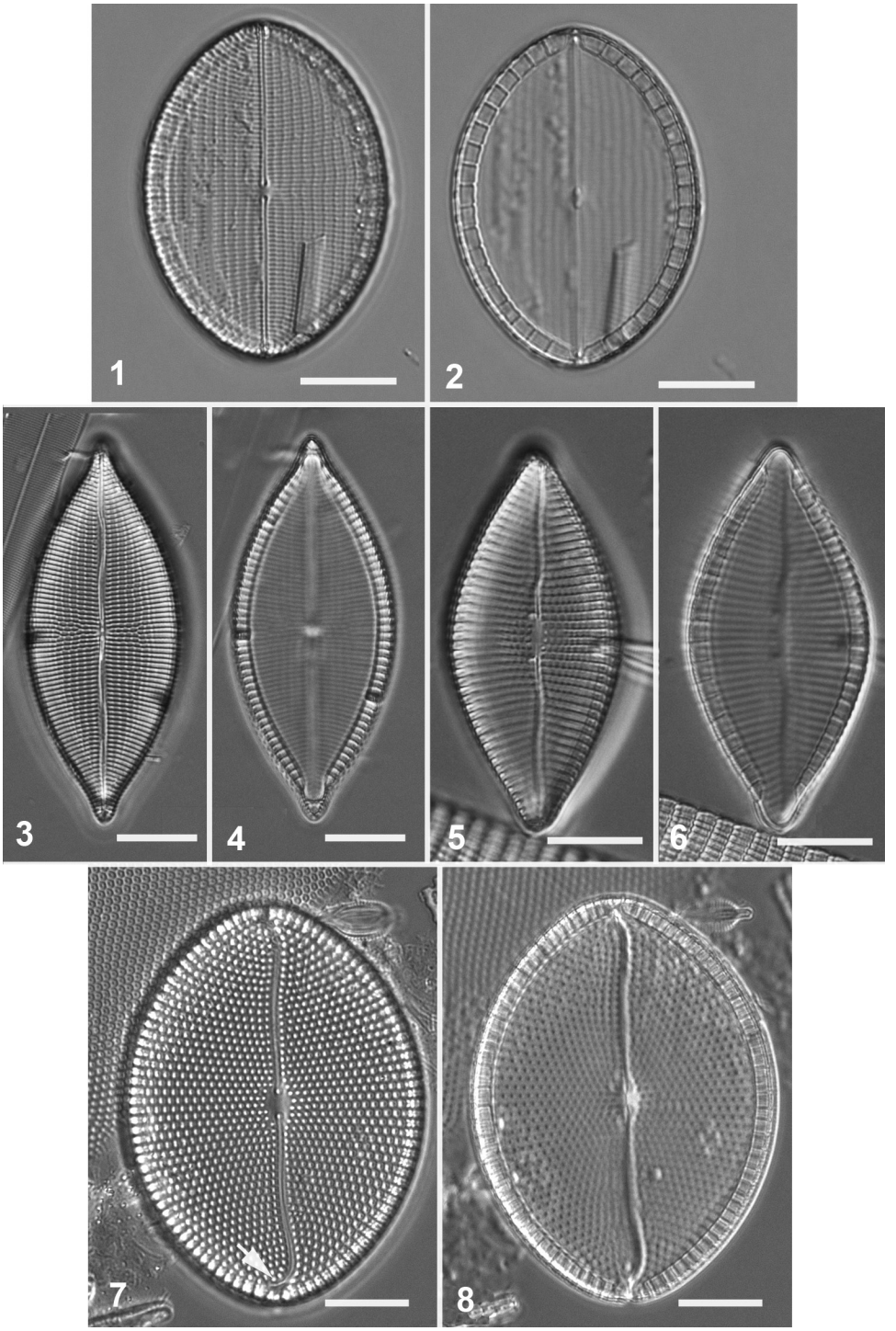

Plate 36.

Figs 1, 2. *Mastogloia rimosa* valve at two focal planes, DIC (GU52P-8).

Figs 3–6. *Mastogloia robusta*.

Figs 3–5. Valve at three focal planes; arrow indicates continuous axial costae across the central area, DIC (GU56A-2).

Fig. 6. Internal view showing axial costae continuous at central area (arrow), SEM (GU44Y-13).

Figs 7, 8. *Mastogloia sergensis* valve at two focal planes, DIC (Gab3C*).

Figs 9, 10. *Mastogloia rostrata* valve at two focal planes showing craticular bars in the rostrate extensions and the duct openings mid-way between partecta and narrowed part (arrowhead), DIC (GU44Z-15).

Scale bars = 10 μm.

Plate 36

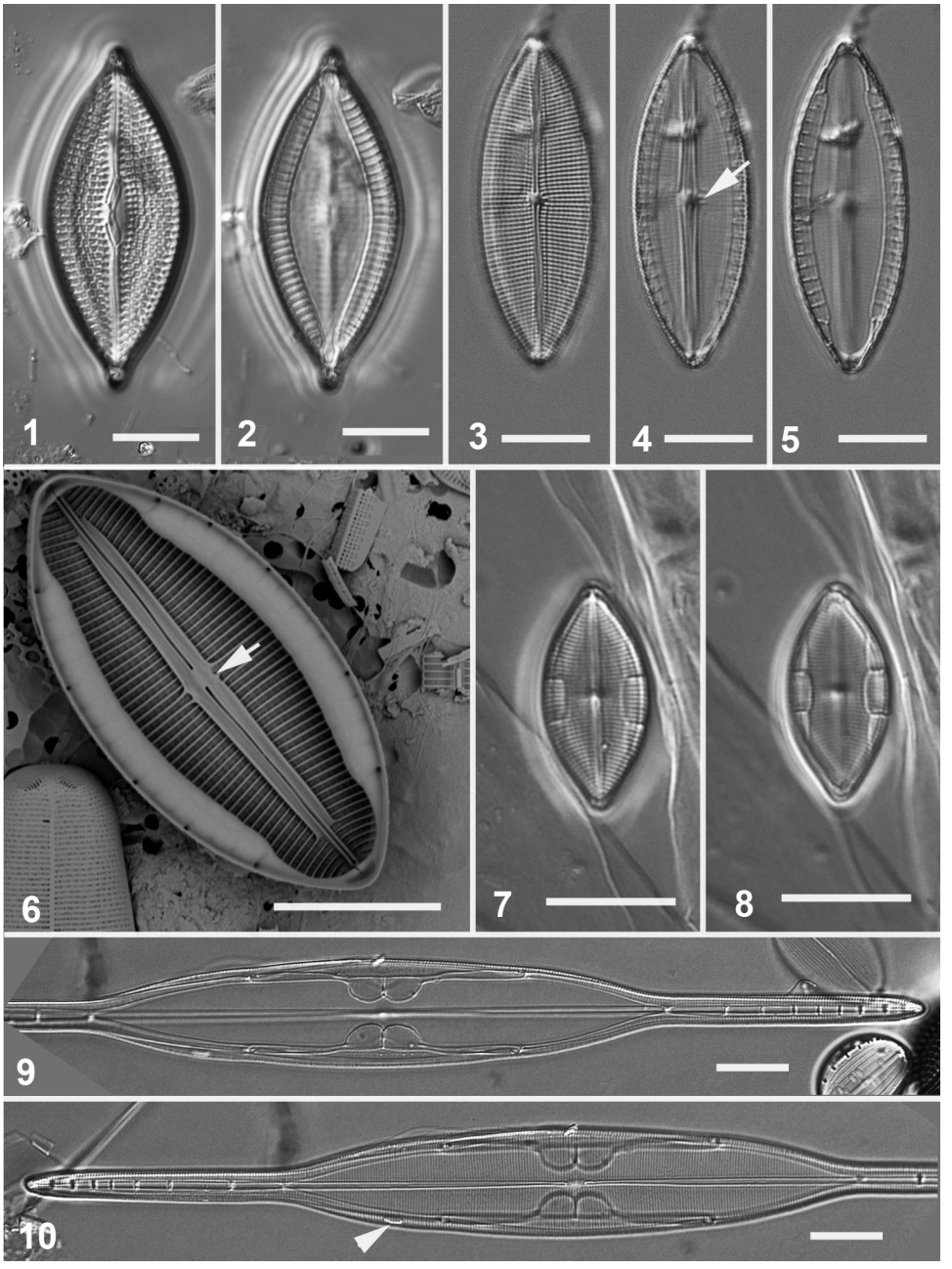

Plate 37.

Figs 1, 2. *Mastogloia sergensis* SEM (GU44P-B).

Fig. 1. External view of broken valve showing part of partectal ring below.

Fig. 2. Internal view of cell with one large chamber on each side.

Figs 3–5. *Mastogloia tautirensis* valve at three focal planes, DIC (GU44I-2).

Figs 6–8. *Mastogloia tenuis*.

Figs 6, 7. Valve at two focal planes (GU44Y-13).

Fig. 8. Internal view SEM, showing longitudinal silica ribs and the partectal ducts leading from the four partecta on each side to paired openings at each apex (arrows) (GU26A).

Fig. 9. *Mastogloia umbra*, external view showing conopeum (arrow), SEM (GU44Y-13).

Scale bars: Figs 1, 2, 6–9 = 5 μm. Figs 3–5 = 10 μm.

Plate 37

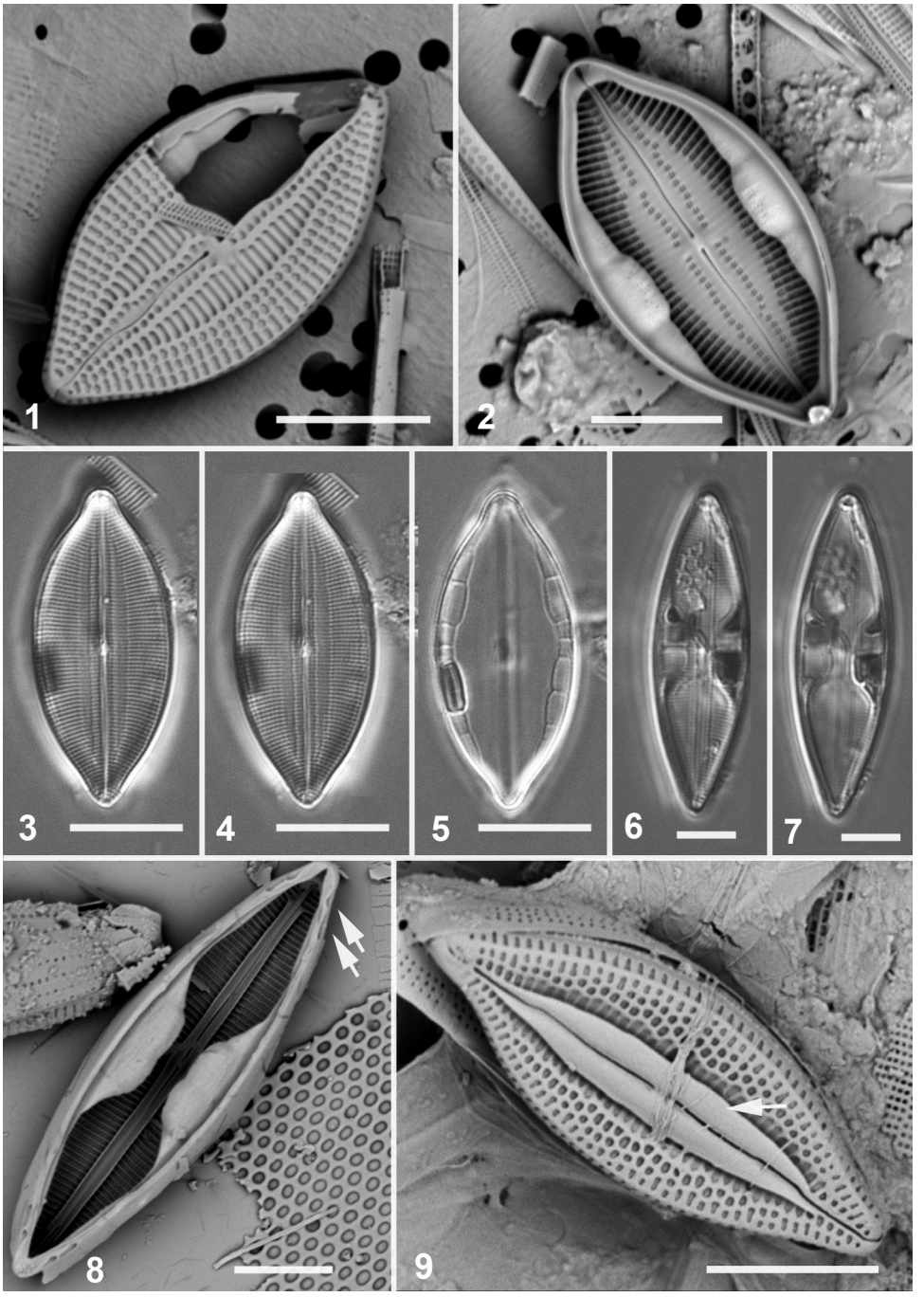

Plate 38.

Figs 1–4. *Achnanthes brevipes*.

Figs 1, 2. Raphe and sternum valves, respectively DIC (GU15C).

Figs 3, 4. Raphe and sternum valves, SEM (GU26A).

Figs 5, 6. *Achnanthes citronella*.

Fig. 5. Sternum valve, DIC (GU6D-2).

Fig. 6, Raphe valve internal view, SEM (GU6D-4).

Fig. 7. *Achnanthes cuneata*, DIC (GU26X).

Scale bars: Figs 1, 2, 5–7 = 10 μm, Figs 3, 4 = 5 μm.

Plate 38

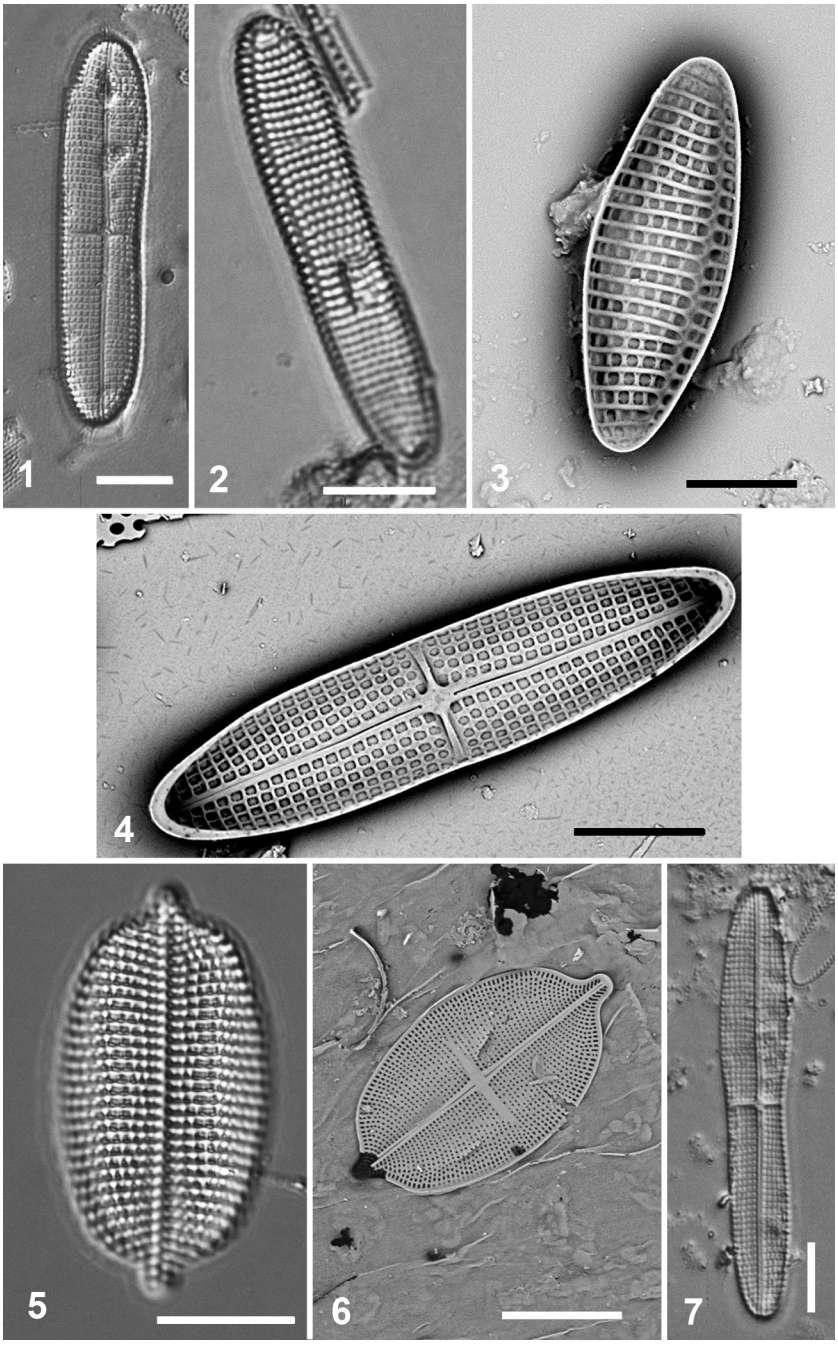

Plate 39.

Figs 1–3. *Achnanthes longipes*.

Fig. 1. Raphe valve, DIC (GU44I-1).

Fig. 2. Valve in girdle view showing striae on raphe and sternum valves (GU44I-1).

Fig. 3. Sternum valve, internal, SEM (GU44Y-13).

Fig. 4. *Planothidium campechianum*, SEM (GU44L-C).

Fig. 5. *Anorthoneis vortex*, DIC (GU44W-5).

Fig. 6. *Cocconeis coronatoides* sternum valve, external view, SEM (GU56A-1).

Scale bars: Figs 1, 2, 3, 5 = 10 μm, Fig. 4 = 2 μm, Fig. 6 = 5 μm.

Plate 39

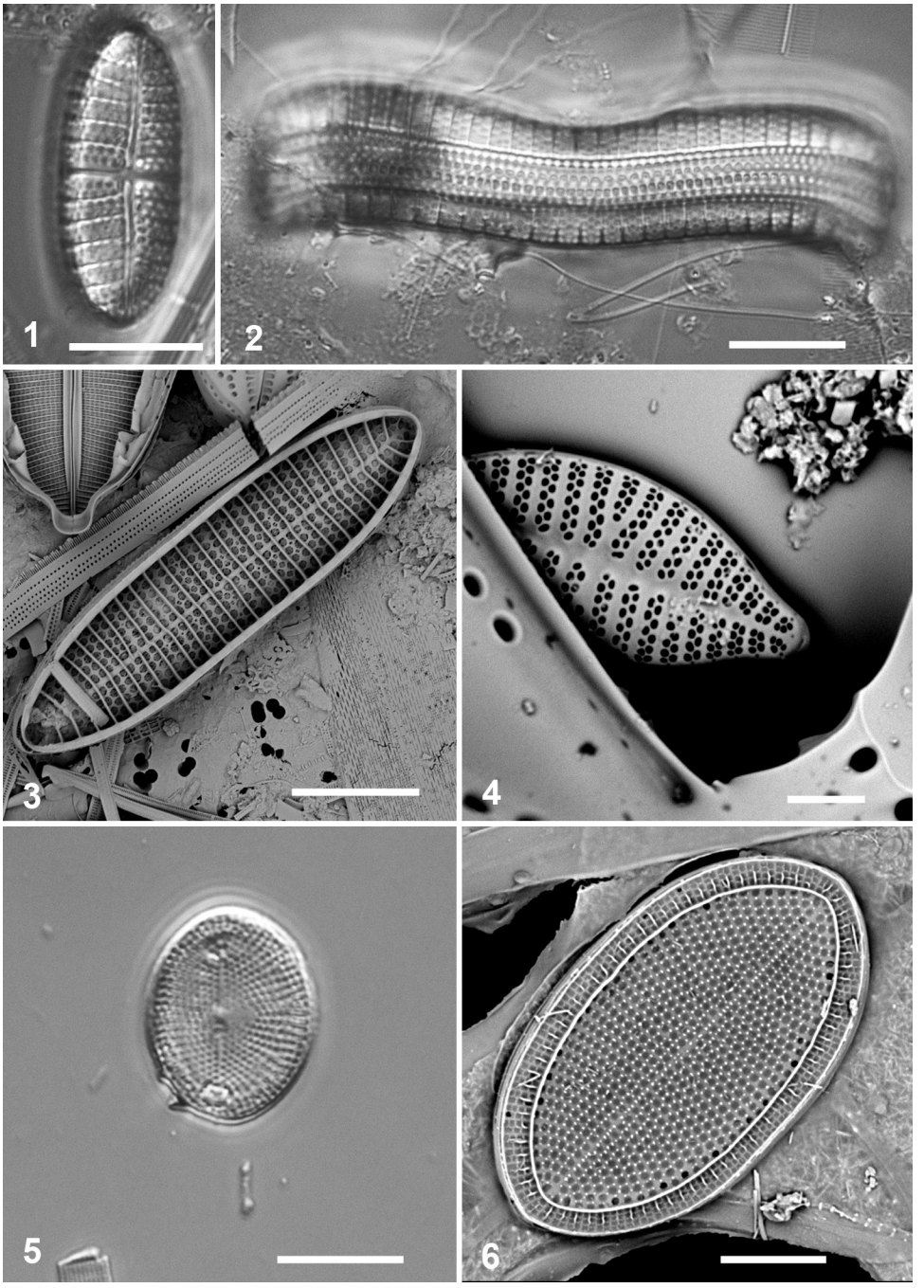

Plate 40.
Figs 1, 2. *Cocconeis dirupta* var. *dirupta*, raphe and sternum valves, DIC (GU44R-2).
Fig. 3. "*Cocconeis* sp. aff. *dirupta*" *sensu* Riaux-Gobin et al., broken frustule, raphe valve uppermost, showing part of sternum valve behind, SEM (GU44Z-15).
Figs, 4, 5. *Cocconeis dirupta* var. *flexella* sternum and raphe valves, SEM (GU44I-1).
Figs 6, 7. *Cocconeis heteroidea* sternum valve at two focal planes, DIC (GU44T-1).
Scale bars: Figs 1–5 = 5 μm, Figs 6, 7 = 10 μm.

Plate 40

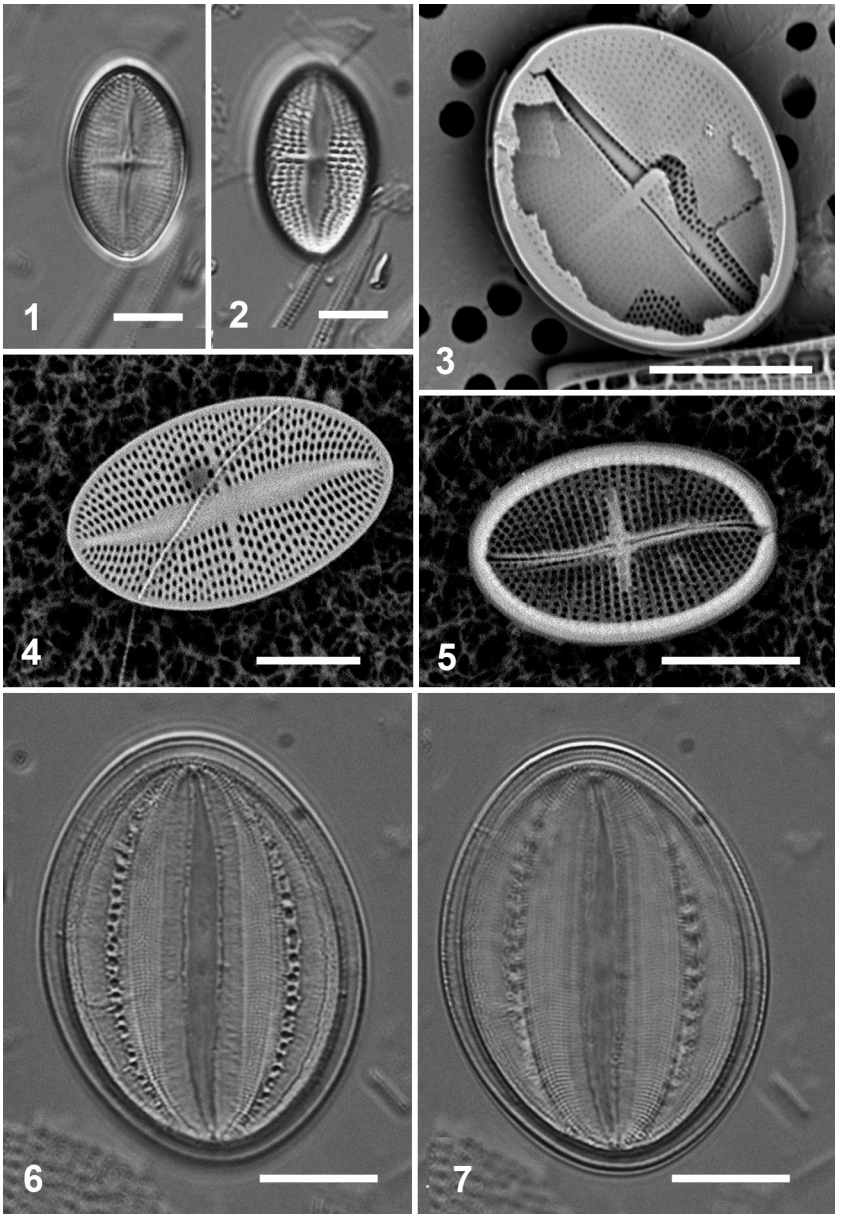

Plate 41.

Figs 1–3. *Cocconeis heteroidea*.

Fig. 1. Sternum valve external view, SEM (GU44AE-2).

Figs 2, 3. Raphe valve, external and detail of apex, SEM (GU44Y-13).

Figs 4, 5. *Cocconeis distans* sternum valve at two focal planes, arrow indicates biseriate striae on margin, DIC (GU12Z).

Fig. 6, 7. *Cocconeis scutellum* var. *scutellum*.

Fig. 6. Sternum valve, DIC (GU44I-1).

Fig. 7. Three sternum valves (possibly whole frustules attached to other diatoms), SEM (stacked images) (GU32B).

Scale bars: Figs 1–5, 7 = 10 μm, Fig. 6 = 5 μm.

Plate 41

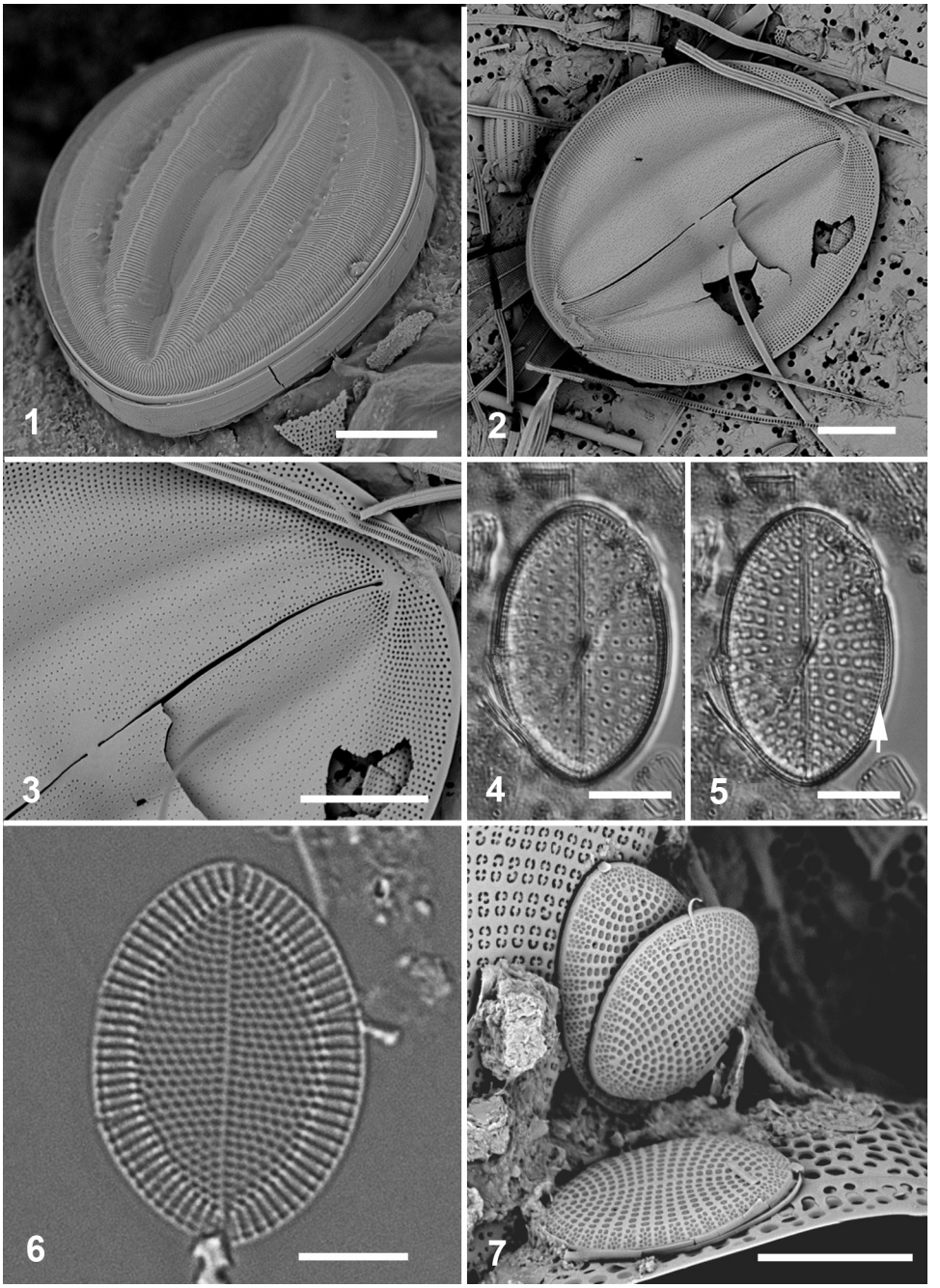

Plate 42.

Figs 1–3. *Cocconeis scutellum* var. *ornata* (GU52P-9).

Figs 1, 2. Sternum valve internal and external views, respectively, SEM.

Fig. 3. Sternum valve, DIC.

Figs 4, 5. *Climaconeis coxii*.

Fig. 4. Half of valve and valvocopula with craticular bars, showing the straight proximal raphe endings (arrow), DIC (GU44L-A).

Fig. 5. Central area, internal view showing valve and craticular bars, SEM (GU6D-2).

Fig. 6. *Parlibellus hamulifer*, valve showing raphe strongly deflected before the apices (arrow), DIC (GU44Z-15).

Scale bars: Figs 1–3, 5 = 5 μm, Figs 4, 6 = 10 μm.

Plate 42

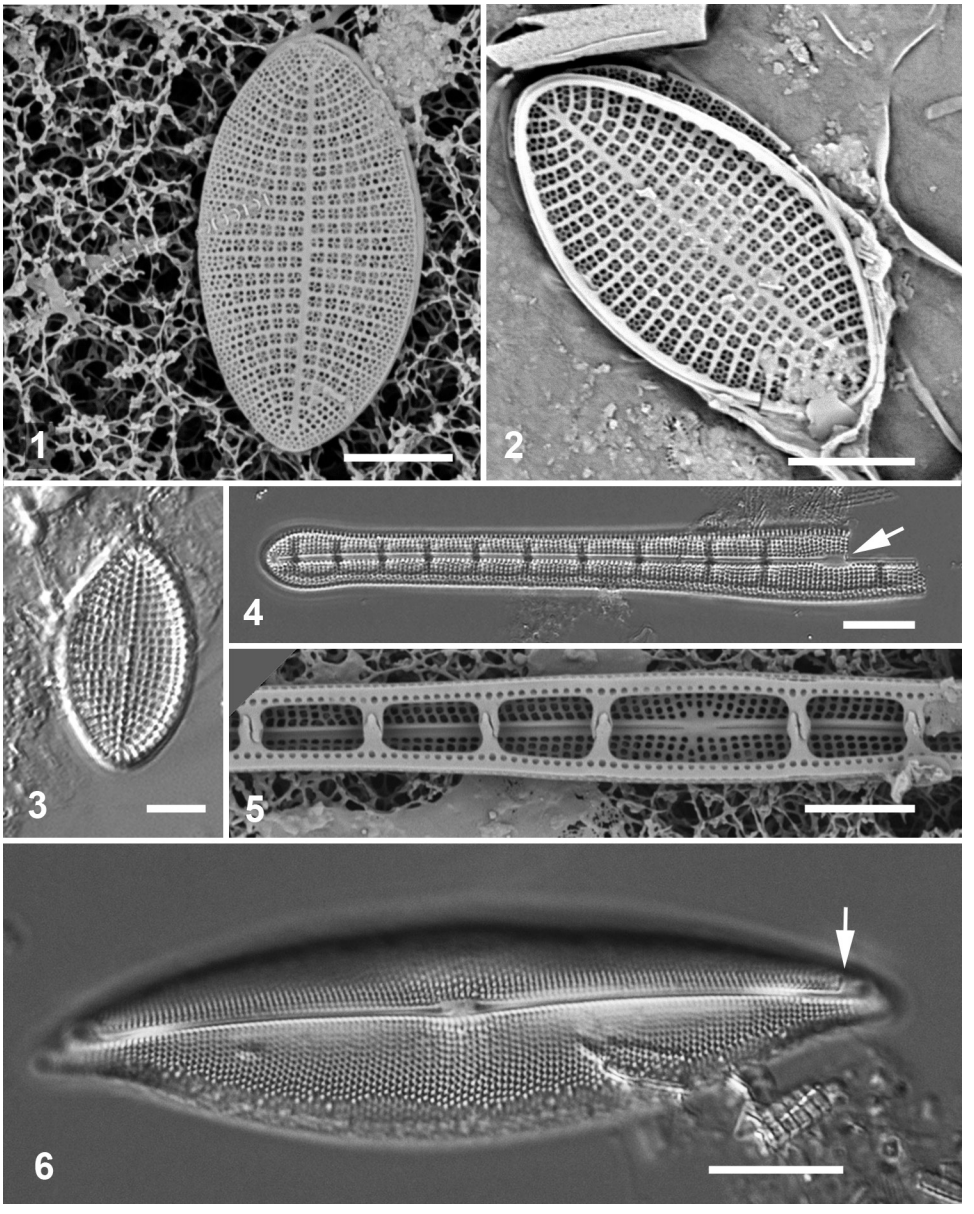

Plate 43.
Figs 1–4. *Diploneis bombus* (GU7N).
Figs 1, 2. Valve in brightfield and DIC respectively.
Figs 3, 4. External and internal views, SEM.
Scale bars = 10 μm.

Plate 43

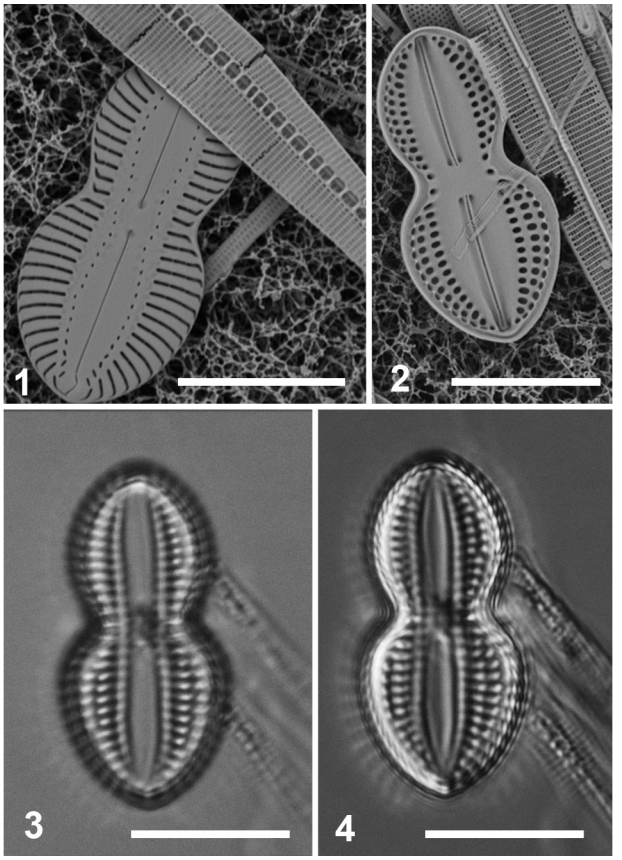

Plate 44.

Figs 1–4. *Diploneis chersonensis*.

Fig. 1. Valve in DIC (GU44Z-15).

Figs 2, 3. Exterior view and detail of central area, SEM (GU44Z-15). [Fig. 2 also shows exterior of *Grammatophora undulata*.]

Fig. 4. Interior view of central area, SEM (GU44Z-15).

Fig. 5. *Diploneis crabro*, brightfield (GU52P-5).

Scale bars: Figs 1, 2, 5 = 10 μm, Figs 3, 4 = 5 μm.

Plate 44

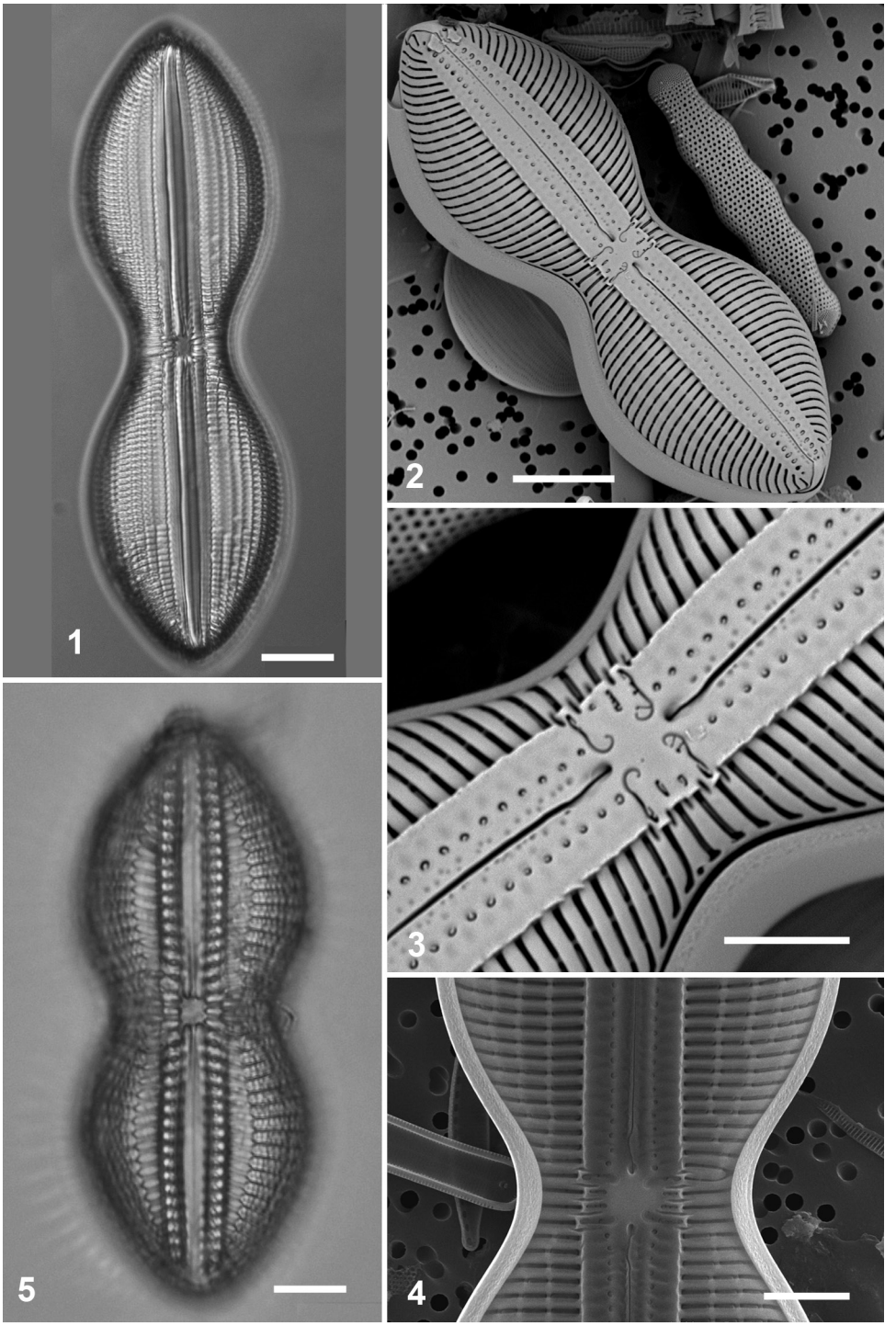

Plate 45.

Figs 1, 2. *Diploneis crabro*, external view showing half of valve and detail of central area, SEM (GU44AK-6).

Figs 3–6. *Diploneis smithii*.

Fig. 3. Valve in DIC (GU52N-7).

Fig. 4. Detail of central area, outer membrane intact, SEM (GU52N-7).

Fig. 5. Internal view, SEM (GU44AK-1).

Fig. 6. Valve in external view, outer membrane eroded, SEM (GU44I-1).

Scale bars: Figs 1, 3, 5, 6 = 10 μm, Figs 2, 4 = 5 μm.

Plate 45

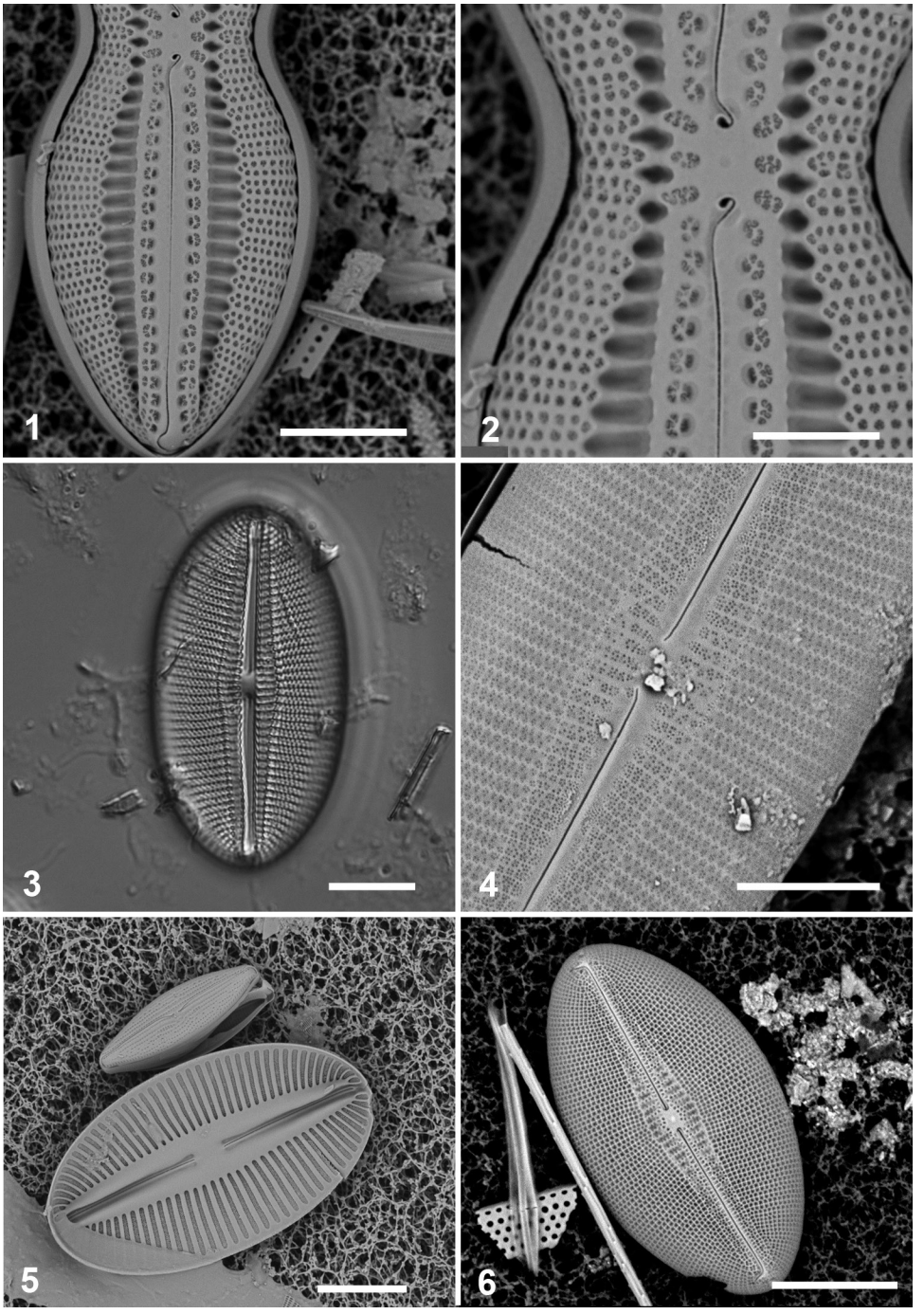

Plate 46.
Fig. 1. *Diploneis smithii* internal view with inner membrane eroded, SEM (GU44I-1).
Figs 2–4. *Diploneis suborbicularis*.
Fig. 2. Valves in DIC (GU52N-7).
Figs 3, 4. External and internal views, SEM (GU52Q-10a, GU52N-7, respectively).
Figs 5–7. *Diploneis weissflogii* (GU44Z-15), DIC, external and internal SEM, respectively.
Figs 8, 9. *Chamaepinnularia clamans*, DIC and external SEM (GU52N-7).
Scale bars: Figs 1, 6, 7, 8, 9 = 5 μm, Figs 2, 3, 4, 5 = 10 μm.

Plate 46

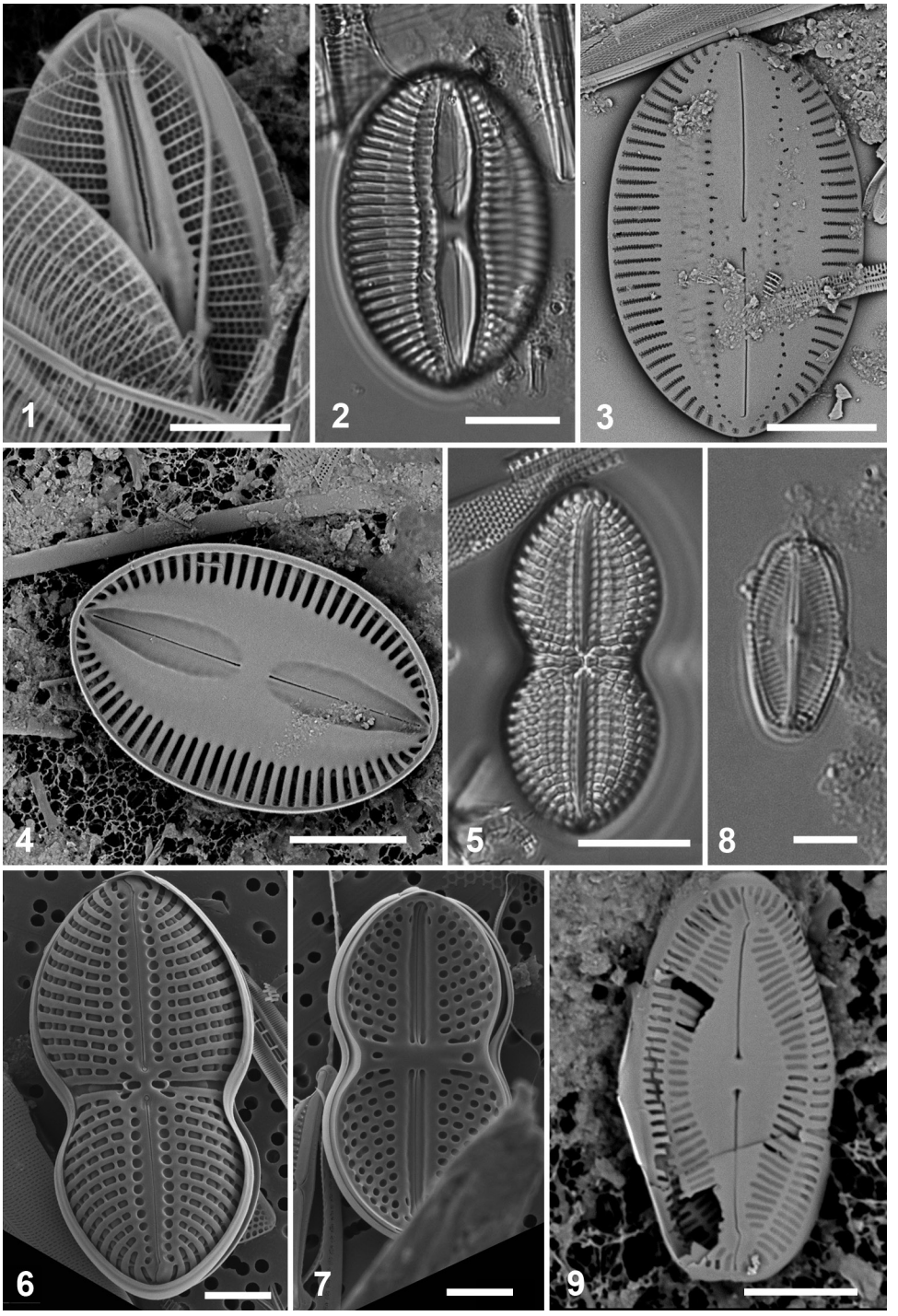

Plate 47.

Fig.1. *Cymatoneis sulcata* oblique external view, SEM (GU55B-4).

Figs 2–5. *Navicula cancellata* (GU6E-9).

Fig. 2. Valve view, DIC.

Fig. 3. Girdle view, DIC.

Fig. 4 Valve external view, SEM.

Fig. 5. Frustule girdle view, SEM.

Figs 6, 7. *Haslea howeana*.

Fig. 6. Valve, DIC (GU44Z-15).

Fig. 7. Detail of central area and striae, external view, SEM, courtesy N. Navarro (GU13AC).

Fig. 8. *Navicula consors*, valve in DIC (GU44Y-13).

Fig. 9. *Navicula mannii,* DIC (GU44Y-13).

Scale bars: Figs 1–6, 8, 9 = 10 μm, Fig. 7 = 1 μm.

Plate 47

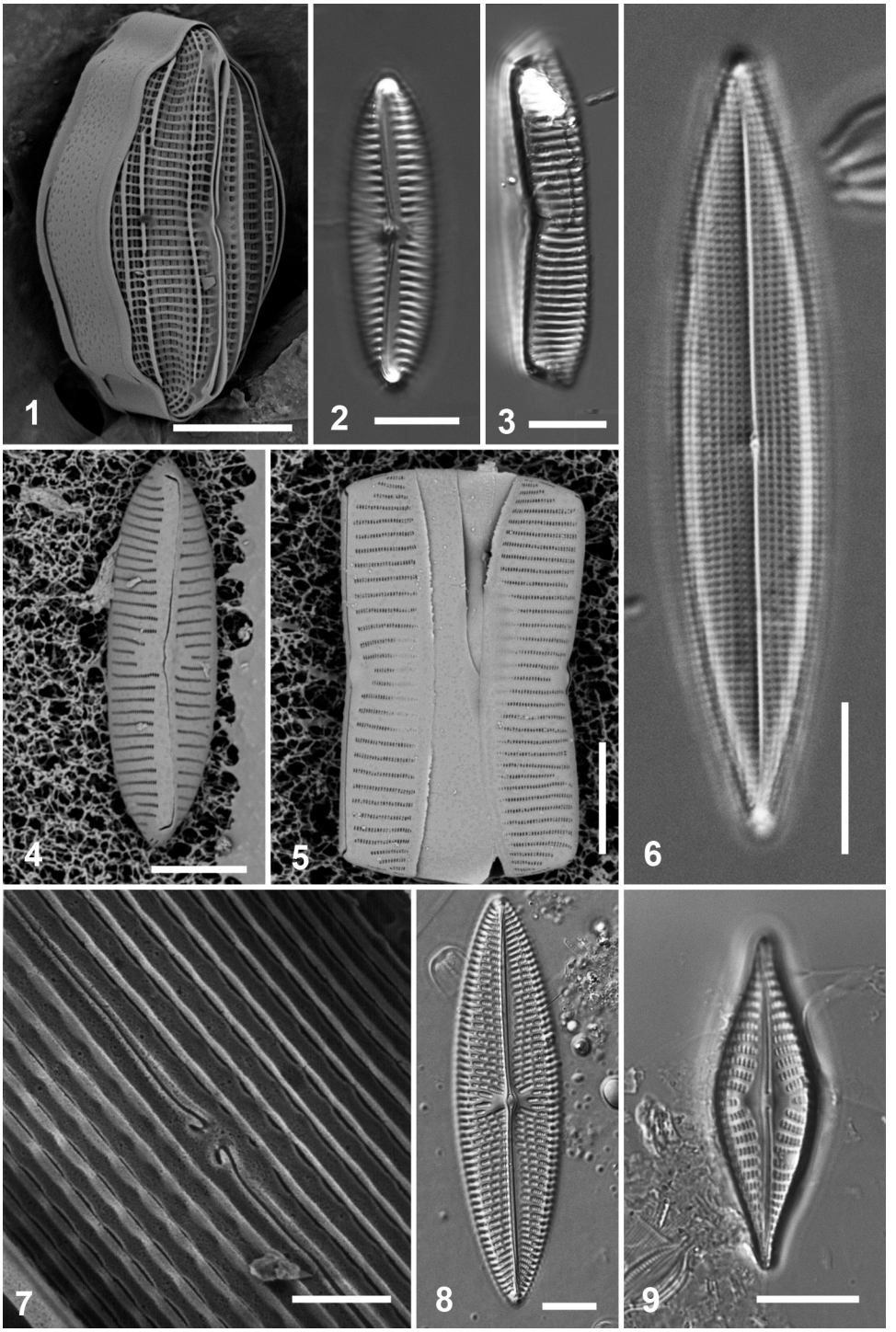

Plate 48.

Figs 1–3. *Navicula plicatula*.

Figs 1, 2. Valve at two focal planes, DIC (GU44U-1A).

Fig. 3. Details of central area and raphe, external, SEM (GU55B-4).

Figs 4–9. *Trachyneis aspera*.

Figs 4, 5. Live cell at two focal planes (Fig. 4 plastid, Fig. 5 valve face), showing lobed plastid margins, DIC (GU44U).

Fig. 6. Acid cleaned valve, DIC (GU44Z-15).

Fig. 7. External view, SEM (GU52P-4).

Fig. 8. Internal view, SEM (GU44L/ECT 3588).

Fig. 9. Broken valve showing external (arrow) and internal (arrowhead) faces of the valve and the wall structure, SEM (GU55B-4).

Scale bars: Figs 1, 2, 6–9 = 10 μm, Figs 3 = 5 μm, Figs 4, 5 = 20 μm.

Plate 48

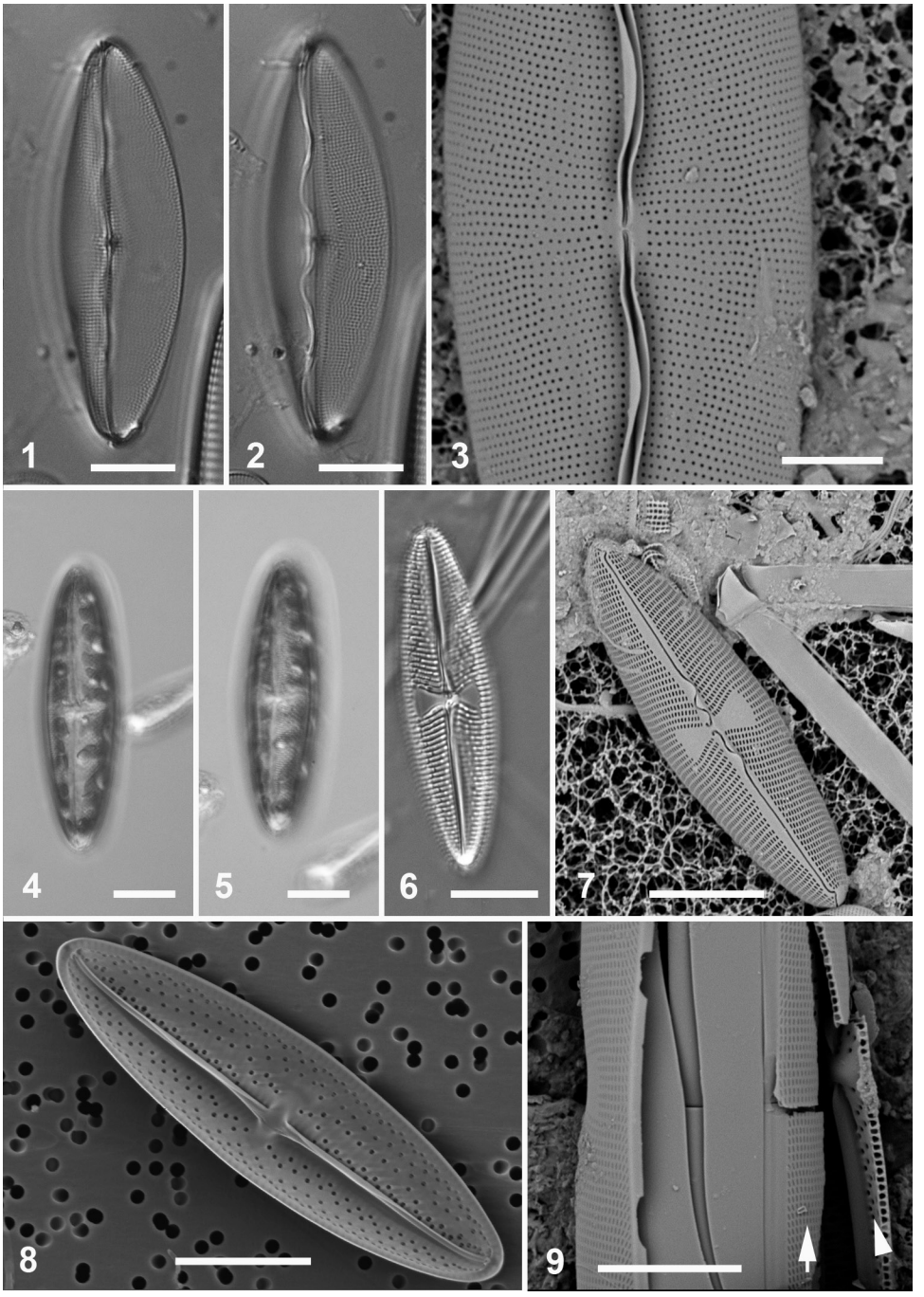

Plate 49.
Figs 1, 2. *Trachyneis velata* valves, DIC (GU52Q-1a).
Figs 3,4. *Caloneis egena*.
Fig. 3. Valve, DIC (GU44I-1).
Fig. 4. Frustule, oblique view, SEM (GU6D-4).
Figs 5, 6. *Caloneis liber* valves, DIC (GU6E-4).
Scale bars = 10 μm.

Plate 49

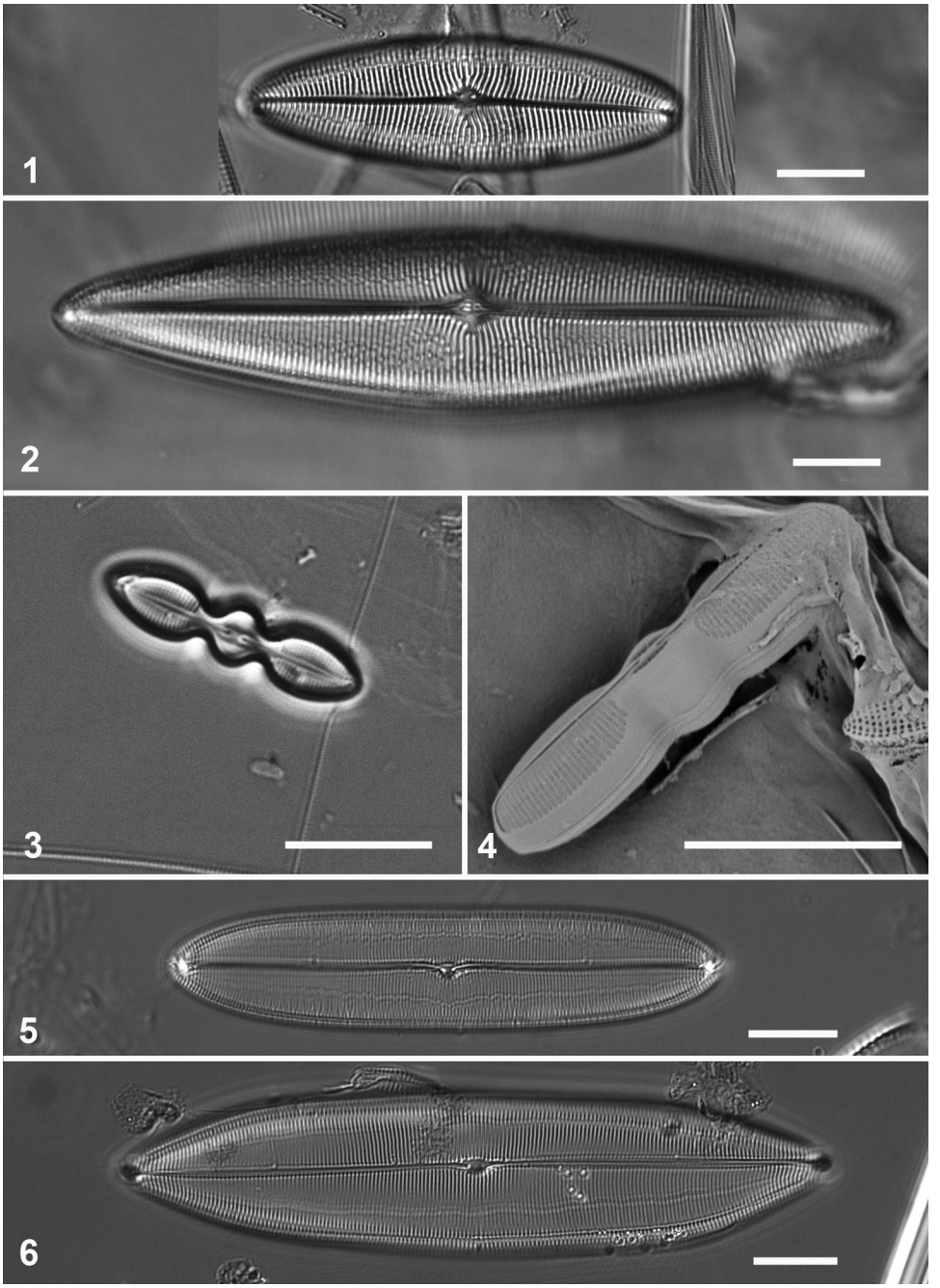

Plate 50.

Figs 1–3. *Caloneis liber.*

Fig. 1. Half of large valve, DIC (GU44I-1).

Fig. 2. Apex of broken frustule in girdle view showing alveolate wall structure and lack of a break in the striae, SEM (GU52P-9).

Fig. 3. Apex of valve, internal showing helictoglossa and single rows of internal alveola openings, SEM (GU55B-4).

Fig. 4. *"Oestrupia* 4" *sensu* Hein et al. 2008, showing line dividing the alveolae (arrow).

Figs 5, 6. *Donkinia minuta* live cell in girdle and valve orientations, respectively, DIC (ECT3739 from GU61).

Scale bars: Figs 1, 2, 4–6 = 10 μm, Fig. 3 = 5 μm.

Plate 50

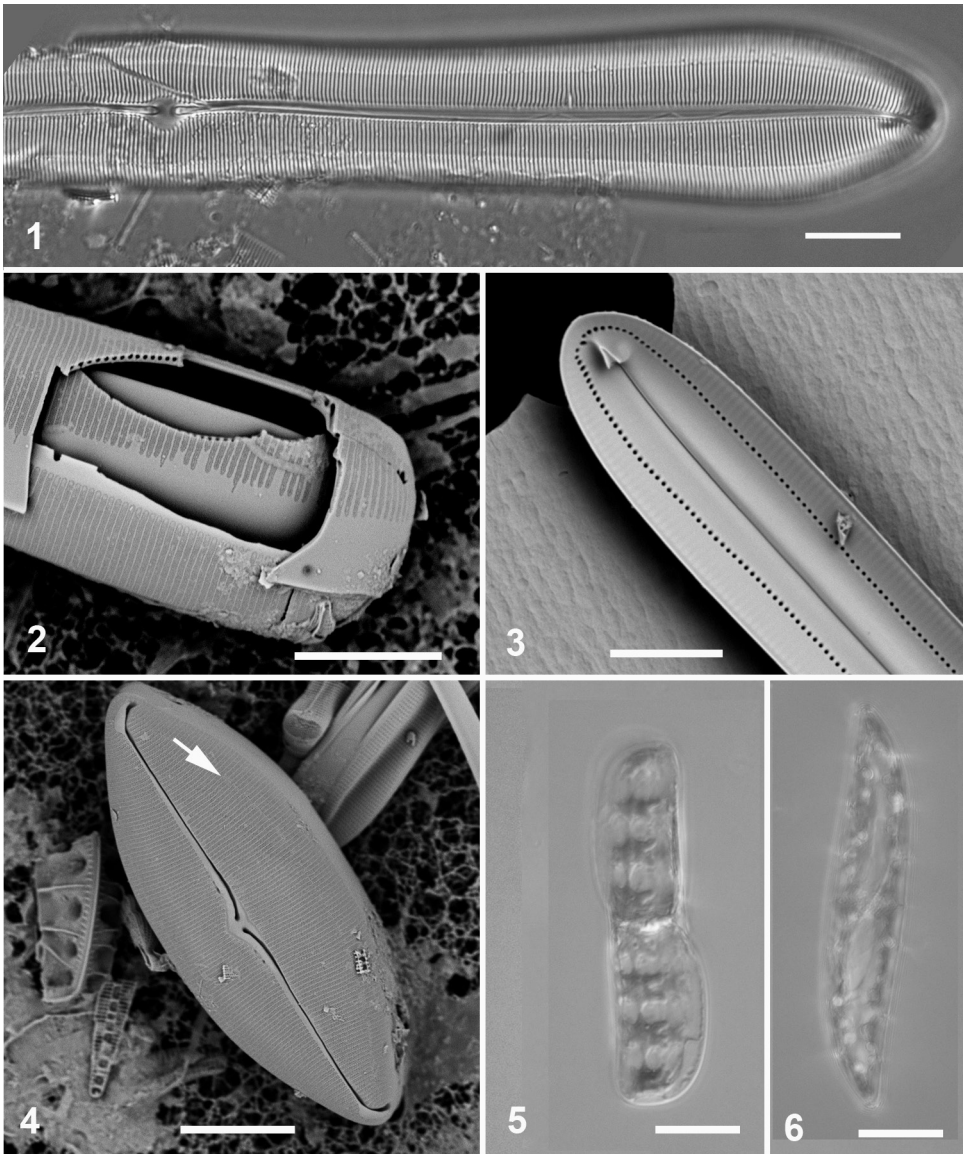

Plate 51.

Fig. 1. *Donkinia minuta* acid cleaned frustule in girdle view, showing unequal keeling in the two halves, DIC (GU44H-15).

Figs 2–4. *Pleurosigma intermedium*.

Fig. 2. Valve, DIC (GU44Z-15).

Figs 3, 4. Internal apex and central area, SEM (GU26A).

Figs 5–8. *Plagiotropis lepidoptera* (GU44R-2).

Figs 5, 6. Valve at two focal planes, DIC.

Figs 7, 8. Valve internal view, half of valve and detail of apex with helictoglossa, SEM.

Scale bars: Figs 1–7 = 10 μm, Fig. 8 = 5 μm.

Plate 51

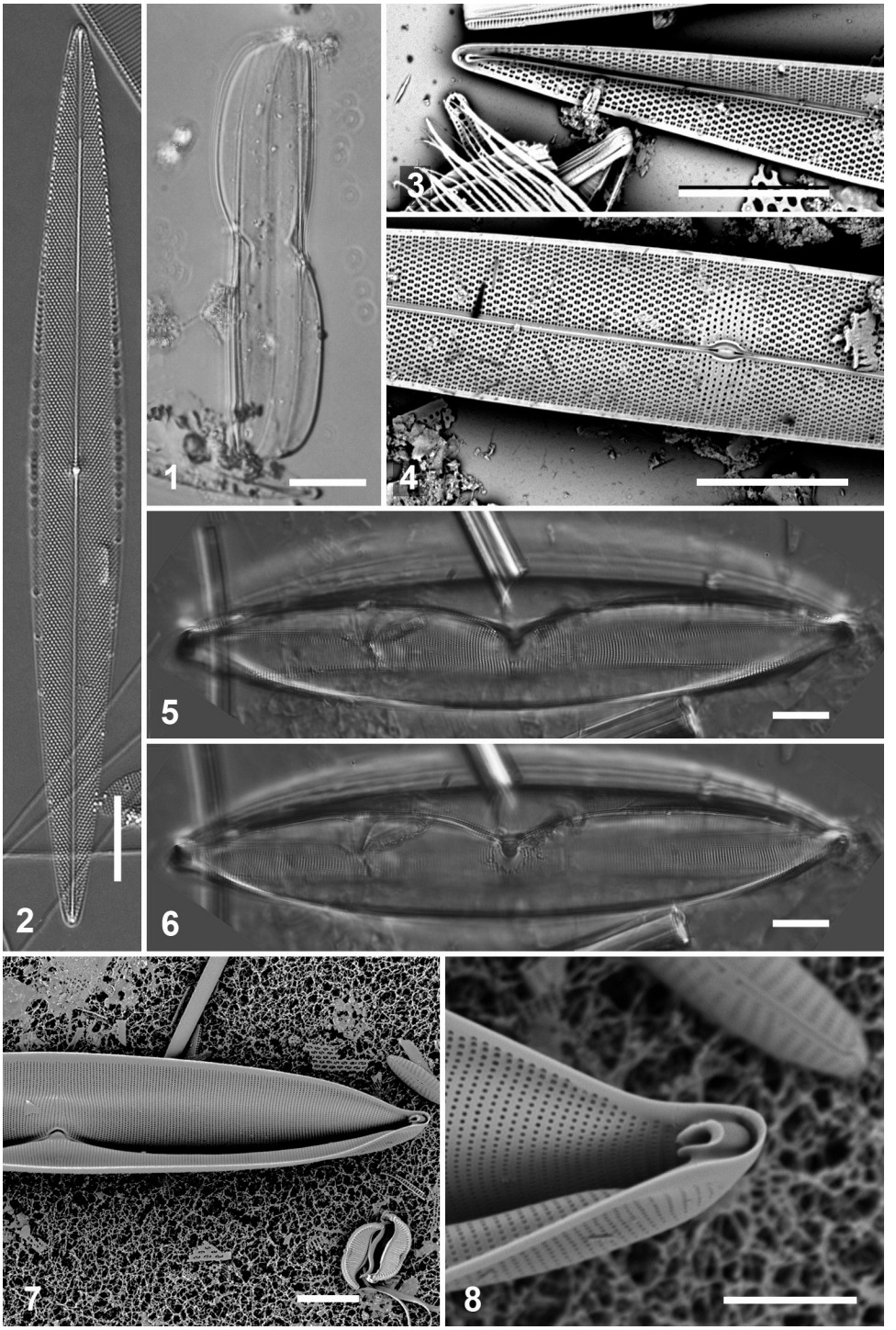

Plate 52.

Figs 1–3. *Staurotropis seychellensis*.

Fig. 1. Frustule in girdle view, cultured cell, DIC (ECT 3721).

Fig. 2. Detail of proximal raphe endings, cultured cell, SEM (ECT 3721).

Fig. 3. Whole frustule with one valve in girdle view, one in valve view, SEM (GU43C).

Figs 4, 5. *Stauroneis retrostauron,* valve in valve view and valve with copulae in girdle view, DIC (GU44Z-15).

Fig. 6. *Proschkinia complanatoides* frustule showing stigma and girdle bands, DIC (GU44Z-15).

Scale bars: Fig. 1 = *ca*. 10 μm, Fig. 2 = 5 μm, Figs. 3–6 = 10 μm.

Plate 52

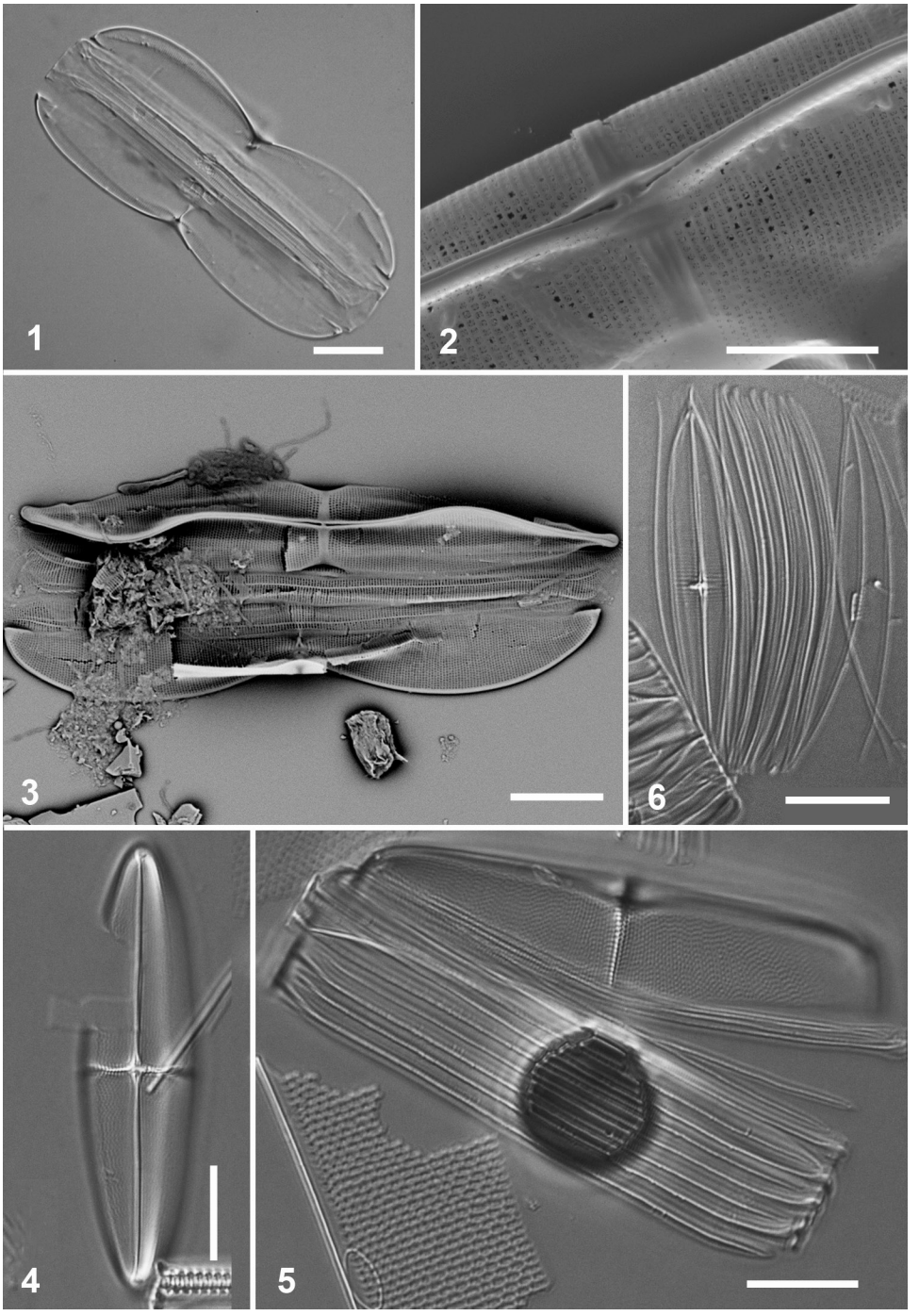

Plate 53.

Figs 1–4. *Proschkinia complanatoides*.

Fig. 1. Valve showing stigma, DIC (GU44Z-15).

Fig. 2. Detail of internal stigma, SEM (GU44Z-15).

Figs 3, 4. Whole mount of valves from live material shown in Pl. 1, Figs 3–5, showing the characteristic folded girdle bands (GU62A-7).

Fig. 5. *Amphora arcuata*, DIC (GU6E-5).

Figs 6, 7. *Amphora arenaria* valve at two focal planes, DIC (GU44I-2).

Scale bars: Figs 1, 3, 5–7 = 10 μm, Fig. 2 = 2 μm, Fig. 4 = 5 μm.

Plate 53

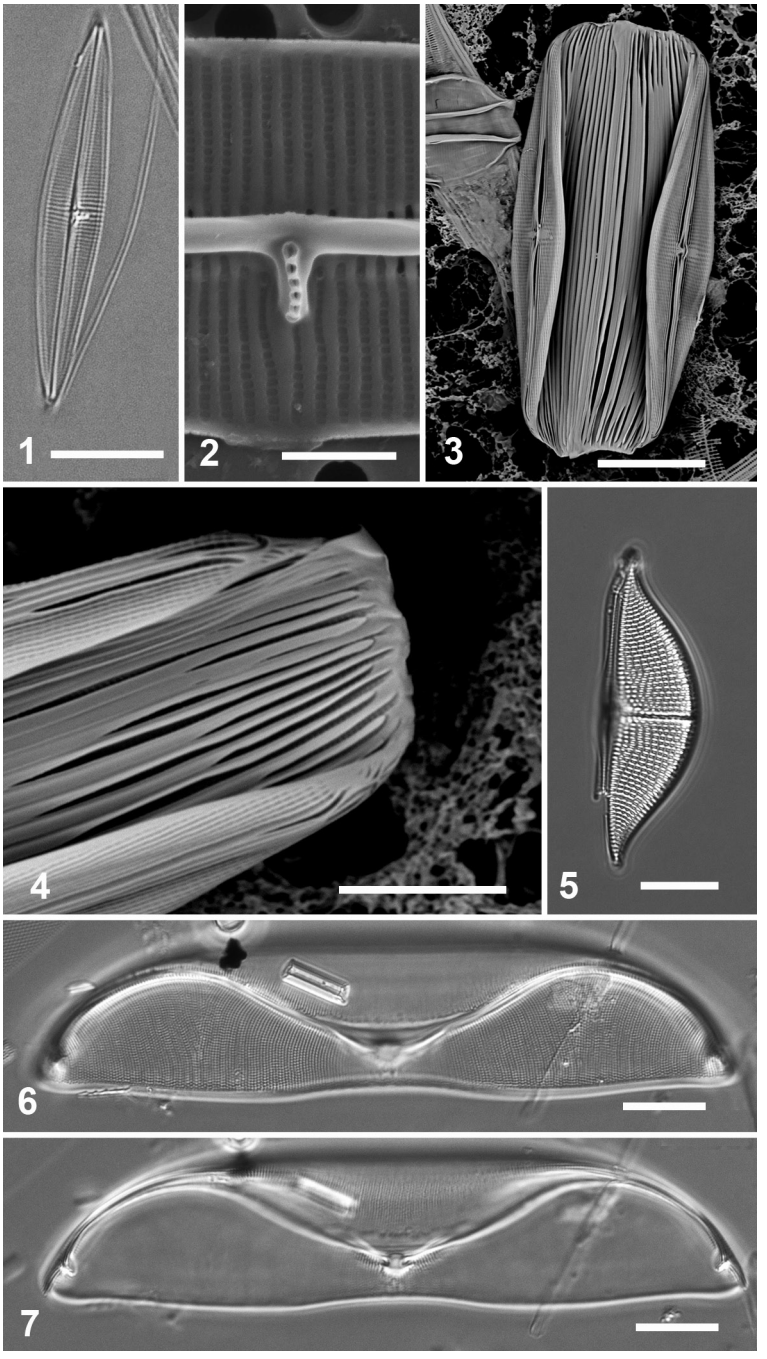

Plate 54.

Figs 1, 2. *Amphora arenaria*.

Fig. 1. Frustule in ventral view showing narrow girdle bands, DIC (GU44AP-2).

Fig. 2. Valve internal view, central detail, SEM (GU44I-2).

Figs 3, 4. *Arenaria obtusa*, valve at two focal planes, DIC (GU44AK-6).

Fig. 5. *Amphora decussata,* two valves, the smaller one with several attached girdle bands, DIC (GU43C).

Scale bars = 10 μm.

Plate 54

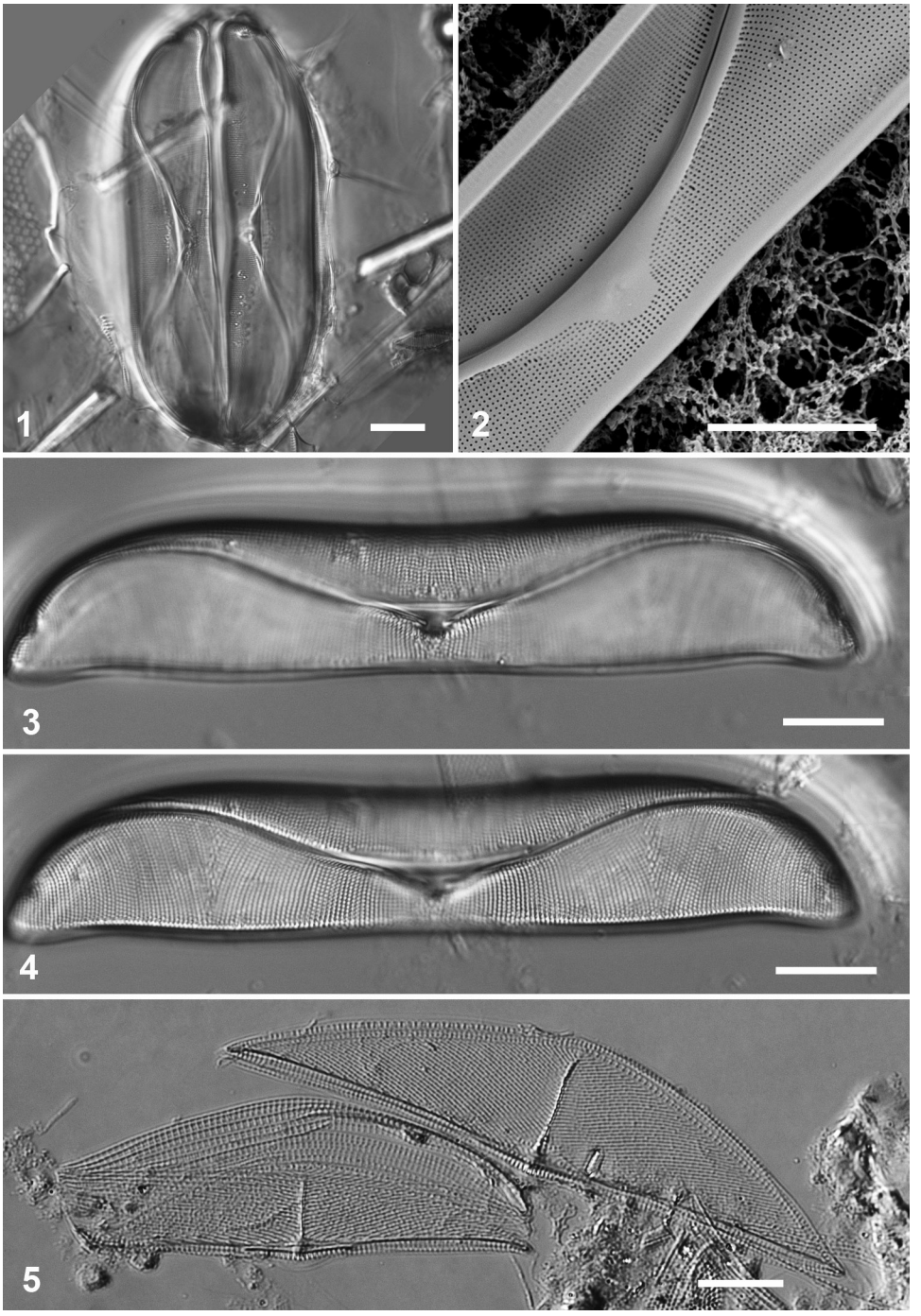

Plate 55.

Figs 1–3. *Amphora decussata,* SEM.

Fig. 1. Portion of valve, internal view; c = conopeum; d = dorsal striae; f = fascia; ms = marginal stria; v = ventral striae; external slits visible in some areolae (arrowhead) (GU44Z-15).

Fig. 2. Whole mount of frustule with shape retained, SEM (GU62A-1A).

Fig. 3. Whole mount of collapsed frustule in ventral view, central area of valves and copulae, external surfaces; arrows indicate conopea over proximal raphe endings (GU62A-1A).

Scale bars = 10 μm.

Plate 55

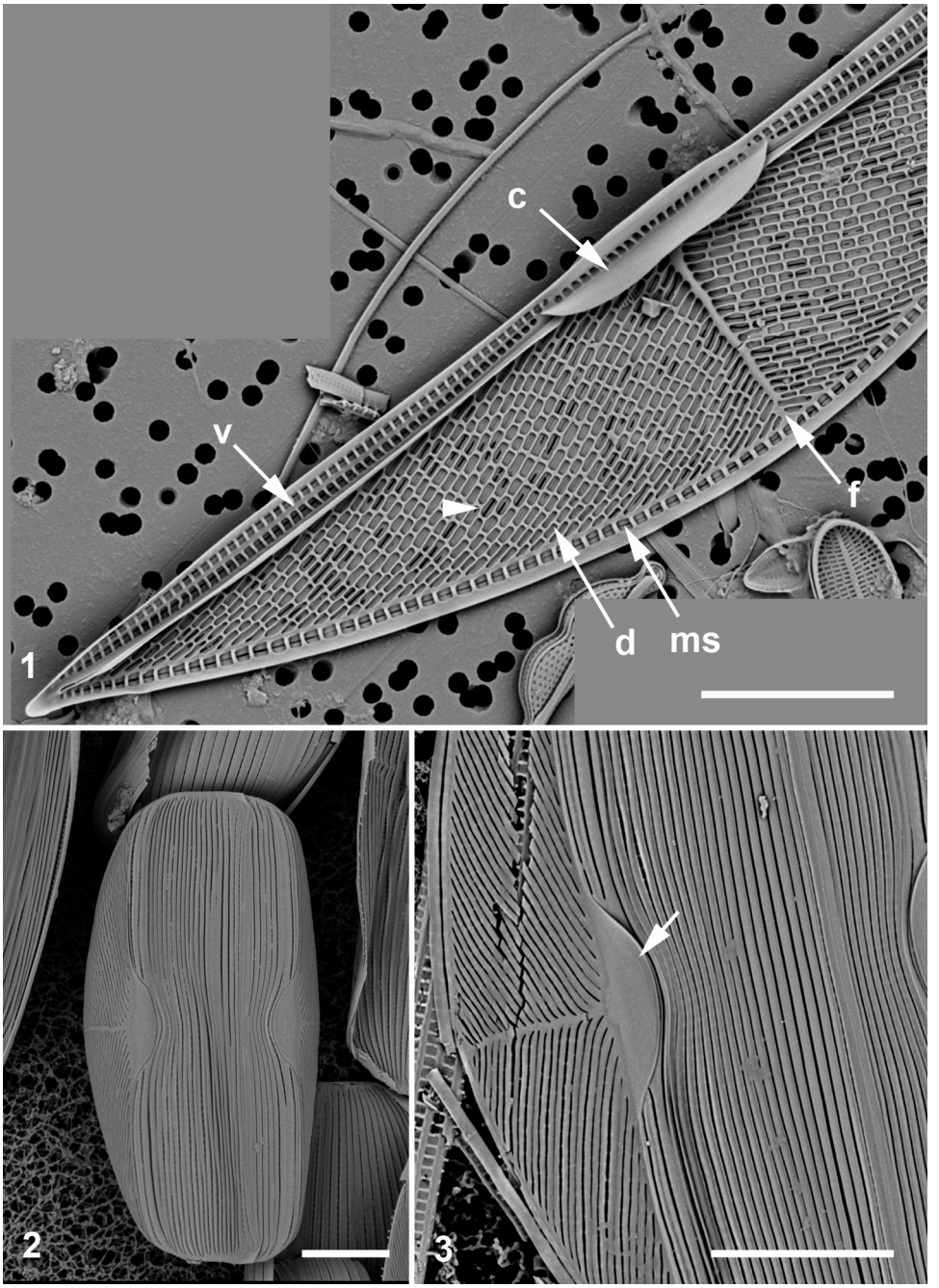

Plate 56.

Figs 1–4. *Amphora immarginata*.

Figs 1, 2. Valves at different angles, Fig. 2 showing "ghost striae" below raphe ledge (arrow), DIC (GU44Z-15, GU44I-1).

Fig. 3. Valve external view showing raphe ledge (arrow), SEM (GU44Z-15).

Fig. 4. Oblique view showing internal aspect of dorsal and ventral striae and external aspect of dorsal striae, SEM (GU54B-4).

Figs 5, 6. *Amphora ostrearia* var. *vitrea*.

Fig. 5. Two frustules in ventral view, DIC (GU44K-6).

Fig. 6. Valve external surface, SEM (GU44Z-15).

Figs 7–9. *Amphora vaughanii*.

Fig. 7. Valve in DIC (GU44Z-15).

Figs. 8, 9. Internal view, details respectively of apex and central area showing central nodule (arrow); the structure indicated by arrowheads is a copula lying on the valve, SEM (GU52J-3).

Scale bars: Figs 1–7 = 10 μm, Figs 7, 8 = 5 μm.

Plate 56

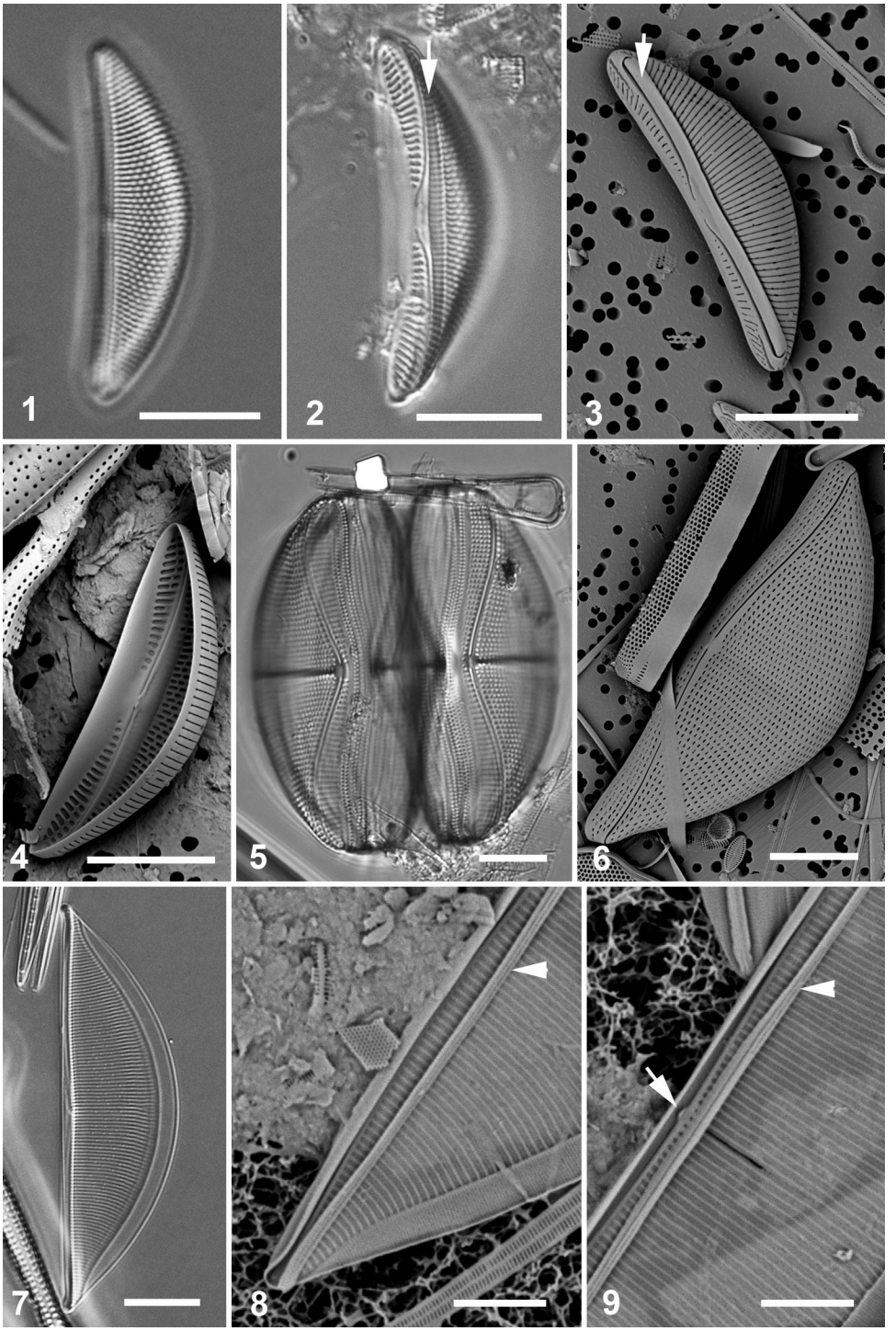

Plate 57.

Figs 1, 2. *Undatella lineata*.

Fig. 1. Valve, girdle view, DIC (GU44I-1).

Fig. 2. Frustule, SEM (GU6D-3).

Figs 3–6. *Undatella quadrata*.

Fig. 3. Living wild cell, showing plastids, DIC (GU7).

Figs 4–6. Cultured cells (ECT 3729 from GU7).

Fig. 4. Cell in valve view, brightfield.

Fig. 5. Valve in girdle view showing the short span of fibulae (arrow), brightfield.

Fig. 6. Frustule, again showing short span of fibulae (arrow), SEM (ECT 3729).

Scale bars: Figs 1, 3–6 = 10 μm, Fig. 2 = 5 μm.

Plate 57

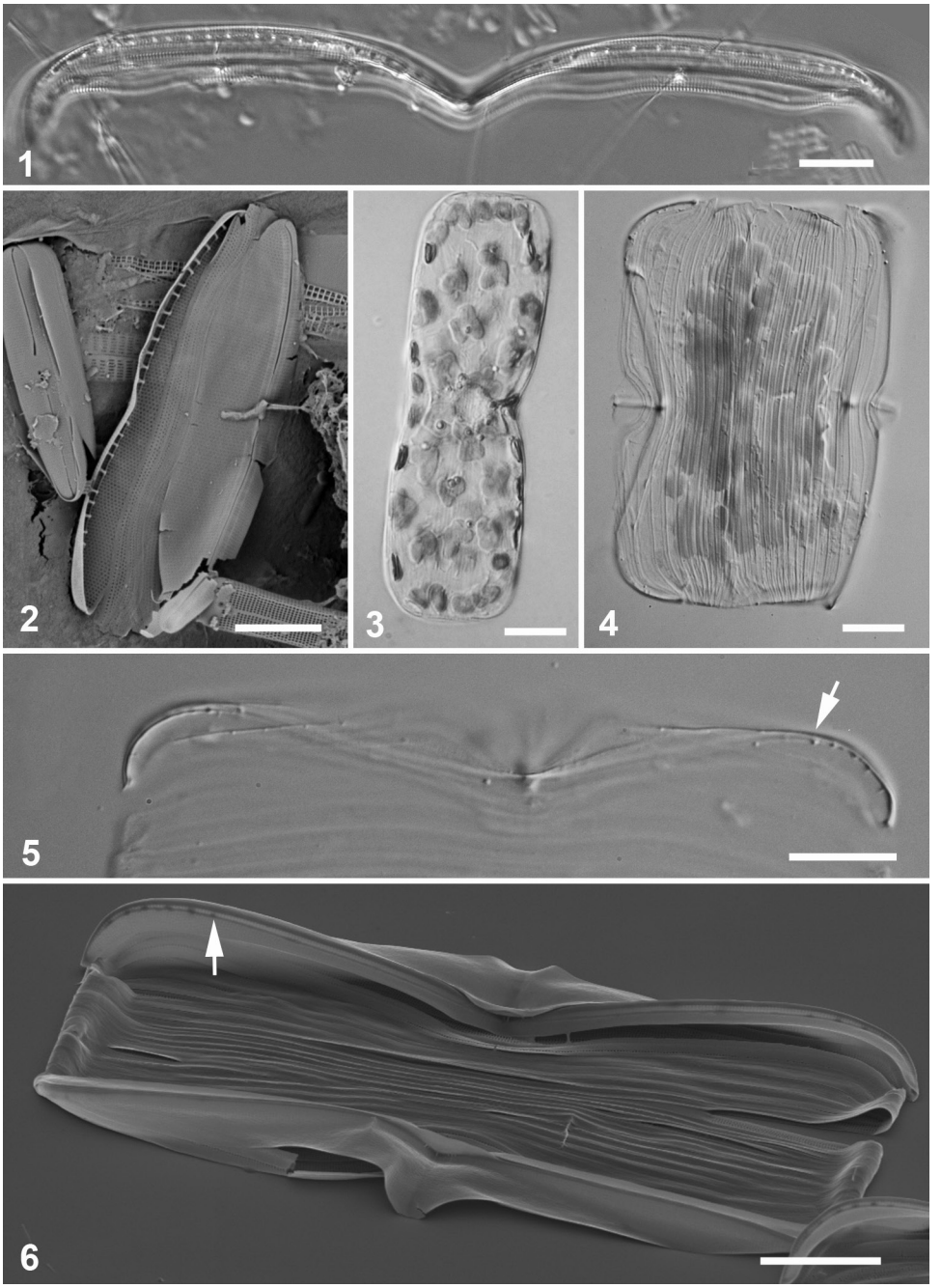

Plate 58.

Fig. 1. *Thalassiophysa hyalina* detail of whole mount showing external features of keel, proximal raphe endings and stria pattern, SEM (GU7S).

Figs 2–6. "*Bacillaria* Group B" *sensu* Schmid.

Figs. 2, 3. Live colonies showing different size cells and different plastid form (GU7N, GU44AC-4 respectively).

Figs 4, 5. Valves, DIC (GU7N); Fig. 5 shows the presence of a few linear cells in the population of largely linear-lanceolate cells.

Fig 6. Valve, DIC (GU44Z-15).

Scale bars = 10 μm.

Plate 58

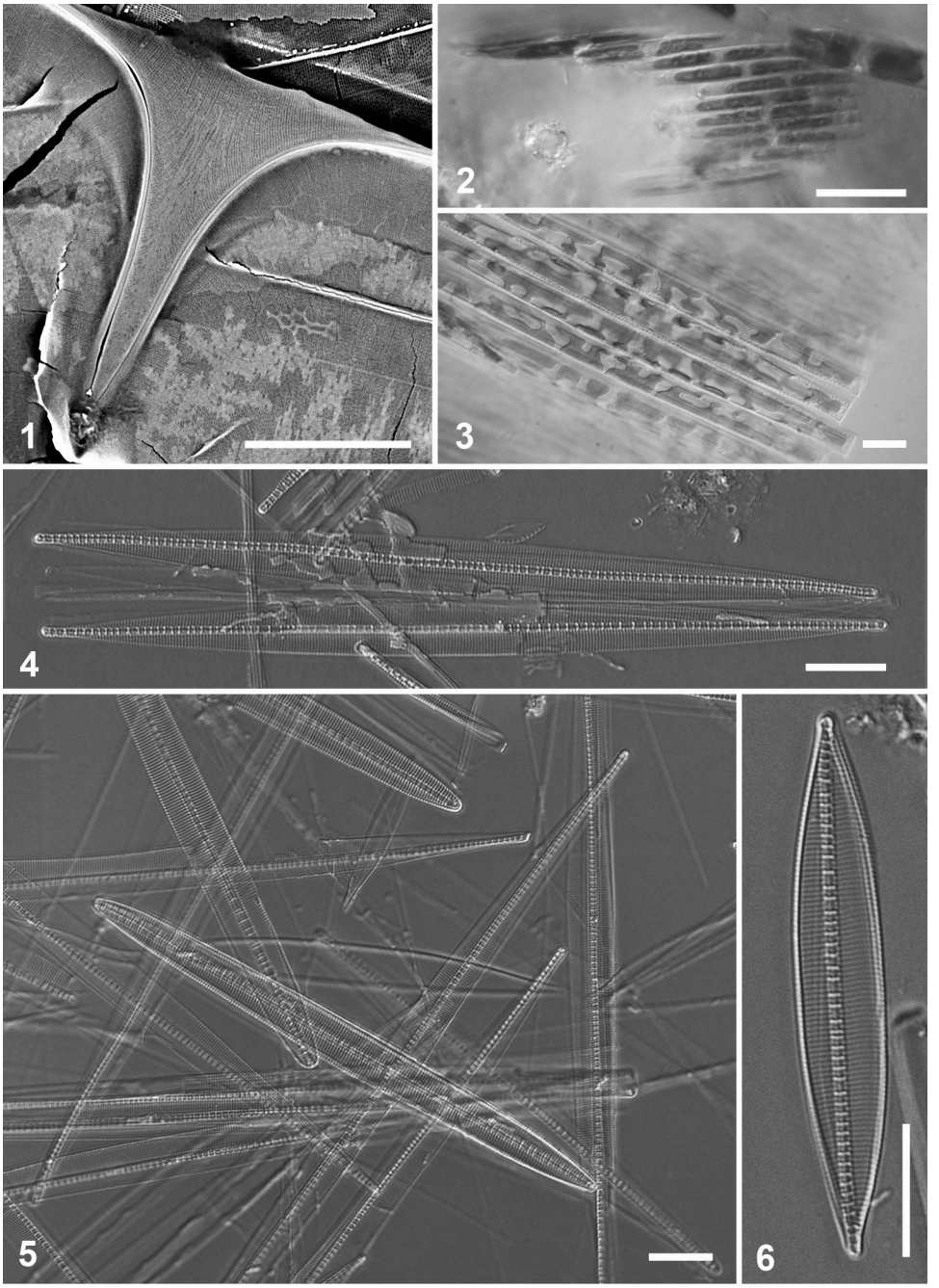

Plate 59.

Figs 1, 2. "*Bacillaria* Group B" *sensu* Schmid, SEM (GU7N).

Fig. 1. Frustule apex showing distal raphe ending.

Fig. 2. Internal view of portion of valve, showing fibulae and biseriate striae.

Figs 3–5. *Nitzschia angularis*.

Figs 3, 4. Whole valve, and enlargement of central area showing conopeum (arrow) and decussate striae, DIC (GU44K-6).

Fig. 5. Internal detail, SEM showing fibulae and decussate striae, SEM (GU44I-1).

Figs 6–8. *Nitzschia constricta*.

Fig. 6. Valve in DIC tentatively identified as *N. constricta* (GU44Z-15).

Fig. 7. External view, SEM (GU44J-2).

Fig. 8. Internal view, SEM (GU44Z-15).

Scale bars: Figs 1, 2, 5, 7 = 5 μm, Figs 3, 4, 6 = 10 μm, Fig. 8 = 2 μm.

Plate 59

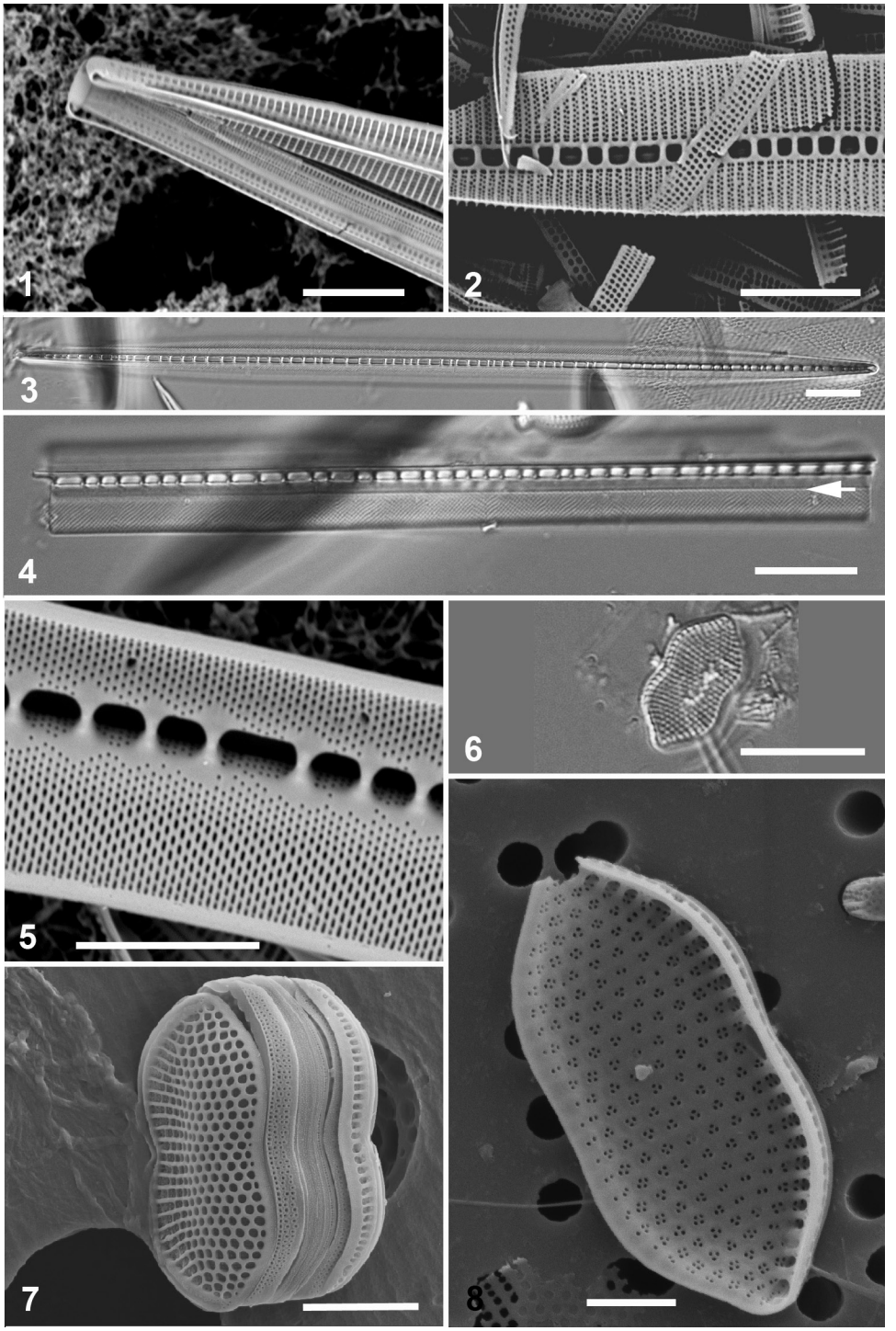

Plate 60.

Figs 1–3. *Nitzschia dissipata*; arrows indicate edge of conopeum.

Fig. 1. DIC (GU44Z-15).

Fig. 2. SEM of frustule showing external and internal faces, SEM (GU26A).

Fig. 3. External valve view showing conopeum, SEM (GU44Z-15).

Fig. 4. *Nitzschia granulata,* DIC (GU4A).

Figs 5–8. *Nitzschia lanceola*.

Fig. 5. Valve, DIC (GU55B-4).

Figs 6, 7. Valve at two focal planes, DIC (GU12G).

Fig. 8. Internal view, SEM (GU55B-4).

Fig. 9. *Nitzschia longissima* central portion, DIC (GU44Z-15).

Scale bars: Figs 1–5, 9 = 10 μm, Figs 6–8 = 5 μm.

Plate 60

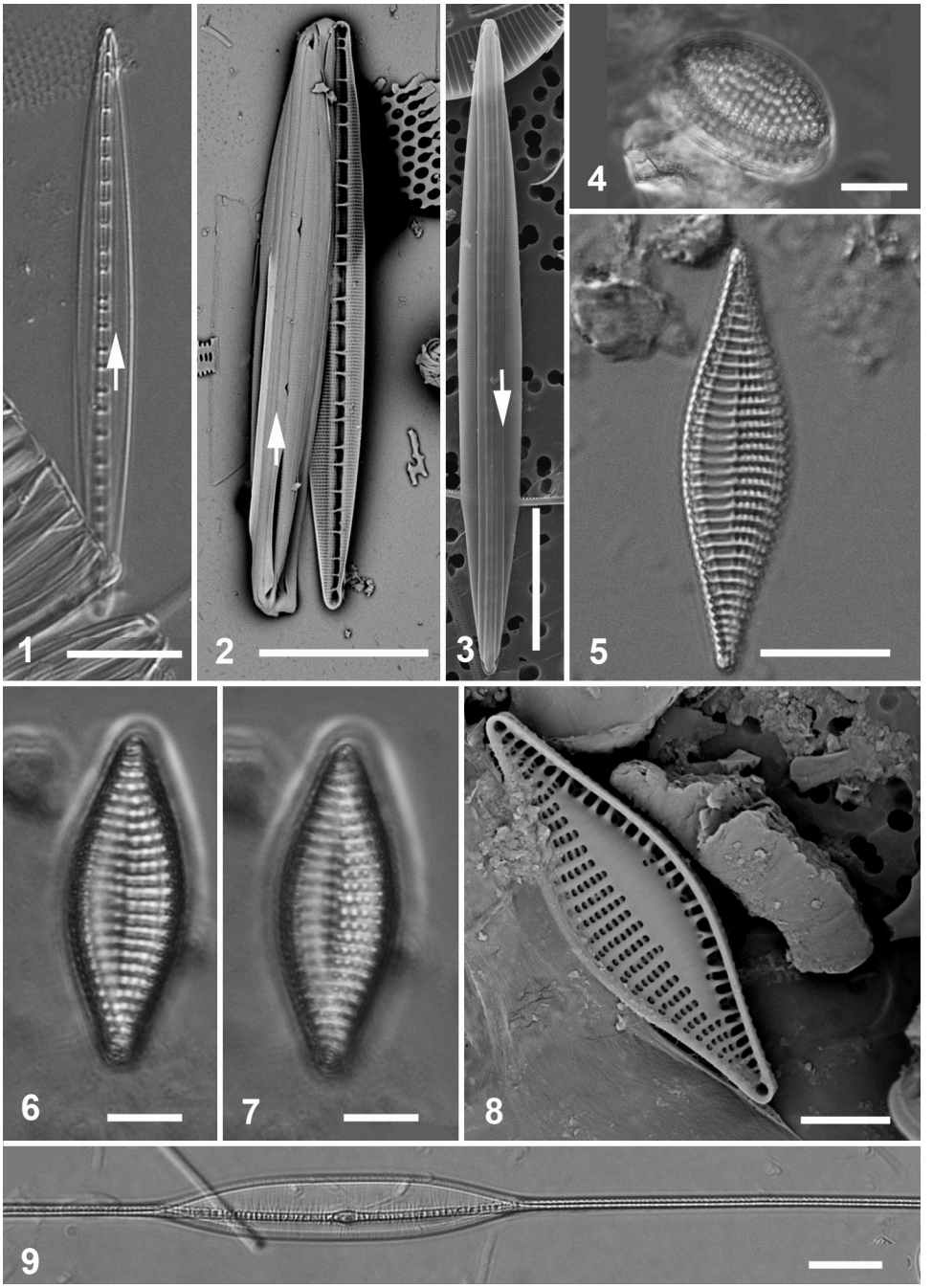

Plate 61.

Fig. 1. *Nitzschia longissima* external central portion, showing proximal raphe endings, SEM (GU52Q-10).

Figs 2, 3. *Nitzschia marginulata* var. *didyma*.

Fig. 2. Valve, DIC (GU44Z-15).

Fig. 3. Whole frustule showing internal surface, SEM (GU44I-1).

Fig. 4. *Nitzschia sigma* var. *intercedens* girdle view, DIC (GU44AR-2).

Scale bars: Fig. 1 = 5 μm, Figs 2–4 = 10 μm.

Plate 61

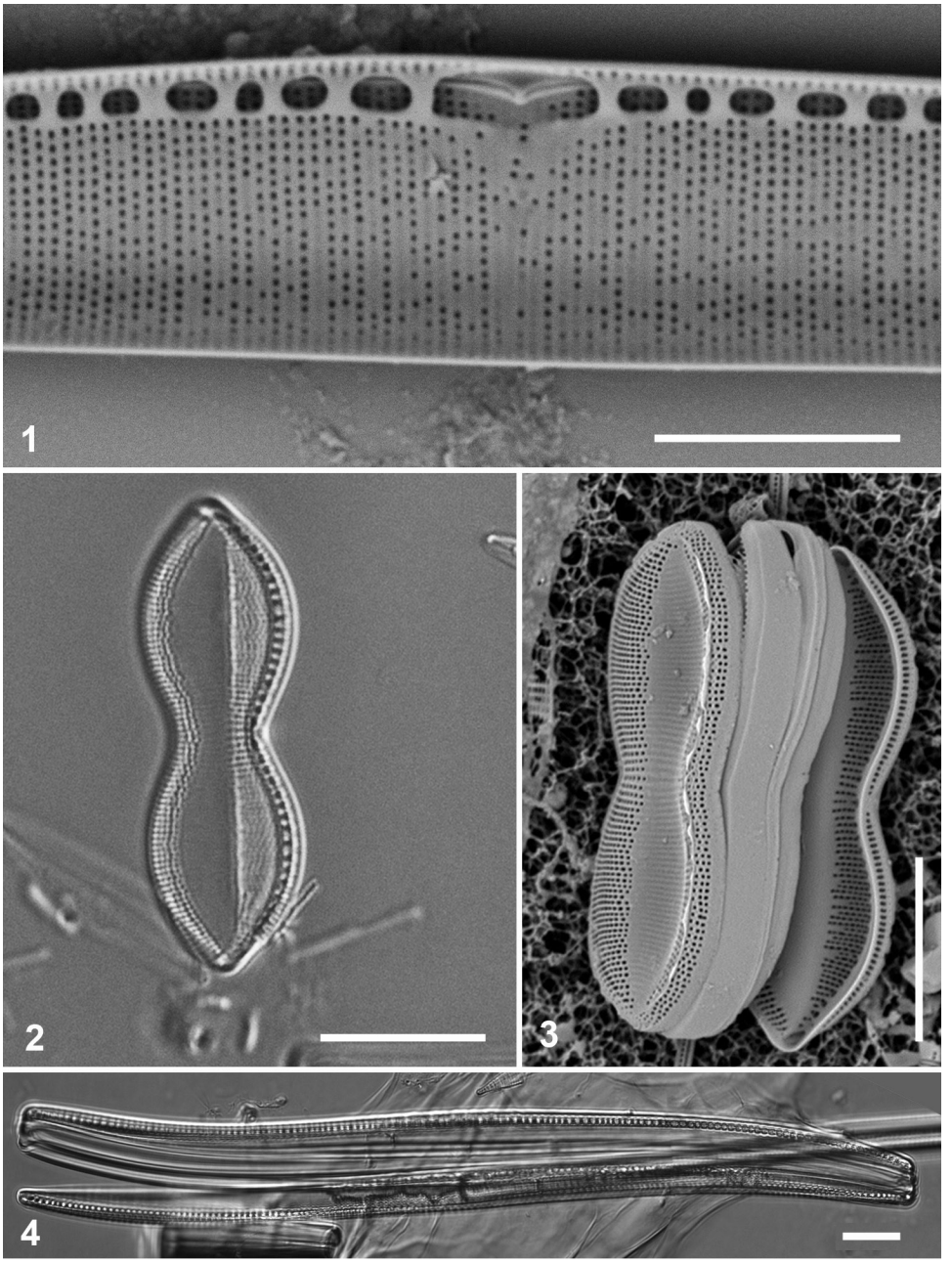

Plate 62.

Figs 1, 2. *Nitzschia ventricosa*.

Fig. 1. Portion of valve, DIC (GU44Z-15).

Fig. 2. Portion of internal valve face including part of the central region (GU26A).

Figs 3, 4. *Psammodictyon panduriforme*.

Fig. 3. Valve, DIC (Gab2D).

Fig. 4. Valve, internal view, SEM (GU44Y-13).

Scale bars = 10 μm.

Plate 62

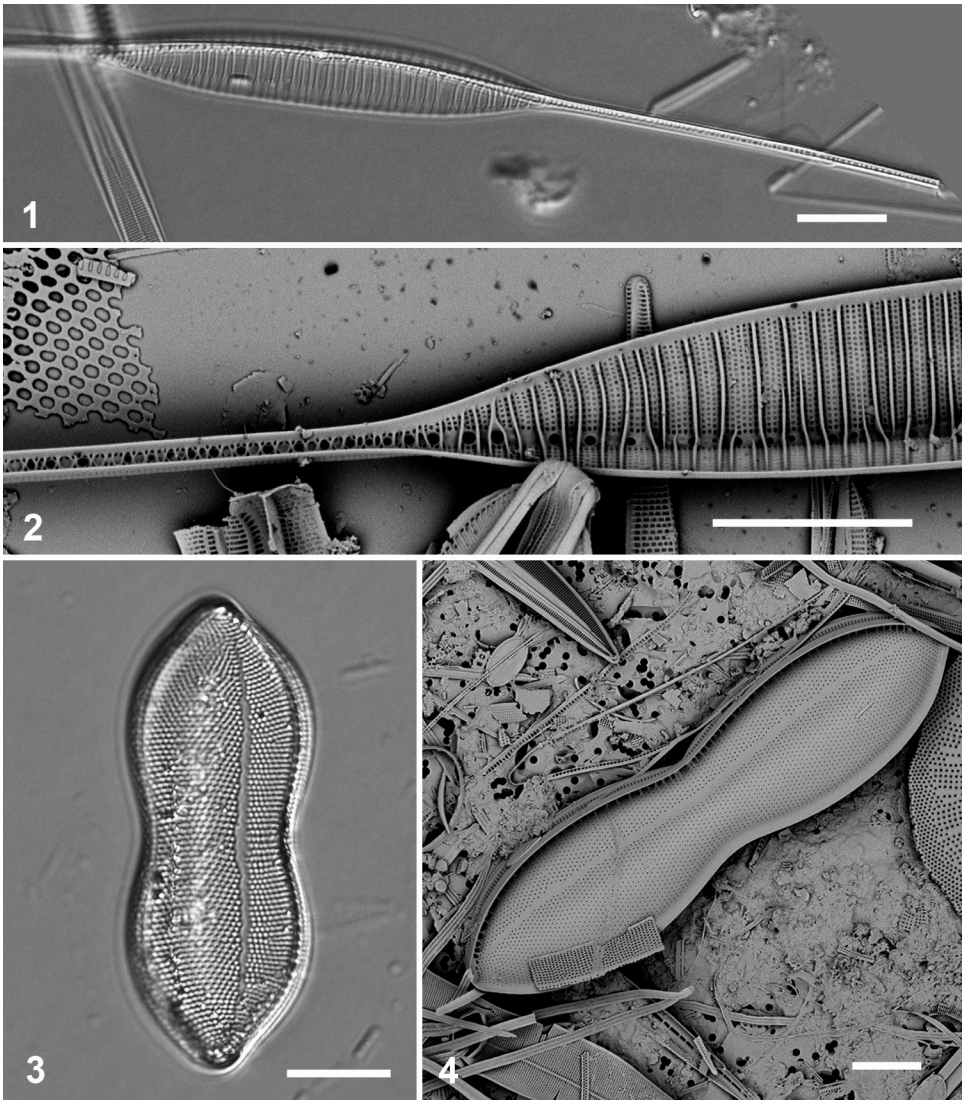

Plate 63.
Figs 1, 2. *Auricula complexa*, DIC (GU44Z-15) and SEM (GU44J-2).
Figs 3, 4. *Auricula intermedia*, DIC (GU55B-4) and SEM (GU44I-2).
Figs 5, 6. *Campylodiscus ambiguus*.
Fig. 5. Valve, DIC (GU44I-2).
Fig. 6. External detail of margin with raphe endings, SEM (GU44Y-14).
Scale bars: Figs 1–5 = 10 μm, Fig. 6 = 5 μm.

Plate 63

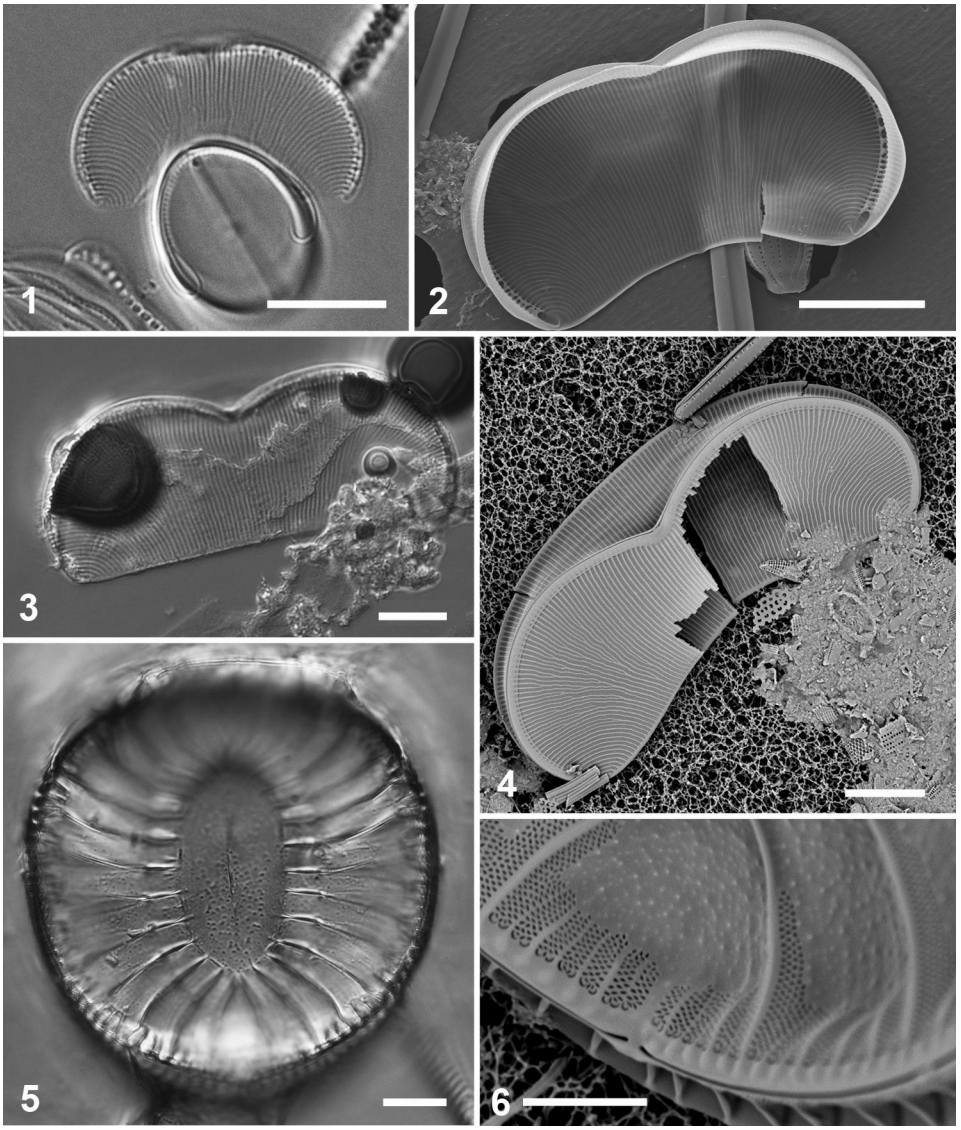

Plate 64.
Fig. 1. *Campylodiscus ambiguus* internal valve view, SEM (GU44R-2).
Figs 2–4. *Campylodiscus brightwellii*.
Fig. 2. Valve, DIC (GU44AN-6).
Figs 3, 4. Valves, external and internal views, SEM (GU44J-2).
Figs 5, 6. *Campylodiscus decorus* nominate variety, frustule at two focal planes showing crossed orientation of the two axial planes, DIC (GU44AR-3).
Scale bars = 10 μm.

Plate 64

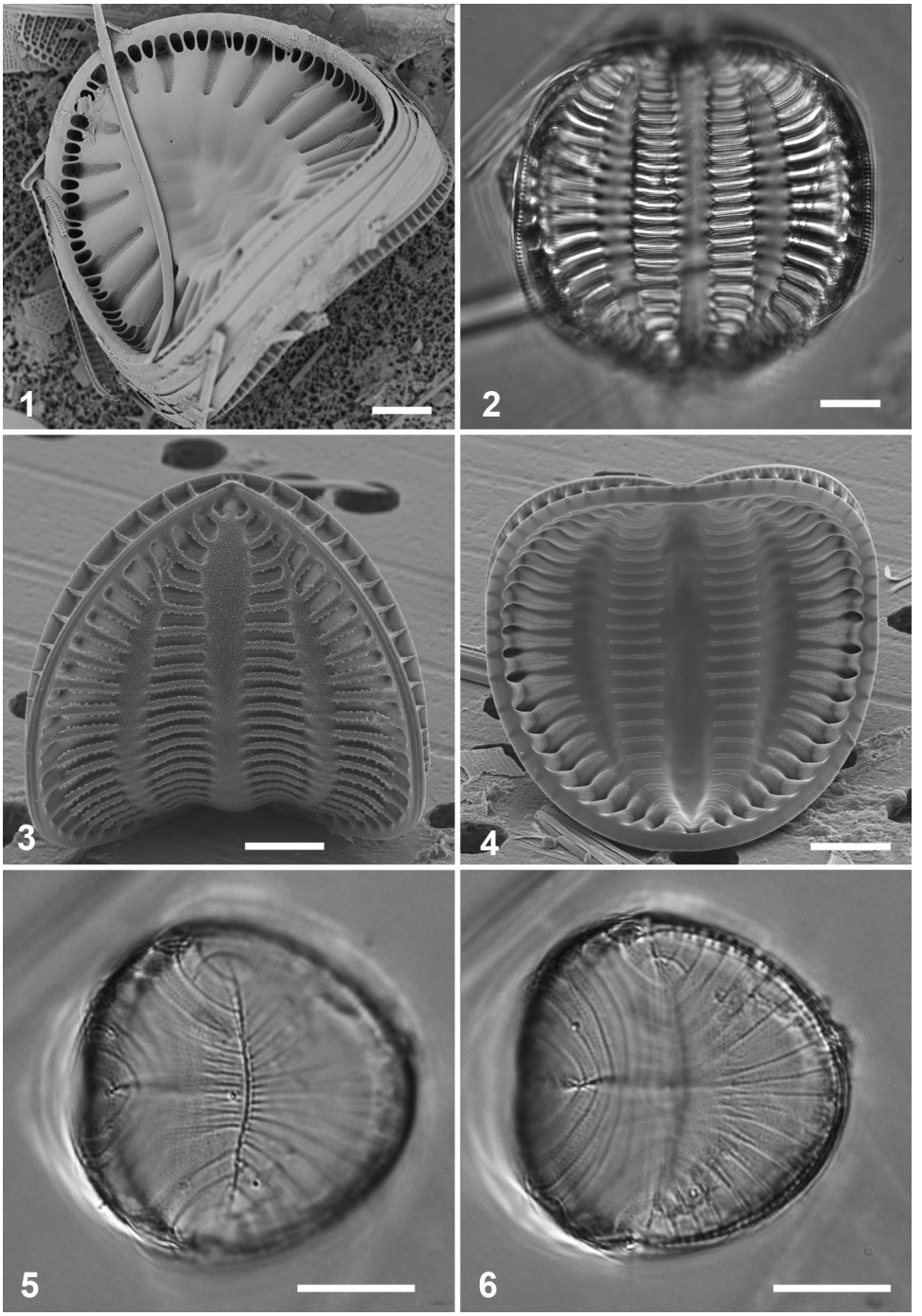

Plate 65.

Figs 1, 2. *Campylodiscus decorus* var. *pinnatus*, DIC (GU44I-1) and SEM (GU44R-2).

Figs 3–6. *Campylodiscus humilis*.

Fig. 3. Valve, DIC (GU44I-2).

Fig. 4. Polar view (external side down), showing parts of external and internal surfaces, SEM (GU44J-2).

Figs 5, 6. Internal and external views, SEM (GU44Y-13).

Scale bars: Figs 1–3 = 10 μm, Figs 4–6 = 5 μm.

Plate 65

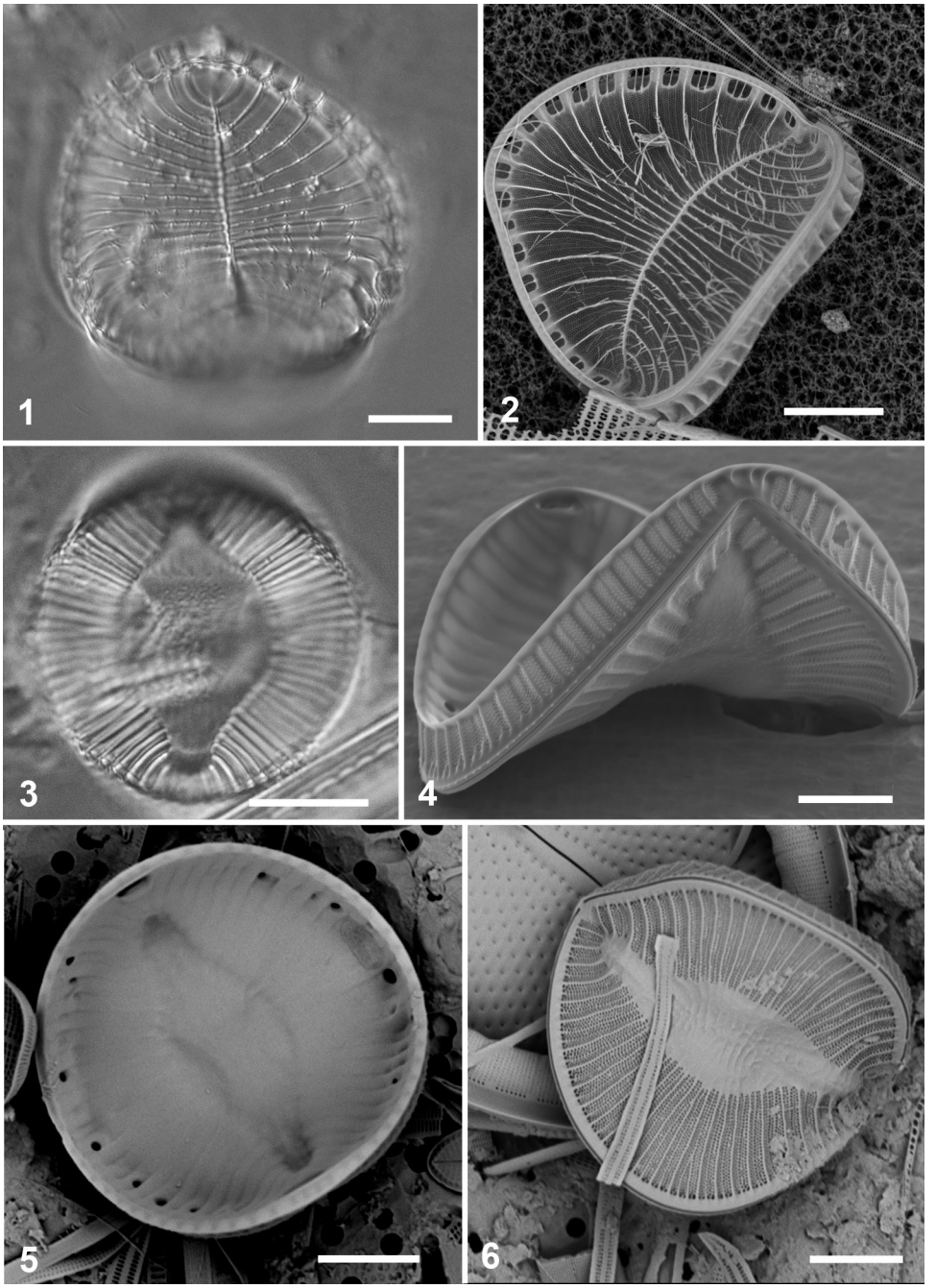

Plate 66.
Fig. 1. *Hydrosilicon mitra*, wet mount, DIC.
Figs 2, 3. *Petrodictyon patrimonii*.
Fig. 2. Living cell in girdle view, DIC (ECT 3681).
Fig. 3. Acid-cleaned valve, DIC (GU26A).
Figs 4, 5. *Plagiodiscus nervatus*.
Fig. 4. Valve showing spur-like process (arrow), DIC (GU55B-4).
Fig. 5. Frustule showing internal and external valve faces, SEM (GU52H).
Scale bars = 10 μm.

Plate 66

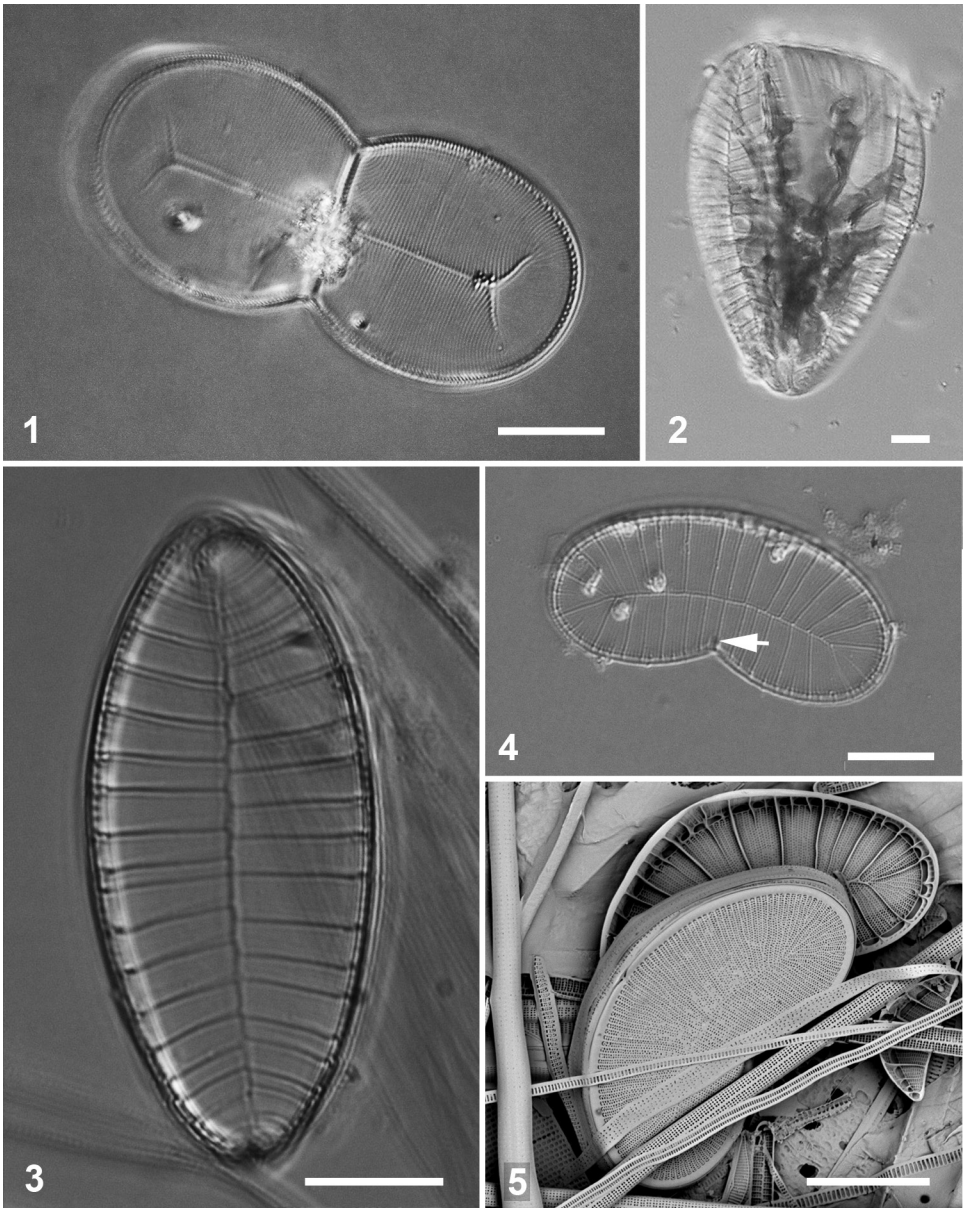

Plate 67.
Fig. 1. *Plagiodiscus martensianus* valve, DIC (GU52P-5).
Figs 2, 3. *Surirella fastuosa* live cell at two focal planes showing plastid and both valves faces with narrower central area on one side than the other (arrows), DIC (GU44AT).
Scale bars = 10 μm.

Plate 67

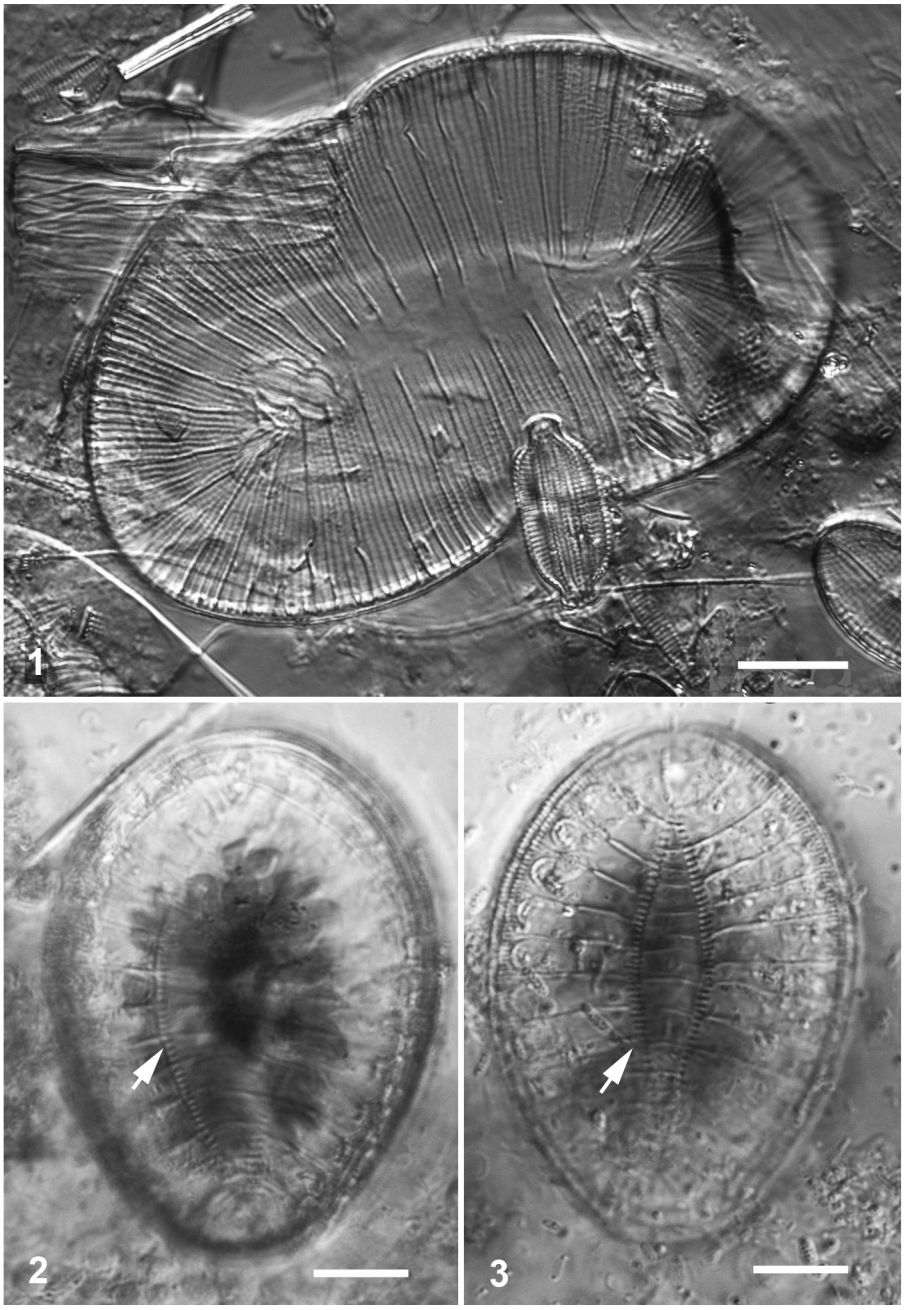

Plate 68.

Figs 1–3. *Surirella fastuosa*.

Fig. 1. Large valve with broad central area, DIC (GU44AN-6).

Figs. 2, 3. Small valve with narrow central area, at two focal planes, DIC. (GU44AN-6).

Figs 4–6. *Surirella scalaris*.

Fig. 4. Valve, DIC (GU52Q-2).

Fig. 5. Two frustules showing external and internal surfaces, SEM (GU52P-9).

Fig. 6. Intact frustule showing parallel orientation of valves, SEM (GU52Q-3).

Scale bars: Figs 1–3 = 10 μm, Figs 4–6 = 5 μm.

Plate 68

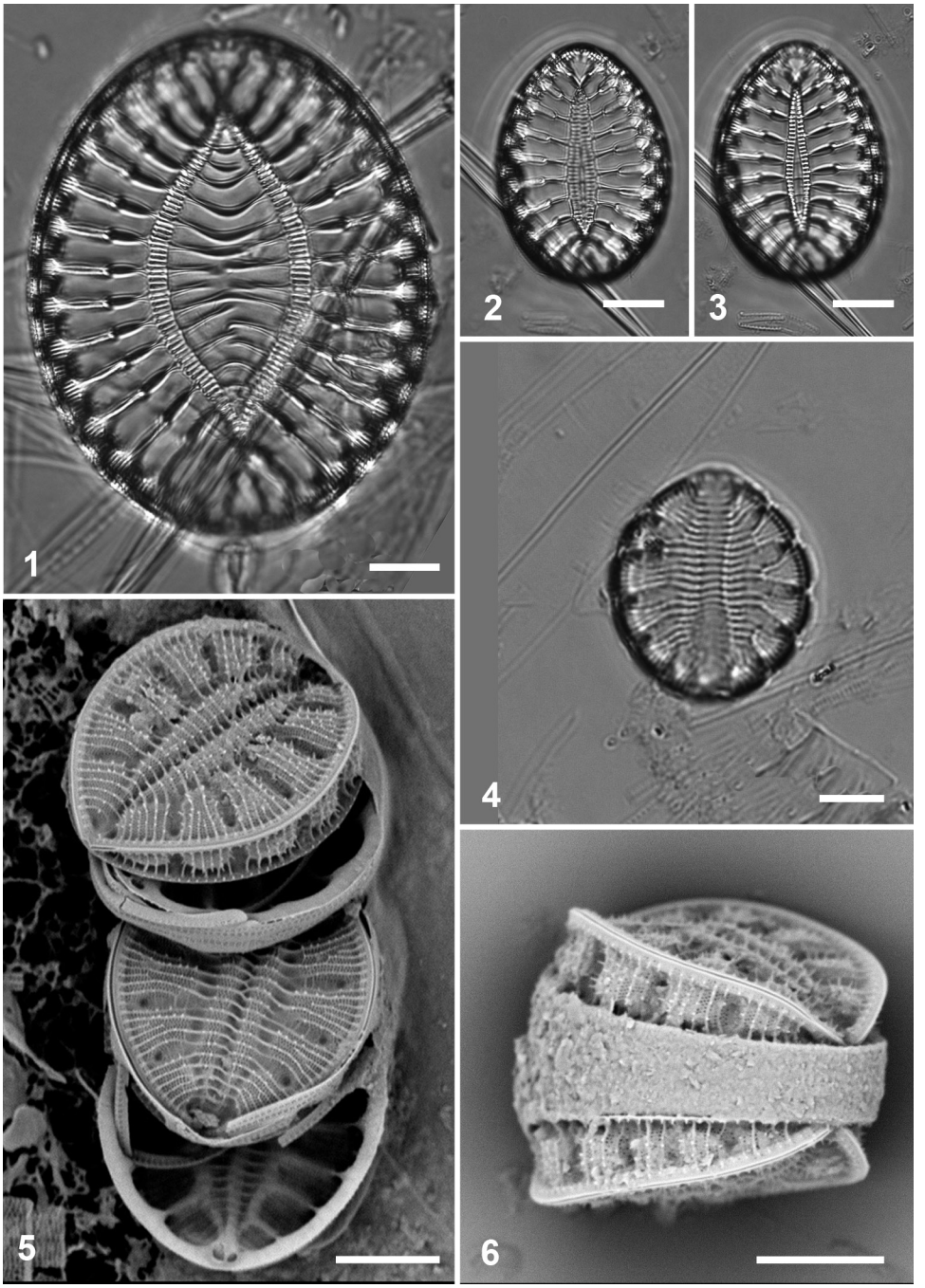

Plate 69.
Figs 1, 2. *Surirella scalaris*, external and internal view, SEM (GU44J-2).
Scale bars = 2 μm.
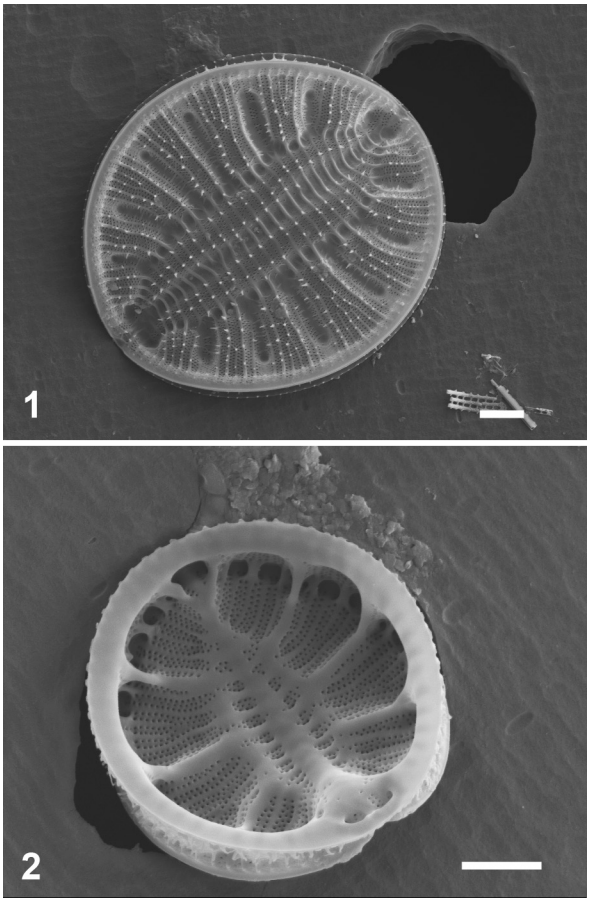
Plate 69